



Corrosion of steel reinforcement in 12 years old concrete: Inspection, evaluation and electrochemical repair of corrosion

Master Thesis

José Pacheco-Farías.

Delft University of Technology
Faculty of Civil Engineering and Geosciences
Materials & Environment
TNO Built Environment and Geosciences

Delft, Netherlands
July 2010

Graduation Committee:

Prof. Dr. R.B. Polder	TU Delft, CiTG, Materials & Environment, TNO Built environment and Geosciences
Dr. A.L.A. Fraaij	TU Delft, CiTG, Materials & Environment
Dr. ir. J.M.C. Mol.	TU Delft, 3ME, Surfaces and Interfaces
Ir. G.A. Leegwater	TNO Built Environment and Geosciences
Ir. L.J.M. Houben	TU Delft, CiTG, Road and Railway Engineering

Preface

This report describes the outcome of a Master Thesis Project at Delft University of Technology, Faculty of Civil Engineering and Geosciences in cooperation with TNO Built Environment and Geosciences. This study was carried out between October 2009 and July 2010. The topic of this project is the inspection, evaluation and electrochemical repair of corrosion of steel in concrete after 12 years of outdoor exposure. In the inspection phase, readers interested in the statistical analysis of results may consult Chapter 5 and Appendix A. Material scientists interested in results of corrosion monitoring may consult Chapter 6 and Appendix B. Engineers and Material Scientists interested in Cathodic Protection of steel in concrete are advised to find work carried out in this project in Chapter 7 and Appendix C.

I want to express my sincere gratitude to the graduation committee for their patience, valuable comments during our meetings and overall interest in the project. Particularly to Prof. Dr. Rob Polder for giving me the opportunity to continue my studies in the field of materials science in Civil Engineering, his guidance and continuous supervision during my work. Also, I want to thank Dr. Alex Fraaij for his most helpful guidance in the field of statistical analysis and comments on the interpretation of results when conducting my project, and to Dr. Arjan Mol for his valuable comments on the electrochemical aspects of corrosion of steel in concrete. I also want to thank Ir. Greet Leegwater for her advice, perspective and critical comments on during the elaboration of the project and report.

I also want to mention the people that helped me during my stage at TNO most satisfactory and assistance with my set of tests. Especially, to Ir. Hans Beijersbergen for his always ready to lend a hand attitude and valuable advice. Also, thanks to Dr. Oswaldo Nápoles for this counsel in the statistical analysis of results during the early stage of my project.

My studies at TU Delft would not be possible at all without the scholarship of Ing. Félix Cantú and UANL Foundation of Universidad Autónoma de Nuevo León. I will always be thankful to them for giving me this great opportunity to study and live in the Netherlands.

Finally but not least, I want to say thanks to my family and friends both in Delft and Mexico for their support during these two years, mostly to my lovely wife Karla for her never-ending patience, love and support. Gracias a todos.

José Pacheco

Delft, 2010.

Abstract

Corrosion of steel in concrete is the most important problem in maintenance of concrete structures. However, this problem has serious effects on infrastructure and economy that may be certainly reduced. The purpose of this research is to study the behavior of corrosion in concrete specimens after 12 years old. In 1998, concrete prisms were cast with four different cement types, three different water/binder ratios, two different cover depths and two different chloride-rich admixtures. Then, several concrete specimens were exposed to separate environmental conditions: salt/drying or carbonation. These differences have influenced the rate of corrosion with regard to the characteristics of each concrete mixture and exposure.

The main aim behind this project was to use as much as possible non-destructive testing (NDT) in order to preserve the highest quantity of specimens for further research. Therefore, description of the behavior of concrete specimens in the propagation phase is mostly based from the results and interpretation of results obtained from these NDT.

Three different aspects were studied in this project with regard to corrosion of steel in concrete. First, labels in concrete specimens were lost due to weathering over time; therefore, inspection of concrete specimens was carried out in order to identify the most probable concrete mixture in all specimens. This stage of study involved a combination of non-destructive testing by the means of visual inspection, electrochemical measurements and statistical analysis. Results showed that it was possible to identify cement types in specimens exposed to salt/dry cycles and mixed-in chlorides. However, for carbonation specimens this approach did not give the same confidence in results.

The second stage of study includes electrochemical measurements over three different time periods, November 2009, February and April 2010. These measurements involved properties like corrosion potential, concrete resistivity and corrosion rate. Results show that in chloride exposure, either salt/dry cycles or admixed-in, specimens containing blended cements (CEM II, CEM III and CEM V) performed better in terms of these properties. In carbonated specimens, Portland cement concrete showed better performance than the rest of concrete mixtures. Influences of environmental conditions, temperature and relative humidity were also studied. It seems that corrosion rate is favored when drier (10 °C and 80% RH) in overall specimens.

Finally, an electrochemical repair technique of Cathodic Protection was proposed in order to study the effect of current in steel bars actively corroding. Special attention was placed in the electrical current demand of steel bars according to their previous corrosion state and different concrete composition. Also, destructive analysis of concrete after CP treatment was carried out to study the visual state of steel reinforcement, the chloride content in concrete and the size of corrosion pits. Results show that the initial current demand and overall charge flow through steel bars during the treatment period are related to the state of steel deterioration by corrosion rate means. Tests done in order to measure the pH in corrosion products did not give reliable results; therefore, an improved test set-up is required. Chloride content profiles show that even after the loading of chlorides in salt/dry specimens stopped during year 1999, internal diffusion of chloride has been still occurring.

Table of contents

Preface	3
Abstract	4
Table of contents	5
1 Introduction	7
1.1 General	7
1.2 Objective of this study	7
1.3 Outline of this report	8
2 Durability and deterioration of concrete structures	9
2.1 General	9
2.2 Service Life of Infrastructure	9
2.3 Deterioration of concrete structures	10
2.3.1 Freeze-thaw	11
2.3.2 Alkali-aggregate reactions	11
2.3.3 Sulphate attack	12
2.3.4 Corrosion of steel in concrete	12
2.4 Concrete properties that are related to corrosion of embedded steel.....	19
2.4.1 Transport of matter in concrete	20
2.5 Inspection and survey of corrosion damage in concrete structures	24
2.6 Evaluation and monitoring of corrosion damage of steel in concrete	25
2.6.1 Steel potential (E_{corr}).....	26
2.6.2 Linear polarization resistance (LPR).....	27
2.6.3 Concrete resistivity	29
2.6.4 Chloride content	30
2.6.5 Carbonation depth	30
2.7 Repair of corrosion of steel in concrete.....	30
2.7.1 Overview	30
2.7.2 Cathodic protection	31
2.7.3 Concrete realkalisation.....	33
2.7.4 Electrochemical chloride extraction.....	33
3 Previous work and reported properties of concrete specimens	35
3.1 Previous work (1998 – 2009).....	35
3.2 Initial state of the project.....	38
4 Experimental program	39
4.1 Visual inspection.....	39
4.2 Concrete resistivity.....	40
4.3 Steel potential.....	40
4.4 Carbonation depth	40
4.5 Schmidt rebound hammer	40
4.6 Statistical Analysis	41
4.7 Linear polarization resistance.....	41
4.8 Chloride content.....	41
4.9 Cathodic protection	41
5 Identification of concrete specimens with the use of non-destructive testing	42
5.1 Overview	42
5.1.1 Visual inspection.....	42
5.2 Concrete Resistivity	43
5.2.1 Salt/dry exposed specimens after 2.5 years.....	43
5.2.2 Salt/dry exposed specimens after 11 years.....	48
5.2.3 Carbonated specimens after 2.5 years.....	51
5.2.4 Carbonated specimens after 11 years.....	54

5.2.5	Mixed-in chloride specimens after 2.5 years.....	57
5.2.6	Mixed-in chloride specimens after 11 years	61
5.3	Schmidt hammer test in hardened concrete.....	65
	Synopsis.....	67
6	Evaluation of corrosion in concrete specimens.....	68
6.1	Electrochemical measurements, November 2009	68
6.1.1	Salt/dry cycles.....	68
6.1.2	Carbonation.....	70
6.1.3	Mixed-in chlorides	71
6.2	Electrochemical measurements, February 2010.....	72
6.2.1	Salt/dry cycles.....	72
6.2.2	Carbonation.....	74
6.2.3	Mixed-in chlorides	76
6.3	Electrochemical measurements, April 2010.....	78
6.3.1	Salt/drying cycles.....	78
6.3.2	Carbonation.....	81
6.3.3	Mixed-in chlorides	82
6.4	Discussion.....	84
6.4.1	General.....	84
6.4.2	Salt/dry specimens	84
6.4.3	Carbonation specimens	88
6.4.4	Mixed-in chloride specimens	91
	Synopsis.....	94
7	Electrochemical repair of concrete specimens deteriorated by corrosion.....	95
7.1	Overview.....	95
7.2	Cathodic protection setup and initial conditions	95
7.3	Monitoring of current in CP system.....	97
7.3.1	General.....	97
7.3.2	Short-term CP results.....	97
7.3.3	Long-term results of CP treatment.....	100
7.3.4	Depolarization.....	104
7.4	Destructive analysis	107
7.4.1	General.....	107
7.4.2	pH measurements.....	108
7.4.3	Carbonation depth.....	108
7.4.4	Chloride profile.....	109
7.4.5	Corrosion pit measurement and volume loss	111
7.5	Discussion.....	113
7.5.1	Corrosion state of steel bars before CP.....	113
7.5.2	Measurements during CP treatment.....	116
7.5.3	Depolarization.....	118
7.5.4	Chloride profiles	118
7.5.5	Corrosion pit measurements and CP	119
	Synopsis.....	121
	Conclusions.....	122
	Recommendations for future research.....	124
	References.....	125
	Appendix A: Inspection of concrete specimens.....
	Appendix B: Evaluation of corrosion of steel in concrete
	Appendix C: Electrochemical repair of corrosion

1 Introduction

1.1 General

In consultancy of civil engineering structures, challenges related to durability of concrete structures can occur during the whole life span. The consultant (engineers, material scientists or operation personnel) finds that many parameters may have influenced the condition of the structure and its remaining service life. Since most concrete structures are exposed to different conditions, several types of degradation mechanisms may be present during their service life. At the same time, important information about the structure -i.e. type of cement used water-binder ratio, curing, etc. - may be lost or was not properly recorded. Which brings the following questions: Which degradation mechanism is affecting the structure? What is causing this degradation? How long will the structure still be in a serviceable condition? What can be done in order to extend its service life?

This challenge is common when dealing with old structures and certainly makes it more difficult for providing an accurate diagnosis of the deterioration problem. Besides this, literature related to the effect of corrosion reinforcement in concrete generally describes results from laboratories where environmental conditions are controlled. However, real structures are subject to conditions that change daily; therefore, the long-term study of concrete is interesting. Results obtained during the early exposure of the structure may provide vital information that may help to identify characteristics of the deterioration mechanism like: the time at which the deterioration started, the length in time that the structure has been under such damage and the causes that originated it.

In the project presented in this report, the performance of reinforced concrete prisms is followed throughout a period of twelve years. The prisms were cast in 1998 and monitored until 2002. In 2006 the specimens were subject to relocation of the laboratory and the labels on their surface were lost. The lack of labels presented a challenge to measure the performance again in the year of 2009. Reports done by TNO personnel gave a broad record of the history of those concrete specimens that made possible to have an initial impression of the probable concrete composition of such specimens. With the use of those reports, visual inspection, some electrochemical measurements and statistical analysis, it was possible to identify the cement type and water cement ratio in most cases with a 95% of confidence. The followed procedure may provide new insights that can be used for the inspection procedure of real structures.

After the identification of concrete specimens was realized, the performance of concrete that contained active corroding steel was monitored in three different time periods, November 2009, February and April 2010. The weather conditions during these testing periods was different, therefore some electrochemical measurements were influenced by changes in temperature and moisture content. However, there was still possible to analyze which specimens have continued corroding since 2002 and some other that have started to corrode more recently over this 8 years time. This part of the research involves comments on literature of corrosion of steel in concrete and a description of different phenomena that have influenced the kinetics of corrosion during such time.

A responsible owner or government should not only address and measure the corrosion state of steel in concrete when investigating this degradation; therefore, a proposed repair action is given in the last part of this research study. An electrochemical repair technique was applied on four specimens with different concrete mixtures and damage levels in order to study the effect of neutralization of acidic pools in corrosion pits and the relationship between the damage level and electric current flow in reinforcement. This final part of the project includes a few minor destructive analyses that were necessary in order to provide a determination of the successfulness of such repair procedure.

1.2 Objective of this study

The objective of this research study is focused on the behavior of corrosion of steel reinforcement in concrete specimens after 12 years of environmental exposure. Differences in type of cement, water-binder ratio and exposure conditions are influencing corrosion kinetics; therefore, a study of the development of corrosion with respect to these parameters after 12 years is of interest. The main goal of this project is to report the outcome of the influence of diverse parameters like type of cement, water/binder ratio and exposure conditions into the corrosion kinetics of embedded steel. As additional goals, a short term cathodic polarization treatment is studied as possible repair solution for neutralization of acidic pools in corrosion pits and the behavior of electric current flow for the design of cathodic protection systems.

1.3 Outline of this report

The report is divided into chapters for describing the parameters of study and the results of each stage.

Chapter 2 describes the background of concrete durability, service life and degradation mechanisms. In this chapter a description of degradation mechanisms in concrete, transport of aggressive agents into concrete, principles behind corrosion of steel in concrete and repair techniques is given. The purpose is to explain and comment about the agents that are involved in the corrosion of steel in concrete.

Chapter 3 resumes previous reports by TNO Built Environment & Geosciences from 1998 until 2002. It contains information about the materials that were used during the fabrication of concrete specimens, their properties in fresh mix state and hardened state. A review of non-destructive and destructive tests that were done during the first four years and the condition of the specimens at the beginning of this study is described.

Chapter 4 shows a detailed description of the experiments that were carried out during this study. A three level study was done in order to inspect, evaluate and repair corrosion damage in concrete specimens. Technical information about the experimental techniques that were used can be found in this chapter.

Chapter 5 describes and discusses the results that were obtained during the inspection stage of the project. It contains results and interpretation of different parameters and the outcome of statistical tests that were used in order to identify concrete specimens.

Chapter 6 contains relevant information related to the evaluation of corrosion of steel in concrete. Results of electrochemical measurements are presented and discussion about the agents that influence the measurements is done. The results are divided into three different periods of testing and comments about similarities and differences are made.

Chapter 7 describes the use of cathodic protection as a proposed solution during the repair phase. In this chapter, a brief description of principles behind cathodic protection, the purpose of the repair methodology, results and interpretation are included. Special attention is paid to the behavior of electric current flow in concrete and through bars and the influence of such current on pH of acidic pools inside corrosion pits. Also, results obtained from destructive analysis are compared and related to the corrosion state of concrete specimens before the electrochemical treatment.

Chapter 8 presents final conclusions, recommendations for future work and reference.

2 Durability and deterioration of concrete structures

2.1 General

Since the end of last century, the influence of durability in design codes for civil infrastructure has been present (ACI-201 1991; RILEM 1996). The main purpose was to improve the durability of infrastructure and extend their life-span. The reduction of service life in concrete structures is a significant problem for the construction industry. This has to do with the fact that concrete is the most used construction material in the world. According to ACI 365 committee (ACI 365 2000), the durability of concrete structures is “*the ability of a structure or its components to maintain serviceability in a given environment over a specified time*”. With regard to service life: “*an estimate of the remaining useful life of a structure based on the current rate of deterioration or distress, assuming continued exposure to given service conditions without repair*”.

A first step in order to provide an opinion and possible solutions must include the previous performance and life span of the structure. To determine if the structure remains serviceable or not is a decision that must be made with solid fundamentals, after analyzing data obtained from different tests.

2.2 Service Life of Infrastructure

Civil infrastructure construction deals with different stages according to the age of the structure. Generally, these stages include the design phase, the service life and the end of service life or collapse. The design phase entails the work done during the pre-execution of the structure. In it, the durability aspect is taken into account by means of deterministic (normative) or stochastic (probabilistic analysis of failure) means. Even though engineers and architects do most of the work in this phase, materials scientists may also be involved when the decision of which building materials are required according to the conditions to which the structure will be subject. During the design phase, the prevention of concrete or steel deterioration is the main concern for engineers and scientists. In this sense, there are several ways to achieve this, like proper structural consideration (cover depth, cement type, water/binder ratio, concrete strength, etc.), construction procedures (curing, variations in cover depth), and other preventive measures. Some of those measures that can be taken during this phase are shown in Figure 2.1 (Bertolini 2004).

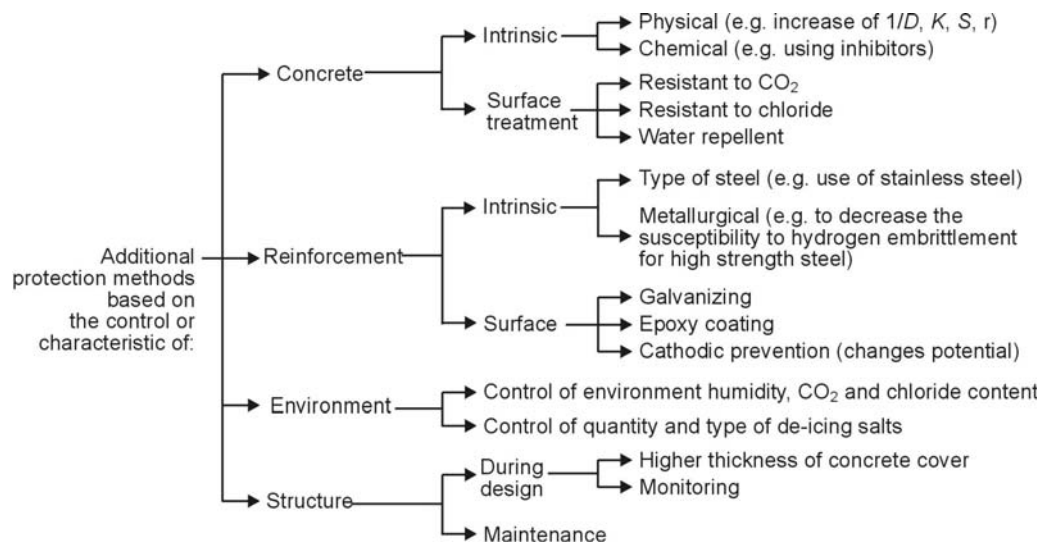


Figure 2.1 Preventive measures for degradation of concrete structures.

The design phase has a significant impact on later stages of prevention and repair of structures during service life as described in ‘De Sitter’s Law of Fives’ (De Sitter 1984), which quantifies the effect on whole-life costs of decisions made at different stages in the life cycle efficiency of a structure. It could be expressed as follows:

€1 spent getting the structure designed and built correctly is as effective as €5 spent in subsequent preventative maintenance in the pre-corrosion phase while carbonation and chlorides are penetrating inwards towards the steel reinforcement. In addition, €1 is as effective as €25 spent in repair and maintenance when local active corrosion is taking place. In turn, this is as effective as €125 when generalized corrosion is taking place and where major repairs are necessary, possibly including strengthening or the replacement of complete members.

After the execution phase has ended, the serviceability of the structure begins to be taken into account. However, the length of the serviceability phase is much higher than the other two previous stages. Right after the moment that the structure is built (and in some cases during the execution phase) the environmental action takes place. The influence of aggressive action on early age concrete structures has been recently addressed in a previous work (Caballero 2009), and shows that material selections is very important when the structure is subject to aggressive conditions since the very beginning of its service life.

After the structure is subject to evident deterioration and the performance of it does not have an ‘acceptable’ level, maintenance or repair actions are required in order to extend the service life of the structure. In principle, the maintenance phase begins with an inspection of the damage in the structure in which characteristic evidence of damage is surveyed like:

- cracking,
- scaling
- spalling
- lime staining on the surface
- leakage through joints
- abrasion, etc.
- efflorescence
- rust staining
- weathering
- honeycombing
- dampness

Data collected from the monitoring or evaluation phase will give important input in order to understand the degradation mechanism that is observed in the structure. A proper repair methodology requires an adequate identification of the problem, in order to provide a successful repair solution. Otherwise, even if repair has been done, there is no certainty that the problem will be stopped and further damage may be present.

Concrete structures have generally service life spans of 20 to 50 years without major damage due to deterioration. During this phase, monitoring of the performance of the structure is recommended in order to identify with precision the time at which significant deterioration occurs in the structure. This is important when identifying the cause of such deterioration, which has significant relevance for possible repairing if required. After doing the first inspection, the damage must be evaluated in order to determine if repair action is necessary.

If proper actions have been taken, the service life of the structure has been increased for a period of time. However, these repair actions involves economical costs that must be reduced as much as possible. Therefore, the influence of decisions made during the design phase is observed during the repair phase as described in De Sitter’s Law.

Corrosion of steel in concrete occurs generally in the serviceability phase and it involves the monitoring of the concrete and steel performance and the repair of such deterioration. In this sense, the detrimental nature of corrosion involves the presence of external agents. By environmental action, the serviceability performance of the structure is reduced due to degradation of concrete structures which is briefly described below.

2.3 Deterioration of concrete structures

The development of reinforced concrete during the 19th century was one of the major advances in the history of construction industry. Reinforcing steel embedded in concrete dramatically improved the tensile strength of concrete structures which led to fabricate slender structures that sustain higher stresses and larger spans. Nevertheless, concrete and steel reinforcement may be subject to several degradation mechanisms that reduce the service life of infrastructure. From a general view, each degradation mechanism requires the presence of different agents and suitable environmental conditions. Nevertheless, in reality things are not so simple. A relevant number of parameters influence the performance of concrete structures in many different ways. Even the contents of concrete itself play a significant role in its behavior during service life. Since degradation of concrete represents high economical costs related to repair and maintenance, deterioration of concrete must be avoided, prevented or repaired.

According to the cause of degradation, concrete may be subjected to diverse deleterious processes. The nature of each particular degradation mechanism is different for each case and an overview of them are shown in Figure 2.2 (Bertolini 2004).

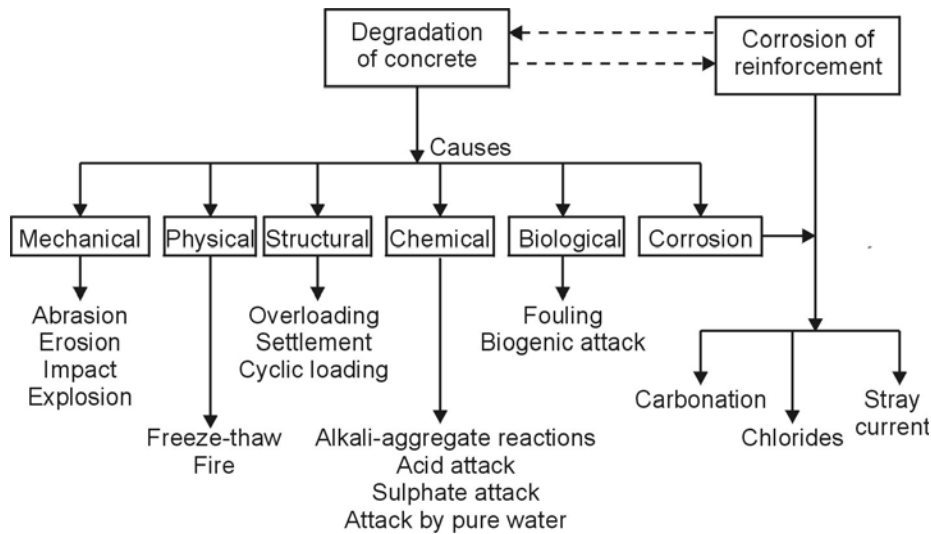


Figure 2.2 Degradation of concrete and their possible causes.

Since concrete structures are present in varied of environmental conditions, several causes of concrete deterioration may be present at the same time. From a point of view in terms of durability, concrete exposed to freeze-thaw, fire, alkali-aggregate reactions, sulphate attack, biological deterioration and corrosion of steel reinforcement are some of the most common mechanisms in concrete degradation. Some of the most common mechanisms of deterioration are briefly described.

2.3.1 Freeze-thaw

In cold climates where the temperature decreases below 0 °C, moisture inside concrete is solidified and an increase in volume is produced (Bertolini 2004). Since the pore matrix is a complex route for moisture transport, water in those pores may not reach outside the specimens. Therefore, internal pressure due to the increase in volume of water inside the pores produce cracking in concrete structures when the stress caused by water is higher than the tensile strength of concrete. When the temperature rise above 0 °C, the ice is melted and moisture is now present again in the structure. The newly-formed crack is now a path for ingress of moisture and the cycle is repeated. For freeze and thaw resistance concrete is considered frost resistance if the durability factor is above 60% after 300 cycles (ASTM C666-08 2008).

The volume of air (different from porosity) that is contained in concrete serves as a pressure reliever for the internal pressures. Also, stress caused by this phenomenon is reduced and will not be higher than the tensile strength. Air-entraining admixtures are now common in concrete industry and they have shown significant improvement in concrete performance under freeze –thawing cycles. Nevertheless, the use of air-entraining agents modifies the mechanical strength of concrete. As a rule of thumb, 1% of entrained air modifies by 5% the 28 day compressive strength of normal strength concrete (Aïtcin 2008).

2.3.2 Alkali-aggregate reactions

Alkali silica reaction (ASR) is a deleterious process, which starts with a reaction between alkaline hydroxides derived from cement alkalis (Na₂O and K₂O) and siliceous minerals from aggregates. As a result, a gel of alkali-silica is formed in some weak planes and pores in concrete or in the aggregate/paste interface. In the latter case, the adhesion force between paste and aggregates is broken. The main characteristic of this gel is its high expansiveness due to water absorption and, therefore, volume increase. Since this gel is confined by the cement paste, internal pressures produce swelling and cracking in concrete when the stress caused by internal pressure is higher than the tensile strength of concrete. Later, the gel is transported by water to the newly formed cracks where it continues its effect. The most important forms of reactive silica are opal, chert, chalcedony and tridymite. Several countries like Canada, Denmark, UK, USA and The Netherlands (Nijland 2002) have reported alkali-silica reaction in concrete bridges and roads. A characteristic map-cracking is observed after this degradation mechanism and leaking of silica-gel may be present on the surface of concrete. The amount of alkali content is also important for alkali-silica reaction. When the aggregates are found to contain amorphous

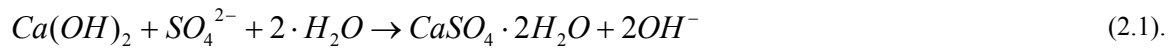
silica and they must be used for concrete fabrication, low alkali Portland cement ($\text{Na}_2\text{O}_{\text{eq}} < 0.6\%$) may be used without the risk of ASR. Also, blended cements like CEM III have higher resistance to ASR.

Alkali carbonate reaction (ACR) occurs when carbonates contained in aggregates react with alkalis of concrete producing a mineral known as brucite. It can be controlled by keeping the alkali content of cement low, adding lithium salts or diluting reactive aggregate with other non-reactive material.

2.3.3 Sulphate attack

Concrete exposed to sulphates contained in water or soil may be subject to reaction between these sulphates (SO_4^-) and cement paste that produce swelling and cracking. Also, loss of bond between aggregates due to dissolution of cement paste may occur.

Two by-products of the sulphate attack reaction may produce either gypsum, (Neville 1995)



or ettringite:



Ettringite is a mineral formed during hydration of concrete (Neville 1995), which is involved in the increase in volume during setting of concrete after cast. Sulphate-produced ettringite is deposited in the pores of hardened concrete and after being in contact with moisture; it swells causing internal stresses and therefore cracking of concrete. The effect of gypsum is of the same nature, but with less magnitude than ettringite.

2.3.4 Corrosion of steel in concrete

Corrosion is a degrading process which involves the dissolution of iron and constitutes the most important problem in durability of concrete, and it is the main degradation problem of maintenance in building industry in the world (Broomfield 2007). Structures exposed to moisture changes in an aerated environment are susceptible to corrosion damage. In an aqueous medium the corrosion of steel is of electrochemical nature. Since concrete may be considered as an aqueous and porous medium, corrosion of steel in concrete is of electrochemical nature.

As described before, concrete cover protects the reinforcement or prestressing cables in a twofold action: first, it provides a physical barrier from the environment. This cover layer has a significant importance for the kinetics of the degradation process. The second one is a chemical protection due to the high pH of the concrete pore solution which provides thermodynamical conditions that prevent or neglect corrosion. Nevertheless, concrete porosity allows moisture, oxygen and aggressive ions penetration, reducing the durability of structures during their service life.

Electrochemistry of corrosion

Some chemical reactions produce electrical flow of current and corrosion follows this behavior similar to a voltaic cell. In this kind of cells, two half-cells are required. In each one, chemical reactions of different nature take place. In aerated conditions, dissolution of material (metal) occurs in the oxidation cell or anodic cell and reduction of oxygen occurs at the reduction or cathodic cell. Both cells are connected by a porous medium (in this case concrete) and the current flow is carried by ions contained in the pore solution, therefore working as an electrolyte. Ions are transported through pores and provide electrical conductivity. These reactions take place only when the electrochemical balance of the metal with its environment is not reached. For this, the concepts of anodic and cathodic corrosion rate are known.

The electrochemical process of corrosion of steel in concrete is made up by the oxidation half-reaction (anode) cell at the steel bar according to:



The reduction half-reaction (cathode) occurs on the steel surface:



Both reactions are in contact due to an electron conductor (steel bar) and an ionic conductor (water-filled pores) forming an electrical circuit. Also, both reactions are related to an electrochemical reaction and the sum of each reaction potential is the electrode electrochemical potential (E). The electrochemical potential of steel occurs due to the difference in potential between the anodic and cathodic regions. This parameter is relevant for knowing the corrosion mechanism that affects the steel reinforcement. Literature has shown that electrochemical potential of steel is related to the possible state of degradation of reinforcement. In this sense, it is possible to determine the corrosion potential at the steel surface and estimate the probability of corrosion.

According to the type of reference electrode the potential has to be compared with normative values for evaluating the probability of corrosion. It must be noted that results of E are influenced by changes in concrete's heterogeneity, moisture, temperature and content of chlorides or pH.

Polarization

Reactions (2.3) and (2.4) only proceed at finite rates. If electrons are provided for (2.4), the potential at the surface of the bar will be more negative due to the presence of electrons in the metal/solution interface and their negative charge. This type of polarization is known as cathodic polarization. When the metal dissolves and electrons are released, a change of the potential towards a more positive one will occur on the surface of the steel bar. This is known as anodic polarization (Jones 1996).

Passivity

During the hydration of cement, soluble alkali oxides (Na_2O , K_2O) produce a highly alkaline solution which provides an environment with kinetically stable conditions for steel bars. After hardening, the pore solution in a hydrated Portland cement matrix remains alkaline with a pH value of around 13. In this environment, steel is protected by a thin but dense layer of protective oxides. This layer is known as "passive layer" which is formed spontaneously (Jones 1996). In these conditions, the passive layer is produced on the surface of reinforcing steel acting as a barrier for the anodic reaction.

In electrochemical terms, when the potential E of a metal is more positive than a specific potential, the corrosion rate at which it dissolves is reduced. This potential is known as passivation potential (E_{pp}). Figure 2.3 shows the reduction in corrosion rate when the potential is changed. In this figure, three main zones are described. The first one is the active zone in which the potential is very negative. As it is named, corrosion occurs when the potential of steel is negative. Dissolution of iron occurs in this zone and its rate is increased when the potential turns more positive. The second zone, called passive zone, is reached when the steel potential is above a certain passivation potential (E_{pp}). In this stage the corrosion rate is very low and dissolution is reduced to a negligible level of loss of material. Finally, the transpassive zone is localized in highly positive potentials and the oxygen concentration regulates the rate at which corrosion rate may occur.

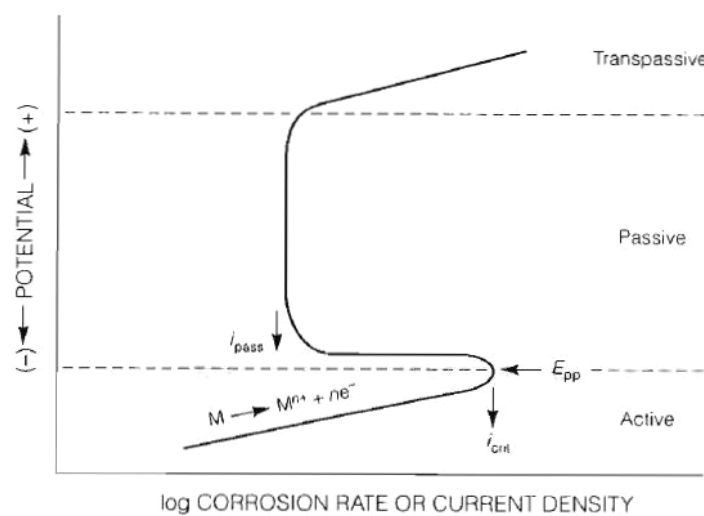


Figure 2.3 Electrode potential curve of embedded steel in concrete.

Nevertheless, when aggressive ions are contained above a threshold level, the passive layer may be destroyed.

This process is called depassivation. When the passive layer breaks down, the protective performance is lost and dissolution of iron may begin.

Corrosion initiation

When a concrete structure is exposed to environmental conditions in which aggressive agents penetrate into concrete in order to react with the embedded steel and oxygen, corrosion of steel reinforcement will occur. Nevertheless, the time that is taken for these agents to reach the bars depends on parameters that may extend the period in which corrosion begins. This period of time is known as corrosion initiation. The service life of a structure in terms of corrosion behavior is shown in Figure 2.4 (Tuutti 1982).

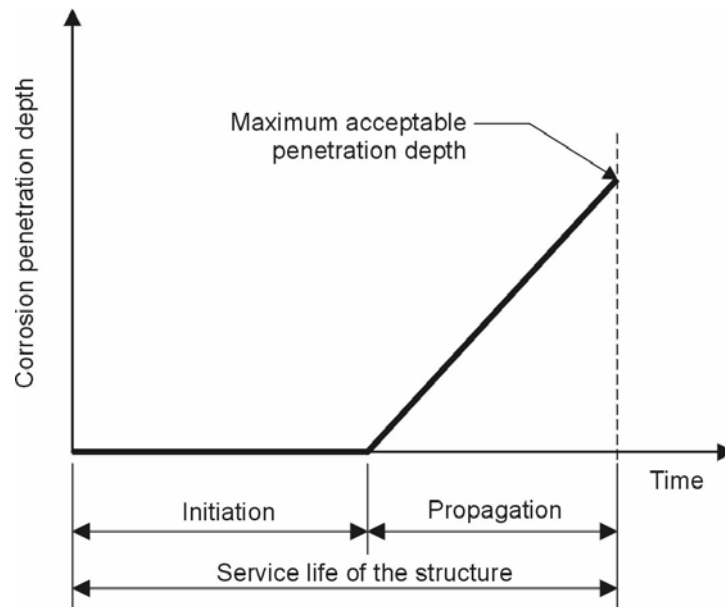


Figure 2.4 Time span of service life in concrete structures subject to corrosion of reinforcement.

Corrosion initiation is considered sometimes as negligible corrosion because the damage or penetration depth of corrosion is very low. Nevertheless, during this period, accumulation of aggressive agents occurs and beyond (above) a specific concentration (threshold), the conditions of stability for the passive layer are not present anymore. During the design phase, the quality of design is significantly important in terms of delaying the ingress of agents into concrete. A proper design should consider the environment that surrounds the structure and which aggressive agents (gasses, ions or currents) may be present and structural and preventive measures should be taken by.

The nature of the agent that causes dissolution of iron of embedded steel determines the mechanism in which the steel will be corroding. In nature, chlorides are responsible of pitting corrosion and carbon dioxide of general corrosion (carbonation). Also, stray currents from other civil infrastructure that are not properly isolated from the steel reinforcement may produce corrosion.

Chlorides

Pitting corrosion is caused by the presence of chloride ions in concrete. These chlorides are generally found in structures exposed to salt/drying cycles caused by sea splash or de-icing salts in cold climates. Also, during the 1950-70's, chlorides were cast into concrete structures as admixture [CaCl_2], in order to accelerate the setting process of fresh concrete. Even though the presence of chlorides does not mean any harm for concrete itself, they are a great threat for steel. The presence of chloride ions in concrete influences the steel potential according to the level of chloride concentration. As the chloride content is increased, the potential shift in the passivity zone is reduced, meaning in an increase in the potentiodynamic anodic current density in the cell. Figure 2.5 shows the performance of steel potential when chlorides are present in concrete (Bertolini 2004)..

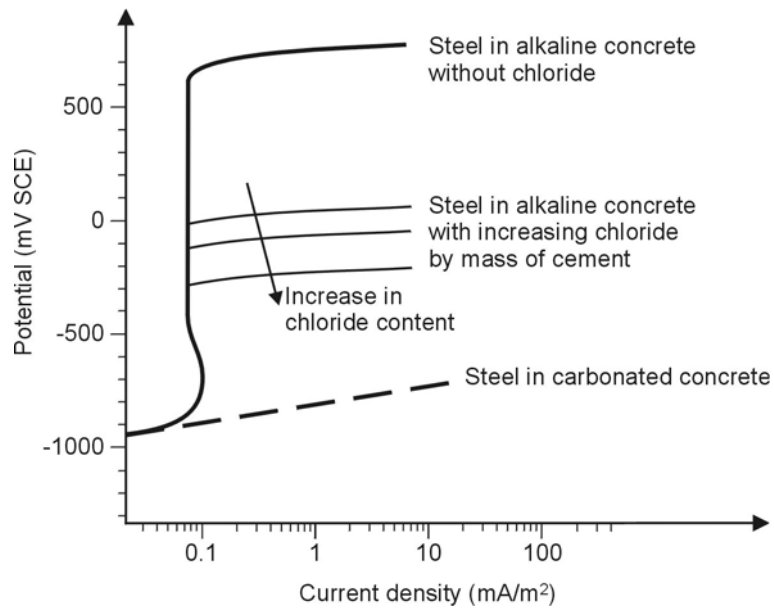


Figure 2.5 Influence of chloride concentration in steel potential of embedded reinforcement.

An increase in the chloride content does not only influence the steel potential, but at a particular concentration (chloride threshold), produces localized breakdown(s) of the passive layer. When the passive layer is destroyed, the thermodynamical conditions that produced its formation are no longer present and dissolution of steel occurs. Nevertheless, there is not a clear specific value for the chloride threshold in general, but each structure may have its own. The chloride threshold required for corrosion of steel may be increased in blended cements (Thomas 1994)

The presence of chlorides also affects the current as shown in Figure 2.6 (Jones 1996). The presence of chlorides induces changes in the current density in the anodic reaction. These changes are significant in the active zone where the current which is associated to the passive potential (E_{pp}) is higher than without the presence of chlorides. As this current is increased, the rate at which dissolution of iron occurs in the anodic cell is increased as well; therefore, when pitting corrosion is affecting reinforcing steel, the presence of chlorides will result in more detrimental conditions for corrosion of steel.

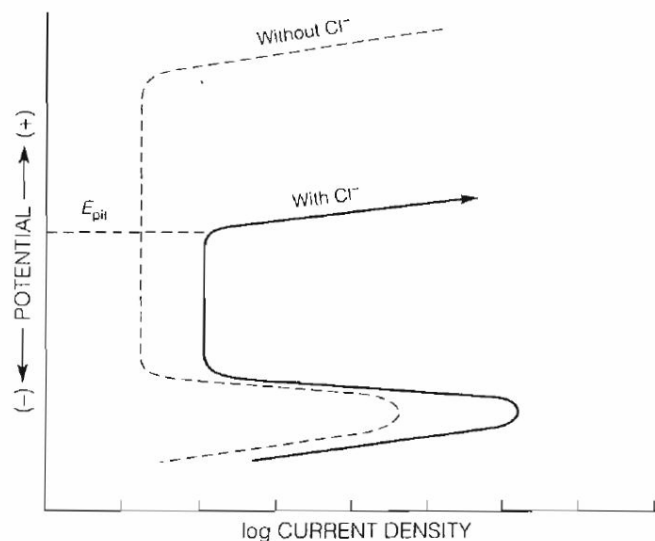


Figure 2.6 Influence of chlorides in current density of steel in concrete.

The rate of chloride ingress depends on the microstructure properties of the pore structure in concrete. Therefore, the most common way to delay the ingress of chlorides into concrete is through densification of the

pre structure. In this sense, fly ash and blast furnace slag (BFS) are common additions in the fabrication of cement and literature has shown that concrete specimens cast with these blended cements can hold higher concentrations of chloride before any corrosion process starts.

Chlorides inside hardened concrete are found and considered to be either:

- fixed, i.e. they are chemically or physically bound to cement minerals and hydration products.
- free, i.e. they are present in the pore solution.

The presence of oxygen and sufficient quantities of free chloride ions in the pore water of concrete can produce corrosion of reinforcement. Chlorides in the pore solution can cause localized breaking of the passive layer. Hydroxyl ions counter this process by repairing the damaged film, but above the chloride threshold, the breakdown is irreversible and dissolution of iron does not stop without repair methods. Binding of chlorides occurs when minerals present in the hydrated matrix react with chlorides forming chloride-containing phases, for example, as Friedel's salt. These chlorides are immobilized and cannot contribute to breaking of the passive layer

When chlorides are present in sufficient concentration – above the chloride threshold – the passive layer on the surface of steel bars is destroyed, forming localized deterioration on the surface of steel. This type of deterioration is known as pitting corrosion, in which the anodic zones are concentrated in those pits. The transfer of electrons is driven through the electrolyte to the cathodic zone on the adjacent non-corroding steel surface (cathode). Because the ratio of anodic/cathodic area is often low, the corrosion inside the pit is intense. Figure 2.7 shows the effect of chlorides in corrosion pits (Bertolini 2004).

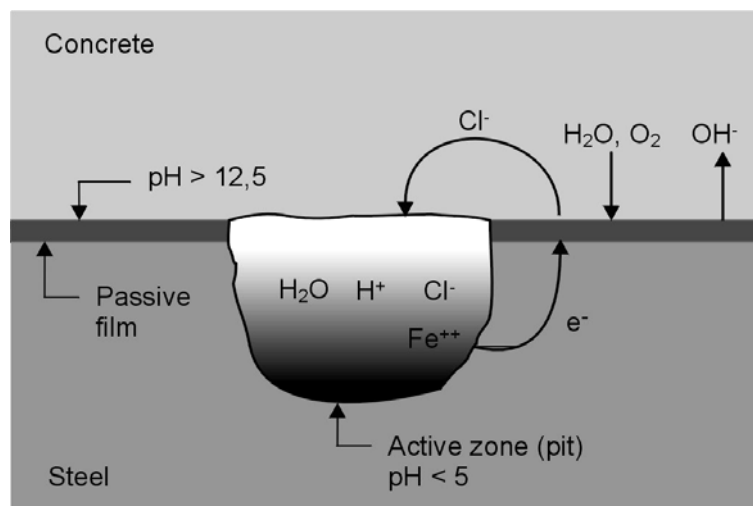


Figure 2.7 Pitting corrosion due to chlorides.

Inside the corrosion pit, the following reaction takes place:



The reaction between iron and chloride ions with water results in the formation of hydrochloric acid which is responsible of acidity inside the pit. The pH inside the pit may decrease significantly to acidic values which constitute an aggressive environment for steel (Arup 1983). When hydrochloric acid is separated again in hydrogen and chloride ions, the process takes again place and is known as auto-catalytic. The availability of oxygen and chloride concentration in those corrosion pits has a significant influence in the rate of iron dissolution. Such loading of chlorides is increased over time (use of de-icing salts or marine splash), resulting in an increase of the chloride content in concrete.

Carbonation

General corrosion of steel in concrete is caused by carbon dioxide present in the atmosphere. This degradation process is known as carbonation and reduces the alkalinity of concrete down to values of pH around 9. In the case of unreinforced concrete, this reaction does not mean any loss in durability. However, the thermodynamic conditions that produced the passive layer are no longer present in the concrete-steel interface; therefore, the

passive layer is destroyed and the surface of steel is in contact with a neutralized pore solution. The carbonation reaction occurs in all the volume of concrete that is in contact with carbon dioxide. As carbonation occurs, the depth of its penetration increases over time. When the concrete surrounding the reinforcement is carbonated, the passive layer is lost and dissolution of steel begins and corrosion products develop on the whole surface of the bar. The loss of alkalinity in concrete due to carbonation occurs as the following reaction:



Reaction products of calcium carbonate are deposited in pores or voids inside the concrete matrix. For concrete cast with Portland cement, this means that the porosity of the concrete is reduced after the reaction occurs; however this is not the case for blended cements like slag cement (CEM III) or fly ash cements (CEM II and CEM V). The consumption of calcium hydroxide is the cause of reduction in concrete alkalinity. The rate of carbonation is a function of concrete properties like cement type, water-binder ratio and curing. Environmental conditions like CO₂ concentration and relative humidity are important as well. Relative humidity strongly influences the carbonation depth when values of RH are between 60-70%, the reason is that CO₂ can diffuse easily through pores when they are not fully saturated. In saturated conditions, the availability of water and lack of enough carbon dioxide prevents carbonation, while in dry concrete, the moisture condition is not sufficient for this reaction. There are several models that predict the depth of carbonation over time, however a commonly accepted equation for describing this phenomenon is:

$$D = A\sqrt{t} \quad (2.7).$$

where D is the carbonation depth measured in mm, A is the carbonation rate coefficient measured in mm-year^{-0.5} and t is the time measured in years (Broomfield 2007). As the carbonation depth increases, the rate of carbonation is modified by changes in the pore structure of concrete itself. In Portland cement-based concrete, the production of calcium carbonate after the carbonation reaction is deposited in pores and air voids contained in the pore network. The presence of these newly formed products, result in an increase of tortuosity and therefore a densification of the pore matrix. However, this is not the case for concrete cast with blended cements in which the presence of carbonation products increase the porosity of such concrete matrix (Neville 1995).

Corrosion propagation

After the passive layer is destroyed dissolution of steel begins and the cross section of the steel bar is reduced over time. In the case of pitting corrosion due to chlorides, the destruction of the passive layer is localized, where the anodic surface (dissolution) is small compared to the cathodic one (reduction). When corrosion propagation has started, the rate of corrosion will depend only on the exposure conditions and availability of oxygen and moisture. In this sense, temperature and moisture changes influence measurements of corrosion rate with notable significance. In electrochemical terms, corrosion propagation is related to an electrochemical potential and corrosion current; both parameters are shown in Figure 2.8 (Bertolini 2004).

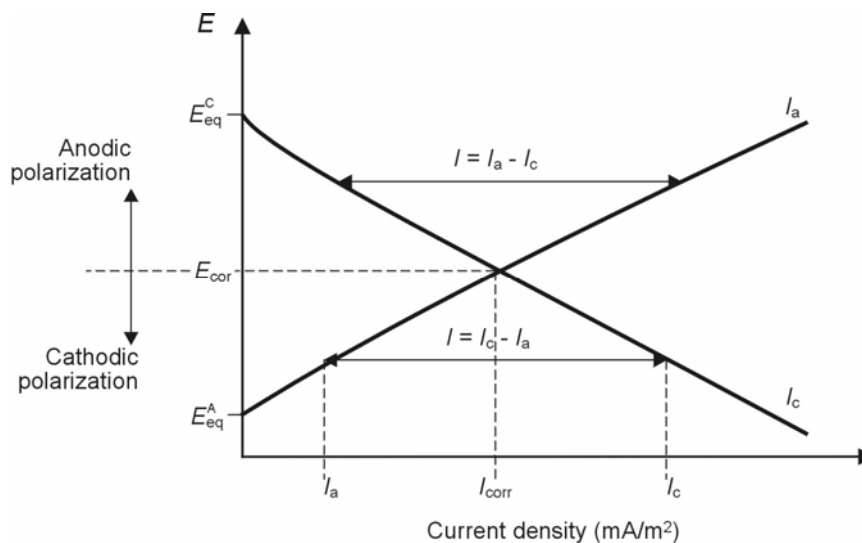


Figure 2.8 Corrosion potential and corrosion current of steel.

Corrosion potential (E_{corr}) is found in the intersection of polarization curves of anodic and cathodic reactions. Only when both reactions have the same potential, the corrosion current is determined. Corrosion current is the sum of both anodic (negative) and cathodic (positive) currents. The slope of polarization curves depends on the environmental conditions that are surrounding the steel like temperature and relative humidity. Nevertheless, when the corrosion current is high (shifted towards the right hand side of Figure 2.6) the potential of the steel will drop to more negative values in order to fulfill the requirement of equal electrode potentials.

The corrosion rate, i_{corr} , is defined as the amount of metal loss due to corrosion per unit of exposed surface and time (COST-521 2003). The weight loss, that is the amount of corrosion accumulated over time, can be transformed to electrochemical units with the use of Faraday's law:

$$\frac{I \cdot t}{F} = \frac{\Delta W}{W_m / Z} \quad (2.8).$$

Where I is the corrosion current in A, t is the time in seconds, F is Faraday's constant (96500 coulomb/mole), ΔW the weight loss due to corrosion, W_m the molecular weight (56) of the metal in g/mole and Z the valence (2) of steel in reaction (2.5).

When referred to corrosion, the current is divided by the surface area and the term corrosion rate or corrosion current density is defined. The results of i_{corr} are generally reported in A/m^2 for homogeneous corrosion and it may be converted to penetration attack in $\mu\text{m}/\text{year}$. Also, other equivalent units that are used include mA/m^2 or $\mu\text{A}/\text{cm}^2$ in more practical cases.

Consequences of damage by corrosion

The net reaction is the production of ferrous hydroxide which, in the presence of oxygen and water, is converted to $\text{Fe}_2\text{O}_3 \cdot n\text{H}_2\text{O}$ (rust). Iron dissolved at the anode, is deposited nearby in the vicinity of the pits as rust. These corrosion products occupies a volume several times that of the parent metal and its formation creates internal stresses that, after time, will be sufficient to exceed the tensile strength of the concrete cover, leading to cracking and finally to spalling. Cracking of concrete cover is the most important consequence of this process. Three different types of cracking may occur due to corrosion of steel

- Cracking in the direction of the reinforcement;
- Spalling of concrete cover over the bars;
- Delamination of concrete cover

The presence of any of these types of cracking depends on the rate of corrosion, the tensile strength of concrete, the geometry (diameter and depth of cover) and the moisture conditions to which specimens are subjected.

The presence of cracking leads to loss in bonding between steel reinforcement and concrete. This behavior reduces the load-bearing capacity of the structure in significant terms. When the loss of bond is very high, delamination of concrete and spalling may be present and the structure is no longer serviceable.

Reduction of the cross-section of reinforcement is an important problem in terms of durability and safety. In the case of general corrosion, the reduction of the cross section is distributed over the complete area of the bar. Even if this reduction might be considered as slow, experience in structures where the carbonation depth has passed the cover depth shows that general corrosion may be very aggressive. In pitting corrosion, the reduction of the cross section is localized in the corrosion pits. This process is faster than in general corrosion, and may be more dangerous because of failure in the reduced cross section since the mechanical capacity of the reduced section may be lower than necessary for serviceability and ultimate service life.

Hydrogen embrittlement is a consequence of a specific type of corrosion where hydrogen diffuses into the metal producing atomic hydrogen at the surface during corrosion or cathodic over protection. Hydrogen embrittlement is predominant in high strength steel like prestressing cable reinforcement. Other side-effects caused by corrosion in reinforced and prestressed concrete structures are shown in Figure. 2.9 (Bertolini 2004).

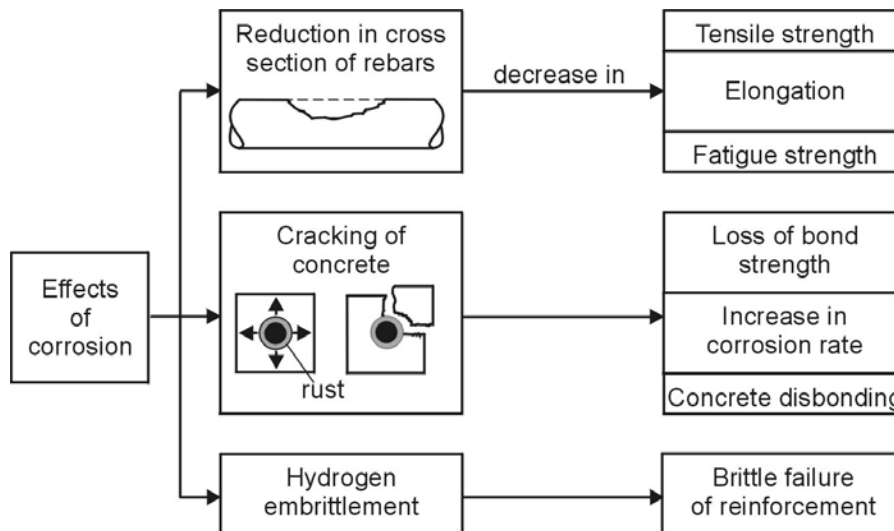


Figure 2.9 Effects of corrosion of steel in concrete.

2.4 Concrete properties that are related to corrosion of embedded steel

Several properties of concrete may influence the kinetics of steel corrosion. During the design phase of a concrete structure, they represent important parameters for the duration of the service life of the structure and possible predictions of the remaining time in case of a damaged structure. Experience reported in literature has proven that the influence on the kinetics of corrosion of steel by these properties is significant. Concrete cover has a major influence on the time-to-corrosion. The depth of cover is usually based on recommendations for concrete strength and exposure conditions. Concrete quality in terms of adequate water-binder ratio, compaction, mix design and mix components with regard to total cement content, concrete strength grade, the inclusion of supplementary cementitious materials and admixtures influence the resistance properties against environmental action.

The concrete pore network is a conductive medium for agents, moisture and thermal energy. The presence of these pores provides ingress routes to aggressive agents like chlorides or sulphates. In these pores, size is a relevant factor that is related to the nature of the pore. Generally, the pore size range varies from 1 nm to millimeters providing a wide array of pore size distribution (Neville 1995). Gel pores are the smallest pores (between 1 and 10 nm) that can be found in concrete. They are present in the CSH gel that is formed during hydration of cement and they are so small that their contribution to transport is negligible. Capillary pores are in the range of 10 to 1000 nm, they are responsible for transport of aggressive agents, moisture and heat. Air and compaction voids are generally in the order of magnitude of mm and are caused by air-entraining admixtures or inadequate compaction during casting.

Some of these pores are interconnected and others remain isolated as shown in Figure 2.10 (Bertolini 2004). Transport of agents in concrete occurs in interconnected capillary pores of sufficient size to allow transport of these agents.

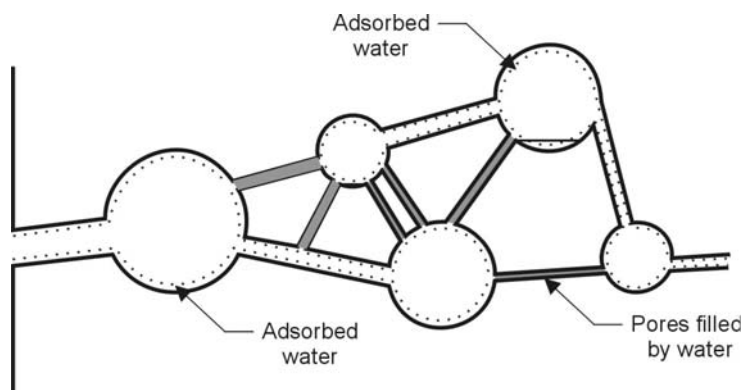


Figure 2.10 Pore network connectivity in concrete.

The term porosity refers to the ratio between the pore volume and the total volume. This property is greatly influenced by the water/binder ratio in a directly linear correlation, therefore, when the water/binder ratio is high, the porosity will be high as well. Porosity may be evaluated as the percentage volume of penetrated voids in concrete by water. In normal conditions, in a low porosity concrete <10% is penetrated by water for the densest concrete while >15% for the least dense as shown in Table 2.1 (ACI 2008).

Table 2.1 Classification of porosity.

Concrete quality	Classification	Percentage volume of penetrated voids
Good	Good or low porosity	< 10%
Average	Medium porosity	10 – 15%
Poor	Highly porous concrete	> 15%

2.4.1 Transport of matter in concrete

Since concrete is a porous material, transport of matter through its pore network has significant relevance in mechanisms of deterioration in concrete structures. All transport processes through concrete matrix depend on their respective driving force. These processes are influenced by many parameters like the type of penetrating agent, the driving force, the concrete cover, the type of cement used, the environmental conditions and the mechanisms involved in the transport, to name a few. In concrete, transport processes depend on the magnitude and type of driving force and the tortuosity of the porous medium. A brief description of transport agents and media is shown in Figure 2.11 (Bertolini 2004).

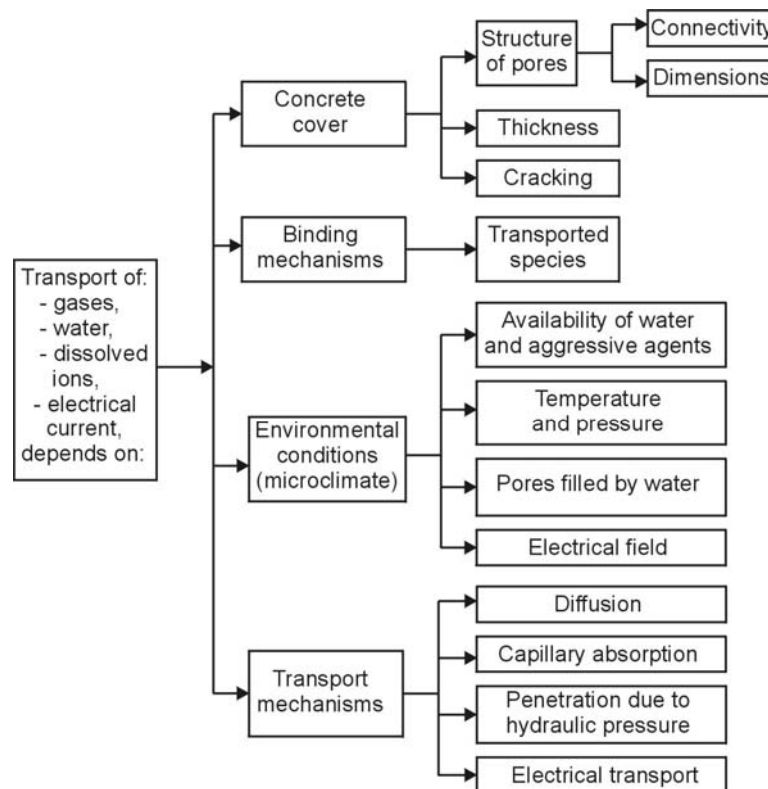


Figure 2.11 Transport of mass in concrete pore network.

Concrete cover has a significant relevance when considering the kinetics in degradation mechanisms. The pore structure of the cover depth is important when considering transport of matter by diffusion or permeability. The thickness of the cover depth is important because it provides a physical barrier against environmental conditions. Unfortunately, cracks in the cover depth decrease significantly the protection quality of the cover in terms of durability.

Binding mechanisms depend of the nature of matter that flows through concrete. Chlorides may be bound to the matrix by the chemical composition of the matrix and pore solution.

Transport mechanisms depend of the nature of the driving force that is acting on the structure. Diffusion is caused by the driving force of concentration gradients of matter. Most common diffusion mechanisms in concrete involve chlorides and sulphates. Capillary absorption depends on the pore volume and the absorbed matter in contact with the concrete. Hydraulic pressure may be caused by gravity or in water-retaining structures. Water containing aggressive agents (chloride or sulphates) may penetrate into concrete. Electrical transport is caused by electrical field that is applied on the structure.

Diffusion

Diffusion is the process by which matter is transported from one part of a system to another as a result of random molecular motions caused by a concentration gradient. Diffusion depends on the state of the substance (gas, liquid) and the diffusive media. Gases diffuse more rapidly through air than in water, and ions like chloride and sulphates diffuse more rapidly when dissolved in water through water contained in pores. Diffusion may be under one of two regimes: steady state or constant regime, and non steady state.

For isotropic substances under steady state conditions, the rate of transfer per unit area of section, J , is given according to Fick's First Law of Diffusion:

$$J = -D \frac{\partial C}{\partial x} \quad (2.9).$$

Where J is the flux in $\text{kg/m}^2\text{s}$, D is the diffusion coefficient in m^2/s and $\frac{dC}{dx}$ is the concentration gradient in kg/m^4 . Since the concentration of ions in a $d_x + \Delta_x$ interval is lower than in d_x , the sign of Fick's First Law will be negative in physical terms, but for simplicity will remain without this sign. When the concentration gradient and the diffusion coefficient are constant, the flux of ions through concrete also becomes constant. This constant flow is called steady state.

However, in most cases diffusion in concrete is not constant, so a non steady-state regime controls the ingress of aggressive agents. This mechanism is the same as in heat transfer and it is modeled by Fick's Second Law:

$$\frac{\partial C}{\partial t} = D \frac{\partial^2 C}{\partial x^2} \quad (2.10).$$

A solution of Fick's Second Law into a semi-infinite medium with the choice of appropriate boundary conditions, gives the following (Colleparidi 1972):

$$C_x - C_b = (C_s - C_b) \left(1 - \text{erf} \frac{x}{2\sqrt{Dt}} \right) \quad (2.11).$$

Where C_x = is chloride content at depth x , [% m/m cement],

C_s = chloride content at surface, [% m/m cement],

C_b = background chloride content (from mixing ingredients), [% m/m cement],

x = distance from exposed surface, [m],

D = diffusion coefficient, [m^2/s],

t = time of exposure, [s],

erf = the error function.

Since the concrete pore network is interconnected, it may be considered a semi-infinite medium where transport of matter may occur. Nevertheless, the nature of the pore system modifies the total transport of ions since they must find a way through the pore solution in the tortuous system which has a larger distance than the geometrical one. Besides, ions move where the concrete pores are filled with water. These conditions reduce the effective diffusion of ions by 3-4 orders of magnitude when compared to pure aqueous solutions, because transport of gasses is easier in filled pores. Typical values of oxygen diffusion coefficients at 28 days for concrete at 55% RH is given in Table 2.2 (The Concrete Society 1988).

Table 2.2 Gas diffusion coefficients in concrete at 55% RH after 28 days and 5 bar pressure.

Concrete quality	Rate of diffusion	Gas diffusion coefficient (m ² /s)
Good	Low	< 5 x 10 ⁻⁸
Average	Average	5 x 10 ⁻⁸ – 50 x 10 ⁻⁸
Poor	High	> 50 x 10 ⁻⁸

Since chloride is an important agent for corrosion of steel reinforcement, diffusion of chloride ion is important for concrete durability. Values of chloride diffusion coefficients for Portland cement concretes is given in Table 2.3 (The Concrete Society 1988).

Table 2.3 Chloride ion diffusion coefficients of concrete at 28 days.

Concrete quality	Rate	Chloride diffusion coefficient (m ² /s)
Good	Low	< 1 x 10 ⁻¹²
Average	Average	1 x 10 ⁻¹² – 5 x 10 ⁻¹²
Poor	High	> 5 x 10 ⁻¹²

Capillary absorption

Water in contact with concrete is absorbed by capillary action. This phenomenon is caused by surface tension, viscosity and density of liquid, the contact angle between liquid and walls from the pores. In concrete, the angle is small due to the presence of molecular attraction between the liquid and the substrate. Because of this, a drop will be spread over concrete surface.

Sorptivity (S), is a property that is related to capillary action in porous materials. The constant S is expressed in g/(m²·s^{1/2}) for mass change measurements or m/(s^{1/2}) if absorbed volume is determined. Typical values of sorptivity for concrete vary from 5 g/(m²·s^{1/2}) in normal strength concrete (compressive strength of 43 MPa and 0.50 w/b ratio) to 1.5 g/(m²·s^{1/2}) for high strength concrete (compressive strength of 67 MPa and 0.4 w/b ratio) (Vries 1998).

Penetration due to hydraulic pressure

Since gases or liquids may move through concrete by its pore, concrete. Permeability becomes relevant. Permeability is the property that relates the rate of ingress of substances into concrete to the driving force. Typical values of water permeability for concrete is shown in Table 2.4 (The Concrete Society 1988). An important keynote is that the permeability will change with time and the value obtained will be a function of the test regime as well as the concrete. In general terms, the flow rate will reduce with time; hence tests run for a long period will yield lower values than short-term tests.

Table 2.4 Water permeability of concrete at 28 days.

Concrete quality	Rate	Water permeability (m/s)
Good	Low	< 10 ⁻¹²
Average	Average	10 ⁻¹² – 10 ⁻¹⁰
Poor	High	> 10 ⁻¹⁰

Oxygen permeability coefficients at 28 days for concrete at 55% RH and tested at 5 bar are given in Table 2.5 (The Concrete Society 1988).

Table 2.5 Gas permeability of concrete at 28 days, 55% RH and 5 bar pressure.

Concrete quality	Rate	Gas permeability (m/s)
Good	Low	< 2 x 10 ⁻¹⁸
Average	Average	2 x 10 ⁻¹⁸ – 2 x 10 ⁻¹⁷
Poor	High	> 2 x 10 ⁻¹⁷

Electrical flow in concrete

The transport of ions in solution caused by the application of electrical fields is called migration. The magnitude of such movement is proportional to the strength of the applied electrical field and the mobility of the ion. Ionic mobility is a property related to the size of an ion including its hydration shell (adherent water molecules). This relationship between the ion transport and the applied electrical field is described by

$$s = uE \quad (2.12).$$

Where s is the drift velocity in m/s, u the ion mobility in $\text{m}^2\text{s}^{-1}\text{V}^{-1}$ and E the electric field strength in V/m. The term mobility refers to the property of each ion to move due to an electric force in a solution. Therefore:

$$u = \frac{ze}{6\pi\eta a} \quad (2.13).$$

Where z is the charge of the ion, e is the elementary charge ($1.602176 \times 10^{-19} \text{ C mol}^{-1}$), η is the viscosity of water at 25°C (298 K) in $\text{kgm}^{-1}\text{s}^{-1}$ and a is the hydrated ionic radius in Angstrom (\AA). It can be seen that the ionic mobility depends only on the properties of each ion. Therefore, the effect of an electrical field on a mixture of ions will affect each ion in a different way.

Since ions in nature have different hydrated sizes, the mobility of each ion is relevant. In fact, ionic mobility is related to diffusion. The diffusion of an ion is determined by the equation:

$$D_i = RT * \frac{u_i}{z_i F} \quad (2.14).$$

Where R is the gas constant in $\text{J}/(\text{K} * \text{mole})$, T the absolute temperature in (K), u_i the ionic mobility, z_i the ion valence and F Faraday's constant (96490 C/mole). The transport number is the contribution of an ion to the total current in the solution and it is related to the concentration and mobility of the ion. The equation that determines the transport number of ions is:

$$t_i = \frac{c_i \cdot u_i \cdot z_i}{\sum (c_j \cdot u_j \cdot z_j)} \text{ for different ions (e.g. 1..j);} \quad (2.15).$$

Because concrete is a porous material, the transport of ions in solution also applies for concrete. Nevertheless, concrete porosity modifies the total transport of ions since these must find a way through pores causing that the effective distance is larger than the geometrical one. Besides, ions can only migrate where the concrete pores are filled with water. These conditions reduce the effective diffusion of ions by 2-3 orders of magnitude when compared to pure aqueous solutions. The flux of ions during migration in concrete is important for electrochemical techniques. Table 2.6 gives values of ionic mobility of various ions including Li^+ , Na^+ and K^+ (Atkins 2006).

Table 2.6 Ionic mobility in water at 25°C , u ($\times 10^{-8} \text{ m}^2\text{s}^{-1}\text{V}^{-1}$)

Cation ⁽⁺⁾		Anion ⁽⁻⁾	
Ag^+	6,24	Br^-	8,09
Ca^{2+}	6,17	CH_3CO_2^-	4,24
Cu^{2+}	5,56	Cl^-	7,91
H^+	36,23	CO_3^{2-}	7,46
K^+	7,62	F^-	5,70
Li^+	4,01	$[\text{Fe}(\text{CN})_6]^{3-}$	11,4
$[\text{N}(\text{CH}_3)_4]^+$	4,65	NO_3^-	7,40
Rb^+	7,92	OH^-	20,64
Zn^{2+}	5,47	SO_4^{2-}	8,29

As a result, drift velocities of ions differs from high (H^+ , OH^-), to medium (K^+ , Cl^-), to low (Na^+ , Li^+). With the application of electrical currents, electrons flow through the steel reinforcement. Ions may be transported through the water-filled pores in the cement matrix. When a driving electrical field is applied on concrete, ions move towards the electrode with the opposite sign, i.e. ions like chloride (Cl^-), hydroxyl (OH^-) or sulphate (SO_4^{2-}) will migrate to the positive electrode (generally, an electrode on the surface of concrete). These ions are also known as anions. Cations like sodium (Na^+), potassium (K^+) or calcium (Ca^{2+}) will move towards the negative electrode which is in most cases the embedded steel. Ionic flow in an electrical field is related to the resistivity of concrete, which is one of the electrochemical properties of concrete that will be studied in this project. When steel reinforcement is subject to an electrical field, a change in the polarization at the surface of the bar will

occur. This means that electrons are available in the vicinity of the surface and they produce changes in the rate of the electrochemical reactions that are occurring inside concrete.

2.5 Inspection and survey of corrosion damage in concrete structures

Corrosion of steel in concrete is a problem that has to be subjected to different stages in order to observe, understand and predict behavior of steel and concrete. First, Inspection is important to determine (at first instance) the possible causes of degradation of concrete.

Cracking of concrete is one of the most helpful features when diagnosing damage of concrete structures. The nature and extent of cracks on the surface of the concrete element is best observed when the surface is dry. Cracks are symptomatic of different deterioration mechanisms, either of mechanical, physical, structural or chemical nature. The location, orientation, length and width give important clues that must not be underestimated.

Spalling is commonly seen in cases of damage by corrosion of steel when the deterioration is high. When steel corrodes, products of corrosion reaction (rust) generate internal pressures which, when are higher than the tensile strength of concrete, may produce cracking and when are distributed over a large area spill off the concrete cover.

Leaking or moisture is relevant for water containing structures, tunnels and basements where moisture is present. Since water is a catalyst of most processes of degradation, the damage may be concentrated near the water accumulation location.

Rust staining is a visible effect of corrosion of steel in concrete. Nevertheless, corrosion damage may be significant even without producing visible rust stains. Therefore, the study of corrosion damage, monitoring and repair is relevant.

A resume of the most important defects in terms of cracking is shown in Table 2.7 (RILEM TC 104 1994) and a scheme of workflow for survey of concrete structures is shown in Figure 2.12 (ACI 2008).

Table 2.7 Examples of classification of defects (after RILEM TC 104)

Damage	Damage rating				
	1 (very slight)	2 (slight)	3 (moderate)	4 (severe)	5 (very severe)
Corrosion in prestressed concrete due to overloading	Width < 0.05 mm	Width 0.05 – 0.1 mm	Width 0.1 – 0.3 mm	Width 0.3 – 1.0 mm	Width 1.0 – 3.0 mm and spalling
Cracks in reinforced concrete due to overloading	Width < 0.1 mm	Width 0.1 – 0.3 mm	Width 0.3 – 1.0 mm	Width 1.0 – 3.0 mm and spalling	Width > 5.0 mm and widespread spalling
Cracks in unreinforced concrete	Width < 1 mm	Width 1 – 10 mm	Width 10 – 20 mm	Width 20 – 25 mm	Width > 25 mm and spalling
Shrinkage or settlement cracks	Single small crack	Several small cracks	Many small cracks	Few large cracks	Many large cracks
Effects of reinforcement corrosion	Barely noticeable	Light rust stains	Heavy rust stains	Heavy rust stains and cracking along line of bars	Heavy rust stains and spalling along the line of bars
Pop-outs	Barely noticeable	Noticeable	Holes up to 10 mm diameter	Holes between 10 and 50 mm diameter	Holes > 50 mm diameter
Spalling	Barely noticeable	Clearly noticeable	Larger than coarse aggregate	Areas up to 150 mm across	Areas larger than 150 mm

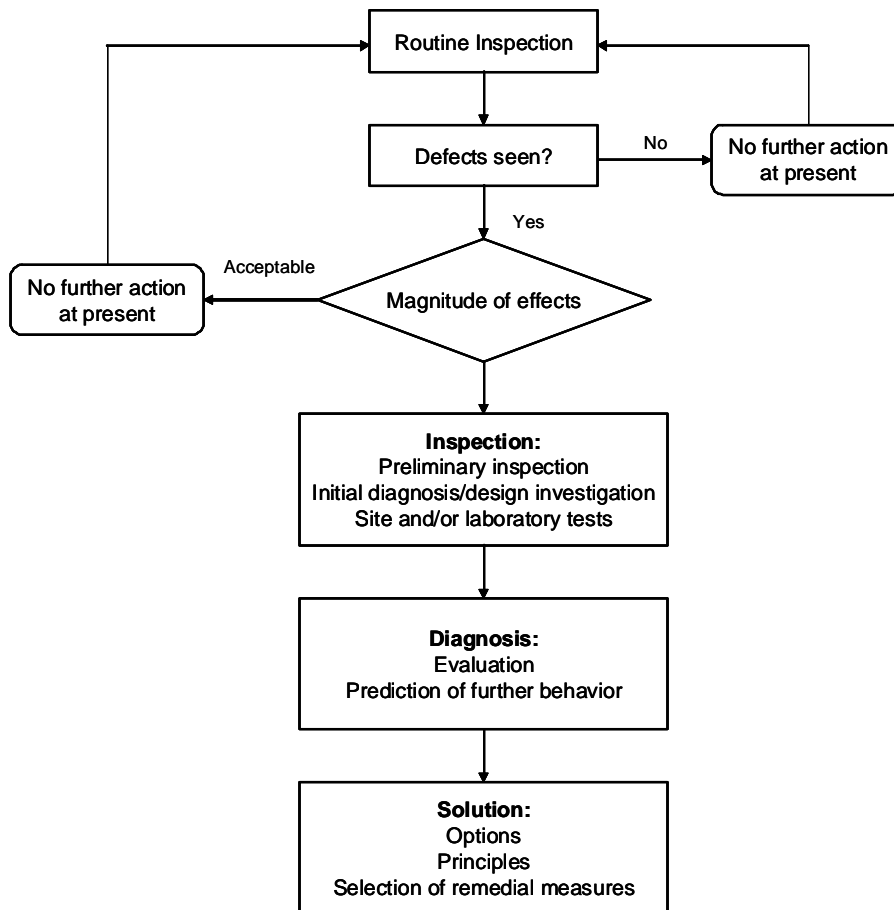


Figure 2.12 Survey procedure for inspection of concrete structures with deterioration (ACI 2008).

2.6 Evaluation and monitoring of corrosion damage of steel in concrete

After the inspection of the structure is done, evaluation of damage is required in order to determine if repair is required. The diagnosis or evaluation of damage is important for this feature. A proposed action for evaluation and diagnosis of service life in civil infrastructure is shown in Figure 2.13 (Bertolini 2004).

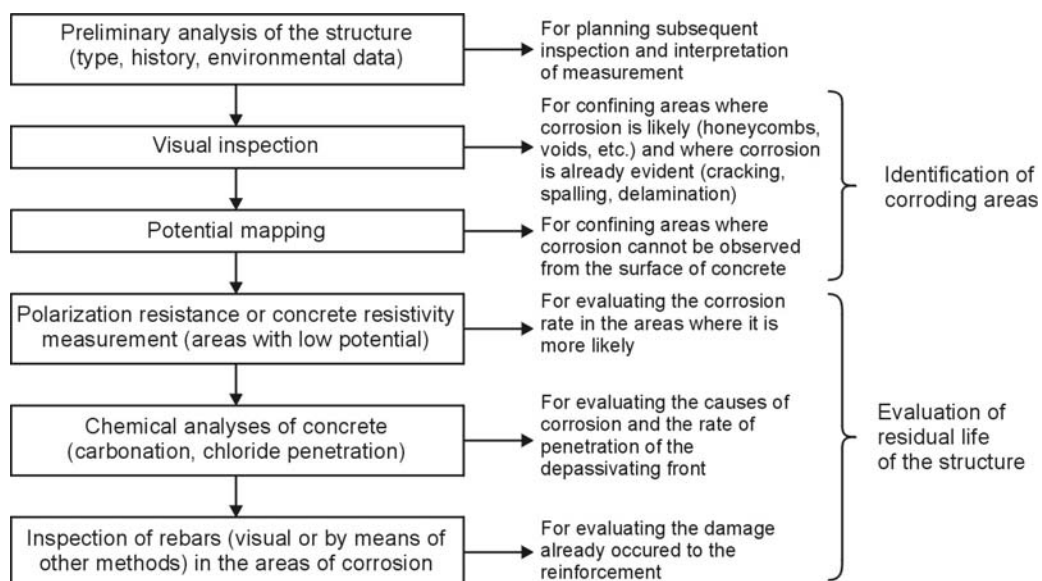


Figure 2.13 Procedure for evaluating deterioration of concrete structures.

When evaluation of deterioration is required, several techniques are available for that purpose. However, the nature of those techniques may be different and this fact has to be taken into account. Non-destructive testing includes evaluation and monitoring techniques that are intrusive for the structure on a negligible level. Common non-destructive testing used in evaluation of concrete structures include: potential mapping, linear polarization resistance, rebound hammer testing, electric pulse velocity and acoustics. Each technique works behind different principle that allow, to a certain degree, to evaluate the damaged state.

Destructive testing involves permanent alteration of the structure itself that allows measurements only once and the sample is destroyed. Destructive testing includes core extraction, chloride content, carbonation depth and gravimetric measurements of steel reinforcement.

In this project, use of destructive testing was reduced as much as possible in order to preserve the concrete specimens for future research. In this sense, special attention to non-destructive testing principles and procedures was carried out during the elaboration of this project is required. Nonetheless, a few destructive testing were done when no other option was available, those destructive tests include chloride content and carbonation depth.

2.6.1 Steel potential (E_{corr})

The electrochemical potential of steel in concrete is a useful parameter when identification and monitoring of corrosion of steel is required. As described before, the potential of steel in concrete is an indicative of the passivity state of steel. The measurement was applied with the use of either embedded reference electrodes (i.e. activated titanium) or external reference electrodes (i.e. saturated calomel electrodes or silver chloride). Electrical connection with the reinforcement must be carried out and, in the case of an external reference electrode, electrolytic connection must be obtained with a wet-soaked sponge. Also, a high impedance voltmeter ($>10\text{ M}\Omega$) is required for a stable measurement. Figure 2.12 shows a schematic figure of a steel potential measurement (Bertolini 2004).

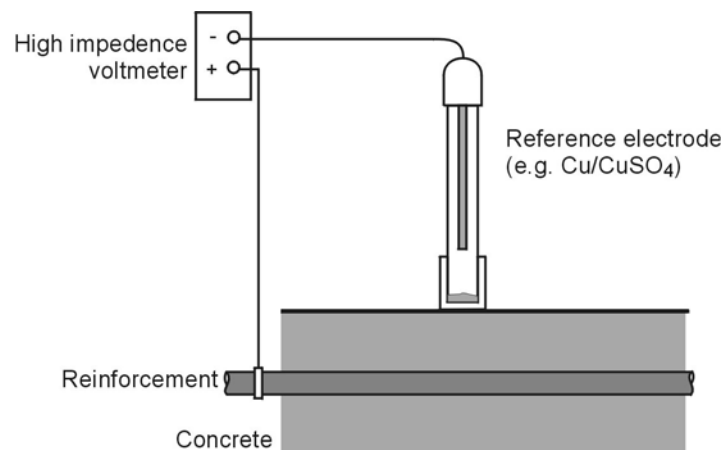


Figure 2.14 Electrode potential of embedded steel in concrete.

The ‘absolute’ value of the reading depends on the reference electrode that was used during the measurement. As described above, each electrode has different potential differences with regard to standard hydrogen electrode (SHE). Table 2.8 shows common values of electrochemical potential for electrodes used during measurements of potential (Vennesland 2007).

Table 2.8 Standard potentials of reference electrodes for use in concrete.

Electrode	Potential vs SHE (mV)
Saturated calomel electrode (SCE)	+244
Silver/Silver chloride (SSE) Ag/AgCl	+199
Copper/Copper sulphate (CSE) Cu/CuSO ₄	+316
Manganese dioxide	+365
Graphite	+150±20
Activated titanium	+150±20
Stainless steel	+150±20
Lead	-450

Changes in potential of electrodes (graphite, activated titanium and stainless steel) are due to changes in the pH of the pore solution of concrete over time. For example, carbonation of concrete in the vicinity of the reference electrodes may produce shifts in the potential values of them in a range of 200 mV (ACI 2008)

The measurement of steel potential is helpful when its value is compared to information reported in literature and an estimation of the probability of corrosion is done. Figure 2.13 shows a schematically scale for determining the state of embedded steel in concrete with reference to a saturated calomel electrode (SCE) (Bertolini 2004).

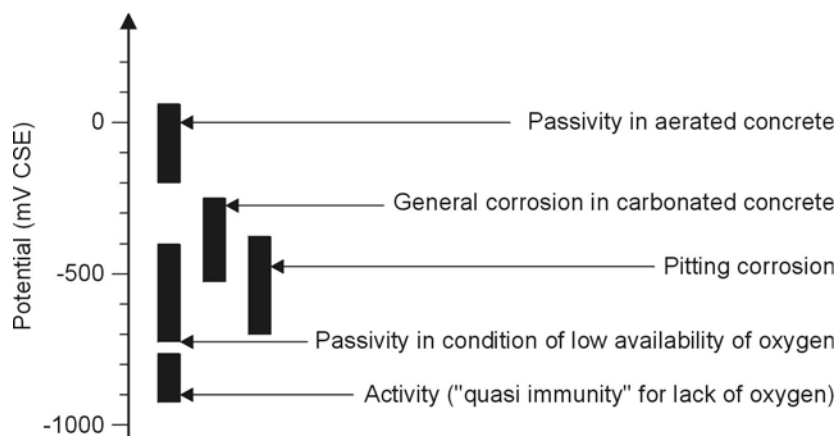


Figure 2.15 Interpretation of potential measurements of embedded steel in concrete.

The previous figure shows that measured values of corrosion potential are related to different conditions in the corrosion state of steel. For example, more positive values (0 to -200 mV) are commonly associated to a passive state of steel, independent to the environmental conditions. More negative values between -300 and -500 mV are found in general corrosion of steel, however, there are also reports of values in this corrosion state between -450 and -600 mV vs SCE (Arup 1983). Pitting corrosion is mostly found when values of corrosion potential are between -400 and -700 mV due to the presence of chlorides is contributing to the negative magnitude of pitting corrosion.. However, it is not possible to assure which mechanism is deteriorating the steel only by measuring corrosion potential. Additional tests like, concrete resistivity or linear polarization resistance (see below) will give additional outcome to identify the most probable degradation mechanism. In this sense, values of probability of corrosion according to measured values of electrochemical potential are shown in Table 2.9 (ASTM C876-09 2009)

Table 2.9 Probability of corrosion of steel reinforcement according to electrochemical potential values.

Measured potential E (mV vs CSE)	Probability of corrosion
$E > -200$	< 10%
$-200 < E < -350$	Unknown
$E < -350$	> 90%

2.6.2 Linear polarization resistance (LPR)

Linear polarization resistance (LPR) is a technique which estimates indirectly the corrosion rate (i_{corr}) from a metal. Corrosion rate is a term that may be expressed in terms of area (A/m^2) or loss of material ($\mu m/year$). The use of this technique is based in the application of potential increase and interpretation of current variations for such potentials. A current-potential plot is generated that represents a quasi-linear relationship between i_{corr} and E_{corr} . The slope of this curve is known as polarization resistance.

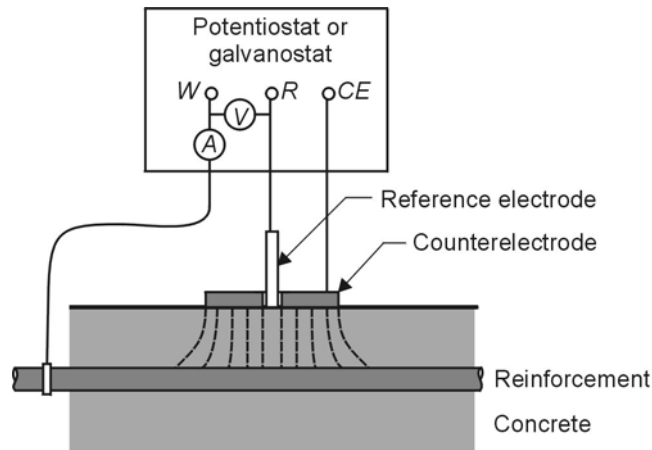


Figure 2.16 Linear polarization resistance of embedded steel in concrete in-situ.

The technique consists of applying small potential differences around the corrosion potential (E_{corr}) and current changes are recorded. The application of the technique is derived from the anodic and cathodic curves proposed by Stern and Geary (Stern 1957). The equation of Stern – Geary is defined as:

$$i_{corr} = \frac{\beta_a \beta_c}{2.3(\beta_a \beta_c)} * \frac{1}{R_p} \quad (2.16).$$

Where i_{corr} is the corrosion rate, β_a is the anodic slope of the R_p curve and β_c is the cathodic slope. Since the rate of change of (7) shows the instantaneous corrosion rate that is occurring in the steel when subjected to polarization. Because β_a and β_c are constant, then Stern-Geary's equation may be redefined as:

$$i_{corr} = B * \frac{1}{R_p} \quad (2.17).$$

The value of B in (7) is related to the slopes of both β_a and β_c and is generally found in the range of 12 to 52 mV depending on the system (Andrade 1996). For embedded steel in concrete, a value of B for a passive state is 52 mV and 24 mV for an active state. A proper way to determine which state is most probable is described in (Andrade 1996).

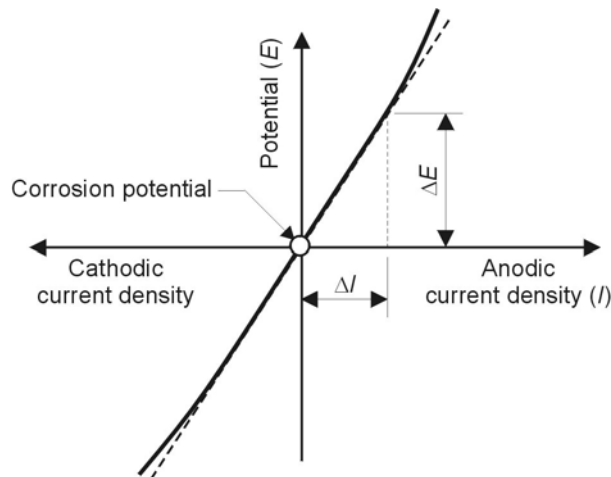


Figure 2.17 Linear polarization resistance.

In general terms, corrosion rates above of $1.0 \mu\text{A}/\text{cm}^2$ indicate active corrosion (Rodriguez 1994; Andrade 1996). Table 2.10 shows criteria for evaluation of corrosion rate in concrete structures.

Table 2.10 Criteria for interpretation of corrosion rate.

Corrosion rate	Classification
< 100 to 200 mA/cm ²	Passive
200 to 500 mA/cm ²	Low to moderate
500 to 1000 mA/cm ²	Moderate to high
> 1000 mA/cm ²	High

2.6.3 Concrete resistivity

The electrical resistivity of concrete is a material property that is useful for monitoring and inspection of concrete structures with regard to reinforcement corrosion in combination with other non-destructive techniques (Polder 2001b).

Concrete resistivity is a geometry-independent property that describes the electrical resistance, which is the ratio between a voltage applied on the specimen and resulting current in a unit cell (Polder 2001b). In concrete, the current is carried by ions in the pore solution. More pore water (wet concrete) as well as more and larger pores with a high degree of connectivity and a low tortuosity (high water-binder ratio) cause a lower resistance to ionic and electric flow. For a constant relative humidity and in stationary conditions, resistivity is increased by a lower water-binder ratio, extended curing time or the addition of supplementary cementitious materials e.g. fly ash, blast furnace slag or silica fume (Polder 2001b).

Resistivity is influenced by both moisture content inside the specimen and the porosity of the cement matrix. As it was discussed before, moisture transport in concrete is relatively slow for the bulk specimen. In the surface (down to approx. 20 mm depth) the moisture content depends mostly on the environmental conditions (exposure) of the specimens. Temperature also has a significant impact in the behavior of concrete electrical resistivity. When temperature is low near or below freezing point, the mobility of ions is reduced. Therefore, ionic flow is decreased. This behavior is opposite when temperature is high. Fig. 2.7 shows the set-up for measuring concrete resistivity (Bertolini 2004).

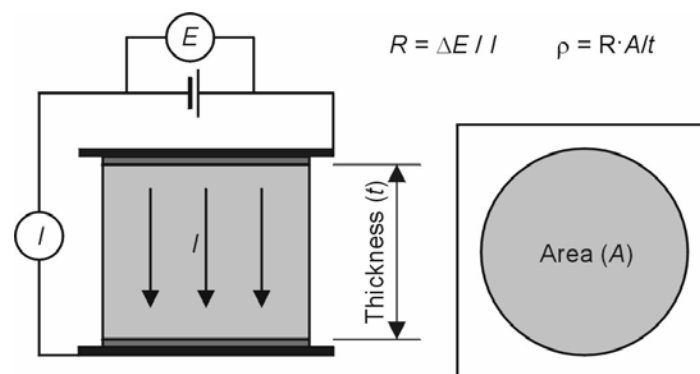


Figure 2.18 Measurement of concrete resistivity.

The resistivity is calculated by using the formula (COST 509, 1997):

$$\rho = A \cdot R_2 \quad (2.18)$$

With ρ as the concrete resistivity (Ωm), A is a cell constant which depends on the geometry of the specimen and the arrangement of steel reinforcement and R_2 is the electrical resistance measured with a voltmeter in AC to avoid electrode polarization. Concrete resistivity values according to the environment and cement type are shown in Table 2.11 (Polder 2001b).

Table 2.11 Electrical resistivity of existing concrete structures (> 10 years) and comparable laboratory climates.

Environment	Concrete resistivity (Ωm)		
	Ordinary concrete (CEM I)	Portland cement	Blast furnace slag (>65% slag, CEM III/B) or fly ash (>25%) cement or silica fume (>5%) concrete
Very wet, submerged, splash zone, [fog room]		50 – 200	300 – 1000
Outside, exposed		100 – 400	500 – 2000
Outside, sheltered, coated, hydrophobised [20C / 80%RH], not carbonated]		200 – 500	1000 – 4000
Carbonated	1000 and higher		2000 – 6000 and higher
Indoor climate (carbonated), [20C / 50% RH]	3000 and higher		4000 – 10000 and higher

Because of the non-destructive nature of this test, measurements of concrete resistivity may be done over time in a serviceable structure on site, in order to have a record of changes in this property and identify turning points where changes in the corrosion state of steel may occur. Also, these results may be correlated to measurements of corrosion potential and corrosion rate for a better analysis of the current condition and predictions on the possible evolution of corrosion of steel in such structure.

2.6.4 Chloride content

As described before, chlorides may be present in concrete due to transport process or during the casting process. To study and interpret the behavior of chloride content, a chloride profile is required. A chloride profile is obtained by sawing slices of concrete at different depths from the exposed surface. These slices should be extracted over the whole depth of the structure, in order to find the depth at which chlorides have penetrated. The content of chloride is of particular importance due to the threshold value described before. When the content of chlorides that have penetrated into concrete near the steel reinforcement is equal or higher than the chloride threshold, corrosion of steel may be taking place.

Chloride content determination in serviceable structures is generally obtained by sawing cores and taking them to a laboratory. Each core must be identified carefully and then concrete slices are sawed at different distances from the exposed face and then grounded to powder. Diverse chemical techniques are available for chloride content determination, but the procedure is not part of this study. However, the most common technique for measuring chloride content in concrete is Volhard's titration. The destructive nature of chloride content determination reduces the number of tests that can be done on a serviceable structure.

2.6.5 Carbonation depth

Carbonated concrete is the result of the reaction between carbon dioxide and the alkaline pore solution. This reaction implies a loss of alkalinity of the pore solution to values of pH below 10. Measurement of carbonation depth is a destructive technique in which a solution of phenolphthalein is commonly used. This solution is a pH indicator which has a change value of around 10 and concrete with pH above this value will turn into a red-pink color. In order to obtain a reliable measurement, fresh-broken concrete is best used for this purpose. Mechanical breaking of specimens may be obtained with appropriate equipment and the phenolphthalein solution must be sprayed afterwards immediately. Measurement of carbonation depth should include the location of the reinforcement and if the carbonation front has surpassed the steel, it is recommended to consider repair techniques in order to extend the service life of the structure.

2.7 Repair of corrosion of steel in concrete

2.7.1 Overview

The study of corrosion of steel reinforcement is generally made by materials scientists interested in the performance of concrete in terms of durability and remaining service life. However, the reach of this problem is

beyond that aim. The importance of such deterioration is not merely in terms of material or structural behavior, but in sum, it affects the industry and society in a broader manner.

Repair, maintenance and replacement of concrete structures damaged by corrosion, require a high amounts inversion that must be reduced to the lowest possible value. In this sense, degradation of concrete represents has a significant impact on economy.

Only in the U.S. the total cost of repair, rehabilitation, strengthening and protection of concrete structures rise up to €14 to €16 billion per year (Emmons 2006). Most of repair in concrete structure implies more cement consumption. Portland cement industry has grown in an exponential way during the past century, due to the development of infrastructure and increase of world population. In the US, it is estimated that over 380 million cubic meters of concrete are installed each year. Therefore, extending the time for repair as much as possible implies a reduction of costs of repair and consumption of construction materials.

In the case of corrosion of steel in concrete, this problem is the most important concern for construction industry. In the US, costs related to corrosion of infrastructure are about 16.4 % brute national product (BNP), around €18.5 million (Corrosion costs 1997). Meanwhile, in the Netherlands, the costs of corrosion ascend to 4% of BNP which is around €17.5 million (Schiring 2008). The indirect costs caused by corrosion are more difficult to quantify but may be the same, or higher, than direct costs. Indirect costs are related to downtime in the structure for repair, loss of value of the structure, loss of efficiency while the repairing is done, contamination and additional consumption of construction materials.

If the damage is considered as significant actions must be taken and repair is needed. When repair is considered, several solutions are available and some of them are shown in Figure 1.5 (Bertolini 2004). Maintenance is considered only necessary when the damage in the structure threatens the serviceability of the structure and/or the service life of the structure is required to be increased.

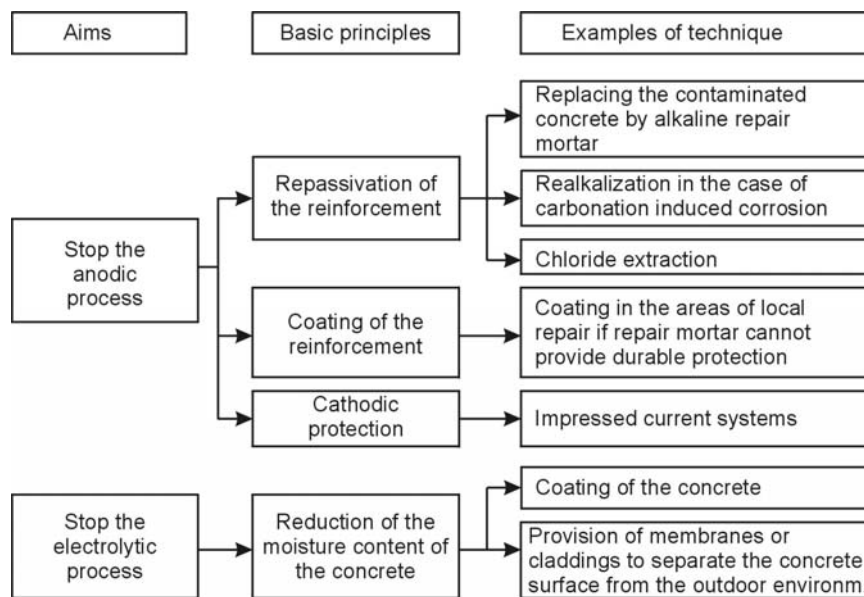


Figure 2.19 Possible repair techniques for corrosion of steel in concrete.

2.7.2 Cathodic protection

When current is impressed to concrete structures, several benefits may be obtained. This principle has been applied during time in electrochemical techniques for repair of concrete structures. Cathodic protection (CP), concrete realkalisation and electrochemical chloride extraction are techniques that involve the application of electrical current to the steel reinforcement (Bertolini 2004). Cathodic protection has been used for the past 30 years and has become very helpful when repairing concrete structures from corrosion damage (Chess 1998). The principle of cathodic protection is to apply an electrical field between the steel reinforcement (cathode) and an external electrode (anode) to form a circuit through the ions in the pore solution. Steel reinforcement is polarized with the negative terminal of a DC power supply, while the external anode is polarized with the positive terminal. The electrical flow will force electron into the steel reinforcement, turning its potential

towards a more negative one and preventing further iron dissolution. However, CP is still a somewhat empirical technique and negative effects may rise from improper application of this technique like concrete degradation, loss of bond and hydrogen embrittlement in prestressing tendons (Pedferri 1995). Cathodic prevention (CPre) refers to a protective system that is applied on concrete structures before any damage of corrosion has occurred. These CPre systems are permanent and they imply higher costs during the construction phase, nonetheless, costs related to repair are significantly reduced (Chess 1998). Both techniques, CP and CPre, are permanent which is different from other repair techniques (see below).

In this project a repair solution of Cathodic Protection was studied. Cathodic protection of steel reinforcement can be schematized as Fig. 2.8. It is obtained by applying an electrical field between the reinforcement and an external anode on the surface of concrete. A CP system comprises a number of basic components which include an anode, a DC electric supply, the protected steel and the concrete surrounding it. Additional required elements include reference electrode and monitoring instruments. The circuit is closed through the ionic flow in the pore solution and transfer of current is possible. This produces a flow of electric current from the anode through the concrete to the reinforcement. Figure 2.20 shows a schematic cathodic protection system.

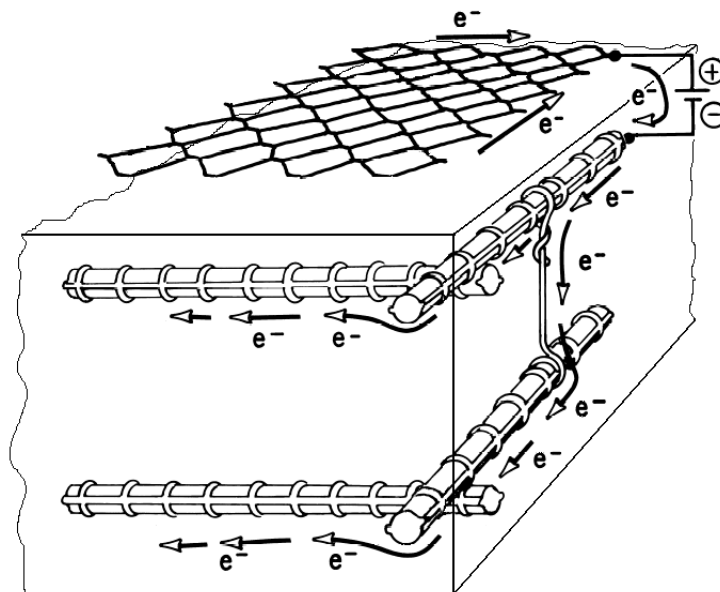


Figure 2.20 Cathodic Protection system for steel reinforcement in concrete.

The design of CP systems has evolved during time. Though, each structure is subjected to different environmental conditions, geometry and material characterization which mean that the design of CP system must be different as well. The voltage applied for cathodic protection depends on the environment and the aggressive agents that may be present; Table 2.12 shows a brief description of alternative current density requirements for different conditions (Chess 1998).

Table 2.12 Practical CP current density requirements.

Environment surrounding steel reinforcement	Current density in mA/m ² of reinforcement
Alkaline, no corrosion occurring, low oxygen resupply	0.1
Alkaline, no corrosion occurring, exposed structure	1-3
Alkaline, chloride present, dry, good quality concrete, high cover, light corrosion observed on the rebar	3-7
Chloride present, wet, poor quality concrete medium-low cover, widespread pitting and general corrosion on steel	8-20
High chloride levels, wet fluctuating environment, high oxygen level, hot, severe corrosion on steel, low cover	30-50

In the case of CPre systems the electric current demand is generally between 1 and 2 mA/m², which is considerably lower than that required by other repair techniques. However, the beneficial long-term effect of CPre provides solid evidence of the efficiency of such system.

2.7.3 Concrete realkalisation

When current flows through concrete, the cathodic surface of steel is subjected to reduction reactions which produce OH⁻ ions. An increase of the concentration of hydroxyl ions in the pore solution, leads to an increase in the pH of the pore solution. Also, migration of alkalis like Na⁺, K⁺ or Li⁺ ions is possible due to a repulsive force (positive polarization in the external anode) and an attractive force (negative polarization in the steel reinforcement). In general terms, slabs that are subjected to this repair technique have a system similar to Figure 2.21.

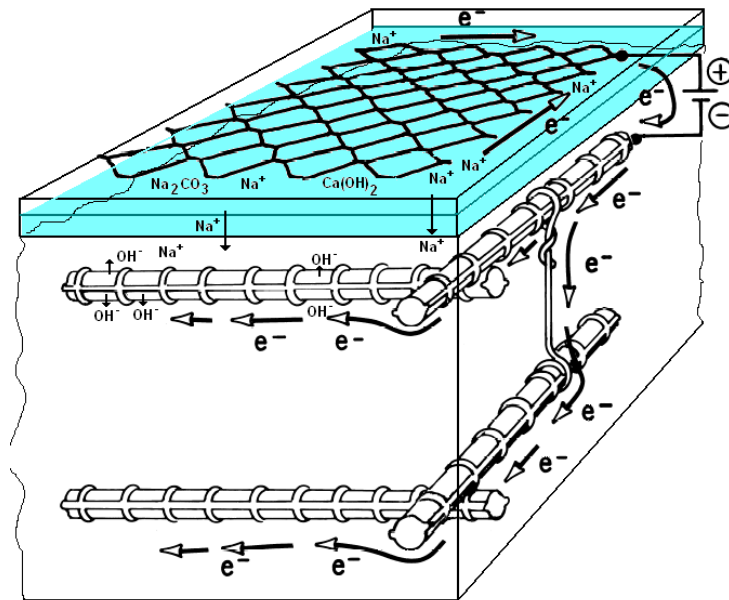


Figure 2.21. Electrochemical realkalisation of concrete.

In this temporary repair technique, the anode is commonly surrounded by a sodium-carbonate solution. The solution must remain in contact with the surface of concrete during the treatment period. The concentration of sodium carbonate, or other solution, is generally of 1 M. The current required for a successful realkalisation is generally between 1 or 2 A/m². With this level of current, concrete realkalisation takes place in the concrete-steel interface and the cover depth; nonetheless, the required treatment period depends on the pH in the pore solution before this technique is applied, the mobility of ions in the pore structure and the structure of the pore matrix. Contractors empirically use a treatment period between 8 and 18 days with a current density of 1 A/m² (COST-521 2003). Values related to total charge after the treatment varies between 200 and 450 Ah/m². After the concrete cover has been realkalised in the vicinity of the reinforcement and the cover depth the treatment may be stopped and removed from the structure.

2.7.4 Electrochemical chloride extraction

Electrochemical chloride extraction (ECE) is a temporary technique in which chlorides are extracted from concrete by the use of an imposed current between the reinforcing steel and an external electrode, thus reducing the chloride content and, consequently the probability and/or the rate of corrosion of reinforcement. In this technique, the anode is surrounded by water or a saturated calcium hydroxide solution. Common electrical currents applied are between 1 and 2 A/m². Figure 2.22 describes the schematical process of ECE.

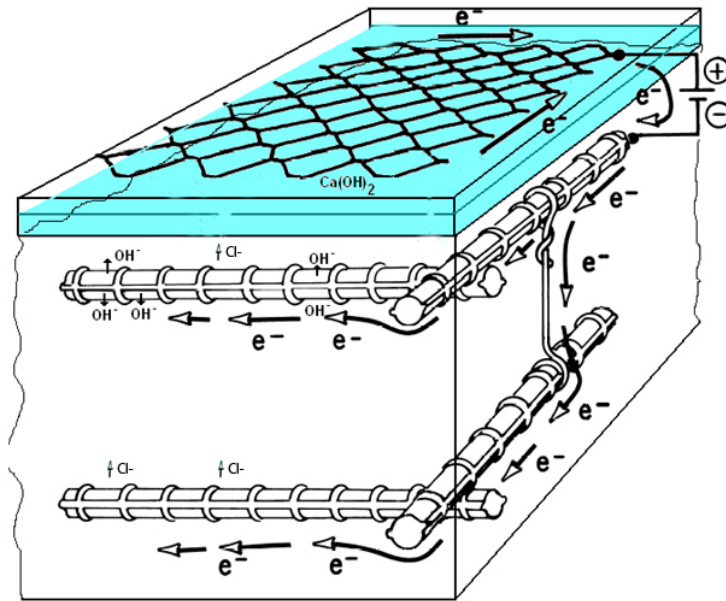


Figure 2.22 Electrochemical chloride extraction in concrete.

In ECE, a direct current is applied between the reinforcement and the temporary anode on the surface of concrete. This anode is surrounded by an electrolyte, which is an aqueous solution in general. In this technique a current density between 1 and 2 A/m² is used, over a treatment period of 6 to 10 weeks (COST-521 2003). The migration of chloride ions (Cl⁻) to the anode is forced by the electrical field that is applied on the structure; however, the total amount of removed chlorides is determined by the total charge that has passed between the reinforcement and the anode and the transport number of chloride, influenced by temperature and chloride content.

The time required for this temporary treatment is dependent of the initial chloride content of concrete and the chloride distribution over it. In literature, reports about removing 50% of total chloride content are found (Mietz 1998).

3 Previous work and reported properties of concrete specimens

3.1 Previous work (1998 – 2009)

In the year 1998, reinforced concrete prisms were cast for studying the behavior of corrosion of steel in concrete. The composition of specimens was defined as a combination of four different cement types and three water/binder ratios (Polder 1998). The cement types that were used according to ENV 197-1:1992 are:

- CEM I 32.5 R Portland cement
- CEM II/B-V 32.5 R fly ash cement
- CEM III/B 42.5 N blast furnace slag cement
- CEM V/A 42.5 N fly ash and slag composite cement

The water/binder ratio:

- 0.40
- 0.45
- 0.55

And the mixed-in chloride content (added as $\text{CaCl}_2 \cdot 2\text{H}_2\text{O}$ to the fresh mix)

- 0 % chloride ion by mass of cement
- 2% chloride ion by mass of cement

All mixes were designed to have similar paste volumes. The aggregate was siliceous river material with a maximum size (D_{max}) of 8 mm. Table 3.1 shows the cement types, water-binder ratios and cement content used for the cast of concrete specimens (Polder 2002).

Table 3.1 Concrete mixes, cement type, w/b ratios and cement content of concrete specimens.

Mix Code	Cement type	w/c	Cement content (kg/m ³)	Aggregate content (kg/m ³)	Water content (kg/m ³)	Admixture (% by mass of cement)
1400	CEM I 32.5 R	0.40	338	1780	143	4.0
1450	Portland cement	0.45	318	1790	149	3.0
1550		0.55	287	1827	163	2.0
2400	CEM II/B-V 32.5 R	0.40	333	1807	141	4.0
2450	Portland fly ash cement	0.45	314	1818	145	2.0
2550	(27% fly ash)	0.55	280	1830	158	2.0
3400	CEM III/B LH HS 42.5	0.40	339	1836	141	2.5
3450	Blast furnace cement (75%)	0.45	316	1831	146	2.0
3550		0.55	286	1864	161	2.0
5400	CEM V/A 42.5	0.40	333	1827	137	2.0
5450	composite cement (25% fly	0.45	322	1882	149	2.0
5550	ash, 25%) slag	0.50	279	1839	157	2.0

According to Table 3.1, there are slight differences in cement and aggregate content of concrete mixes. Also, the calcium chloride admixture dosage is higher in the 1400 mix. While all specimens are considered to have a dosage of 2% by mass of cement, changes in the activation time and corrosion state of specimens cast with this mixture may be significant during the rest of the study. Since the volume of the paste was designed for similar volumes, this means that the workability properties may be different for each mix. Table 3.2 shows a resume of properties (slump, specific gravity of mix and air content) of concrete mixes in fresh state and in hardened state (compressive strength and specific gravity).

Tabla 3.1 Properties of fresh concrete and hardened concrete after 280 days

Cement type	w/b	Chloride content (%)	Slump (mm)	Flow (mm)	Specific gravity fresh mix (kg/m ³)	Air content (% V/V)	Compressive strength (MPa)	Specific gravity cube (kg/m ³)
CEM I	0.40	0	10	360	2267	3.9	45.7	2338
	0.40	2	20	310	2068	6.8	44.4	2290
	0.45	0	4	n.b.	2260	2.1	42.0	2314
	0.45	2	55	360	2042	12.5	39.3	2229
	0.55	0	10	290	2280	4.3	23.4	2256
	0.55	2	120	440	1986	12.0	27.4	2227
CEM II/ B-V	0.40	0	120	420	2287	4.4	53.2	2345
	0.40	2	37	335	2238	5.5	48.7	2250
	0.45	0	70	380	2280	4.0	40.8	2337
	0.45	2	100	400	2230	7.4	37.4	2225
	0.55	0	20	320	2270	4.6	36.5	2339
	0.55	2	200	500	2091	11.5	25.6	2197
CEM III/B	0.40	0	10	320	2319	3.7	43.0	2345
	0.40	2	10	280	2222	6.7	50.8	2276
	0.45	0	10	300	2296	4.3	41.5	2335
	0.45	2	70	360	2126	9.0	36.8	2218
	0.55	0	110	460	2313	3.5	34.6	2357
	0.55	2	250	540	2176	8.3	38.1	2247
CEM V/A	0.40	0	10	270	2300	n.b.	60.8	2329
	0.40	2	0	280	2290	4.4	51.1	2275
	0.45	0	70	370	2355	1.9	46.2	2322
	0.45	2	130	420	2259	5.0	47.3	2244
	0.55	0	120	460	2278	3.0	35.8	2327
	0.55	2	220	510	2096	10.0	32.9	2202

In this table, it is shown that CaCl₂ admixture influenced the properties of the fresh mixes and also in the hardened state of concrete. The presence of this admixture has produced changes in the slump, flow and air content in fresh state and of specific gravity of the fresh mix, compressive strength and hardened cube specific gravity. Increase in slump and flow is attributed to the improved workability effect of calcium chloride in fresh concrete. However, the specific gravity of those mixes is significantly lower than those without chlorides. For a similar paste volume, this probably means an increase in the porosity of the cement matrix during fresh state and later confirmed by the specific gravity of cubes in hardened state. A significant change in the fresh mixture state due to chlorides is visible in the air content in all mixtures. It is then possible; to assume that the pore matrix of specimens cast with chlorides is significantly different to the ones without this admixture.

Casting of all concrete specimens was carried out between August and October 1998 (Polder 1998). After casting, the specimens remained in their moulds for 24 hours, covered with plastic foil. After removing the specimens from the moulds, they were stored in a fog room (20 °C, RH ≥ 95%) for one week. Then, they were moved to a climate room with 20 °C and 80% RH and remained there for three weeks.

The geometrical representation of specimens is shown in Figure 3.1. Prisms of 100 x 100 x 300 mm were cast with two groups of three embedded steel bars of 6 mm in diameter located at 10 mm and 30 mm of cover depth from one mould face. The mild steel bars had an exposed length of 45 mm, resulting in an exposed surface of about 1090 mm² with a variation coefficient of 3%. Stainless steel bars with 6 mm in diameter were placed at both 10 and 50 mm in depth for resistance measurements. Two activated titanium electrodes with length of 20 mm were cast-in for each group of embedded mild steel bars as reference electrodes.

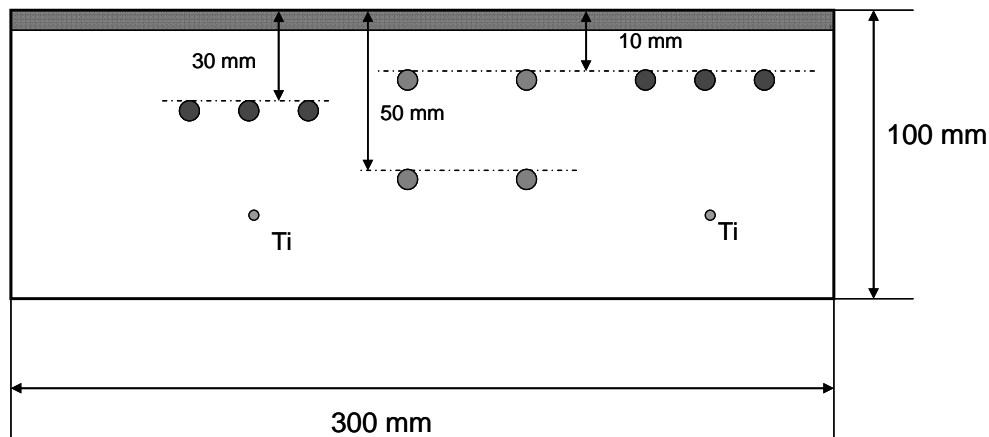


Figure 3.1 Geometrical representation of concrete specimens, (top view).

For each concrete mixture without added chlorides, ten prisms were cast for measurements of concrete resistivity, steel potential, corrosion rate, chloride profile (see below) and carbonation depth. Of those ten specimens, four were subject to accelerated carbonation exposure (labeled as carbonation specimens) and the remaining six were exposed to salt/dry cycles (labeled salt/dry specimens) for 30 weeks. Another group of six specimens were cast with the addition of 2% of chloride by mass of cement. Also, four concrete cubes for mixes without chloride and three for mixes with chloride with dimensions of 100 x 100 x 100 mm were cast for resistivity measurements.

The ‘salt/dry specimens’ were exposed to cycling exposure the face with the lowest cover depth for the steel bars to a 3.5% NaCl solution for 24 hours and then stored in a 20 °C and 50% RH environment for six days, this cycle was applied during six months. ‘Carbonation specimens’ were stored in a 5% CO₂, 20 °C and 50% RH environment for six months.

‘Mixed in chloride specimens’ were stored in three different environments, with two specimens in each environment. These environments were a fog room, outside (unsheltered) and 20C 80%RH room for six months. Table 3.2 shows the distribution of specimens over the exposure environments.

Table 3.2 Exposure conditions of specimens until 32 weeks; numbers in () are specimen subcodes.

Week	1	2-4	5-32
0% chloride	Fog room (all 10)	20C 80% RH (all 10)	5% CO ₂ 50% RH (1-4) (carbonation specimens) 24 hrs in NaCl solution (5-10) Six days at 20C 50% RH (salt/dry specimens)
2% of chloride	Fog room (all 6)	20C 80% RH (all 6)	Fog room (1-2) (mixed-in chloride specimens) Outside (3-4) 20C 80% RH (5-6)

The concrete specimens were labeled by four digits with the following codes:

- The first one indicating the cement type (1 for CEM I, 2 for CEM II, 3 for CEM III and 5 for CEM V).
- The second and third digits for the water/binder ratio (40 for 0.40, 45 for 0.45 and 55 for 0.55).
- The last digit for the chloride content (0 for 0% of Cl⁻ and 2 for 2% of Cl⁻ by mass of cement).

In this sense, a specimen labeled 3452 corresponds to CEM III/B 42.5 N cement with 0.45 water/binder ratio and 2% of mixed in chloride. A fifth number was marked as a sub-code on the specimens indicating the exposure conditions as described in Table 3.1, fourth column between parentheses.

At 32 weeks, chloride penetration profiles were determined on specimens that had been subjected to salt/dry cycles (“first chloride profile”); and carbonation depths were determined in specimens that had undergone accelerated carbonation. At an age of 32 weeks, all specimens were moved into three climates: fog room, outside (unsheltered) or 20C & 80%RH. During those works, reported values of carbonated depth after 2.5 years are shown in Table 3.4 (Polder 2000).

Table 3.3 Carbonation depth of carbonation specimens after 2.5 years.

Cement type	w/b	Carbonation depth (mm)			Down to 10 mm	Down to 30 mm
		Lowest	Middle	Highest		
CEM I	0.40	9	17-38	100	yes	some
	0.45	10	13-22	30	yes	no
	0.55	23	27-40	100	yes	yes
CEM II/B-V	0.40	8	13-19	20	yes	no
	0.45	21	26-32	34	yes	some
	0.55	32	34-37	42	yes	yes
CEM III/B	0.40	21	27-32	40	yes	some
	0.45	33	35-50	100	yes	yes
	0.55	Completely carbonated			yes	yes
CEM V/A	0.40	14	15-18	20	yes	no
	0.45	20	21-24	27	yes	no
	0.55	36	43-100	100	yes	yes

During the year 2000, thus at about 2.5 years age, partial destructive analysis of concrete specimens was carried out resulting in a reduction of the amount of specimens. Table 3.3 shows the amount of specimens left after (Polder 2000; Polder 2001a; Guerreri 2002; Peelen 2003). The total amount of specimens left after this work is 151. In 2002 and 2003, specimens were stored and moved a few times due to relocation of the TNO Laboratory. During this phase, some specimens were lost. Specimens have been exposed on the roof of TNO Lab since early 2004.

Table 3.4 Total amount of remaining specimens after 2.5 years.

w/b ratio	0.40		0.45		0,55	
	0%	2%	0%	2%	0%	2%
CEM I	7	5	7	3	7	3
CEM II/B-V	10	5	7	3	7	3
CEM III/B	10	5	10	5	7	3
CEM V/A (S-V)	10	5	10	5	7	3

3.2 Initial state of the project

During the months of October and November 2009, the specimens were studied in order to know their current state after 11 years. At this time, most of the labeling of the specimens was lost due to environmental action. Also, the current amount of specimens did not correspond to that reported in (Polder 1998) among others due to relocation of the lab. Therefore, the work required to fulfill the goals of this project is:

- Identification of the specimens according to their cement type and water binder ratio.
- Electrochemical measurements (Ecorr, icorr, concrete resistivity) for describing the kinetics of the current state of the specimens.
- Apply short-term cathodic protection on selected specimens with high corrosion rates and different cement types and water/binder ratios.
- Chloride content, carbonation depth measurements after CP in selected specimens.

4 Experimental program

Inspection, monitoring and evaluation of corrosion of steel in concrete were done in extensive studies over the last 50 or 60 years. With regard to techniques of inspection and evaluation of concrete structures, two different types are used: Non-Destructive Testing (NDT) and Destructive Testing (DT). In the consulting and repair industry it is important to preserve as much as possible the current state of the structure in order to avoid that the testing stage influences the results, therefore NDT are preferable. The use of NDT has the purpose of describing the nature and the current state of degradation mechanisms that are present in concrete structures. In the case of DT, this kind of techniques studies parameters that cannot be described with the use of NDT. Also, DT output is used for modeling of service life design in concrete structures.

In this report, NDTs were used for two different purposes. First, to identify the most probable concrete mix of specimens and then, to monitor the current state and the progress of corrosion during time. NDTs that were used during this study were visual inspection, corrosion potential of steel, corrosion rate, electrical resistance of concrete and rebound hammer. With the use of these, the stages of inspection and evaluation of corrosion are studied. As an additional tool statistical analysis was used during the inspection stage to identify concrete specimens. Short term cathodic protection was applied to a selected group of specimens in order to study the behavior of current flow, corrosion potential, corrosion rate and concrete resistivity over the period of four weeks. After that, study of the size and pH in corrosion pits was done. It is important to note the CP and NDT are of different nature and therefore, they belong to different stages in the workflow. CP belongs to the repair stage in where (after evaluating results of NDT) the purpose is to modify the state of corrosion degradation. Destructive testing of chloride content and carbonation depth measurements were made as well.

4.1 Visual inspection

At first, a preliminary temporal label was made according to their position on the roof. They were stored up to 8 different rows of 15 to 18 specimens each. In this way, the first new-labeling system was determined from specimen 1-1 to 8-15. All rows were composed of 15 specimens each, except for row 4 which had 18 prisms. The total amount of specimens on the roof was of 123. The results of concrete resistivity, visual inspection, steel potential and rebound number are shown in Appendix 1.

A visual inspection on the specimens was carried out in order to identify at first instance specimens that probably contained different cement types. According to earlier reports (Polder 1998; Polder 2000; Polder 2001a), some characteristic signs were corresponding to different mixes in the concrete specimens. First, a rough distinction was made between specimens that were exposed to wet-dry cycles, mixed-in chlorides and carbonation exposure with the following criteria:

- Specimens that were exposed to penetrating chlorides (wet-dry cycles) had a seal on the perimeter of the exposed face. In addition, the length of those specimens was not of 300 mm but rather of 250 mm, indicating that some destructive analysis has been made on them (first chloride profile). The surface of this face was smooth due to saw-cut.
- Specimens exposed to carbonation did not have the seal as the penetrating chloride specimens but had the same length of 250 mm. Nevertheless, the surface of the lateral face on which the destructive analysis was made, was a rough one when compared due to mechanical splitting for carbonation depth measurement.
- Specimens with mixed-in chlorides showed a rough finish on the upper part of the specimen (the face from where concrete was cast). According to reports, the presence of chlorides during the mix reduced the setting time of the concrete mixes and leveling was incomplete in many cases.
- A small group of specimens which were not tested with destructive analysis during previous work (Polder 2001a) were tested for carbonation and chloride content (November 2009) in order to identify them.

An independent group of specimens which is part of a previous research program (COST 509 1997) was also tested for identification. An important note is that this group will not be subjected to further tests after its identification.

4.2 Concrete resistivity

Resistivity measurements were carried out using a two-point electrode method (2P). In this method, the electrical resistance of concrete was measured between two stainless steel bars at 10 and 50 mm of cover. These measurements were made with an ESCORT instrument with 120 Hz AC.

The cell constant has a different value depending on which pair of stainless steel electrodes is used. For the bars at 10 mm the cell constant is 0,093 m and for 50 mm is 0,106 m as reported (Polder 1998). These values were obtained by measuring the resistance between steel plates fixed in opposing faces of 100 mm concrete cubes and comparing to resistance measured between the electrodes in prisms of identical compositions when exposed in the fog room. This calibration procedure is described in (Polder 2001b). Results of concrete resistivity are reported in (Polder 1998; Polder 2000; Polder 2001a).

Since both of these factors are completely out of control in an outdoor exposure, but all the specimens are exposed to the same conditions, the electrical resistivity may be considered as a continuous variable that may be dependant only of cement type and water binder/ratio. The resistivity measurements were done on the roof of TNO Lab during the same day, such that, all the specimens had the same exposure conditions of temperature and relative humidity. Hence, the variation of resistivity measurements are influenced by the density of cement matrix which is a property related to water/binder ratio and cement type. Measurements of concrete resistivity were carried out in October 2009, February and April 2010.

4.3 Steel potential

Measurements of steel potential were done in concrete prisms with the use of a high impedance voltmeter HP-972A, between each mild steel bar and the closest activated titanium (Ti*) reference electrode embedded in the concrete specimen. Activated titanium is a piece of pure titanium coated with noble metal oxides of the platinum group. Results of steel potential in concrete specimens are reported in (Polder 1998; Polder 2000; Polder 2001a).

The convention is to connect the positive terminal of the voltmeter to the steel bar and the negative terminal to the reference electrode. The steel potential was recorded in mV with respect to the Ti* reference electrode. In 1998, reference electrodes were calibrated against the standard Ag/AgCl reference electrode in a bath with saturated Ca(OH)₂ solution for 24 hours in laboratory conditions. The standard potential of the reference electrode is similar to the Ag/Ag/Cl (saturated KCl) with an average potential difference of ± 10 mV. Measurements of steel potential were carried out in October 2009, February and April 2010.

4.4 Carbonation depth

The depth of carbonation in concrete was obtained after mechanically breaking one side of the specimen and spraying the fresh cut sample with a pH indicator (phenolphthalein). This procedure was made on 15 unknown specimens that did not have any signs of either exposure to wet-dry cycles or mixed-in chlorides. The carbonation depth was measured and recorded (RILEM CPC-118 2006). Carbonation depth measurements were made in November 2009.

4.5 Schmidt rebound hammer

Test on hardened concrete with the use of Schmidt hammer was carried out in order to study the elastic properties of the concrete prisms after according to NEN-EN 122504-02. The hammer test consists of a hammer which contains a spring loaded mass impacting against the surface of the sample. The hammer hits the specimen with a specific energy which produces a rebound of the mass which records a number. This number is known as rebound number and relates to the hardness of the concrete surface. The rebound number can be converted to the mechanical resistance of concrete with the use of a plot which is made for each particular hammer. The procedure of use of the Schmidt hammer is described in (NEN-EN 2001). The results of this test are affected by different parameters like the surface texture of the specimen, the moisture content and the temperature during the test. The Schmidt hammer used for this test is property of TNO and is identified as number 1. Schmidt-hammer was used during the inspection stage to make a distinction between water:binder ratio in terms of compressive strength (Malhotra 1976) of a known concrete mix. In this sense, specimens may be divided in their most probable mix design in terms of cement type and water binder ratio. All measurements done with the Schmidt hammer were done during the same day, November 25 2009, in order to reduce the influence of environmental conditions like temperature and relative humidity.

4.6 Statistical Analysis

A statistical test was carried out in order to make a distinction according to their results of concrete resistivity and visual inspection between cement types for specimens that were exposed to the same conditions during the first years of the project. A Nested Factorial Design (NFD) statistical test was used to determine the most important parameter influencing values of concrete resistivity or electrochemical measurements. A Kolmogorov-Smirnov two sample test analyzes data collected from the non-destructive test and proves (or rejects) the null hypothesis which is that two different groups of specimens belong to the same empirical cumulative distribution function (ECDF) (Bedford 2001). The Kolmogorov-Smirnov two sample test can be used for groups which have different lengths and continuous variables (e.g. resistivity). This test gives a result in terms of accepting or rejecting the null hypothesis, the significance value of the test and the maximum difference between ECDF of each group.

For the realization of this test, a short program that uses the data of resistivity measurements as input was used in MatLab software. The theoretical background of the Kolmogorov-Smirnov test is described briefly in Appendix 2.

4.7 Linear polarization resistance

Measurements of corrosion rate were made during the month of February 2010. During this time, the specimens were exposed on average to environmental conditions of 1 C and >90% RH. All measurements were done on-site with a device from CorrOcean Multicorr MKII, this was the same instrument as used before, that was newly calibrated by the manufacturer. The R_p test was carried out using the (three) bars of the same cover depth as alternatively working, reference and counter electrodes, without correction for ohmic drop as reported in (Polder 2001a). No correction was made for ohmic drop. The exposed area of the bar (10 cm²) and B value of 24 were given as input for the Multicorr device.

4.8 Chloride content

Chloride content of concrete samples was obtained from concrete slices sawed from the exposed face of concrete. Then those slices were grounded to powder and chloride content was determined by titration in acid dissolution. Results are reported as the average chloride content in slice of 10 mm depth.

4.9 Cathodic protection

Short term cathodic polarization was applied to selected (corroding) bars in order to better understand the effects of electrochemical treatment on pH in corrosion pits, aimed at improving modeling of such treatments. A carbon fiber anode was attached to the exposed face of each specimen with a layer of mortar with a thickness of 5 mm with a water-binder ratio of 0.50 and CEM I. The electrical current flow to each individual bar contained in the specimens was recorded. One bar per each cover depth in every specimen was left as a reference for comparing the pH of pits when CP is not applied. Linear polarization resistance, electrochemical potential and cell resistivity were measured before, during and after the treatment period. Depolarization measurements were done at 1 day, 3 days, 1 week, 2 weeks and 3 weeks. After 3 weeks the current flow was stopped; destructive testing for corrosion pits, chloride profiles, carbonation depth were done. For measuring the corrosion pits, the bars were exposed to a neutralized acid solution of 15% sulfuric acid (H₂SO₄) and 5% Hexamethylenetetramine (C₆H₁₂N₄) during 24 hours and then, the corrosion products were removed with a steel brush.

5 Identification of concrete specimens with the use of non-destructive testing.

5.1 Overview

Identification of concrete specimens was an important part of this project. As described before, labels on the surface of concrete specimens have disappeared due to weathering during the past 8 years. Beside this, some specimens were lost during the movement of the specimens from the lab in Rijswijk to Delft during 2004.

This chapter is divided in three different levels with a different goal or resolution. First, visual inspection combined with information from previous reports of the concrete specimens was done and in order to separate the specimens into broadly four major groups. Each one of those groups considered specimens containing a different type of cement. The second level defined a more detailed inspection of the concrete specimens. In this level, the concrete resistivity values of specimens were analyzed with the use of two different statistical tests. The values recorded during the month of November 2009 were compared with those reported during the year 2002. The last level of the identification of specimens aimed to make a distinction between water-binder ratios in each group of specimens that was determined in the second level of inspection

5.1.1 Visual inspection

Concrete specimens were visually inspected during the months of October and November 2009. Since the original labels were lost, the specimens were temporary labeled according to their position on the roof. They were stocked in a matricidal form of 8 columns and 15 rows (except for column 4 which contained 18 rows). In this form, all the specimens were labeled for a first trial. After that, it was noticed that some specimens belong to a different project, since they had the reinforcement bars perpendicular to the longest face. These specimens were excluded from any experiment or study during in this project.

The outcome of the visual inspection of concrete specimens is given in Appendix 1. The most characteristic signs used for identification are: apparent color of concrete surface, geometrical dimensions of the specimen, presence or absence of sealing on the longest direction, finishing of the casting face and smoothness of the broken or cut face. Each property will be discussed in more detail below.

The type of cement contained in concrete specimens related to an apparent color is shown in Table 5.1. When evaluating the color of concrete specimens, the final decision was made as a combination of apparent color from visual inspection and reports of previous work (Polder 1998; Polder 2000; Polder 2001a; Guerreri 2002).

Table 5.1 Most common color of concrete specimens according to cement type.

<u>Cement type</u>	<u>Color</u>
CEM I	Gray
CEM II	Dark gray
CEM III	Light gray
CEM V	Very dark-spotted gray

Length of specimens is relevant because it gave the certainty that they were either analyzed for chloride content or carbonation depth. Specimens with length of 250 mm were named as “tested” and specimens with length of 300 mm as “unknown”.

Specimens that had a length of 250 mm had either a rough or smooth surface. When chloride profiles are required, the specimens went under a saw cutting and then grinding to obtain the profile (Polder 2000; Polder 2001a; Guerreri 2002). In the same documents, it is reported that some specimens were subjected to mechanical breaking in order to obtain a clean surface for measuring carbonation depth.

Rubber sealing in one of the longest faces in the specimens was a clear indicative of salt/drying cycles, because the sealing was used while the wetting of concrete specimens in NaCl solution (Polder 1998; Polder 2000; Polder 2001a).

The finish of the casting face was important to identify specimens that contained mixed-in chlorides. A solution of CaCl_2 was added as 2% of cement weight in concrete specimens. This compound accelerated the setting time of concrete, and in this sense, there was not enough time to make a smooth finish in the upper face of the

specimens. After the visual inspection, the three major groups are found with the characteristics shown in Table 5.2.

Table 5.2 Environmental exposure of concrete specimens.

Group	Characteristics
Salt/drying NaCl	Sealing, 250 mm length
Carbonation	No sealing, 250 or 300 mm length, rough finish of lateral face
2% mixed-in Cl	Rough casting surface, 250 or 300 mm

5.2 Concrete Resistivity

5.2.1 Salt/dry exposed specimens after 2.5 years

Measurements of concrete resistivity after 2.5 years of exposure are shown in Table 5.3 (Polder 2001a). In this table, the measured values of concrete resistivity with stainless steel electrodes at 10 and 50 mm depth are shown. In these results, the specimens were fully identified. As described in the experimental program, six specimens of each type of cement and water/binder ratio were exposed to penetrating chloride from salt/drying cycles. Each column is labeled with a code that shows the type of cement and the electrode depth. Therefore, the code 3R50 means CEM III and 50 mm depth.

Table 5.3 Concrete resistivity of salt/dry specimens after 2.5 years, kΩm.

w/b	Environment	CEM I		CEM II		CEM III		CEM V	
		1R10	1R50	2R10	2R50	3R10	3R50	5R10	5R50
0.40	Outside	0.6	0.5	1.3	1.5	3.0	2.4	2.3	2.4
		0.6	0.4	1.5	1.4	2.6	2.3	2.3	2.4
	20 °C – 80% RH	0.8	0.6	1.9	2.6	2.7	3.3	3.2	3.5
		0.7	0.6	2.0	2.8	2.3	3.1	3.1	3.7
	Fog room	0.2	0.2	0.9	1.3	1.8	1.7	1.7	1.9
		0.2	0.2	1.0	1.3	1.8	1.7	1.7	2.0
0.45	Outside	0.4	0.3	1.5	1.7	2.7	2.3	1.7	2.0
		0.4	0.3	1.6	1.7	3.2	2.4	1.9	2.0
	20 °C – 80% RH	0.6	0.6	1.8	2.8	2.2	3.3	2.4	3.5
		0.5	0.5	1.5	2.7	2.2	3.1	2.4	3.5
	Fog room	0.2	0.2	0.7	1.2	1.8	1.7	1.4	1.6
		0.2	0.2	0.7	1.2	1.8	1.7	1.4	1.7
0.55	Outside	0.4	0.2	1.1	1.4	2.3	2.3	1.4	1.6
		0.2	0.2	1.2	1.5	2.8	2.5	1.3	1.7
	20 °C – 80% RH	0.3	0.5	0.9	2.0	1.0	1.9	1.3	3.8
		0.3	0.5	0.8	1.8	0.8	1.3	1.2	3.1
	Fog room	0.1	0.1	0.7	1.0	1.7	1.6	1.1	1.3
		0.1	0.1	0.7	1.0	1.5	1.4	1.2	1.4

Results shown in Table 5.3 show that the environment at which each specimen was exposed, has a significant influence in the values of concrete resistivity in general terms.

With measurements of concrete resistivity after 2.5 years, a nested factorial design (NFD) probabilistic tool was used to analyze the data and identify the influence of and possible interaction between parameters that affect the results of resistivity. These parameters are: cement type, water binder ratio and cover depth as shown in Table 5.4.

Table 5.4 Nested Factorial Design parameters.

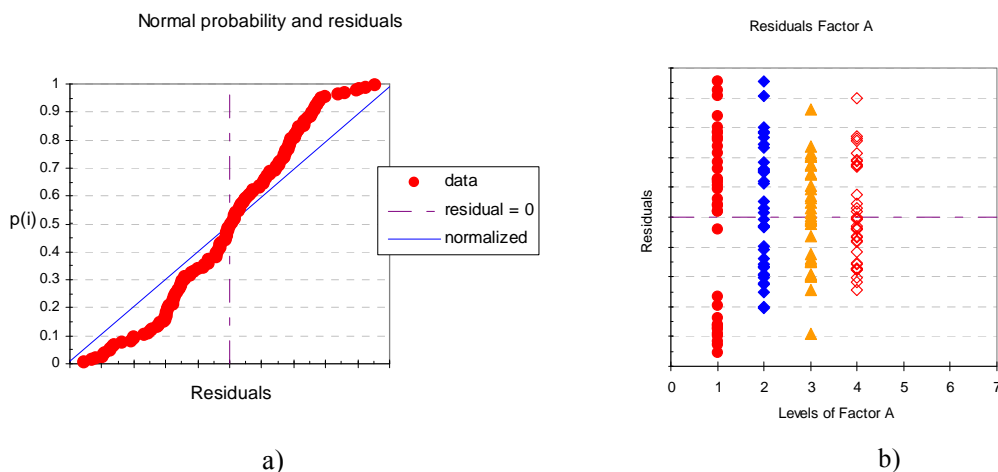
Factor A	Type of cement		Factor B	w/c	Factor C		Concrete cover (mm)	
$(\tau$ is Fixed) counter = i	A1	CEM I	$(\beta$ is Fixed) counter = j	B1	0.40	$(\gamma$ is Random) counter = k C is nested in Factor B	C1	10
	A2	CEM II		B2	0.45		C2	30
	A3	CEM III		B3	0.55		C3	
	A4	CEM V		B4			C4	

The null hypothesis of the NFD test is that each parameter does not influence the values of concrete resistivity. By rejecting the null hypothesis, the NFD test identifies which of these three parameters had influenced values of concrete resistivity in a higher degree. The partial outcome of the test is shown in Table 5.5, while complete results of NFD test are shown in Appendix 2.

Table 5.5 Results of NFD test on values of concrete resistivity after 2.5 years.

F-value	F crit	P-value	Conclusion
207.5914	3.862548	1.26E-08	Reject Ho: 'There is no influence of Factor A'
6.134869	9.552094	0.087083	Accept Ho: 'There is no influence of Factor B'
2.657066	2.680168	0.051483	Accept Ho: 'There is no influence of Factor C'
0.42792	3.373754	0.843137	Accept Ho: 'There is no influence of AB-interaction'
0.943975	1.958763	0.490017	Accept Ho: 'There is no influence of BC-interaction'

Table 5.5 shows that the most important parameter that has significant influence in values of concrete resistivity after 2.5 years is cement type. This is confirmed by the high value in variable F-value compared to those obtained for water-binder ratio or concrete cover. This result is validated because of results reported in literature and in the reports from TNO (Bedford 2001). Figure 5.1a shows the normal distribution of resistivity values as a function of their residuals. Figure 5.1b shows the residuals of values of concrete resistivity with respect to the values of Factor A (Cement type), in which Level 1, 2, 3 and 4 represent CEM I, CEM II, CEM III and CEM V, respectively.

**Figure 5.1** Distribution of concrete resistivity values according to NFD test.

In Figure 5.1a, the line of measured values of concrete resistivity is labeled as data, and the path of the line is deviated from a normal distribution line in both sides of the curve. However, this difference is small and when looking at Figure 5.1b, the scatter of resistivity values, according to their cement type, shows similar range in values when statistical treatment of the results was carried out. As a statistical treatment of results, the logarithm of values of resistivity was analyzed in order to reduce the bigger scatter in the results without treatment. Since the logarithm was applied on all results of resistivity, it is allowed to do a NFD test on those results without affecting the final outcome.

Figure 5.2a shows the impact level of the Factor A (cement type) in terms of resistivity values. It is clear that the impact of cement type in values of concrete resistivity in specimens cast with blended cements (CEM II, CEM III and CEM V) is significantly bigger than for Portland cement. CEM II has an intermediate influence in concrete resistivity when compared to CEM III and CEM V. The impact level of CEM III and CEM V are very similar to each other, meaning that with only statistical analysis, it is not possible to identify them with certainty. For this, a combination of statistical analysis and visual inspection was required.

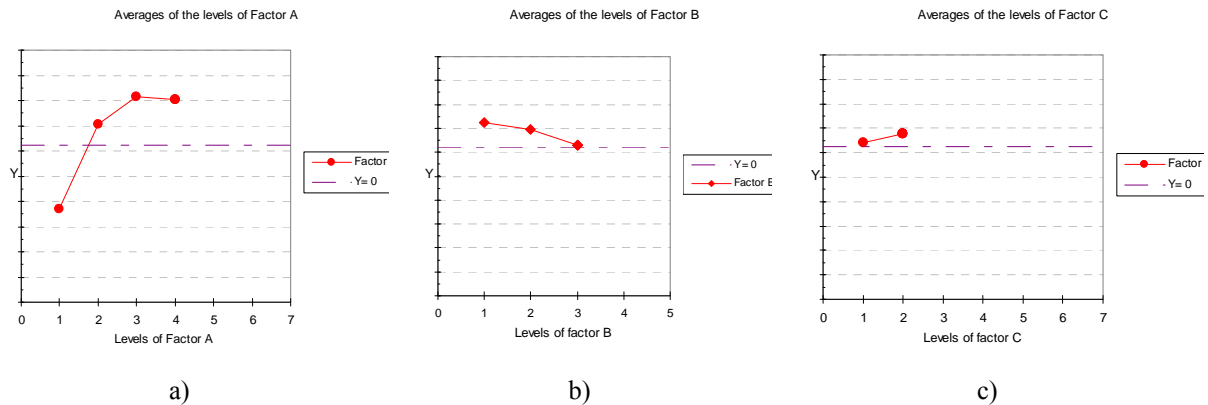


Figure 5.2 Impact level of cement type, w/b ratio and cover depth in values of resistivity after 2.5 years.

In Figure 5.2b, the influence of water/binder ratio is shown in values of concrete resistivity is shown. The Levels of Factor B are 0.40, 0.45 and 0.55 respectively. Results of NFD show that as the water/binder ratio is increased, the values of concrete resistivity decrease in a similar proportion. This effect has been recorded in literature, where the effect of high water/binder ratios in the structure of the pore network (and indirectly, concrete conductivity and resistivity) resulted in a decrease of durability properties (Neville 1995; Polder 2001b; Bertolini 2004). Finally, the influence of cover depth shown in Figure 5.2c is not as strong as the other parameters that were investigated for this research.

The NFD conclusion shows that the strongest influence in values of concrete resistivity in specimens exposed to salt/dry cycles is attributed to the cement type contained in them.

However, a disadvantage of the use of NFD test is that the number of replicates (specimens) must be the same in the investigated groups. While this holds true in 2000, it is not in after 12 years; therefore an additional test that can be done in a set with a different number of replicates is required. Since the cement type is the most influencing factor with regard to concrete resistivity, it is possible to use the measured values of this property in order to identify the cement type with a confidence of 95%. For this, a statistical tool Kolmogorov-Smirnov for two sample test is adequate. The Kolmogorov-Smirnov test compares the values of concrete resistivity of two groups at the time. The null hypothesis in this test is that a group of samples with values of a continuous variable (i.e. concrete resistivity) with the same empirical cumulative distribution function (ECDF), will belong to the same type of group (i.e. cement type). By comparing the empirical cumulative distribution function (ECDF) of resistivity values, it is possible to find differences between each line that would lead to the conclusion that both groups contain different cement types.

With the use of Matlab[®] software, a Kolmogorov-Smirnov two sample test was carried out with the values of concrete resistivity after 2.5 years as input. The statistical analysis of these data is shown in Table 5.6. In this table, three different variables are given. The first, [H] represents the acceptance or rejection of the null hypothesis, can only give values of 1 (rejection) or 0 (acceptance). In this case, a positive outcome in terms of identification of cement type is a [H] value of 1. This means that the ECDF of a group of samples tested against another one are different, ergo, they contain different cement type. This confirms the outcome of the factorial nested test described above. The second variable [P] shows the probability of a sample that has been labeled incorrectly. Since the null hypothesis can only be rejected when the value of P is lower than 5% (significance value of the test), [H] is a function of [P]. The Kolmogorov-Smirnov test gives the maximum difference between ECDF lines for two different groups. When the third variable [kst] shows values high enough to make a clear distinction between groups, [P] will be low and [H] may be rejected.

Table 5.6 Kolmogorov-Smirnov test results for 10 mm cover, 2.5 years.

	2R10		3R10		5R10	
1R10	H	1	H	1	H	1
	P	2.90E-07	P	3.81E-08	P	4.43E-09
	kst	0.8889	kst	0.9444	kst	1
2R10	-		H	1	H	1
			P	2.85E-04	P	0.039
			kst	0.6667	kst	0.4444
3R10	-		-		H	0
					P	0.0982
					kst	0.3889

Results shown in Table 5.6 are described graphically in Fig. 5.3. In this figure, it is clear that the difference between the ECDF lines for each type of cement is located at different values of resistivity, indicating the difference between cement types. It is important to note that the values of resistivity in specimens made with CEM III and CEM V are significantly closer to each other. This corresponds to the result of the Kolmogorov-Smirnov test between these cements ($H=0$, $P=0,09$). Even when the specimens are identified accurately, the closeness in results leads to a degree of uncertainty. Thus, all groups could be distinguished statistically, except for CEM III and CEM V.

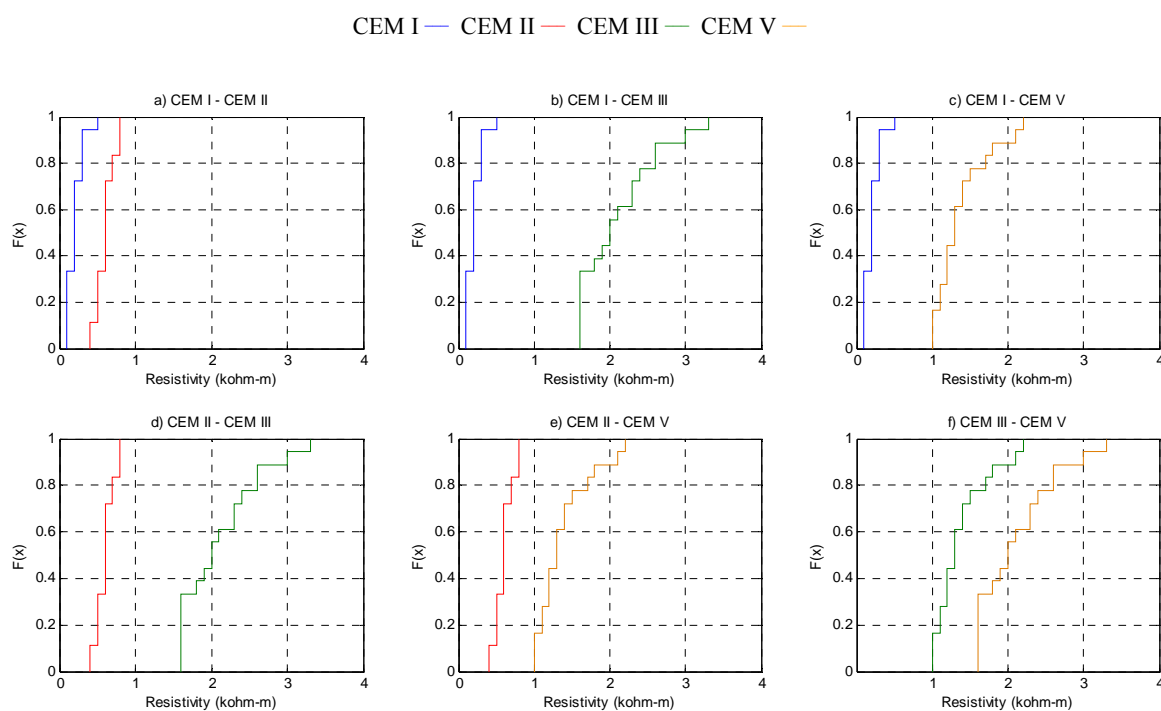


Figure 5.3 ECDF plots of concrete resistivity in salt/dry specimens at 10 mm depth.

Using the Kolmogorov-Smirnov test on concrete resistivity at 50 mm depth measured at 2.5 years, the outcome is shown in Table 5.7. In this table, it is seen that the confidence of the test is higher than for 10 mm. This can be explained as the influence of the outdoor conditions on the moisture content in the outer layer of concrete which is more sensitive to change. At 50 mm, the moisture content remains more stable over time due to relatively slow transport of moisture through the cement matrix when compared to evaporation in the outer layer.

Table 5.7 Kolmogorov-Smirnov result of salt/dry specimens at 50 mm depth, 2.5 years.

	2R50		3R50		5R50	
1R50	H	1	H	1	H	1
	P	4.43E-09	P	4.43E-09	P	4.25E-10
	kst	1	kst	1	kst	1
2R50	-	-	H	1	H	1
	-	-	P	0.039	P	0.039
	-	-	kst	0.44	kst	0.44
3R50	-	-	-	-	H	0
	-	-	-	-	P	0.4255
	-	-	-	-	kst	0.27

The Kolmogorov-Smirnov test was used also for values of resistivity at 50 mm cover depth. After 2.5 years, the difference between the resistivity at 10 and 50 mm depth for a single specimen is relatively small. This difference may be relevant after 11 years due to changes in exposure conditions, moisture content, temperature and differences between the outer concrete layer and the bulk concrete specimen producing a so-called skin effect (Polder 2001a).

The comparison between ECDF lines for concrete resistivity at 50 mm is shown in Fig. 5.4. This behavior is proved by the Kolmogorov-Smirnov test outcome in Table 5.7. Again, the ECDF lines of CEM III and CEM V are very similar. The influence of slag (CEM III), and slag + fly ash (CEM V) is visible in the minimum value of resistivity in those sets of specimens. While for CEM I and II the values of resistivity are below 1 kΩm, for CEM III and CEM V the lower boundary for CEM III and for CEM V is even higher. Again, it is possible to identify those specimens which belong to different mixture compositions with this statistical tool, except for CEM III and CEM V as with 10 mm of cover depth.

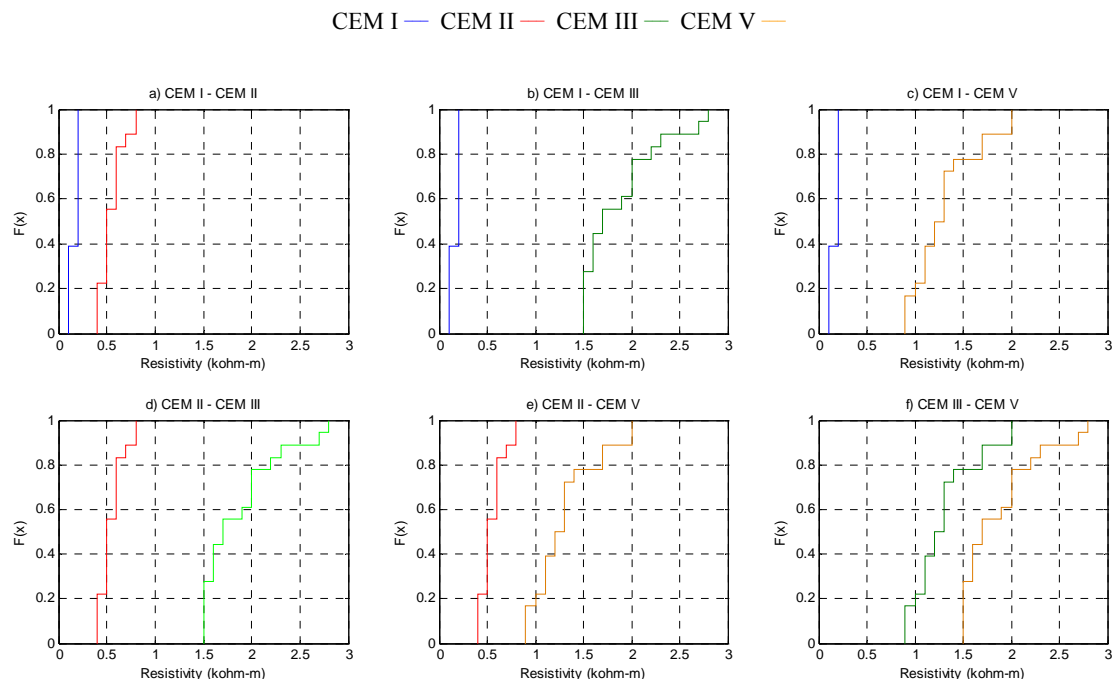


Figure 5.4 ECDF plots of concrete resistivity of salt/dry specimens at 50 mm depth.

Results of both Kolmogorov-Smirnov and NFD show that cement type is most favorable parameter to be investigated after 12 years, in order to identify concrete mixtures. In this sense, a combination of visual inspection and Kolmogorov-Smirnov test was used in specimens after 12 years, since the NFD can not be used due to the differences in the number of specimens as either destructively analyzed (Polder 2000; Polder 2001a; Guerreri 2002) or lost.

5.2.2 Salt/dry exposed specimens after 11 years.

Measurements of concrete resistivity in 2009 are shown in Tables 5.8 to 5.11 for specimens that are identified as part of the group subjected to salt/dry cycles. These specimens were selected according to a combination of visual inspection and probabilistic analysis with the Kolmogorov-Smirnov test.

Table 5.8 Probable CEM I salt/dry specimens, November 2009.

Specimen	Cement type	Concrete resistivity (kΩm)	
		10 mm	50 mm
6-8	I	0.8	0.6
3-12	I	0.8	0.4
4-13	I	1.5	1.0
1-7	I	1.5	0.9
2-11	I	0.7	0.8
4-5	I	0.9	0.6

Table 5.9 Probable CEM II salt/dry specimens, November 2009.

Specimen	Cement type	Concrete resistivity (kΩm)	
		10 mm	50 mm
4-8	II	1.9	1.7
3-3	II	1.8	1.6
3-10	II	1.9	1.5
4-17	II	3.2	2.9
4-3	II	2.1	2.6
1-8	II	2.2	3.4

Table 5.10 Probable CEM III salt/dry specimens, November 2009.

Specimen	Cement type	Concrete resistivity (kΩm)	
		10 mm	50 mm
4-9*	III	2.2	2.1
4-7*	III	2.7	2.8
8-8	III	2.0	1.9
4-11	III	3.9	2.4
8-6	III	5.7	4.3
4-18*	III	9.6	5.5
5-7	III	6.5	4.9
8-5	III	7.6	5.1
7-5	III	8.5	5.4
6-15	III	4.1	2.9
1-9*	III	4.4	3.8

Table 5.11 Possible CEM V salt/dry specimens, November 2009.

Specimen	Cement type	Concrete resistivity (kΩm)	
		10 mm	50 mm
4-5	V	3.6	4.9
5-9	V	3.0	4.0
2-4	V	3.3	3.7
3-7	V	3.9	3.6
4-14	V	8.9	6.4
6-10	V	4.7	3.9
4-16	V	5.1	4.4
3-11	V	6.3	6.4
5-4	V	5.6	5.8
6-7	V	6.0	4.2
5-5	V	7.5	6.6
5-10	V	3.7	4.2
3-15	V	6.2	4.0

With the Kolmogorov-Smirnov test, the values of resistivity for each group with regard to their cement type

* Specimens with mark * belong to a different batch that was cast in 1999. However, this was found in a report on the latter stage of the study and, therefore, remained in it as part of the group.

were compared with the other cement types for both electrode pair depths. Table 5.12 shows the outcome of the KS test at a depth of 10 mm.

Table 5.12 Kolmogorov-Smirnov result of salt/dry specimens at 10 mm depth, 11 years.

	2R10		3R10		5R10	
1R10	H	1	H	1	H	1
	P	0.0013	P	1.55E-04	P	1.25E-04
	kst	1	kst	1	kst	1
2R10	-		H	1	H	1
			P	0.0298	P	5.21E-04
			kst	0.66	kst	0.923
3R10	-		-		H	0
					P	0.4104
					kst	0.33

An important remark is that the range of resistivity values in the group of CEM III and CEM V is much higher than for CEM I and CEM II. This may be caused by a difference between the number of specimens and the measured values that may be influenced by the position of each specimen on the roof, since specimens were stored in clusters of five specimens followed by an empty space of the size of one specimen roughly. This may lead to different exposure conditions of moisture in the specimens that had one side uncovered. Also, there is a probability that few specimens belong to a different group with regard to where they were considered for the Kolmogorov-Smirnov test. Nevertheless, the results given in Table 5.12 have a similar pattern as those reported on Table 5.6 (based on perfect identification) with differences in the significance value and the [kst]. Therefore, the confidence by which one may assume that each specimen is correctly placed in its corresponding cement group is above 95%. Only in the case of CEM III and CEM V this is not true, but then again, even in the well-known specimens reported in (Polder 2001a), the KS test result could not assure a statistical difference between them.

The outcome of the Kolmogorov-Smirnov test shows the comparison between ECDF of each group of specimens with different cement type. Figure 5.5 shows this test for each combination possible for four different cement types at a depth of 10 mm. The ECDF lines for CEM I and CEM II are shown in Fig. 5.3a. The numerical results are given in the left upper part of Table 5.10. For the combination of CEM I (1R10) and CEM II (2R10), the maximum difference between the ECDF lines is 1 for resistivity values of about 1.8 kΩm according to Figure 5.3a.

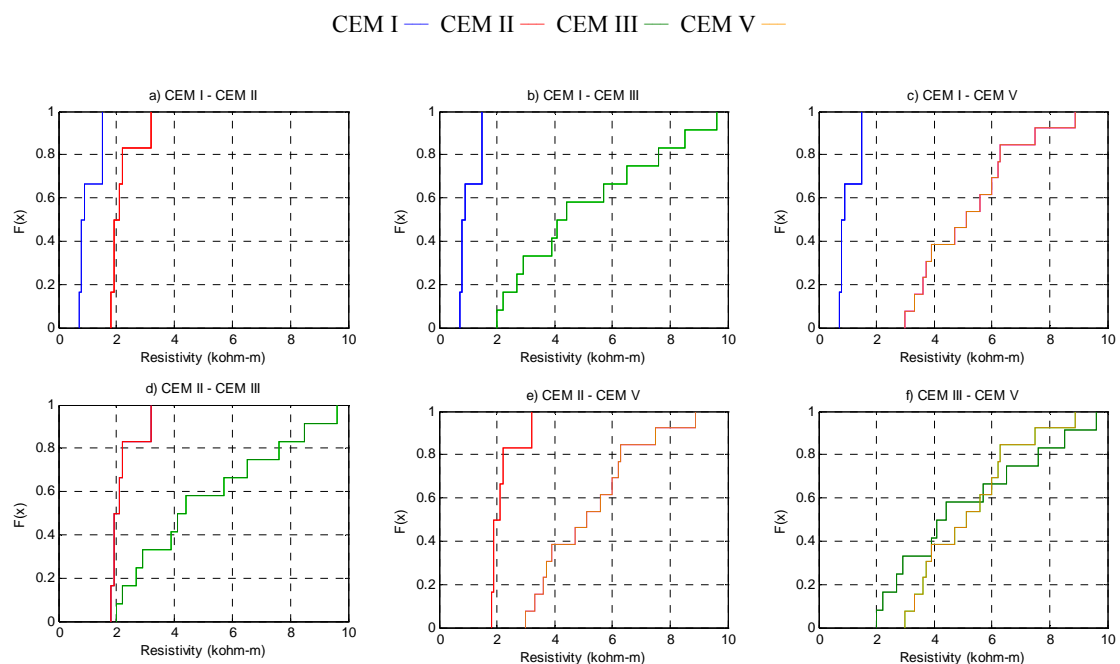


Figure 5.5 ECDF plots of salt/dry specimens at 10 mm depth, 11 years.

At first instance, it is clear that the minimum value of resistivity in all the specimens has increased significantly from 2000 to 2009. This behavior may be caused by continuous hydration of the cement. Nevertheless, the increase in resistivity is not the same in all specimens. Prisms cast with CEM III and CEM V shows a more significant increase (by a factor of two), while for CEM I and CEM II the increase is not so high. Results of the Kolmogorov-Smirnov test applied to values of concrete resistivity at 50 mm depth are shown in Table 5.13.

Table 5.13 Kolmogorov-Smirnov result of salt/dry specimens at 50 mm depth, 11 years.

	2R50		3R50		5R50	
1R50	H	1	H	1	H	1
	P	0.0013	P	1.55E-04	P	1.25E-04
	kst	1	kst	1	kst	1
2R50	-		H	0	H	1
			P	0.1876	P	1.25E-04
			kst	0.5	kst	1
3R50	-		-		H	0
					P	0.578
					kst	0.5

Results show that the difference between ECDF lines from CEM I and CEM II remain at lower resistivity values. On the other hand, CEM V shows a more dispersed range of resistivity values but, nevertheless, the lower boundary is still higher than for the CEM I and CEM II groups. CEM III differs from CEM I, but not from CEM II. Resistivity values of CEM II and CEM III are in the range between 1.8 and 3.5 kΩm. This interval is uncertain for the KS test to reject the null hypothesis. This is shown when the groups 2R50 and 3R50 are compared. Plots of ECDF lines are shown in Fig. 5.6.

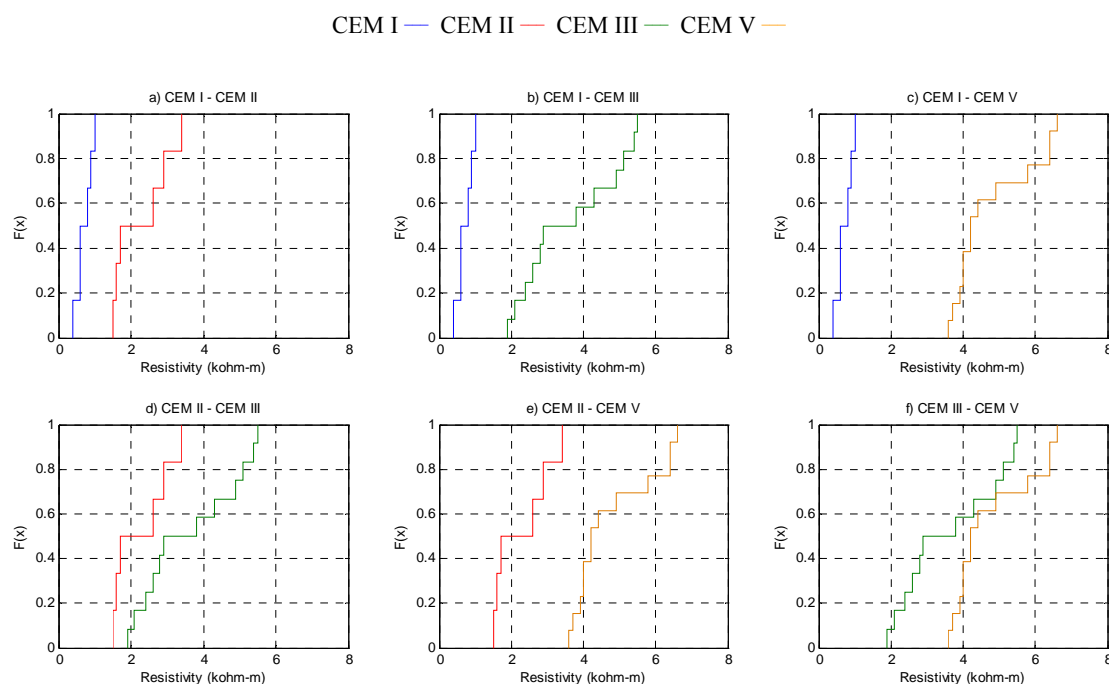


Figure 5.6 ECDF plots of salt/dry specimens at 50 mm depth, 11 years.

After evaluating the results obtained from the KS test and the ECDF plots, it is possible to assure with 95% confidence that the specimens that were considered for each group of cement type are correctly identified. The increase in concrete resistivity of CEM II can be explained as the further hydration of cement due to the influence of fly ash. This behavior is also observed in CEM V. While CEM III and CEM V had similar resistivity during the first years after casting, the resistivity in CEM V is more developed after 10 years. This is observed as a displacement to the right hand side of the CEM V ECDF in Fig. 5.4f. In contrast, the minimum value of CEM III is closer to the maximum value as measured after 2.5 years.

The Kolmogorov-Smirnov test has made possible to identify the cement type in specimens exposed to salt/dry cycles after 12 years. In most cases, it was possible to determine the difference between cement type (except between CEM III and CEM V) but not with water-binder ratio. For this, additional tests of Schmidt hammer for hardened concrete were required.

5.2.3 Carbonated specimens after 2.5 years.

The specimens that were exposed to accelerated carbonation were recognized easily because of the rough finish on the surface of the broken cross section (for carbonation depth measurement). Apart from the obvious specimens, a few of them apparently had not been tested and the complete specimen was available for this test. The values of concrete resistivity of the specimens after 2.5 years (Polder 2001a), that were exposed to accelerated carbonation are shown in Table 5.14.

Table 5.14 Concrete resistivity of carbonated specimens after 2.5 years, kΩm.

w/b	Exposure	CEM I		CEM II			CEM III		CEM V
		1R10	1R50	2R10	2R50	3R10	3R50	5R10	5R50
0.40	Outside	4.0	1.0	5.4	2.2	7.0	4.4	2.6	2.0
		2.7	0.8	4.9	2.0	8.6	4.0	2.6	1.9
	20°C/80%RH	10.8	1.6	15.8	4.9	19.4	8.4	11.2	5.5
		8.5	1.6	16.8	5.3	19.3	8.6	10.0	5.2
0.45	Outside	4.9	0.8	7.1	2.0	2.2	2.3	2.0	1.9
		3.5	0.7	6.8	1.9	2.5	2.3	1.7	1.9
	20°C/80%RH	16.2	1.5	30.6	6.9	13.2	11.0	13.1	5.1
		16.5	1.4	32.8	7.9	13.6	9.6	12.8	6.0
0.55	Outside	8.0	2.8	4.0	2.4	3.9	1.7	1.3	1.9
		7.0	2.1	3.6	2.6	3.7	1.9	1.9	1.6
	20°C/80%RH	42.9	25.5	14.4	6.1	17.8	15.2	18.5	16.3
		37.8	8.2	15.5	6.3	17.6	16.0	17.6	14.5

In the case of carbonated specimens, the parameters that may influence differ from those studied in the salt/dry exposure. The outcome of the NFD test using the parameters of cement type, water-binder ratio and cover depth did not brought any significant conclusion. This was caused because the most important parameter that influences the values of concrete resistivity is the exposure to accelerated carbonation or outside exposure. Therefore, the third parameter was fixed for the climate exposure of the specimens as shown in Table 5.15.

Table 5.15 NFD parameters of carbonated specimens.

Factor A	Type of cement		Factor B	w/c	Factor C	Cover depth		
(τ is Fixed) counter = i	A1	CEM I	(β is Fixed) counter = j	B1	0.40	(γ is Random) counter = k	C1	10mm
	A2	CEM II		B2	0.45		C2	50mm
	A3	CEM III		B3	0.55		C3	
	A4	CEM V		B4			C4	
						C is nested in Factor B		

The NFD outcome was done in values of specimens that had been exposed to an outside environment. In this sense, Table 5.16 shows the outcome of the NFD test outcome for those specimens.

Table 5.16 NFD test outcome of carbonated specimens at after 2.5 years.

F-value	F crit	P-value	Conclusion
2.052981	3.862548	0.176969	Accept Ho: 'There is no influence of Factor A'
0.129184	9.552094	0.883449	Accept Ho: 'There is no influence of Factor B'
116.6031	3.008787	1.92E-14	Reject Ho: 'There is no influence of Factor C'
1.51677	3.373754	0.275437	Accept Ho: 'There is no influence of AB-interaction'
26.18505	2.300244	2.65E-10	Reject Ho: 'There is no influence of BC-interaction'

The results of the NFD show that in the case of carbonated specimens, the influence of cement type in values of concrete resistivity is not as strong as the cover depth. This behavior has two different causes; first, the influence of carbonation itself affects results of concrete resistivity due to the production of carbonates after the reaction. Second, the carbonation depth of specimens is not the same for all concrete mixtures as shown in Table 3.3; therefore, the identification of carbonation specimens becomes more complicated. Since the intention of this project is to use as much as possible the non-destructive testing, the statistical analysis of such specimens will still be carried out. However, an important remark on the results of carbonation specimens must be applied.

Figure 5.7a shows the distribution of values of concrete resistivity and their residuals against a normalized distribution. When comparing this figure with the one obtained with specimens exposed to salt/dry cycles, it is clear that the distribution of values follows a more erratic behavior. In Figure 5.7b, the distribution of values of concrete resistivity with respect to their cement type is even more difficult to identify. Even though the specimens are fully identified, the nature of the deterioration of concrete due to carbonation is affecting the values of resistivity in such a way that by only analyzing those results, is not possible to come to a certain conclusion.

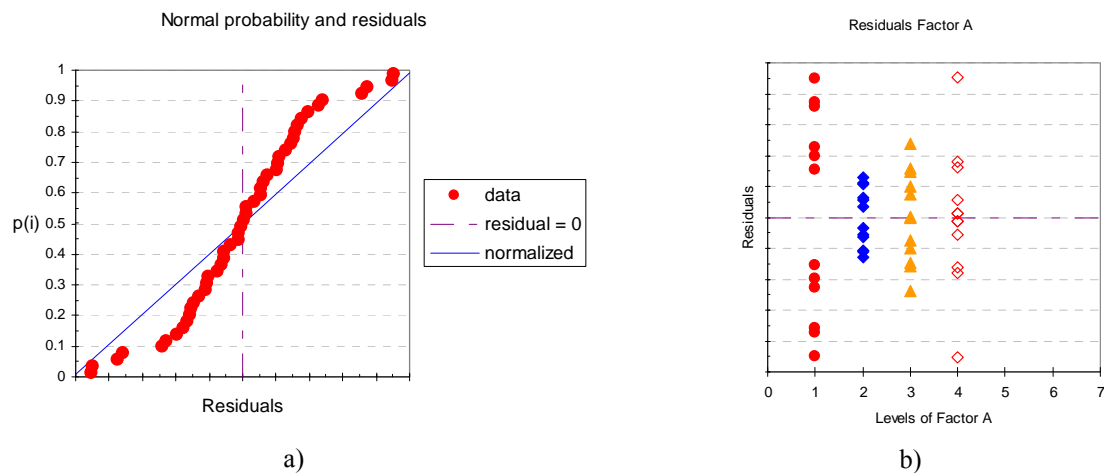


Figure 5.7 NFD outcome of carbonation specimens after 2.5 years.

Figure 5.8a shows the impact level of cement type in values of concrete resistivity in carbonated specimens after 2.5 years. Values of concrete resistivity of Portland cement concrete are slightly below those found with concrete containing CEM II and CEM III. This was unexpected, since the presence of cementitious materials (fly ash, slag) generally results in an reduction of pH in the pore solution, favoring the carbonation process as shown in Table 3.3.. This behavior was found in concrete with CEM V. With respect to water/binder ratio, Figure 5.8b shows the influence of this parameter in the concrete resistivity. There are not significant differences between each water/binder ratio; nonetheless, for a ratio of 0.45 the lowest values of concrete resistivity are found. This is probably related to a faster diffusion of carbon dioxide due to favorable conditions of connectivity of pores and water content. Finally the cover depth influence is shown in Figure 5.8c. It is clear that this parameter has the strongest influence on values of concrete resistivity. However, the reasons behind this phenomenon have been discussed above.

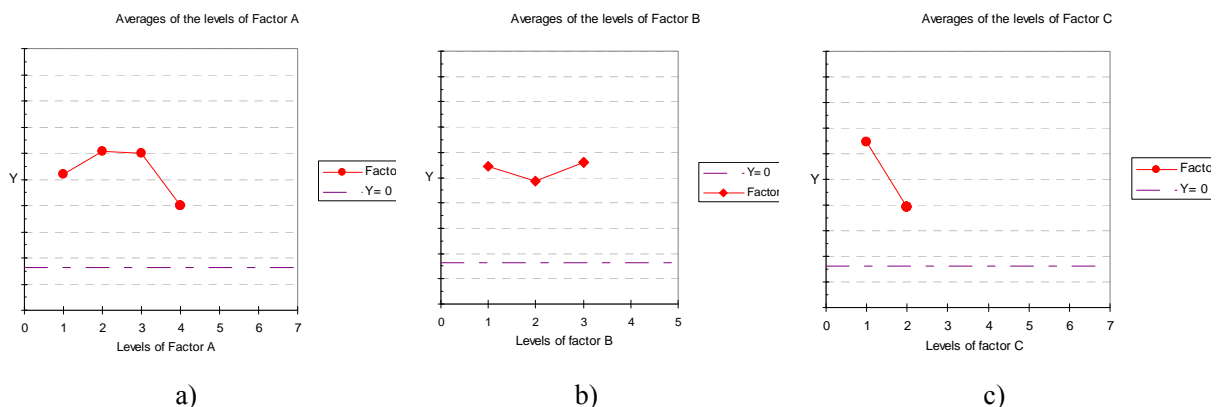


Figure 5.8 Impact level of parameters in concrete resistivity of carbonation specimens after 2.5 years.

The most parameter that has the strongest influence in values of concrete resistivity of carbonation specimens is the concrete cover depth.

Values of concrete resistivity in Table 5.17 show significant scatter in results for each cement type and water/binder ratio. The carbonation depth in these specimens also reflected this scatter (Polder 2000). When the Kolmogorov-Smirnov test is applied to these values, the outcome of the test shows the difference between the resistivity values at 10 and 50 mm depth. This behavior occurs due to differences in the environmental conditions from the initial exposure climate (5% CO₂, 50% RH) for the first 26 weeks and then outside and unsheltered for 2 more years. When concrete is carbonated, the pore volume is reduced due to deposition of carbonate by-products of carbonation reaction and therefore, resistivity is increased (Neville 1995; Bertolini 2004; Broomfield 2007). High values of resistivity at 10 mm and low values at 50 mm indicate that the cover depth of 10 mm has been carbonated, while at 50 mm the carbonation front has not reached the stainless steel bars. The outcome of Kolmogorov-Smirnov test on carbonation specimens after 2.5 years is given in Table 5.17.

Table 5.17 Kolmogorov-Smirnov result of carbonated specimens at 10 mm depth, 2.5 years.

	2R10		3R10		5R10	
1R10	H	0	H	0	H	0
	P	0.9913	P	0.9913	P	0.0656
	kst	0.1667	kst	0.1667	kst	0.5
2R10	-	-	H	0	H	0
	-	-	P	0.7864	P	0.0656
	-	-	kst	0.25	kst	0.5
3R10	-	-	-	-	H	0
	-	-	-	-	P	0.4333
	-	-	-	-	kst	0.333

The plot of ECDF lines for a cover depth of 10 mm is shown in Fig. 5.9. In this figure, ECDF lines show clearly the range of resistivity values for each cement type. The greatest range was found in CEM I which is twice as big as those reported for CEM III and CEM V. The maximum value of concrete resistivity found in groups of specimens with CEM III and CEM V is under 20 kΩm. These results correspond to the increase of carbonation depth in specimens cast with CEM I and CEM V as reported in (Polder 2000). On the other hand, the values for CEM I and CEM II are higher than 30 kΩm.

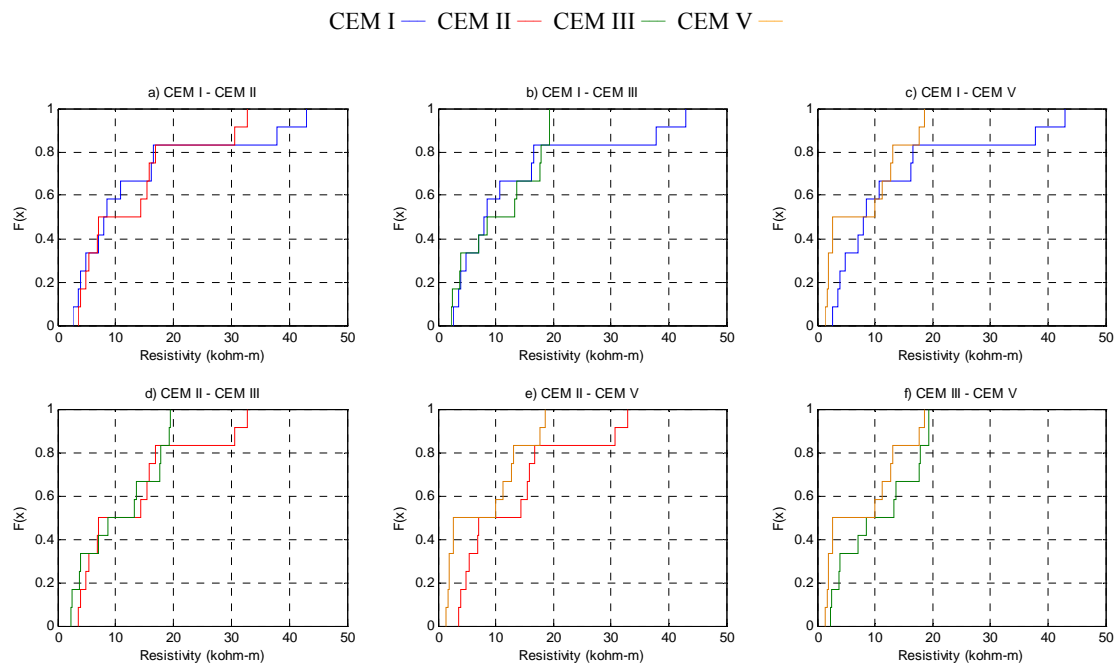


Figure 5.9 ECDF plots of carbonated specimens at 10 mm depth, 2.5 years.

The outcome of Kolmogorov-Smirnov test for a cover depth of 50 mm is given in Table 5.18. In contrast with Table 5.17, the Kolmogorov-Smirnov test on CEM I with the rest of the specimens is clearly identified. Nevertheless, this is not the case for CEM II, CEM III and CEM V. It is important to note that, the absolute values of resistivity at 50 mm are different from those recorded at 10 mm. The difference between concrete resistivity values at different depths in specimens of CEM I and CEM II are higher than in CEM III and CEM V. The cause of this is the non-carbonated concrete at 50 mm depth.

Table 5.18 Kolmogorov-Smirnov result of carbonated specimens at 50 mm depth, 2.5 years.

	2R50		3R50		5R50	
1R50	H	1	H	1	H	1
	P	0.0046	P	0.0046	P	0.0191
	kst	0.6667	kst	0.6667	kst	0.5833
2R50	-		H	0	H	0
			P	0.0656	P	0.4333
			kst	0.5	kst	0.333
3R50	-		-		H	0
					P	0.4333
					kst	0.333

The ECDF plots of concrete resistivity at 50 mm depth in specimens exposed to carbonation are shown in Fig. 5.10. Again, the range of resistivity values of CEM I is the highest of all. Nevertheless, the probabilistic test shows that CEM I specimens are identifiable when compared to the rest of the cement types. It is important to note that the maximum resistivity values at 50 mm are around 25 kΩm, when for 10 mm they are around 50 kΩm.

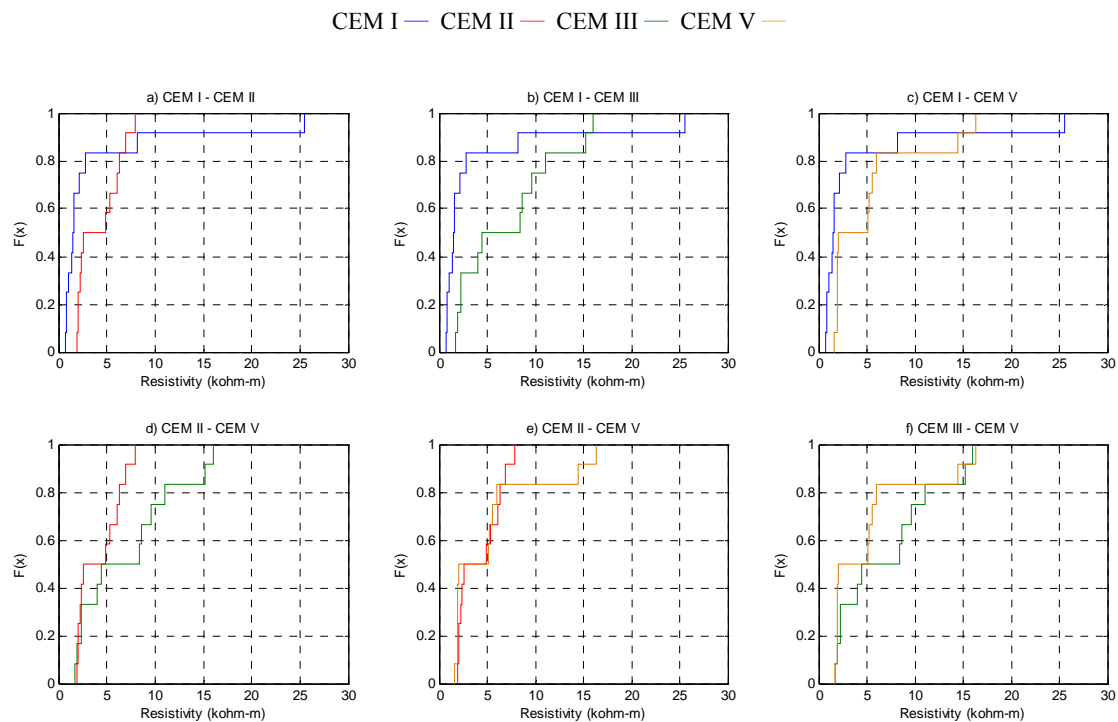


Figure 5.10 ECDF plots of carbonated specimens at 50 mm depth after 2.5 years.

5.2.4 Carbonated specimens after 11 years.

After doing the visual inspection and measurements of concrete resistivity, concrete specimens with a rough side surface (where a slice was broken off for carbonation depth measurement) were separated according to these two parameters. It should be noted that the distribution of specimens among the different cement types is given in Table 5.19 to Table 5.24.

Table 5.19 Concrete resistivity of carbonated specimens with CEM I after 11 years.

Specimen	Cement type	Concrete resistivity (k Ω m)	
		10 mm	50 mm
8-13	I	4.4	2.9
7-12	I	5.8	3.4
8-14	I	7.2	1.4
2-13	I	3.6	4.0
3-6	I	7.6	1.1
3-9	I	3.7	1.3
1-2	I	5.6	1.1

Table 5.20 Concrete resistivity of carbonated specimens with CEM II after 2.5 years.

Specimen	Cement type	Concrete resistivity (k Ω m)	
		10 mm	50 mm
3-13	II	2.5	2.4
5-3	II	2.1	2.6
5-11	II	0.9	0.9
3-1	II	1.2	1.3
1-10	II	3.7	3.5
5-1	II	2.2	3.2
2-10	II	3.3	4.2

Table 5.21 Concrete resistivity of carbonated specimens with CEM III after 2.5 years.

Specimen	Cement type	Concrete resistivity (k Ω m)	
		10 mm	50 mm
2-12	III	1.0	0.8
3-14	III	0.8	0.9
5-12	III	1.2	1.5
8-7	III	1.2	1.7
1-15	III	5.9	1.8
8-4	III	3.3	2.5

Table 5.22 Concrete resistivity of carbonated specimens with CEM V after 2.5 years.

Specimen	Cement type	Concrete resistivity (k Ω m)	
		10 mm	50 mm
5-2	V	1.0	0.9
4-1	V	1.4	2.0
7-3	V	0.9	0.9
2-3	V	1.3	1.6
3-2	V	1.8	2.1
8-1	V	2.7	2.8
3-8	V	1.0	0.8

The Kolmogorov-Smirnov test was applied for concrete resistivity values at 10 mm cover depth, and the outcome is shown in Table 5.23. In this table, the results between CEM I and the rest of the groups are clearly visible. This difference is not visible for a comparison between the other cement types. Therefore, the null hypothesis cannot be rejected in these cases.

Table 5.23 Kolmogorov-Smirnov outcome of carbonated specimens at 10 mm depth.

	2R10		3R10		5R10	
1R10	H	1	H	1	H	1
	P	0.0041	P	8.70E-3	P	4.48E-4
	kst	0.8571	kst	0.833	kst	1
2R10	-	-	H	0	H	0
	-	-	P	0.61084	P	0.1286
	-	-	kst	0.38	kst	0.5
3R10	-	-	-	-	H	0
	-	-	-	-	P	0.777
	-	-	-	-	kst	0.333

The ECDF plots for concrete resistivity values at a cover depth of 10 mm are shown in Fig. 5.11. Like in the results shown in the KS test outcome after 2.5 years, the concrete resistivity of CEM I have higher values than the rest of the cement types. Concrete specimens with CEM II and CEM V show similar values of resistivity, which may be caused by the influence of fly ash in these two cement types. CEM III shows the lowest values, which is the same behavior found in the results of (Polder 2001b).

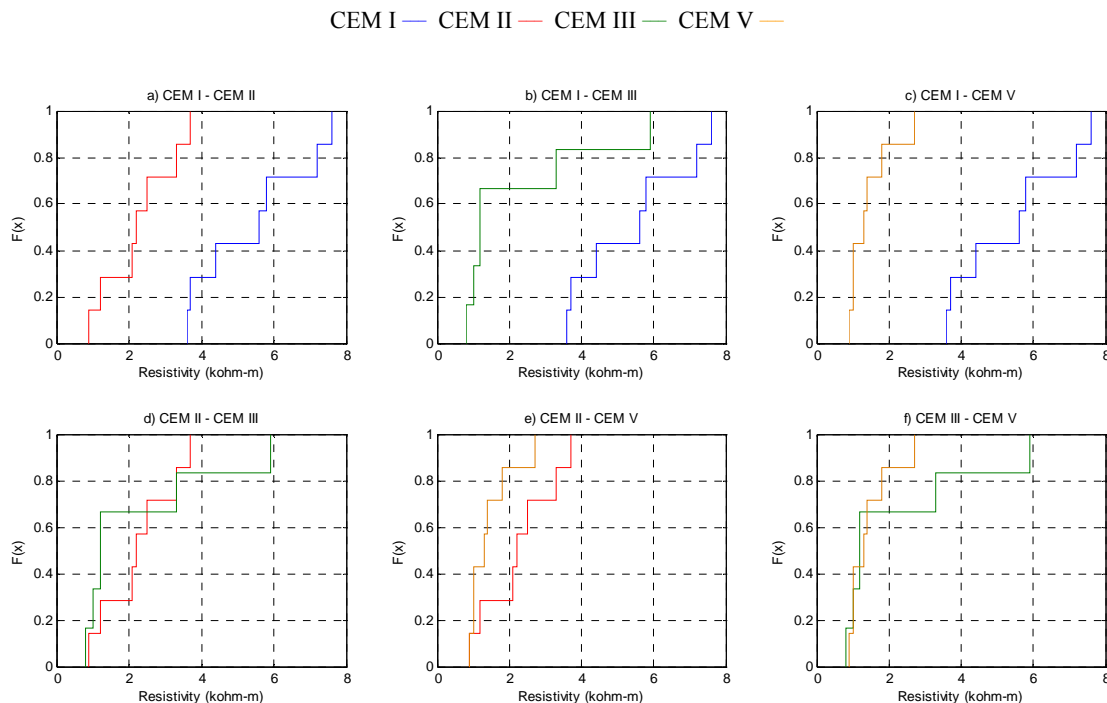


Figure 5.11 ECDF plots of carbonated specimens at 10 mm depth after 11 years.

The results of the Kolmogorov-Smirnov test for concrete resistivity at 50 mm depth are shown in Table 5.24. In this case, it is not possible to reject the null hypothesis in any combination of concrete resistivity values. Values of resistivity at this cover depth are significantly lower than those measured at 10 mm. This behavior may be caused by internal moisture in the specimens after many years of outdoor exposure. Because of carbonation, this moisture cannot be evaporated easily due to a reduction in the transport kinetics in the carbonated layer. It is (also) possible that specimens were not fully carbonated until a depth of 50 mm. This is supported by the observation that resistivity are lower than measured using electrodes at 10 mm depth.

Table 5.24 Kolmogorov-Smirnov test outcome of carbonated specimens at 50 mm depth after 11 years.

	2R50		3R50		5R50	
1R50	H	0	H	0	H	0
	P	0.8827	P	0.4681	P	0.4235
	kst	0.2857	kst	0.4285	kst	0.4285
2R50	-		H	0	H	0
			P	0.155	P	0.1286
			Kst	0.5714	kst	0.5714
3R50	-		-		H	0
					P	0.951
					kst	0.2618

Results of the probabilistic test are shown in Fig. 5.12 for concrete resistivity at 50 mm. Again, resistivity values are lower than those reported at 10 mm. As seen previously, CEM I has values with bigger scatter than the CEM III and CEM V cement types. Nevertheless, in this case CEM II also has resistivity values similar to CEM I. CEM III and CEM V show similar values that are below those measured for CEM I and CEM II.

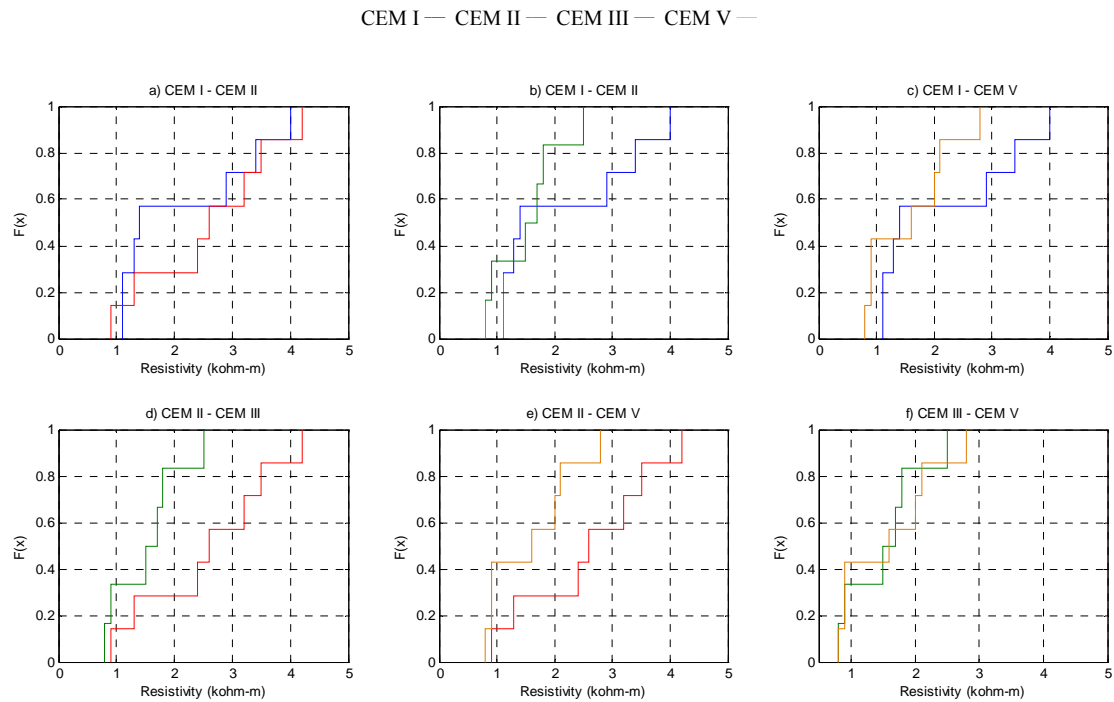


Figure 5.12 ECDF plots of carbonated specimens at 50 mm depth after 11 years.

With the results of the KS test for resistivity at 10 and 50 mm depth it can be concluded that it is not possible to assure that specimens subjected to accelerated carbonation are identified with certainty in this manner. Nevertheless, even when the specimens were perfectly identified, the KS test was not able to distinguish in some group of specimens. This may be caused by the influence of the carbonation depth in through the specimen, which modifies the resistivity and therefore makes it difficult to distinguish them.

Specimens cast with CEM III showed the highest carbonation depth after 2 years when compared to the other specimens with different type of cement. Once that the carbonation depth has surpassed the 50 mm cover depth, values of resistivity make the outcome of the test negative due to the influence of carbonation. CEM II and CEM V reported values of carbonation depth lower than specimens containing CEM III. In this case, Portland cement

The identification of concrete specimens exposed to carbonation after 12 years is not possible with a confidence value of 95%. In this sense, the author suggests a microscopy analysis of such specimens. However, the destructive nature of that investigation is not part of this study.

5.2.5 Mixed-in chloride specimens after 2.5 years.

Six specimens of each cement type and water/binder ratio were cast with added chloride and exposed to different environmental conditions (Polder 2001b). After 2.5 years, concrete resistivity measurements were made in those specimens at depths of 10 and 50 mm (Polder 2000). Table 5.25 shows the values of concrete resistivity after 2.5 years.

Table 5.25 Concrete resistivity of mixed-in chloride specimens after 2.5 years, kΩm.

w/b	CEM I		CEM II		CEM III		CEM V	
	1R10	1R50	2R10	2R50	3R10	3R50	5R10	5R50
0.40	0.1	0.1	0.6	0.6	1.6	1.5	1.3	1.3
	0.1	0.1	0.6	0.6	1.6	1.5	1.3	1.2
	0.2	0.2	0.6	0.5	2.0	1.7	1.4	1.3
	0.2	0.2	0.6	0.5	1.8	1.6	1.5	1.3
	0.3	0.2	0.8	0.8	2.0	1.9	2.2	2.0
	0.3	0.2	0.8	0.8	2.1	2.0	2.1	2.0
0.45	0.1	0.1	0.6	0.6	1.6	1.6	1.1	1.1
	0.1	0.1	0.6	0.6	1.6	1.5	1.2	1.1
	0.2	0.2	0.8	0.5	2.3	2.0	1.2	1.1
	0.5	0.2	0.5	0.5	2.4	2.0	1.2	1.2
	0.2	0.2	0.7	0.6	2.6	2.2	1.7	1.7
	0.2	0.2	0.7	0.7	2.6	2.3	1.8	1.7
0.55	0.1	0.1	0.4	0.4	1.6	1.5	1.1	1.0
	0.1	0.1	0.4	0.4	1.6	1.5	1.0	0.9
	0.2	0.2	0.5	0.4	1.9	1.6	1.0	0.9
	0.2	0.1	0.5	0.4	2.3	1.7	1.0	0.9
	0.3	0.2	0.5	0.5	3.0	2.7	1.4	1.4
	0.3	0.2	0.6	0.5	3.3	2.8	1.3	1.3

The parameters that were studied in these specimens with the NFD test are shown in Table 5.26. Again, the influence of cement type, water-binder ratio and cover depth were on values of concrete resistivity was studied.

Table 5.26 NFD parameters of mixed-in chloride specimens.

Factor A	Type of cement		Factor B	w/c	Factor C	Cover depth		
(τ is Fixed)	A1	CEM I	(β is Fixed)	B1	0.40	(γ is Random)	C1	10 mm
counter = i	A2	CEM II	counter = j	B2	0.45	counter = k	C2	50 mm
	A3	CEM III		B3	0.55	is nested in Factor B	C3	
	A4	CEM V		B4			C4	

The outcome of the NFD test is shown in table 5.27. In this table, it is clear that the most important parameter in terms of influence in resistivity is the cement type. This result is similar to that found in the salt/dry specimens and confirms that in the case of non-carbonated concrete, the cement type is the most important parameter that influences values of concrete resistivity.

Table 5.27 NFD outcome of mixed-in chloride specimens after 2.5 years.

F-value	F crit	P-value	Conclusion
2673.909	3.862548	1.37E-13	Reject Ho: 'There is no influence of Factor A'
3.725945	9.552094	0.153776	Accept Ho: 'There is no influence of Factor B'
1.77869	2.680168	0.154882	Accept Ho: 'There is no influence of Factor C'
11.46415	3.373754	0.000893	Reject Ho: 'There is no influence of AB-interaction'
0.195954	1.958763	0.994233	Accept Ho: 'There is no influence of BC-interaction'

However, there was also found an interaction between Parameter A and B, meaning in an interaction between cement type and water/binder ratio. The significance of this interaction is probably related to the relationship between the binding capacity of cement type and the structure and connectivity of the pore network that has been modified by the accelerating effect of the chlorides in the mixture.

Figure 5.13a shows the distribution of values with respect to their residuals. The line of data collected from the NFD test is strongly deviated from the normalized curve for such values. This behavior is also found in the distribution of values according to their cement type as shown in Figure 5.13b. Even after the logarithmic treatment of the results, the scatter for values of Portland cement concrete is still higher when compared to the other cement types.

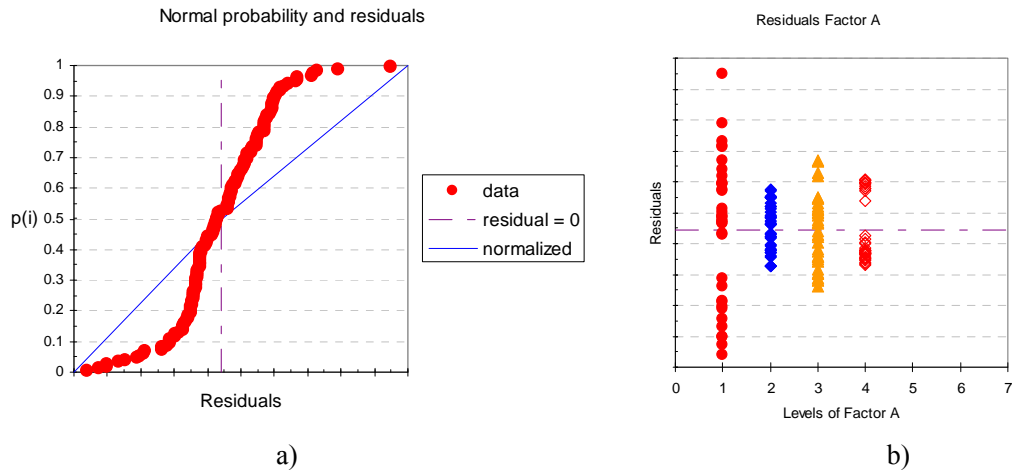


Figure 5.13 NFD outcome of mixed-in chloride specimens after 2.5 years.

The influence of cement type in values of concrete resistivity is shown in Figure 5.14a. This figure shows clearly the influence of cement type in the values of resistivity. Portland cement concrete has the weakest influence in such property, while the specimens containing slag (CEM III and CEM V) have the strongest. This again, suggests that the chloride-binding capacity influences the construction of the pore structure while the setting of fresh concrete. Figure 5.14b shows the impact of water/binder ratio; clearly, the water binder ratio has a weak influence by itself on the values of concrete resistivity. On the other hand, a combination of cement type and water binder ratio may provide a stronger influence of these two parameters as suggested by the NFD test outcome. Finally the influence of cover depth is shown in Figure 5.14c. This parameter has a weak influence on the values of concrete resistivity.

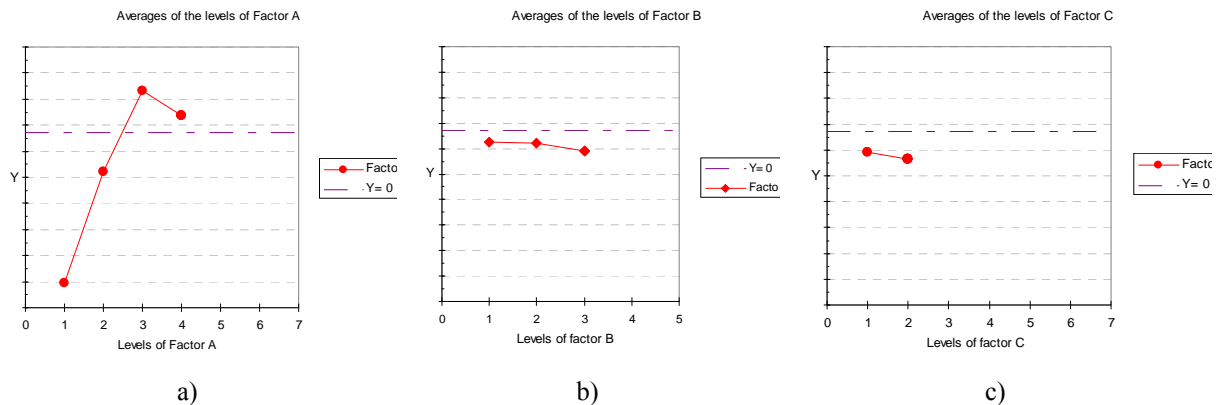


Figure 5.14 Impact level of parameters in concrete resistivity of carbonation specimens after 2.5 years.

In the case of mixed-in chlorides, the cement type is the most influencing parameter on values of concrete resistivity. However, some interaction with water/binder ratio was found.

The results of Kolmogorov-Smirnov test for a depth of 10 mm after 2.5 years are shown in Table 5.28. It clearly shows that each cement type is identified correctly during that time. Therefore, the null hypothesis may be rejected in all cases for a depth of 10 mm. These results are similar to those reported in the penetrating chloride exposure, with only minor differences in the results between CEM III and CEM V.

Table 5.28 Kolmogorov-Smirnov result of mixed-in chloride specimens at 10 mm depth after 2.5 years.

	2R10		3R10		5R10	
1R10	H	1	H	1	H	1
	P	3.81E-8	P	4.43E-9	P	4.43E-4
	kst	0.944	kst	1	kst	1
2R10	-		H	1	H	1
			P	0.43E-9	P	4.43E-9
			kst	1	kst	1
3R10	-		-		H	1
					P	4.24E-4
					kst	1

The ECDF plots for resistivity values at 10 mm depth are shown in Fig. 5.15. In these plots each group of different cement type has its own particular range of values for which the null hypothesis may be rejected. First, CEM I and CEM II measurements reported lower resistivity than CEM III and CEM V. The order of the distribution of concrete resistivity values at this depth is CEM III > CEM V > CEM II > CEM I.

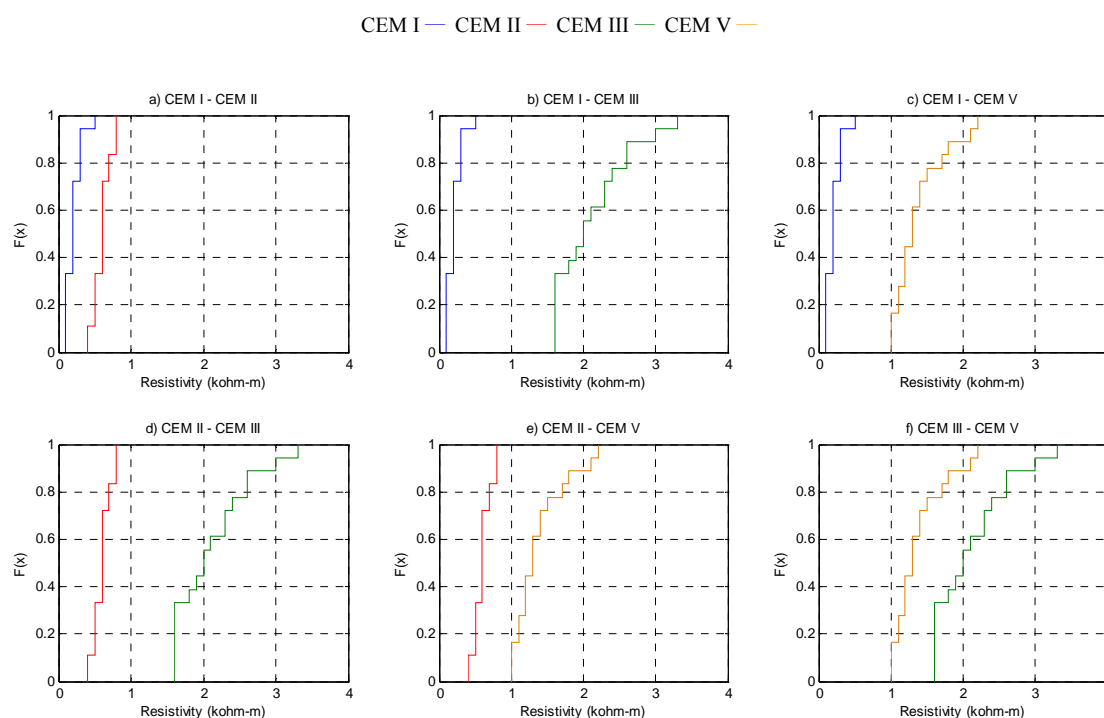


Figure 5.15 ECDF plots of mixed-in chloride specimens at 10 mm depth after 2.5 years.

After applying the probabilistic tool to the values of concrete resistivity at a depth of 50 mm, each group of cement type can be clearly identified with regard to the other types of cement. The results of the Kolmogorov-Smirnov test are shown in Table 5.29.

Table 5.29 Kolmogorov-Smirnov result of mixed-in chloride specimens at 50 mm depth after 2.5 years.

	2R50		3R50		5R50	
1R50	H	1	H	1	H	1
	P	4.43E-9	P	4.43E-9	P	4.43E-9
	kst	1	kst	1	kst	1
2R50	-		H	1	H	1
			P	4.43E-9	P	4.43E-9
			kst	1	kst	1
3R50	-		-		H	1
					P	1.16E-5
					kst	0.7778

The plots of ECDF lines for concrete resistivity after 2.5 years at 50 mm of cover depth are shown in Fig. 5.16. A similar behavior of this analysis and the one for the penetrating chloride specimens is found with regard to the order of maximum resistivity values. Then again, CEM III shows higher values than the rest of the cement types. An important remark about the resistivity in CEM I when mixed-in chlorides are present, is that the values are very low.

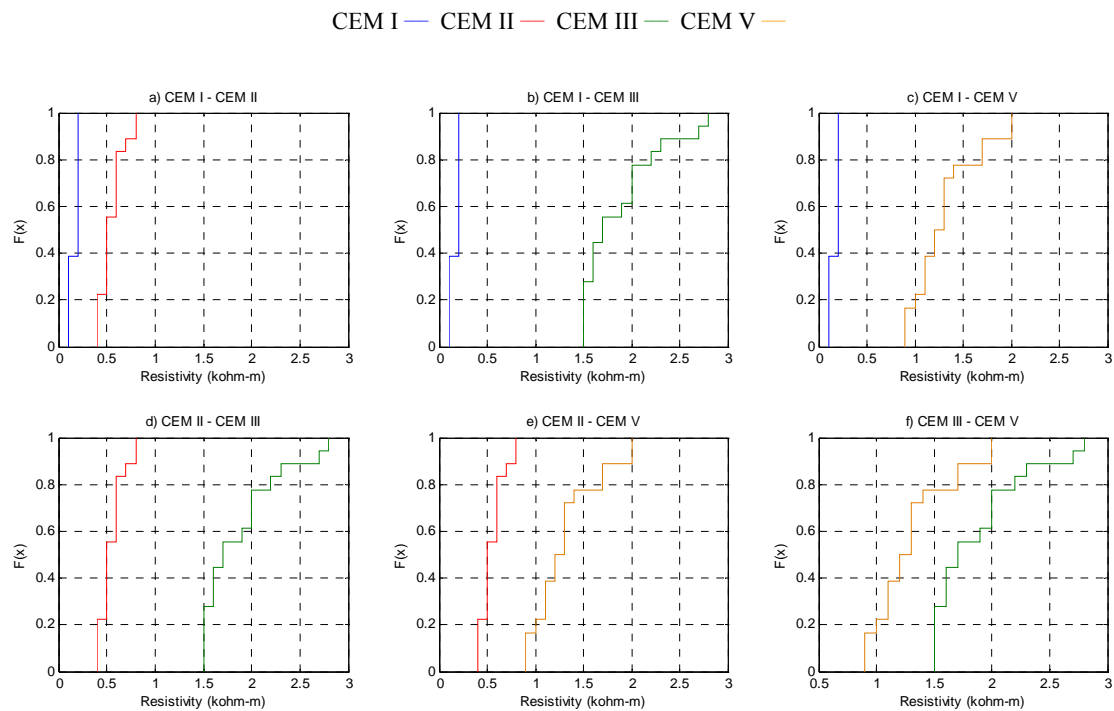


Figure 5.16 ECDF plots of mixed-in chloride specimens at 50 mm depth after 2.5 years.

5.2.6 Mixed-in chloride specimens after 11 years

Specimens with mixed in chlorides were visually identified with a rough surface in the casting face of the specimen. This surface was produced due to the reduced setting time in the specimens caused by the presence of chlorides. The specimens considered for this analysis according to their cement type are given in Table 5.30 to Table 5.33.

Table 5.30 Concrete resistivity of mixed-in chloride specimens with CEM I after 11 years.

Specimen	Cement type	Concrete resistivity (k Ω m)	
		10 mm	50 mm
3-5	I	0.6	0.5
8-12	I	0.6	0.6
5-13	I	0.3	0.3
8-10	I	0.4	0.3
2-6	I	0.3	0.3
6-9	I	0.2	0.2
7-9	I	0.3	0.2
7-8	I	0.8	1.0

Table 5.31 Concrete resistivity of mixed-in chloride specimens with CEM II after 11 years.

Specimen	Cement type	Concrete resistivity (k Ω m)	
		10 mm	50 mm
1-1	II	3.3	3.1
2-8	II	2.7	3.3
6-6	II	1.4	1.6
4-10	II	1.9	2.1
6-2	II	2.3	2.4
6-11	II	1.7	2.3
2-7	II	1.7	1.6
7-7	II	1.7	1.8
6-1	II	2.7	2.7
7-11	II	2.8	3.4

Table 5.32 Concrete resistivity of mixed-in chloride specimens with CEM III after 11 years.

Specimen	Cement type	Concrete resistivity (k Ω m)	
		10 mm	50 mm
2-14	III	5.9	3.7
4-12	III	2.1	2.7
6-5	III	3.7	2.9
8-9	III	2.1	2.5
5-14	III	3.8	4.3
1-5	III	4.1	4.2
8-2	III	2.2	1.9
1-4	III	2.9	3.2
5-6	III	2.8	3.2
6-13	III	1.8	1.9
6-14	III	1.9	1.8
8-3	III	4.7	3.0
4-2	III	3.2	3.9

Table 5.33 Concrete resistivity of mixed-in chloride specimens with CEM V after 11 years.

Specimen	Cement type	Concrete resistivity (k Ω m)	
		10 mm	50 mm
2-9	V	3.2	2.9
1-13	V	2.8	4.2
4-4	V	3.0	3.4
7-6	V	4.3	4.9
6-12	V	3.6	3.7
7-10	V	8.1	4.5
2-15	V	10.2	5.7
3-4	V	5.1	2.7
5-15	V	2.8	3.2
6-3	V	3.6	1.7
7-4	V	2.5	2.7
7-1	V	3.1	2.4
2-1	V	3.2	3.9

The outcome of the KS test of resistivity measured using electrodes at a depth of 10 mm is shown in Table 5.34.

Comparing these results with the outcome of the test after 2.5 years, it is seen that there is some uncertainty with regard to the distinction between CEM II and CEM III and between CEM III and CEM V. This behavior may be attributed to hydration of cement in specimens containing fly ash (CEM II and CEM V) which may have increased their respective resistivity towards the values of CEM III.

Table 5.34 Kolmogorov-Smirnov result of mixed-in chloride specimens at 10 mm depth after 11 years.

	2R10		3R10		5R10	
1R10	H	1	H	1	H	1
	P	6.09E-04	P	2.09E-05	P	2.09E-05
	kst	1	kst	1	kst	1
2R10	-		H	0	H	1
			P	0.166	P	0.0023
			kst	0.43	kst	0.723
3R10	-		-		H	0
					P	0.2241
					kst	0.3846

The outcome of the Kolmogorov-Smirnov test may be verified with the use of the ECDF plots shown in Fig. 5.17. For specimens cast with CEM II and CEM V, the increase in resistivity according to the values reported in (Polder 2000), is about 1.5 times. Nevertheless, specimens with CEM I do not show this behavior and their resistivity remains almost in the same range as eight years before. In the case of CEM III the increase in resistivity is less pronounced than for CEM V.

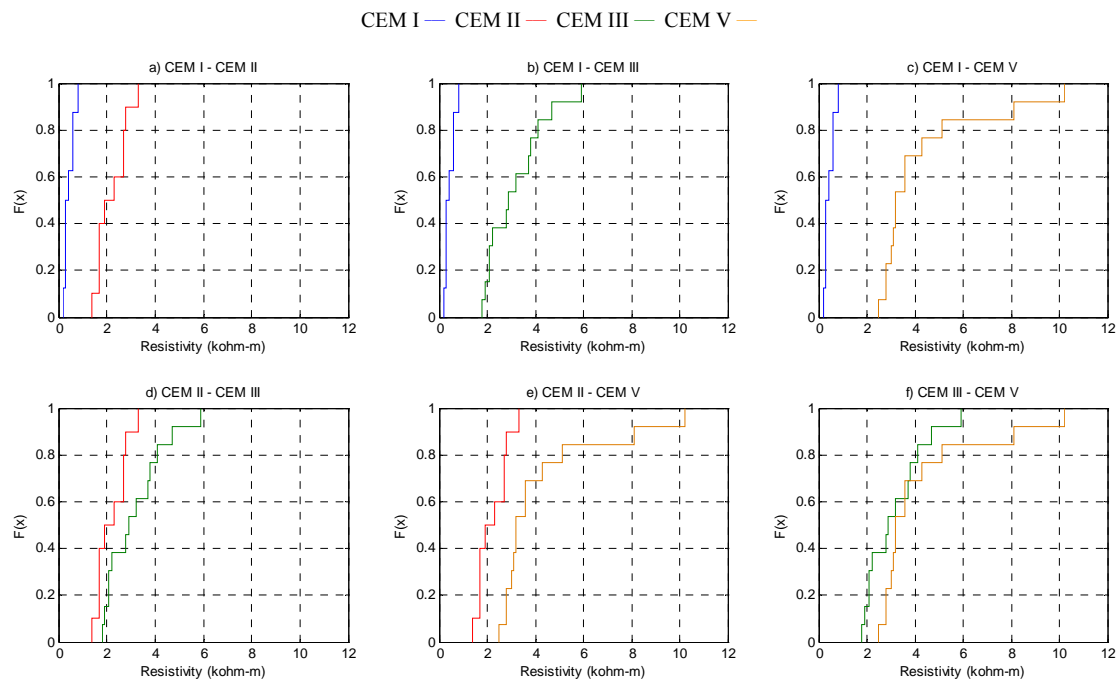


Figure 5.17 ECDF plots of mixed-in chloride specimens at 10 mm depth after 11 years.

The outcome of Kolmogorov-Smirnov test for 50 mm of depth is shown in Table 5.36. The same behavior of uncertainty when comparing CEM II with CEM III and CEM III with CEM V is observed. But in this case, also the rejection of the null hypothesis when comparing CEM II and CEM V is not possible. The values of concrete resistivity at 50 mm depth of CEM II specimens are lower than for a depth of 10 mm. This would imply that, the specimens contain more moisture inside.

Table 5.35 Kolmogorov-Smirnov result of mixed-in chloride specimens at 50 mm depth after 11 years.

	2R50		3R50		5R50	
1R50	H	1	H	1	H	1
	P	6.09E-05	P	2.09E-05	P	2.09E-05
	kst	1	kst	1	kst	1
2R50	-		H	0	H	0
			P	0.3409	P	0.126979
			kst	0.3692	kst	0.4615
3R50	-		-		H	0
					P	0.8281
					kst	0.2307

The plots of ECDF lines for 50 mm cover depth are shown in Fig. 5.18. In these plots, it is clear that the distribution of resistivity values of CEM II does not permit to distinguish them from CEM III and CEM V. It would be expected that CEM II values would be nearer to values of CEM I but this was not the case. Hydration of the fly ash in the matrix may be the cause of this behavior.

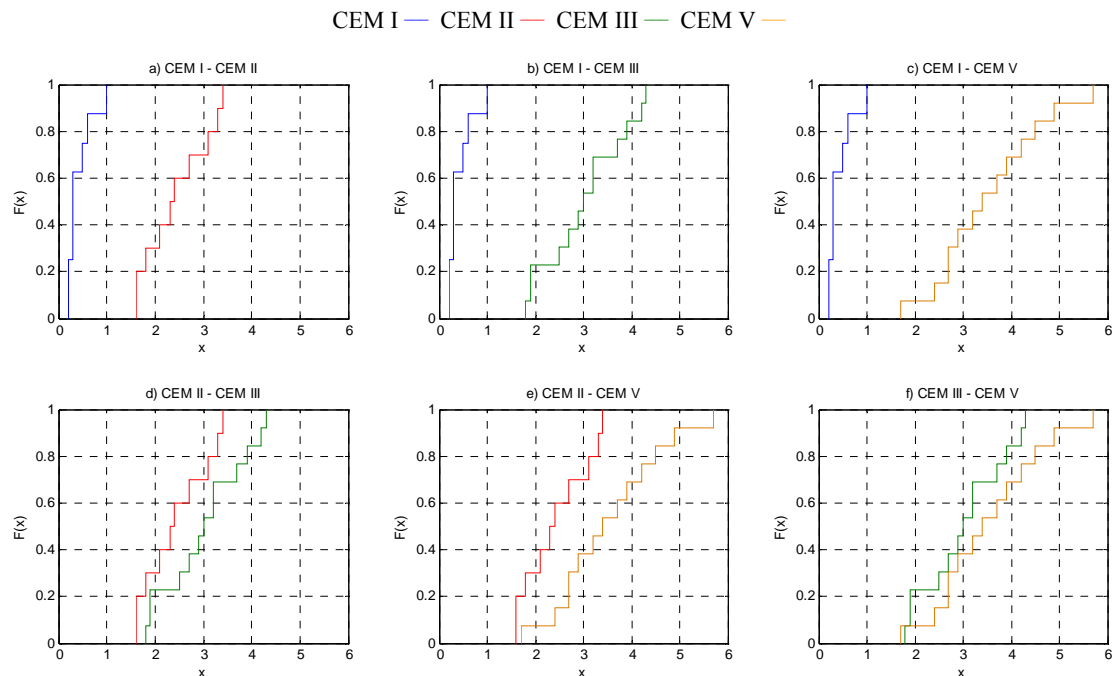


Figure 5.18 ECDF plots of mixed-in chloride specimens at 50 mm depth after 11 years.

The identification of concrete mixtures in mixed-in chloride specimens was successful with both NFD and Kolmogorov-Smirnov with respect to values of concrete resistivity.

Summary of the identification of concrete specimens after 11 years

The use of Kolmogorov-Smirnov test has proven to be successful in concrete specimens exposed to chlorides either from salt/dry cycles or mixed-in. In these conditions, the identification of cement type for these concrete specimens is possible. However, for carbonation specimens is not possible to identify with the same degree of certainty. The next and final step in this part of the study is to identify the most probable water/cement ratio and combine it with visual inspection and the outcome of statistical tests. For this, the use of Schmidt hammer results is important.

5.3 Schmidt hammer test in hardened concrete.

Although the rebound number provides a quick, inexpensive means of checking uniformity of concrete, it has several limitations that must be recognized. The results of the Schmidt hammer are affected by:

- Smoothness of surface under test,
- Size, shape and rigidity of the specimen,
- Age of the specimen,
- Surface and internal moisture condition of the concrete,
- Type of coarse aggregate,
- Type of cement,
- Type of mould,
- Carbonation of the concrete surface.

Of these agents, the most relevant for this project are the age of the specimen, surface and internal moisture condition, type of cement and carbonation of the concrete surface. In theory, the hydration of cement inside concrete structures is still ongoing – at a lower rate – than shortly after casting, even in terms of years (Neville 1995; Kosmatka 2004; Aïtcin 2008). In this sense, after more than 10 years, the hydration of cement (particularly of blended cements) remains active. Surface and internal moisture is a parameter that must be considered as the most important influence for changes in the results of Schmidt hammer. Since all the specimens have been on the roof of TNO Lab since early 2006, it is allowed to assume that all of them have the same exposure conditions. Now that the specimens have been divided in specific groups where their most probable cement type has been identified, Schmidt hammer results will give an idea of the most probable water:binder ratio in terms of rebound number results of each group of specimens. In literature, there is a general correlation between compressive strength of concrete and the rebound hammer number (Kolek 1958; Malhotra 1968), and since the compressive strength is heavily influenced by water:binder ratio (Neville 1995; Kosmatka 2004; Aïtcin 2008), it is possible to give the most probable water:binder ratio.

Results of Schmidt hammer rebound number are given in Appendix 1. The outcome of the test is the average of 10 tests with a deviation of less than 5 as in (Malhotra 1968; NEN-EN 2001). In this terms, the final mark and labeling (and the identification of specimens in this report and afterwards) is given for each specimen according to its group as shown in Table 5.36 for salt/dry specimens, Table 5.37 for carbonation specimens and 5.38 for mixed-in chloride specimens.

Table 5.36 Final labeling of concrete salt/dry specimens.

Water:binder	CEM I		CEM II		CEM III		CEM V	
	Old label	Final label	Old label	Final label	Old label	Final label	Old label	Final label
0.55	7-9	1550-A	4-5	2550-A	2-11	3550-A	3-2	5550-A
	6-8	1550-B	6-11	2550-B	8-8	3550-B	1-8	5550-B
			3-3	2550-C	4-9	3550-C	4-17	5550-C
					4-7	3550-D	2-4	5550-D
					5-6	3550-E	6-3	5550-E
							5-10	5550-F
0.45	3-12	1450-A	3-10	2450-A	1-4	3450-A	3-7	5450-A
	7-8	1450-B	4-3	2450-B	1-6	3450-B	6-10	5450-B
					6-5	3450-C	4-16	5450-C
					4-11	3450-D	5-4	5450-D
					6-15	3450-E	6-7	5450-E
					1-9	3450-F		
0.40	4-13	1440-A	5-9	2400-A	8-3	3400-A	3-15	5400-A
	1-7	1440-B	2-1	2400-B	8-6	3400-B	3-11	5400-B
	4-8	1400-C	4-15	2400-C	5-7	3400-C	5-5	5400-C
					8-5	3400-D	7-10	5400-D
					7-5	3400-E	4-14	5400-E
					4-18	3400-F	2-15	5400-F

Table 5.37 Final labeling of carbonated specimens.

Water:binder	CEM I		CEM II		CEM III		CEM V	
	Old label	Final label	Old label	Final label	Old label	Final label	Old label	Final label
0.55	3-9	1550-A	5-11	2550-A	3-14	3550-A	7-3	5550-A
	2-13	1550-B	3-1	2550-B	2-12	3550-B	3-8	5550-B
					5-12	3550-C	5-2	5550-C
0.45	8-13	1450-A	5-3	2450-A	8-7	3450-D	2-3	5450-D
	1-2	1450-B	5-1	2450-B	8-4	3450-E	4-1	5450-E
	7-12	1450-C						
0.40	8-14	1400-A	3-13	2400-A	1-15	3400-A	8-1	5400-A
	3-6	1400-B	2-10	2400-B			3-4	5400-B
			1-10	2400-C				

Table 5.38 Final labeling of mixed-in chloride specimens.

Water:binder	CEM I		CEM II		CEM III		CEM V	
	Old label	Final label	Old label	Final label	Old label	Final label	Old label	Final label
0.55	6-9	1552-A	6-6	2552-A	6-13	3552-A	7-4	5552-A
	2-6	1552-B	2-7	2552-B	6-14	3552-B	5-15	5552-B
			7-7	2552-C	4-12	3552-C	1-13	5552-C
			4-10	2552-D				
0.45	5-13	1452-A	8-9	2452-A	8-2	3452-A	4-4	5452-A
	8-10	1452-B	6-2	2452-B	4-2	3452-B	7-1	5452-B
			6-1	2452-C	5-14	3452-C		
0.40	3-5	1402-A	2-8	2402-A	1-5	3402-A	2-9	5402-A
	8-12	1402-B	7-11	2402-B	2-14	3402-B	6-12	5402-B
			1-1	2402-C			7-6	5402-C

As a remark, several important remarks must be made: First, the identification of concrete specimens with only non-destructive testing described before is statistically possible in most cases. Nevertheless, the reliability of the identification is only of 95% for salt/dry and mixed in chloride specimens. In carbonation, this is not possible. Second, results of Schmidt hammer did not give any useful outcome when using statistical analysis on them. This was caused by the fact that Schmidt hammer test is influenced by many parameters that cannot be controlled like temperature and moisture changes. Also, the initial exposure conditions (fog, outside and 20C 80%RH) were not possible to be identified on the specimens with non-destructive testing. One possible solution for more precise identification would be microscopy analysis or complete saturation of the specimens and measurements of corrosion potential, concrete resistivity and corrosion rate. However, these two options were not considered due to their permanent alteration to the specimens.

Synopsis

Identification of concrete specimens was carried out in a three level experimental setup of non-destructive testing. This was done with the help of visual inspection, statistical analysis of concrete resistivity and Schmidt hammer testing. Visual inspection of concrete specimens provided an initial point where each specimen had a preliminary label and the most characteristic features of them were matched with their recorded. Reports provided by TNO described 3 different deterioration mechanisms, 4 different types of cement, 3 water-binder ratios and 2 admixed chloride contents. After the visual inspection of the specimens was carried out, groups of concrete specimens were separated into their “apparent” cement type and deterioration mechanism.

Two statistical tests were used; Nested Factorial Design and Kolmogorov-Smirnov Two Sample Test, in order to analyze data collected during the year 2000 and 2009. The NFD test was carried out in results of concrete resistivity recorded in previous reports and found that the cement type was the most influencing parameter for concrete resistivity values exposed to either penetrating or admixed chlorides. In the case of salt/dry exposure, the cement type determined that differences in values of concrete resistivity were attributed to cement type exclusively, while in mixed-in chlorides to an interaction between cement type and water/binder ratio. In the case of carbonation specimens, the statistical test proved that the most influencing factor was the cover depth. This evidence suggests that in this case, measurements of concrete resistivity are not relevant when inspecting concrete structures subject to carbonation. It would be a better choice to apply another non-destructive technique like ultrasonic pulse velocity.

After cement type was identified in concrete specimens, Schmidt hammer testing was carried out in order to find the most probable water/binder ratio according to the rebound number result. This technique was useful in general terms, however, a significant scatter was also found while conducting this research.

The outcome of this research may be interesting for engineers and materials scientists involved in repair and rehabilitation of monuments and old civil infrastructure in which records related to cement type and water-binder ratios are lost. Also, this kind of study may be suitable for quality-control of concrete casting-in site. Standard values of contractors in concrete casting may be provided to the client in order to assure with a 95% of confidence that the provided concrete match the required one.

6 Evaluation of corrosion in concrete specimens.

In this chapter, measurements of electrochemical parameters of concrete specimens that were done during this project will be described. Results of corrosion potential, corrosion rate and concrete resistivity of concrete specimens will be divided into three time-span periods: November 2009, February and April 2010; and also into their exposure conditions: salt/dry cycles, carbonation and mixed-in chlorides. It is important to note that the environmental conditions are significantly different from each testing stage. In November 2009 the measurements of corrosion rate were not done because the instrument needed repair. Therefore, during that month only results of corrosion potential and concrete resistivity are described. In February 2010 corrosion potential, corrosion rate and concrete resistivity measurements were done in all concrete specimens. During that month, the temperature was significantly lower than the previous testing period and important differences between values of corrosion potential and concrete resistivity were found. Also, during that time, the first measurements of corrosion rate were done with the use of the MultiCorr device. Finally, in the month of April 2010 measurements were made again in order to study the effect of the environmental conditions in the results that were obtained during November 2009 and February 2010. Again, temperature and moisture change effects are particularly noticeable in all measurements. The environmental conditions in Delft during each testing time span is shown in Table 6.1 (Koninklijk Nederlands Meteorologisch Instituut 2010).

Table 6.1 Environmental conditions in Delft from November 2009 to April 2010.

Month	Average temperature (°C)	Average relative humidity (%)
November 2009	9	85
February 2010	2	87
April 2010	10	73

6.1 Electrochemical measurements, November 2009

In the first period of electrochemical testing (November 2009), measurements of corrosion potential (E_{corr}) and concrete resistivity (ρ) were made for identification purposes as described in Chapter 5. At this time, the instrument for measuring corrosion rate was not available, because it required maintenance from the manufacture company CorrOcean®. Nevertheless, testing was done for the purpose of identification and to have a reference value for further testing.

6.1.1 Salt/dry cycles

Concrete specimens exposed to salt/drying cycles with chlorides that were identified as according to Chapter 5 will be studied. First, corrosion potential of steel (E_{corr}) is an important parameter for evaluating the condition of the embedded steel bars with regards to the probability of corrosion. However, corrosion potential is only an indicator of the presence of corrosion in the steel, but it must be matched with other techniques or test to assure with certainty the rate at which the steel bars are corroding. There are several factors that affect measurements of corrosion potential. The chemical composition of concrete with regards to the type of cement that was used has an influence in the value of corrosion potential after 11 years. The activated titanium electrodes that were embedded in the specimens may experience changes in the pore solution chemistry after being exposed to carbonation. The availability of oxygen for the cathodic reaction in the surface of the steel bars that is required for the process of corrosion is determined by the density of the cement matrix. This property is related to two different agents; first, the type of cement that was used during the cast of the concrete specimens and the water-binder ratio that was used. Literature has shown that specimens containing blended cements with the same water-binder ratio that specimens fabricated with Portland cement showed more resistance to the corrosion process.

Results of corrosion potential of embedded steel in concrete specimens exposed to salt/drying cycles for six months and then stored in the roof of TNO lab for 8 years are shown in Table 6.2. Only mean values are shown and full results may be consulted in Appendix A. In this table, results show that most of the bars during the month of November 2009 showed potentials that indicate a high probability of corrosion with values more negative than -300 mV vs Ti* (Andrade 1996). Bars in which the potential was more positive than -300 mV vs Ti* are shown in italics. This behavior is contrary to what was inferred from previous reports, in which was stated that bars were under an active corrosion state. Since once that corrosion has been initiated, this suggests that the current rate of corrosion is lower when compared to that found during the year of 2002 (Polder 2000; Polder 2001a).

Table 6.2 Corrosion potential and concrete resistivity of salt/dry specimens, November 2009.

Specimen	Corrosion Potential vs Ti* (mV)				Resistivity, kΩm	
	10 mm		30 mm		10 mm	50 mm
	Mean	STD	Mean	STD		
1550-A	-482	40	-485	40	0.3	0.2
1550-B	-474	75	-407	84	0.8	0.6
1450-A	-328	37	-393	14	0.8	0.4
1450-B	-527	52	-604	61	0.8	1.0
1400-A	-328	60	-295	20	1.5	1.0
1400-B	-296	31	-298	81	1.5	0.9
1400-C	-242	43	-227	24	1.9	1.7
2550-A	-324	26	-419	24	0.9	0.6
2550-B	-505	39	-480	44	1.7	2.3
2550-C	-433	37	-322	64	1.8	1.6
2450-A	-448	51	-222	24	1.9	1.5
2450-B	-384	49	-195	9	2.1	2.6
2400-A	-279	134	-227	35	3.0	4.0
2400-B	-518	51	-506	29	3.2	3.9
2400-C	-480	35	-361	11	3.6	4.9
3550-A	-519	51	-404	87	0.7	0.8
3550-B	-458	17	-376	38	2.0	1.9
3550-C	-473	43	-351	48	2.2	2.1
3550-D	-462	53	-321	36	2.7	2.8
3550-E	-483	36	-426	45	2.8	3.2
3450-A	-421	13	-420	34	2.9	3.2
3450-B	-91	31	-138	10	2.9	2.6
3450-C	-534	25	-461	36	3.7	2.9
3450-D	-237	29	-228	32	3.9	2.4
3450-E	-454	65	-303	89	4.1	2.9
3450-F	-141	68	-282	57	4.4	3.8
3400-A	-193	60	-145	50	4.7	3.0
3400-B	-396	62	-359	37	5.7	4.3
3400-C	-384	76	-225	58	6.5	4.9
3400-D	-140	45	-128	47	7.6	5.1
3400-E	-153	89	-214	109	8.5	5.4
3400-F	-316	50	-243	16	9.6	5.5
5550-A	-471	30	-466	64	1.8	2.1
5550-B	-440	19	-196	62	2.2	3.4
5550-C	-451	125	-380	94	3.2	2.9
5550-D	-401	12	-242	13	3.3	3.7
5550-E	-346	59	-245	24	3.6	1.7
5550-F	-486	19	-221	86	3.7	4.2
5450-A	-316	11	-154	54	3.9	3.6
5450-B	-414	31	-295	88	4.7	3.9
5450-C	-355	64	-256	61	5.1	4.4
5450-D	-373	56	-146	32	5.6	5.8
5450-E	-386	79	-183	50	6.0	4.2
5400-A	-267	8	-348	15	6.2	4.0
5400-B	-307	68	-221	2	6.3	6.4
5400-C	-401	56	-181	66	7.5	6.6
5400-D	-381	9	-374	41	8.1	4.5
5400-E	-166	9	-188	36	8.9	6.4
5400-F	-516	46	-435	25	10.2	5.7

The number of bars that have potential values more positive than -300 mV is small compared to the total amount of bars. This behavior is similar to reported previously (Polder 2001a), showing that even after the loading of chlorides was stopped, the corrosion process continues over time. It can be seen that the amount of active bars in relation to the total amount of bars of each group of concrete mix is higher for CEM I and CEM II than CEM III and CEM V. This behavior is caused by the increase of density in the cement matrix, thus, reducing the size and

amount of pores in the specimens caused by the use of blended cements (Neville 1995; Kosmatka 2004; Aïtcin 2008). The kinetics of corrosion is different for these cements than for Portland cement. Another important feature is the capacity of chloride-binding of blended cements, which is higher than of Portland cement (Thomas 1994; Neville 1995; Guerrerri 2002). However, research has also show that this is not always the case and that corrosion in blended cements might be the same as Portland cement (Byfors 1985; Maslehuddin 1987; Alonso 1988; González 1995; Atiş 2003). The current state of the bars indicates that they are still corroding, but for determining the rate of corrosion, the corrosion potential is not enough.

Results of concrete resistivity in the specimens exposed to salt/dry cycles have been described also in Table 6.2. Concrete specimens that were cast with blended cements CEM II, CEM III and CEM V had higher values of concrete resistivity than specimens with Portland cement as reported previously (Polder 1998; Polder 2000; Guerrerri 2002). This behavior is caused by the reduction of pore size and pore distribution of further hydration of blended cements. The silica contained in supplementary cementitious materials that are used for blended cements (fly ash, slag or silica fume) react with calcium hydroxide Ca(OH)_2 , producing calcium silicate gel C-S-H, so the cement matrix is more dense, stronger and more resistance to penetration of chlorides in general terms. It can be seen in Table 6.1 that specimens cast with CEM III or CEM V have the highest values of concrete resistivity. This is due to the fact that higher percentage of Portland cement is substituted for either slag (CEM III) or a combination of fly ash + slag (CEM V).

6.1.2 Carbonation

Concrete specimens exposed to carbonation reported values of corrosion potential as shown in Table 6.3. In general terms, most of the bars seem to be in an active corrosion state (< -300 mV vs Ti^*), although there are some specimens that remain in an passive state. Values of potential for 10 mm are significantly more negative than values at 30 mm. This behavior is produced by the effect of the carbonation front that has not reached until 30 mm depth. Specimens with CEM I have in general terms values of potential that are more positive than specimens with CEM II and CEM III; and similar to potential values of CEM V..

Table 6.3 Corrosion potential and concrete resistivity of carbonated specimens, November 2009.

Specimen	Corrosion Potential vs Ti^* (mV)				Resistivity ($\text{k}\Omega\text{m}$)	
	10 mm		30 mm		10 mm	50 mm
	Mean	STD	Mean	STD		
1550-A	-163	38	-170	53	3.7	1.3
1550-B	-697	88	-776	85	3.6	4.0
1450-A	-466	79	-441	28	4.4	2.9
1450-B	-294	59	-388	63	5.6	1.1
1450-C	-491	130	-344	89	5.8	3.4
1400-A	-373	16	-285	62	7.2	1.4
1400-B	-566	77	-718	38	7.6	1.1
2550-A	-566	65	-612	21	0.9	0.9
2550-B	-652	40	-639	20	1.2	1.3
2450-A	-426	61	-361	47	2.1	2.6
2450-B	-441	114	-253	50	2.2	3.2
2400-A	-489	38	-485	33	2.5	2.4
2400-B	-542	21	-577	10	3.3	4.2
2400-C	-499	34	-577	58	3.7	3.5
3550-A	-591	60	-684	70	0.8	0.9
3550-B	-609	87	-800	35	1.0	0.8
3550-C	-501	86	-581	23	1.2	1.5
3450-A	-409	66	-457	48	1.2	1.7
3450-B	-317	40	-222	17	3.3	2.5
3400-A	-327	57	-227	46	5.9	1.8
5550-A	-562	30	-555	53	0.9	0.9
5550-B	-474	28	-474	48	1.0	0.8
5550-C	-614	30	-675	44	1.0	0.9
5450-A	-393	90	-343	59	1.3	1.6
5450-B	-485	26	-324	3	1.4	2.0
5400-A	-323	37	-183	65	2.7	2.8
5400-B	-413	18	-249	46	5.1	2.7

The use of supplementary cementing material (fly ash or slag) may increase the rate of concrete carbonation due to the reaction of Ca(OH)_2 and the reduction in pH of the pore solution. Since CEM II, CEM III and CEM V contain fly ash and/or slag as substitution of Portland cement, this phenomenon is accelerated (Maslehuddin 1987; Alonso 1988; Campbell 1991; González 1995). Results of concrete resistivity indicate that specimens with CEM I and CEM II have considerable higher values than CEM III and CEM V, due to the fact that substitution of Portland cement in CEM III and CEM V is higher. Therefore, the pH of the pore solution in CEM III and CEM V specimens is lower than the others. But in the case of mixes 3400 and 5400 the values are around the same than CEM I and CEM II. In this case the effect of higher carbonation rate is balanced with the reduction of the size and volume of the pore network which increases the difficulty for CO_2 to diffuse into the specimens and the carbonation reaction will take place at a much lower rate.

6.1.3 Mixed-in chlorides

Results of corrosion potential for specimens cast with mixed-in chlorides are shown in Table 6.4. Potential values show that almost all bars have potentials more negative than -300 mV vs Ti^* . This indicates that corrosion may be active in the steel bars. Most of the non-active bars are at 30 mm of depth which is related to the fact that oxygen diffusion of oxygen is lower in those mixes (mostly 3402 and 5402). In these specimens, the chlorides have been in contact with the steel since the cast, which might suggest that corrosion has started first in them than in those exposed to salt/dry cycles. In the specimens mixed with chlorides, the binding capacity of the cement has an important role because the amount of 'free' chlorides that will remain after hydration will be the ones available for corrosion (Arya 1989).

Table 6.4 Corrosion potential and concrete resistivity of mixed-in chloride specimens, November 2009.

Specimen	Corrosion Potential vs Ti^* (mV)				Resistivity ($\text{k}\Omega\text{m}$)	
	10 mm		30 mm		10 mm	50 mm
	Mean	STD	Mean	STD		
1552-A	-488	29	-473	42	0.2	0.2
1552-B	-460	32	-475	21	0.3	0.3
1452-A	-467	54	-344	131	0.3	0.3
1452-B	-476	60	-457	35	0.4	0.3
1402-A	-365	23	-285	71	0.6	0.5
1402-B	-338	23	-450	0	0.6	0.6
2552-A	-555	35	-451	101	1.4	1.6
2552-B	-243	15	-301	30	1.7	1.6
2552-C	-402	125	-376	84	1.7	1.8
2552-D	-468	81	-503	17	1.9	2.1
2452-A	-471	51	-397	48	2.1	2.5
2452-B	-528	25	-479	52	2.3	2.4
2452-C	-572	58	-313	35	2.7	2.7
2402-A	-477	56	-488	24	2.7	3.3
2402-B	-513	21	-407	59	2.8	3.4
2402-C	-395	49	-330	0	3.3	3.1
3552-A	-509	42	-494	10	1.8	1.9
3552-B	-540	31	-483	20	1.9	1.8
3552-C	-544	69	-556	91	2.1	2.7
3452-A	-88	61	-206	122	2.2	1.9
3452-B	-514	14	-413	49	3.2	3.9
3452-C	-375	29	-301	78	3.8	4.3
3402-A	-418	80	-363	81	4.1	4.2
3402-B	-180	26	-190	56	5.9	3.7
5552-A	-345	87	-224	25	2.5	2.7
5552-B	-433	19	-369	35	2.8	3.2
5552-C	-411	65	-297	33	2.8	4.2
5452-A	-468	22	-371	57	3.0	3.4
5452-B	-296	155	-194	100	3.1	2.4
5402-A	-475	61	-487	17	3.2	2.9
5402-B	-570	34	-371	95	3.6	3.7
5402-C	-482	25	-434	85	4.3	4.9

Results of concrete resistivity in specimens with mixed chlorides show values that are significantly lower than those exposed to salt/dry cycles. The presence of chlorides since the cast has a crucial effect on this, because the structure of the pore network will not be developed during the same amount of time during setting, but the time of setting will be much shorter because of the ‘accelerating’ effect of the chlorides. Also, the chemical composition of the specimens and pore solution will be mostly different because of the presence of free and bound chlorides (Friedel’s salt) (Arya 1989).

6.2 Electrochemical measurements, February 2010

At the beginning of 2010, the MultiCorr instrument was ready to do measurements which were combined with another round of corrosion potential and concrete resistivity testing. During the month of February 2010, the average temperature in the Netherlands was around 2 degrees according to Table 6.1. Also, the relative humidity of the three testing periods was the highest during that month. These two conditions will induce changes in potential and concrete resistivity values, which will be described as follows.

6.2.1 Salt/dry cycles

Specimens exposed to salt/dry cycles were tested for corrosion potential and concrete resistivity as shown in Table 6.5. Corrosion potential results show that in general terms, almost all potential values have become more negative than those obtained in November 2009. This behavior may be caused by the increase of moisture inside the specimens which will provide differences in oxygen concentration on the surface of the steel that produce zones of anodic and cathodic polarization. In fact, those zones were already there because according to previous reports, most of the bars had become active during the year 2001 (Polder 2001a).

Concrete resistivity of specimens during the month of February showed values that are lower than those reported in November 2009. This behavior is caused by the increase of moisture inside the specimens; therefore the conductivity of the pore network is increased. Changes in moisture and temperature have been identified as important parameters for influencing concrete resistivity (Polder 2001b). However, changes in resistivity are more subtle in mixes with CEM III and CEM V with low water-binder ratio.

Nonetheless, change in potential and resistivity values are not an indicative of how fast the corrosion is taking place. And for that, corrosion rate results are shown in Table 6.6. At first instance, it is clear that corrosion rates are significantly low which contradicts the fact that they have been corroding. When corrosion rates are below 10 $\mu\text{m}/\text{year}$, corrosion is considered low (Andrade 1996; Bertolini 2004; Broomfield 2007). In this case, it seems to be that corrosion rate is reduced during the month of February because of temperature effects and moisture changes. If this is the case, it may be important to remark that the average temperature over the year in the Netherlands is around 10 degrees (Koninklijk Nederlands Meteorologisch Instituut 2010) which will give an overall average temperature for inspection and evaluation of corrosion rate. Another possible cause of low corrosion rate could be bad contact between the instrument and the metallic iron in the bars which is covered by a thick layer of iron oxide. Even though the bars were brushed for removing these oxides, in not all the cases a proper removal was obtained. With these conditions it is possible to infer that these values of corrosion rate are not the ‘real’ corrosion rate that will affect the specimens over the majority of the year.

Table 6.5 Corrosion potential and concrete resistivity of salt/dry specimens, February 2010.

Specimen	Corrosion Potential vs Ti* (mV)				Resistivity kΩm	
	10 mm		30 mm		10 mm	50 mm
	MEAN	STD	MEAN	STD		
1550-A	-532	56	-503	17	0.1	0.2
1550-B	-480	81	-395	69	0.6	0.6
1450-A	-428	110	-420	13	0.7	0.5
1450-B	-518	16	-597	40	0.5	0.5
1400-A	-318	29	-308	63	1.1	0.6
1400-B	-337	12	-342	48	1.5	0.9
1400-C	-293	7	-240	54	1.8	1.8
2550-A	-412	35	-421	67	0.8	0.7
2550-B	-564	64	-508	12	1.8	2.1
2550-C	-484	19	-335	15	1.3	1.5
2450-A	-511	26	-282	24	1.4	1.4
2450-B	-380	61	-235	21	2.0	2.7
2400-A	-345	154	-239	44	2.9	3.8
2400-B	-552	46	-528	64	3.3	4.3
2400-C	-510	12	-368	18	3.6	5.1
3550-A	-567	51	-442	113	0.6	0.6
3550-B	-524	20	-430	51	1.8	1.9
3550-C	-503	28	-383	59	2.0	2.1
3550-D	-472	46	-338	41	2.5	2.8
3550-E	-424	141	-456	40	2.7	3.2
3450-A	-476	11	-460	26	2.7	3.1
3450-B	-198	48	-167	19	2.8	2.7
3450-C	-573	22	-510	29	3.7	2.9
3450-D	-261	35	-402	98	3.9	2.4
3450-E	-551	56	-363	67	4.0	2.8
3450-F	-209	71	-313	99	4.1	3.6
3400-A	-240	45	-191	106	4.6	2.7
3400-B	-420	32	-425	68	5.7	4.5
3400-C	-437	76	-245	43	6.6	5.0
3400-D	-185	67	-127	55	7.4	4.7
3400-E	-201	105	-229	117	8.0	5.4
3400-F	-335	47	-265	13	9.8	5.3
5550-A	-542	23	-537	48	1.2	1.6
5550-B	-507	23	-264	79	2.0	3.3
5550-C	-530	118	-448	100	2.7	3.0
5550-D	-460	40	-342	72	3.1	3.5
5550-E	-358	62	-284	66	3.5	1.8
5550-F	-529	43	-297	107	3.6	4.2
5450-A	-375	21	-193	85	3.9	3.6
5450-B	-441	26	-324	82	4.2	3.4
5450-C	-351	57	-340	155	4.8	4.2
5450-D	-426	39	-214	11	5.4	5.5
5450-E	-453	73	-274	39	5.8	4.3
5400-A	-326	53	-403	8	5.9	3.7
5400-B	-354	41	-234	11	6.1	6.5
5400-C	-443	45	-231	63	7.0	6.1
5400-D	-419	17	-396	19	7.7	4.1
5400-E	-208	12	-223	64	8.5	6.1
5400-F	-521	34	-466	12	9.9	5.7

Table 6.6 Corrosion rate of salt/dry specimens ($\mu\text{m}/\text{year}$), February 2010.

Specimen	10 mm		30 mm	
	Mean	STD	Mean	STD
1550-A	0.1	0.1	0.2	0.1
1550-B	0.6	0.6	0.2	0.1
1450-A	0.6	0.2	0.6	0.3
1450-B	0.5	0.4	0.6	0.2
1400-A	0.3	0.2	0.3	0.1
1400-B	0.2	0.0	0.2	0.1
1400-C	5.2	6.0	0.8	0.4
2550-A	0.2	0.1	0.3	0.0
2550-B	0.3	0.2	0.4	0.0
2550-C	0.3	0.0	0.4	0.0
2450-A	0.3	0.1	1.2	1.4
2450-B	0.1	0.1	0.3	0.0
2400-A	0.3	0.1	0.4	0.0
2400-B	0.4	0.0	0.4	0.0
2400-C	0.4	0.0	0.4	0.0
3550-A	1.7	2.4	0.8	0.8
3550-B	0.4	0.0	0.4	0.0
3550-C	0.4	0.0	0.4	0.0
3550-D	0.7	0.4	0.4	0.3
3550-E	0.4	0.3	0.3	0.1
3450-A	0.4	0.1	0.3	0.1
3450-B	0.4	0.0	0.4	0.0
3450-C	0.3	0.1	0.4	0.1
3450-D	0.1	0.1	0.2	0.1
3450-E	0.2	0.1	0.3	0.0
3450-F	0.5	0.4	0.6	0.2
3400-A	0.3	0.0	0.4	0.0
3400-B	0.4	0.0	0.4	0.0
3400-C	0.6	0.2	0.9	0.3
3400-D	0.3	0.1	0.4	0.1
3400-E	0.3	0.1	0.2	0.2
3400-F	0.3	0.2	0.4	0.0
5550-A	0.4	0.1	0.3	0.0
5550-B	0.3	0.1	0.3	0.1
5550-C	0.3	0.0	0.3	0.0
5550-D	0.3	0.0	0.3	0.0
5550-E	0.3	0.2	0.4	0.1
5550-F	0.5	0.1	0.3	0.1
5450-A	0.3	0.0	0.3	0.0
5450-B	0.3	0.0	0.3	0.0
5450-C	0.4	0.1	0.1	0.1
5450-D	0.2	0.2	1.1	1.0
5450-E	0.3	0.0	0.3	0.1
5400-A	0.2	0.1	0.3	0.0
5400-B	0.2	0.2	0.3	0.0
5400-C	0.2	0.1	0.3	0.0
5400-D	0.3	0.0	0.3	0.0
5400-E	0.4	0.5	0.2	0.0
5400-E	0.3	0.0	0.3	0.0

6.2.2 Carbonation

Results of corrosion potential and concrete resistivity of specimens exposed to carbonation are shown in Table 6.7. Corrosion potential values shown a change towards more negative values than -300 mV vs Ti^* in the

specimens. This shift in potential is caused by changes in moisture which are particularly significant for carbonated specimens. Once that concrete is carbonated, the pore structure and chemical composition of it are permanently changed as well. When moisture penetrates through the altered pore system, conditions of humidity and low pH are very aggressive for iron dissolution.

In the case of concrete resistivity, values of carbonated specimens are quite similar to those obtained during the month of November 2009. These results show that the pore structure has remained unaltered in general terms and that changes in pore solution chemical composition might be responsible of changes in electrochemical potential of the steel.

Table 6.7 Corrosion potential and corrosion rate of carbonated specimens, February 2010.

Corrosion potential vs Ti* (mV)						
Specimen	10 mm		30 mm		Resistivity kΩm	
	Mean	STD	Mean	STD	10	50
1550-A	-217	29	-191	57	3.5	1.3
1550-B	-550	64	-798	87	3.6	3.9
1450-A	-510	52	-490	26	4.3	2.7
1450-B	-319	61	-396	67	5.5	1.1
1450-C	-566	117	-415	155	5.6	3.1
1400-A	-411	38	-368	71	6.8	1.5
1400-B	-622	96	-745	60	7.3	0.9
2550-A	-605	67	-653	27	0.6	0.7
2550-B	-710	13	-677	22	0.9	1.2
2450-A	-485	71	-420	37	2.0	2.2
2450-B	-489	132	-276	28	1.9	2.6
2400-A	-520	52	-519	23	2.3	2.4
2400-B	-598	59	-577	16	3.0	3.9
2400-C	-527	33	-577	46	3.2	3.2
3550-A	-539	221	-709	78	0.6	0.7
3550-B	-635	74	-767	61	0.7	0.8
3550-C	-549	61	-643	31	1.1	1.3
3450-A	-430	79	-402	35	1.1	1.5
3450-B	-332	23	-277	27	2.8	2.4
3400-A	-365	68	-245	36	4.4	1.2
5550-A	-450	132	-249	49	2.1	2.4
5550-B	-483	26	-256	43	4.6	2.1
5550-C	-663	23	-695	31	0.7	0.8
5450-A	-428	67	-365	61	1.2	1.4
5450-B	-530	36	-339	8	1.2	1.6
5400-A	-387	77	-216	72	2.5	2.6
5400-B	-470	29	-280	32	4.8	2.5

Corrosion rate values of carbonated specimens are shown in Table 6.8. As with specimens exposed to salt/dry cycles, low values of corrosion rate were found. This was unexpected since the changes in moisture inside carbonated specimens would have suggested significant increase in corrosion rate. Again, influence of the layer of oxides on the surface of the steel bars might be sufficiently strong to avoid polarization during the polarization resistance test.

Table 6.8 Corrosion rate of carbonated specimens ($\mu\text{m}/\text{year}$), February 2010.

Specimen	10 mm		30 mm	
	Mean	STD	Mean	STD
1550-A	0.3	0.1	0.3	0.1
1550-B	0.4	0.0	0.4	0.0
1450-A	0.2	0.1	0.3	0.1
1450-B	0.4	0.2	0.3	0.1
1450-C	0.6	0.3	0.4	0.0
1400-A	0.5	0.2	0.3	0.0
1400-B	0.4	0.3	0.3	0.1
2550-A	0.3	0.1	0.4	0.0
2550-B	0.4	0.0	0.4	0.0
2450-A	0.3	0.1	1.2	1.4
2450-B	0.4	0.0	0.4	0.0
2400-A	0.2	0.1	0.3	0.0
2400-B	0.6	0.2	0.6	0.3
2400-C	0.1	0.1	0.3	0.0
3550-A	0.3	0.0	0.3	0.0
3550-B	0.3	0.0	0.2	0.1
3550-C	0.3	0.1	0.4	0.1
3450-A	0.4	0.4	0.4	0.2
3450-B	0.8	0.3	0.8	0.3
3400-A	0.3	0.3	0.8	0.8
5550-A	0.3	0.0	0.6	0.5
5550-B	0.3	0.1	0.2	0.1
5550-C	0.4	0.2	0.3	0.1
5450-A	0.3	0.1	0.3	0.1
5450-B	0.5	0.4	0.4	0.1
5400-A	0.4	0.1	0.5	0.1
5400-B	0.2	0.1	0.3	0.0

6.2.3 Mixed-in chlorides

Results of corrosion potential and concrete resistance of specimens mixed with chlorides are shown in Table 6.9. Corrosion potential in these specimens is significantly high in almost all mixes. Since chlorides were present since the cast, the loss of passivity in them had occurred after 2.5 years. By now, the passive film (if it was made) has been lost in the embedded bars. Even mixes with low water-binder ratio have potentials that indicate corrosion activity.

Concrete resistivity values show the lowest results of all. As seen before, resistivity in concrete specimens with chlorides was low because of the accelerated setting of concrete after casting, which produces a porous cement matrix. These results suggest that corrosion in these specimens is completely dependent of the diffusion of oxygen towards the surface of the steel bars.

Table 6.9 Corrosion potential and concrete resistivity of mixed-in chloride specimens, February 2010.

Specimen	Corrosion potential vs Ti* (mV)					
	10 mm		30 mm		Resistivity kΩm	
	Mean	STD	Mean	STD	10	50
1552-A	-506	49	-515	35	0.1	0.1
1552-B	-507	22	-507	42	0.2	0.3
1452-A	-478	55	-379	108	0.2	0.2
1452-B	-514	42	-496	35	0.3	0.3
1402-A	-387	34	-320	49	0.4	0.5
1402-B	-420	45	-503		0.5	0.4
2552-A	-578	32	-508	125	1.3	1.5
2552-B	-265	17	-346	43	1.5	1.6
2552-C	-427	147	-402	81	1.7	1.6
2552-D	-494	77	-520	14	1.7	1.8
2452-A	-512	50	-429	66	1.9	2.4
2452-B	-567	53	-587	56	2.2	2.1
2452-C	-607	53	-342	42	2.5	2.6
2402-A	-533	48	-506	38	2.6	2.9
2402-B	-539	31	-441	54	2.7	3.5
2402-C	-427	99			3.2	3.1
3552-A	-568	7	-540	24	1.5	1.6
3552-B	-525	77	-370	52	3.8	2.5
3552-C	-597	49	-585	100	1.9	2.1
3452-A	-234	103	-258	124	2.1	1.5
3452-B	-577	49	-431	41	3.1	3.1
3452-C	-427	16	-365	35	3.4	4.0
3402-A	-503	72	-406	67	3.9	3.8
3402-B	-237	19	-220	72	5.5	3.4
5552-A	-397	89	-316	25	2.1	2.2
5552-B	-456	24	-438	56	2.4	2.5
5552-C	-460	73	-373	28	2.3	4.0
5452-A	-522	33	-451	39	2.5	2.1
5452-B	-351	135	-285	158	2.7	2.0
5402-A	-514	73	-542	45	3.0	2.6
5402-B	-603	45	-423	73	3.1	3.4
5402-C	-531	38	-495	59	3.8	4.4

Values of corrosion rate are below 1 μm/year, which means it can be considered as negligible. However, reports and values of potential and concrete resistivity indicate the opposite. After finishing the measurements of polarization resistance on these specimens, it was concluded that the effect of the oxide layer was strong enough to interfere with the measurements. Sadly, this conclusion was determined after all the bars were examined.

Table 6.10 Corrosion rate of mixed-in chloride specimens (mm/year), February 2010.

Specimen	10 mm		30 mm	
	Mean	STD	Mean	STD
1552-A	0.2	0.1	0.3	0.0
1552-B	0.3	0.1	0.2	0.1
1452-A	0.3	0.0	0.2	0.2
1452-B	0.0	0.0	0.1	0.1
1402-A	0.2	0.0	0.2	0.2
1402-B	0.3	0.0	0.3	
2552-A	0.2	0.1	0.2	0.0
2552-B	0.5	0.7	0.2	0.2
2552-C	0.5	0.6	0.3	0.1
2552-D	0.2	0.1	0.2	0.1
2452-A	0.1	0.1	0.2	0.1
2452-B	0.3	0.1	0.3	0.1
2452-C	0.5	0.2	0.3	0.1
2402-A	0.2	0.0	0.2	0.0
2402-B	0.2	0.0	0.2	0.1
2402-C	0.2	0.0	0.1	
3552-A	0.3	0.0	0.3	0.1
3552-B	0.2	0.1	0.3	0.0
3552-C	0.7	0.1	0.2	0.1
3452-A	0.7	0.8	0.2	0.1
3452-B	0.3	0.0	0.3	0.0
3452-C	0.3	0.2	0.3	0.1
3402-A	0.4	0.1	0.4	0.2
3402-B	0.2	0.1	0.5	0.2
5552-A	0.2	0.1	0.6	0.7
5552-B	0.2	0.1	0.2	0.0
5552-C	0.2	0.0	0.2	0.0
5452-A	0.2	0.0	0.2	0.0
5452-B	0.2	0.1	0.3	0.2
5402-A	0.1	0.1	0.1	0.1
5402-B	0.2	0.0	0.2	0.0
5402-C	0.2	0.0	0.2	0.0

6.3 Electrochemical measurements, April 2010

The last period of electrochemical testing was done during the month of April 2010. For corrosion rate testing, the bars were subjected to cleaning in order to provide better contact between the MultiCorr instrument and the steel bars. First, mechanical cleaning was made with a steel brush and sandpaper. When these two were not enough, a solution of soap was applied on the surface of the bars and the test was carried out. Even with these measures, some contact problems were still present. Therefore, the last measure was to apply oil on the oxide layer to provide contact between the metallic steel and the instrument. The average temperature in Delft was around 10 C according to Table 6.1. Also, the relative humidity of the three testing periods was the lowest of the project during that month. Again, these two conditions will induce changes in potential and concrete resistivity values. Four specimens were removed from the groups in order to carry out an experiment of repair by means of cathodic protection. These specimens were therefore measured in other conditions and they will be described on the next chapter.

6.3.1 Salt/drying cycles

Results of corrosion potential and concrete resistivity of specimens exposed to salt/dry cycles are shown in Table 6.11. In this table, corrosion potential values have become more negative than those found during February. This behavior is related to the fact of temperature increase and reduction of relative humidity which provides the best conditions for increasing corrosion rate. When specimens are 'drying out', a process that takes a few days, the conditions for corrosion rate increase are found inside the specimens; which will be related to an increase of corrosion rate. Since corrosion potential alone cannot give this information, results of corrosion rate will be required. Concrete resistivity of specimens is also shown in Table 6.11. In general terms, all values of

resistivity have been increased. This is caused by the reduction of relative humidity in the environment and inside the specimens as well. During the process of ‘drying out’, moisture changes inside the specimen would result in higher values of resistivity (Polder 2001b).

Table 6.11 Corrosion potential and concrete resistivity of salt/dry specimens, April 2010.

	Corrosion potential vs Ti* (mV)					
	10 mm		30 mm		Resistivity kΩm	
	MEAN	STD	MEAN	STD	10	50
1550-A	-649	53	-629	127	0.3	0.2
1550-B	-597	165	-651	106	0.7	0.6
1450-A			Cathodic Protection			
1450-B	-612	23	-668	43	0.2	2.0
1400-A	-389	52	-363	56	0.1	0.9
1400-B	-430	70	-441	43	0.1	0.9
1400-C	-399	49	-382	49	0.2	1.7
2550-A	-548	21	-456	50	0.1	0.6
2550-B	-591	48	-600	44	0.6	4.2
2550-C	-554	55	-450	13	0.5	4.1
2450-A	-586	44	-309	31	1.7	1.7
2450-B	-373	31	-377	28	2.6	2.9
2400-A	-444	163	-328	36	3.8	4.1
2400-B	-658	29	-550	58	8.3	6.5
2400-C	-675	158	-403	15	3.8	4.6
3550-A	-577	45	-466	105	10.3	7.4
3550-B	-542	26	-477	42	18.4	8.3
3550-C			Cathodic Protection			
3550-D	-502	41	-369	37	10.0	7.4
3550-E	-413	197	-481	25	7.0	5.9
3450-A	-497	9	-491	21	8.1	5.9
3450-B	-271	74	-308	10	3.4	3.0
3450-C	-609	21	-563	28	6.1	3.5
3450-D	-358	27	-449	86	3.1	1.8
3450-E	-572	55	-407	26	8.0	6.2
3450-F	-291	42	-387	21	4.8	4.2
3400-A	-283	30	-165	354	9.4	6.5
3400-B	-407	42	-455	41	9.8	8.8
3400-C	-431	85	-343	9	8.5	6.1
3400-D	-318	61	-338	51	4.8	3.2
3400-E	-298	54	-274	74	9.5	6.6
3400-F	-384	20	-308	11	9.3	6.2
5550-A	-568	12	-574	38	5.6	4.0
5550-B	-539	42	-364	58	3.0	3.8
5550-C	-552	99	-506	44	4.4	2.9
5550-D	-490	28	-344	36	5.5	5.6
5550-E	-435	55	-328	46	5.6	2.0
5550-F	-551	46	-363	64	4.2	5.0
5450-A	-409	17	-304	14	5.6	5.4
5450-B	-488	12	-380	73	3.9	4.0
5450-C	-172	480	-401	103	4.6	4.5
5450-D	-484	29	-319	8	7.4	5.8
5450-E	-508	59	-333	39	6.3	5.1
5400-A	-363	41	-446	19	6.1	5.0
5400-B	-381	24	-299	10	7.0	6.7
5400-C	-475	33	-284	26	7.5	6.1
5400-D	-438	12	-477	12	16.7	6.1
5400-E	-284	14	-277	29	8.8	7.0
5400-F	-533	34	-473	6	14.1	5.1

Results of corrosion rate are shown in Table 6.12. It is clear that corrosion rate values are much higher than the previous period of testing. Particularly in mixes containing CEM I, the corrosion rate average in each specimen is significantly higher than the rest of the mixes. This was also found during the visual inspection where rust stains were visible in high amounts on the concrete surface of those mixes. Specimens with CEM III and CEM V showed the lowest values for this period. This is caused by the increased density of the cement matrix and the reduction of the diffusion coefficient of chloride in them.

Table 6.12 Corrosion rate of salt/dry concrete specimens ($\mu\text{m}/\text{year}$), April 2010.

	10 mm		30 mm	
	Mean	STD	Mean	STD
1550-A	89.9	59.0	64.7	110.3
1550-B	12.2	8.3	1.8	1.3
1450-A		Cathodic Protection		
1450-B	18.1	21.1	2.6	3.0
1400-A	24.3	16.8	1.4	0.3
1400-B	2.9	1.5	3.1	3.0
1400-C	3.8	2.1	3.6	2.2
2550-A	3.0	1.4	0.9	0.2
2550-B	1.4	0.7	0.9	0.3
2550-C	1.3	0.5	0.7	0.3
2450-A	1.6	1.0	0.9	0.4
2450-B	0.9	0.3	1.9	2.1
2400-A	1.4	0.6	1.1	1.1
2400-B	3.5	4.2	2.2	1.2
2400-C	1.5	0.4	0.5	0.1
3550-A	6.1	4.1	4.7	3.5
3550-B	4.3	5.2	1.2	0.6
3550-C		Cathodic Protection		
3550-D	4.4	5.4	2.9	3.2
3550-E	3.5	4.8	3.3	4.1
3450-A	3.5	2.6	1.2	0.3
3450-B	2.3	1.2	3.0	2.3
3450-C	4.0	1.9	1.8	1.0
3450-D	4.7	3.4	2.6	3.1
3450-E	3.8	1.5	1.8	2.5
3450-F	4.4	1.7	0.4	0.4
3400-A	2.2	0.7	1.0	1.0
3400-B	2.7	2.1	1.5	1.5
3400-C	2.3	0.8	1.2	1.0
3400-D	2.4	0.8	0.7	0.4
3400-E	1.6	1.1	1.5	0.5
3400-F	3.5	1.3	1.2	0.5
5550-A	3.4	2.7	2.1	1.3
5550-B	2.2	0.6	2.9	1.4
5550-C	3.7	1.6	2.2	1.5
5550-D	2.9	2.7	3.7	2.0
5550-E	1.5	1.2	1.5	1.3
5550-F	3.0	1.9	1.4	1.2
5450-A	2.6	0.5	2.9	2.5
5450-B	2.4	1.5	2.5	2.6
5450-C	3.4	0.7	1.8	1.4
5450-D	2.9	0.9	3.6	2.4
5450-E	3.1	2.5	2.1	0.5
5400-A	1.3	1.0	1.7	0.5
5400-B	1.8	1.3	1.6	0.7
5400-C	2.5	1.6	1.4	0.4
5400-D	2.6	0.5	1.3	0.8
5400-E	1.6	1.3	1.3	0.8
5400-F	1.7	2.0	1.8	0.5

6.3.2 Carbonation

Results of corrosion potential and concrete resistivity of carbonated specimens are shown in Table 6.13. Changes in corrosion potential remain subtle when compared to the previous testing time. This behavior is caused by the drying of internal moisture in the specimens. Since the bars have been polarized according to the corrosion activity, these may be considered as the bottom boundary corrosion potential. This means that only an increase in internal moisture would produce more negative potentials.

Concrete resistivity is also shown in Table 6.13. These values show significant increase with regards to the ones found in February. Again, as concrete dries out, concrete resistivity is increased particularly in specimens with CEM III and CEM V with high water-binder ratio. This is because the carbonation front in those specimens has passed 10 and 30 mm of cover depth. Nevertheless, in mixes with low water-binder ratio, the carbonation front has not reached 10 mm and the resistivity is therefore low. Only mixes with CEM II show an opposite behavior. This may be related to the fact of continuous hydration of fly ash that has increased the density of the cement matrix, therefore, reducing the corrosion rate inside them.

Table 6.13 Corrosion potential and concrete resistivity of carbonated specimens, April 2010.

Corrosion Potential vs Ti* (mV)						
	10 mm		30 mm		Resistivity kΩm	
	MEAN	STD	MEAN	STD	10	50
1550-A	-292	14	-302	12	4.6	1.2
1550-B			Cathodic Protection			
1450-A	-520	51	-498	29	20.5	2.8
1450-B	-334	49	-431	63	7.5	1.0
1450-C	-586	88	-382	77	19.2	2.9
1400-A	-442	25	-435	40	7.2	0.9
1400-B	-609	68	-745	61	9.0	7.1
2550-A	-617	61	-674	25	8.0	3.8
2550-B	-713	6	-681	23	9.8	5.4
2450-A	-503	62	-432	33	16.7	5.8
2450-B	-500	112	-268	17	17.7	6.1
2400-A	-525	27	-516	25	20.1	4.1
2400-B	-562	64	-577	13	15.3	4.8
2400-C	-512	26	-577	23	15.7	4.3
3550-A	-568	233	-721	65	13.5	9.7
3550-B	-659	59	-749	27	12.0	7.0
3550-C	-572	58	-673	36	14.2	8.5
3450-A	-471	14	-406	46	12.8	8.1
3450-B	-345	33	-338	77	3.3	2.2
3400-A	-395	47	-312	24	5.3	1.5
5550-A	-487	93	-292	9	1.6	1.4
5550-B	-511	29	-312	25	8.3	4.4
5550-C	-646	5	-686	8	12.2	7.9
5450-A	-445	49	-399	46	13.3	5.7
5450-B	-530	36	-339	8	12.7	5.4
5400-A	-417	60	-316	35	5.3	4.0
5400-B	-487	46	-299	11	2.4	3.6

Table 6.14 shows results of corrosion rate in carbonated specimens. Compared to salt/drying specimens, corrosion rate in carbonated concrete has higher values. Since the carbonation front has reached most of bars at 10 mm, it is clear that this is not the case at 30 mm. Once the bar is surrounded by neutralized pH in the pore solution, the rate of corrosion will be severely increased when moisture is present. Since during the month of February the specimens contained higher internal moisture, the rate of corrosion in the bars has been increased.

Table 6.14 Corrosion rate of carbonated specimens ($\mu\text{m}/\text{year}$), April 2010.

	10 mm		30 mm	
	Mean	STD	Mean	STD
1550-A	2.8	1.6	2.4	0.5
1550-B	Cathodic Protection			
1450-A	1.8	1.6	0.7	0.2
1450-B	2.0	0.6	2.2	1.7
1450-C	2.5	1.4	4.5	3.7
1400-A	3.2	0.5	0.9	0.3
1400-B	1.7	0.7	1.5	0.7
2550-A	3.8	0.9	4.0	3.0
2550-B	2.7	1.6	3.4	1.0
2450-A	3.7	1.5	1.9	1.4
2450-B	4.3	1.4	1.4	1.3
2400-A	3.9	1.4	2.1	1.5
2400-B	3.5	2.2	2.2	1.0
2400-C	2.4	1.7	1.7	1.4
3550-A	5.3	3.0	4.0	1.5
3550-B	4.6	2.4	2.7	1.4
3550-C	4.9	1.5	1.2	0.9
3450-A	3.3	1.1	1.3	0.8
3450-B	2.3	1.2	0.7	0.5
3400-A	2.0	1.3	0.8	0.3
5550-A	2.3	0.8	1.3	0.3
5550-B	2.2	0.3	1.6	0.7
5550-C	2.6	0.8	1.5	1.1
5450-A	1.9	0.4	1.0	0.7
5450-B	2.9	1.3	0.9	1.2
5400-A	2.3	0.9	1.6	1.0
5400-B	3.6	1.4	0.9	0.7

6.3.3 Mixed-in chlorides

Results of corrosion potential and concrete resistivity of specimens exposed to salt/dry cycles are shown in Table 6.15. Results show that potentials are at their most negative values of all concrete specimens. As described before, the presence of chlorides since the cast has an important role in this behavior. Since the bars were found corroding since the year 2001, there is not much difference between the potential at that time and during this project. Once that the bars have started, corroding, the influence of corrosion potential is subtle because the kinetics of corrosion cannot be measured with this experiment.

Concrete resistivity is shown in Table 6.16. An interesting behavior is found on mixes with 0.45 water-binder ratio which had the highest values. Apparently, the influence of chloride as an accelerating admixture is less significant at this water-binder ratio. For mixes with CEM I and CEM II in 0.55, the pore structure is so open and porous that oxygen and moisture can diffuse easily into the specimens. But in 0.40, the chloride accelerating effect prevents concrete from a fully developed cement matrix. Results of concrete resistivity are different for specimens with CEM III and CEM V, which is most probably related to the binding capacity of those cements. It is not clear whether this bound chloride will be free when the pH in the pore solution and in the corrosion pits becomes acidic as reported in literature (Glass 2002).

Table 6.15 Corrosion potential and concrete resistivity of mixed-in chloride specimens, April 2010.

Corrosion Potential vs Ti* (mV)						
	10 mm		30 mm		Resistivity kΩm	
	MEAN	STD	MEAN	STD	10	50
1552-A	-614	41	-586	33	0.2	0.2
1552-B			Cathodic Protection			
1452-A	-545	25	-528	66	0.4	0.3
1452-B	-553	41	-542	39	0.3	0.2
1402-A	-481	19	-449	18	0.4	0.4
1402-B	-414	52	-487		0.4	0.3
2552-A	-608	27	-540	122	1.4	1.3
2552-B	-369	12	-413	33	1.6	1.4
2552-C	-536	83	-482	36	1.8	1.6
2552-D	-559	51	-571	14	1.9	1.8
2452-A	-543	33	-512	13	6.2	4.7
2452-B	-574	32	-589	37	3.1	2.4
2452-C	-598	20	-478	60	2.8	2.6
2402-A	-554	44	-509	43	1.7	1.4
2402-B	-567	12	-466	27	2.0	2.0
2402-C	-492	63	-	-	2.8	2.3
3552-A	-604	17	-660	17	9.9	5.3
3552-B	-590	21	-493	78	8.4	4.9
3552-C	-692	24	-642	60	2.8	2.8
3452-A	-315	28	-327	54	1.9	1.6
3452-B	-508	138	-505	54	5.1	4.7
3452-C	-497	19	-479	32	5.7	5.0
3402-A	-517	71	-424	71	6.2	5.4
3402-B	-321	17	-326	25	5.2	4.7
5552-A	-488	18	-435	28	3.2	2.7
5552-B	-498	28	-480	43	2.5	2.9
5552-C	-494	44	-415	46	5.5	5.2
5452-A	-553	33	-566	13	5.1	4.1
5452-B	-440	100	-367	98	2.9	1.2
5402-A	-548	52	-565	32	5.3	4.2
5402-B	-570	49	-501	26	5.3	4.5
5402-C	-544	41	-545	45	5.8	5.4

Corrosion rate results are shown in Table 6.16, which show high values of corrosion rate among bars with CEM I and CEM II. Since the volume of chlorides that were used for casting concrete was the same, the difference between corrosion rate from CEM I and CEM II when compared to CEM III and CEM V is determined by the difference of chloride binding capacity of each type of cement. In the case of CEM I and CEM II, when the pH inside the corrosion pits is below 11 (Glass 2002), the bound chlorides will be freed and will be available for further iron dissolution or depassivation of more steel surface.

Table 6.16 Corrosion rate of mixed-in chloride specimens ($\mu\text{m}/\text{year}$), April 2010.

	10 mm		30 mm	
	Mean	STD	Mean	STD
1552-A	15.9	5.2	3.2	2.8
1552-B		Cathodic Protection		
1452-A	4.2	2.9	2.6	1.8
1452-B	3.3	2.4	3.7	2.9
1402-A	7.3	3.6	1.6	1.4
1402-B	5.0	0.7	2.5	2.2
2552-A	8.2	3.5	5.2	2.7
2552-B	7.5	4.5	4.1	1.6
2552-C	8.6	9.1	4.0	2.9
2552-D	5.9	3.0	5.5	4.4
2452-A	3.5	2.5	2.7	1.7
2452-B	2.1	2.0	2.1	1.7
2452-C	3.4	3.1	2.2	1.8
2402-A	2.9	1.9	2.6	1.5
2402-B	3.3	1.6	0.6	0.2
2402-C	1.6	1.4	1.0	1.0
3552-A	2.7	2.4	2.3	1.9
3552-B	1.2	0.8	2.5	1.5
3552-C	2.0	1.1	2.0	1.1
3452-A	3.1	0.9	2.1	1.3
3452-B	1.5	1.4	2.2	2.6
3452-C	1.9	0.7	0.7	0.1
3402-A	2.3	1.5	1.8	1.3
3402-B	2.2	0.4	1.4	0.8
5552-A	1.4	0.6	1.2	0.5
5552-B	1.0	0.4	0.9	0.2
5552-C	0.9	0.3	1.6	0.9
5452-A	2.6	1.5	1.0	0.5
5452-B	1.9	1.2	1.3	0.9
5402-A	2.1	0.3	1.3	1.6
5402-B	2.4	1.2	1.0	0.8
5402-C	2.4	0.9	2.4	1.9

6.4 Discussion

6.4.1 General

The results of electrochemical measurements that were carried out during the elaboration of this project, show significant scatter that is representative of measurements done in-site in consulting of civil engineering. Even while this scatter make the task of identifying behaviors more complicated, engineers and materials scientists must interpret such results in order to provide an opinion and possible repair solutions.

6.4.2 Salt/dry specimens

The relationship between concrete resistivity and corrosion potential of specimens exposed to salt/dry cycles during the month of November 2009 is shown in Figure 6.1. In this figure, the distribution of such relationship is distributed over a range of 0 to 12 k Ωm for concrete resistivity and potential between -100 to -600 mV. These values are indicative of high degree of corrosion in these specimens (Alonso 1988; Andrade 1996; Bertolini 2004). Values of concrete resistivity measured at 10 mm have a broader distribution than those for bars at 30 mm. One explanation for this behavior is differences in moisture content at 10 and 30 mm of cover depth. With respect to cement types, CEM I values of resistivity are in general the lowest of the four groups. Also, the potential range between it is broader than the rest because the minimum potentials are around -200 mV vs Ti* and the highest near -600 mV. Values more positive than -300 mV represent a low corrosion probability, as shown in Table 2.8 and Table 2.9. For CEM I the number of bars more positive than -300 mV is 2. The distribution of values for concrete containing CEM II show a more disperse group of results in terms of concrete resistivity. The number of bars more positive than -300 mV is 4 for this type of cement. In the case of slag

cement (CEM III) shows the highest variation of concrete resistivity. In this type of concrete, the increase of density in the hardened pore structure is responsible of such improvement for this property of durability. The number of bars with potentials more positive than -300 mV is 13; which is significantly higher than bars embedded in concrete with CEM I and CEM II. This difference is a clear evidence of the improved behavior of concrete durability. Finally, for CEM V the distribution of concrete resistivity is similar to CEM III. The number of bars with potentials above -300 mV is 13 as well. These results confirm the tendency that was found during the inspection and identification of concrete specimens.

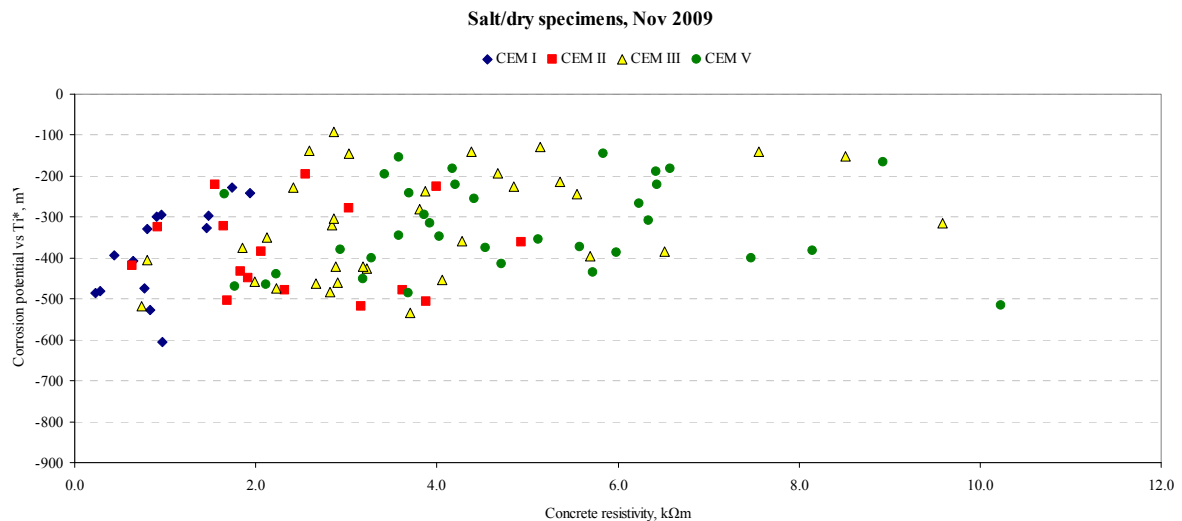


Figure 6.1 Concrete resistivity and corrosion potential of salt/dry specimens, November 2009.

Since during the month of November 2009 the instrument for measurements of corrosion rate was not available, the next period of electrochemical testing for specimens exposed to salt/dry cycles was set at February 2010. As described in Table 6.1, the temperature and relative humidity at this time of the project was different when compared to November 2009. In this sense, changes in measured values of corrosion potential and concrete resistivity are shown in Figure 6.2. After a drop of temperature and an increase in relative humidity, the values of potential for concrete cast with Portland cement show a shift towards more negative values than in November 2009. The number of bars more positive than -300 mV remains at 2, but the bars more negative than -300 mV decreased their potential in a considerable amount. In terms of concrete resistivity, results show a slight reduction in such values because the increase in relative humidity. These conditions favor higher moisture content inside these concrete specimens, thus reducing the resistivity of concrete. In the case of CEM II, the distribution of values of concrete resistivity is also modified by the influence of moisture ingress into the specimens. The number of bars with potentials above -300 mV is still 3 for this type of cement. For CEM III the number of bars without high probability of corrosion has decreased to a value of 12. For cement type CEM V, the distribution of concrete resistivity values is shifted slightly towards lesser values. Also, the number of bars with potential values above -300 mV is reduced to 10. These results show that concrete with lower values of concrete resistivity are more susceptible to moisture changes due to environmental action. These differences should be considered when analyzing the results of corrosion potential and concrete resistivity by the materials scientist, with respect to the conditions at which the measurements were carried out.

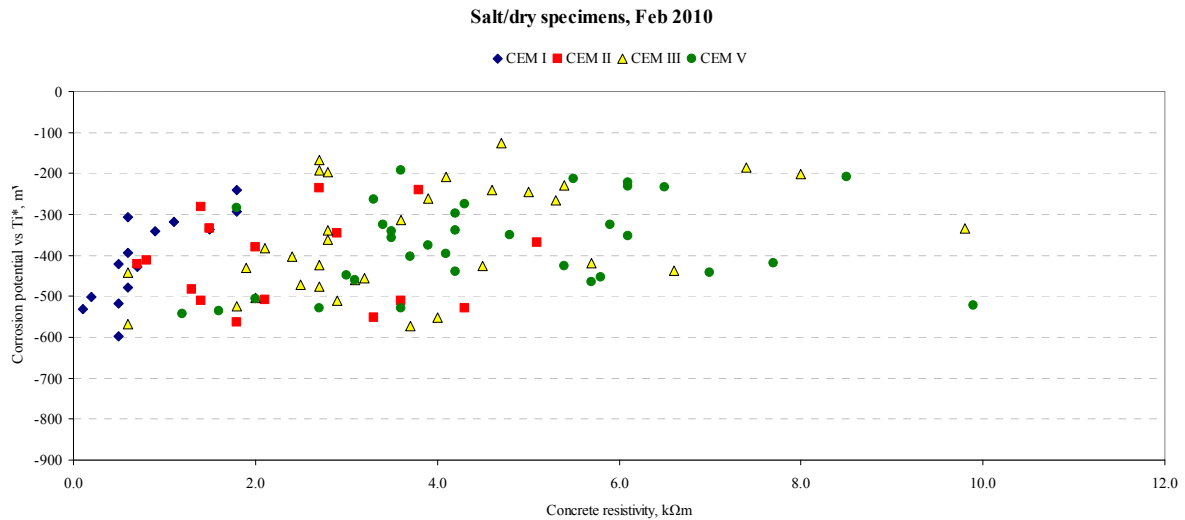


Figure 6.2 Concrete resistivity and corrosion potential of salt/dry specimens, February 2010.

In the month of April 2010, the temperature raised to values near the annual average temperature of the Netherlands and the relative humidity was significantly lower than in the previous measurements. These changes represent a significant difference in terms of the internal conditions of the specimens with regard to ionic transport and availability of oxygen. During the past few months, the specimens were probably near saturation due to rain and snow, which interferes with the oxygen availability at the surface of the steel bars. Therefore, the rate of corrosion (see below) is lower than in drier and higher temperatures.

As shown in Figure 6.3, the behavior of corrosion potential and concrete resistivity is affected by these environmental changes over two months. This figure shows that almost all bars embedded in concrete specimens exposed to salt/dry cycles have become more negative than the potential of -300 mV; therefore an active corrosion rate of steel bars is considered (Alonso 1988; Andrade 1996; Bertolini 2004; Broomfield 2007; ASTM C876-09 2009). Since the year 2000, most of the bars reported potentials more negative than -300 mV and corrosion rates above 10 $\mu\text{m}/\text{year}$. These findings suggest that in cold environment the thermodynamical conditions for corrosion of steel in concrete are affected by such changes.

For specimens cast with CEM I, some bars have reached values of corrosion potential near -650 mV. This shift is produced by the increase of oxygen availability at the surface of the steel bar. However, the most significant change in results obtained in April is found in concrete resistivity. The increase in resistivity is related to a decrease in the moisture content in the specimen, reducing the conductivity through the pore structure. Another possible cause is carbonation of concrete but this hypothesis can only be confirmed with the use of destructive analysis. This will be done in the following chapter. For specimens containing CEM II the decrease of potential values is also observed. On the other hand, concrete resistivity values are also increased. This behavior is also found in specimens with CEM III and CEM V. However, Figure 6.3 shows that the number of bars with potentials more positive than -300 mV in specimens with CEM III and CEM V has decreased to 5 and 3, respectively.

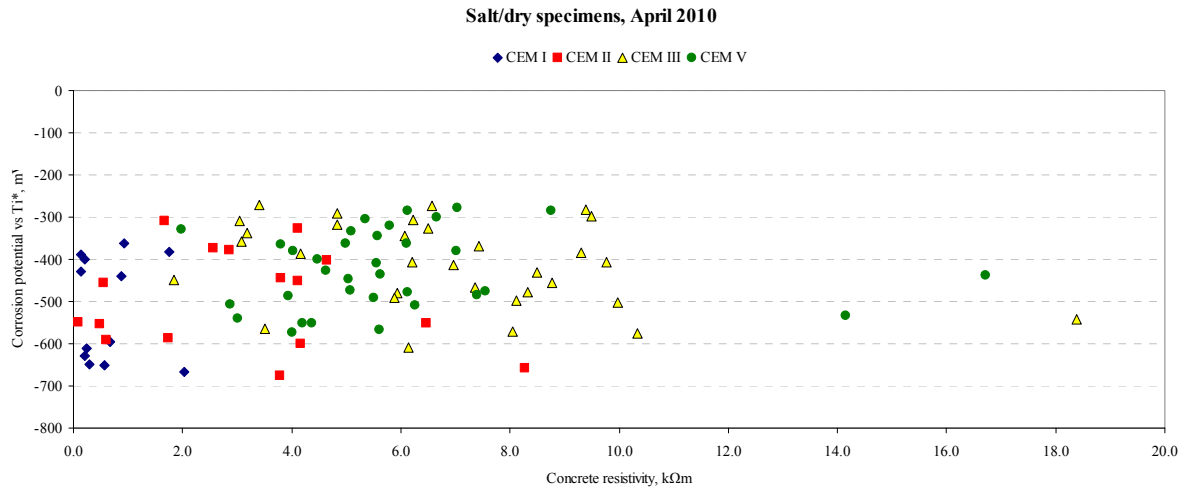


Figure 6.3 Concrete resistivity and corrosion potential of salt/dry specimens, April 2010.

When the MultiCorr instrument was available, measurements of corrosion rate of steel bars embedded in specimens exposed to salt/dry cycles were carried out. Figure 6.4 shows the relation between corrosion rate and the inverse of concrete resistivity. At first instance, it is clear that values of corrosion rate obtained during the month of February are quite low. Independent of cement type, almost all bars have values of corrosion rate below $1 \mu\text{m}/\text{year}$. Most of the bars reported values between 0.2 and $0.6 \mu\text{m}/\text{year}$. Beyond this upper limit, bars with higher corrosion rates were found mostly in specimens cast with CEM I or CEM II.

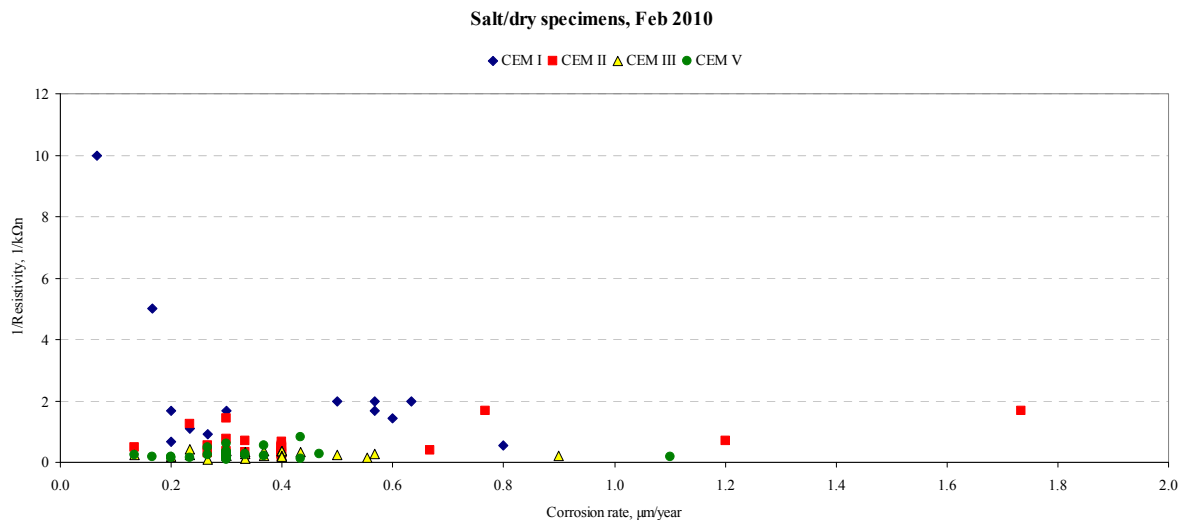


Figure 6.4 Corrosion rate and concrete resistivity of salt/dry specimens, February 2010.

Finally, in the month of April 2010 measurements of corrosion rate were carried out in specimens exposed to salt/dry cycles. Figure 6.5 show the results of such period. At first instance, it is clear that the measured values of corrosion rate are much higher than in February. In the case of CEM I, the difference is most significant and the increase is of an order of magnitude. Specimens containing CEM II also show a high increase in corrosion rate values during this period. In the case of CEM III and CEM V, the difference is not as considerable as with the other two cement types. As discussed before, changes in temperature and moisture content inside the specimens are responsible of these differences. As a remark, it is important to consider this aspect when doing an evaluation of the current state of corrosion of steel in concrete.

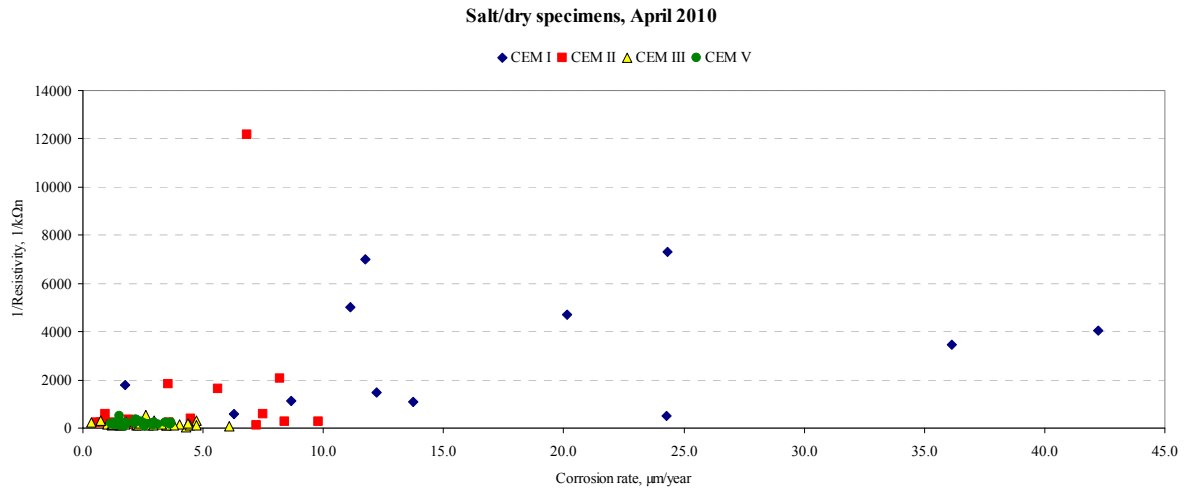


Figure 6.5 Corrosion rate and concrete resistivity of salt/dry specimens, April 2010.

The evidence found during the measurement of corrosion rate and concrete resistivity, shows that resistivity is the controlling factor for corrosion propagation of steel in concrete, as reported in literature (Alonso 1988; Andrade 1996; Polder 1998; Polder 2001b)

6.4.3 Carbonation specimens

Measurements of corrosion potential and concrete resistivity of carbonation specimens were carried out during the month of November 2009. Figure 6.6 show the measured values of such testing. The relationship between concrete resistivity and corrosion potential of specimens show a broad range of corrosion potentials. The most negative potentials have values around -800 mV. In the case of concrete specimens cast with CEM I, results of potential and resistivity are dispersed in the entire chart. In the case of CEM II, values fluctuate between -300 and -600 mV. For CEM III and CEM V, values of concrete resistivity are distributed over lower values than the rest of the concrete mixtures. The differences in values of both resistivity and potential show that results are probably influenced by carbonation some concrete mixes.

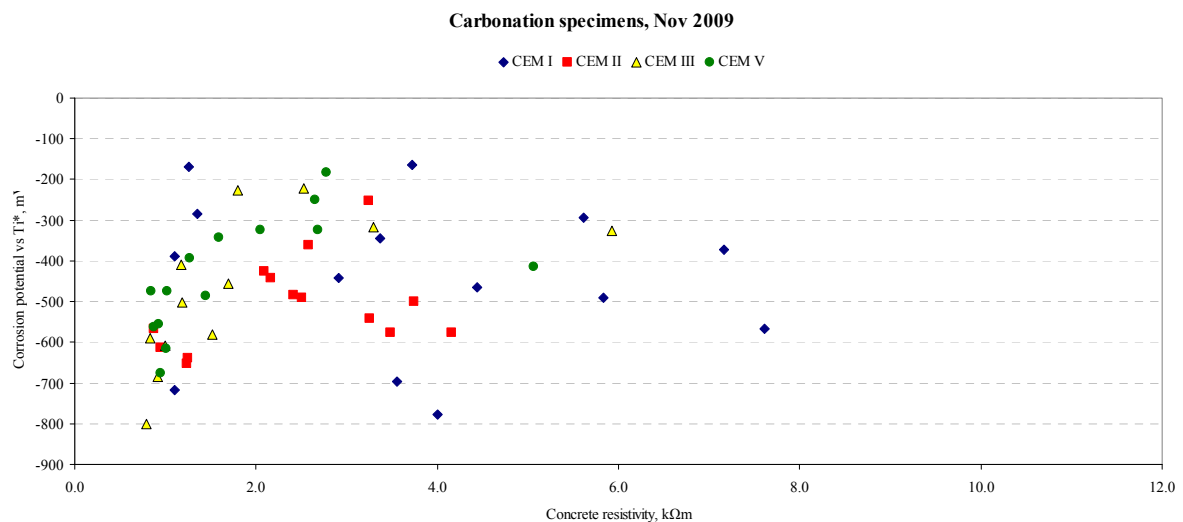


Figure 6.6 Concrete resistivity and corrosion potential of carbonation specimens, November 2009.

Figure 6.7 shows the relationship between values of concrete resistivity and corrosion potential during the month of February 2010. When comparing this figure with Figure 6.6, it is seen that the differences in concrete resistivity between these two periods of testing is not as significant as with specimens exposed to salt/dry. The

influence of temperature and moisture conditions is not as important as in salt/dry specimens. This evidence suggests that carbonation depth has reached the bars and the favorable conditions for corrosion are dependant of the drop in pH in the pore solution and changes in the microstructure of hardened concrete.

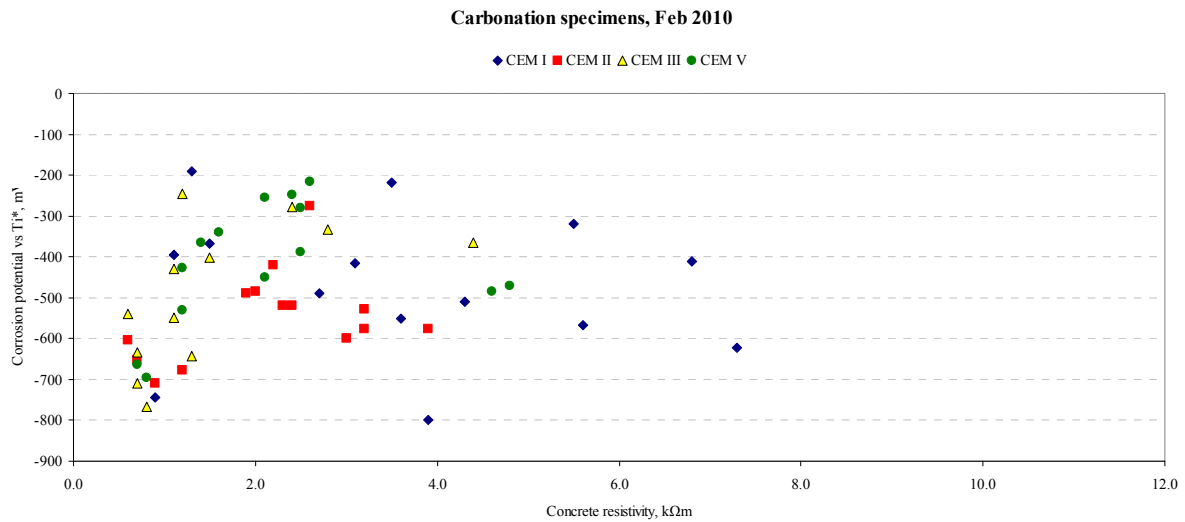


Figure 6.7 Concrete resistivity and corrosion potential of carbonation specimens, February 2010.

Results of concrete resistivity and corrosion potential during the month of April 2010 are shown in Figure 6.8. In this period, the influence of environmental conditions implies significant changes in the specimens in terms of both resistivity and potential. For CEM I, increased results of concrete resistivity are found, while values of corrosion potential remain in the same range. The increase in resistivity is about one and a half times in the highest case. This is most probably related to changes in the pore structure due to moisture increase during the winter and drying out during spring. For CEM II, the same behavior of increased resistivity is found. Like with CEM I, potential values remain almost constant in each bar, however, values of concrete resistivity show significant increases. On the other hand, for specimens cast with CEM III, changes in both resistivity and potential are observed. The reason behind this behavior is the change in the chemistry of the pore solution of this concrete due to carbonation of each specimen through its complete depth. For concrete cast with CEM V, the specimens show a behavior that is in between those found for CEM III (changes in both resistivity and potential) and CEM I and CEM II (changes mostly in resistivity). This evidence suggests that fly ash, as in contrary with slag, does not contribute to significant reduction of pH in the pore solution during hydration and therefore, carbonation is not as severe as with slag cement. This confirms the findings of Table 3.3 at 2.5 years, while after 12 years a carbonation depth measurement would assure if this behavior has prevailed after this period. Unfortunately, this measurement was not considered for this project.

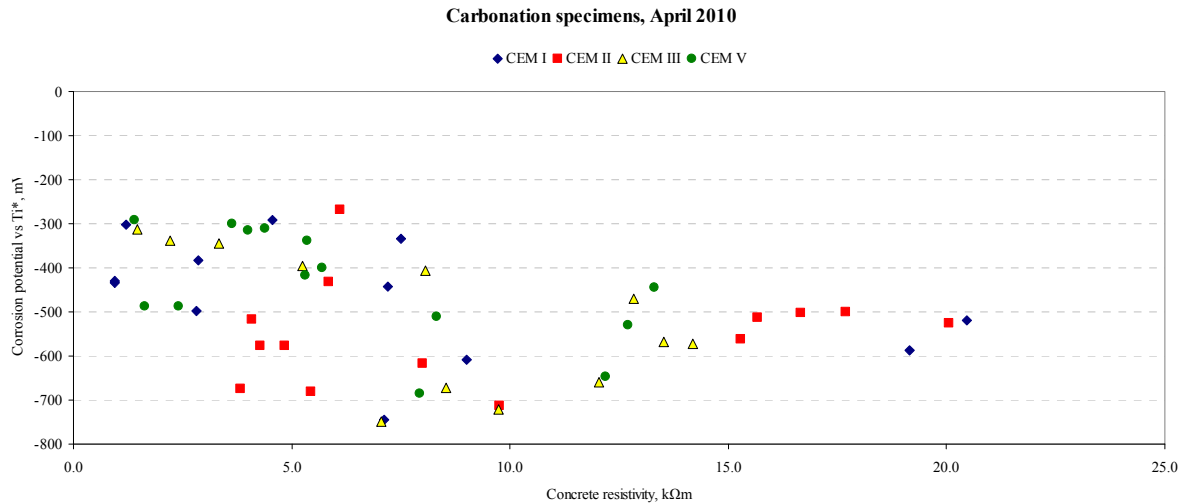


Figure 6.8 Concrete resistivity and corrosion potential of carbonation specimens, April 2010.

Figure 6.9 shows the relationship between corrosion rate and concrete resistivity during the month of February 2010. As with specimens exposed to salt/dry cycles, measurements of corrosion rate in carbonation specimens reported values of corrosion rate between 0.2 and 0.8 $\mu\text{m}/\text{year}$ for almost all bars. Environmental conditions of high relative humidity and low temperature seem to be unfavorable for corrosion propagation in both cases, as reported in literature (Haque 1992; Khunthongkeaw 2006). During this month, measurements of corrosion rate and concrete resistivity for all concrete mixtures are similar, independent of cement type or water binder ratio (as then proved by the identification of concrete).

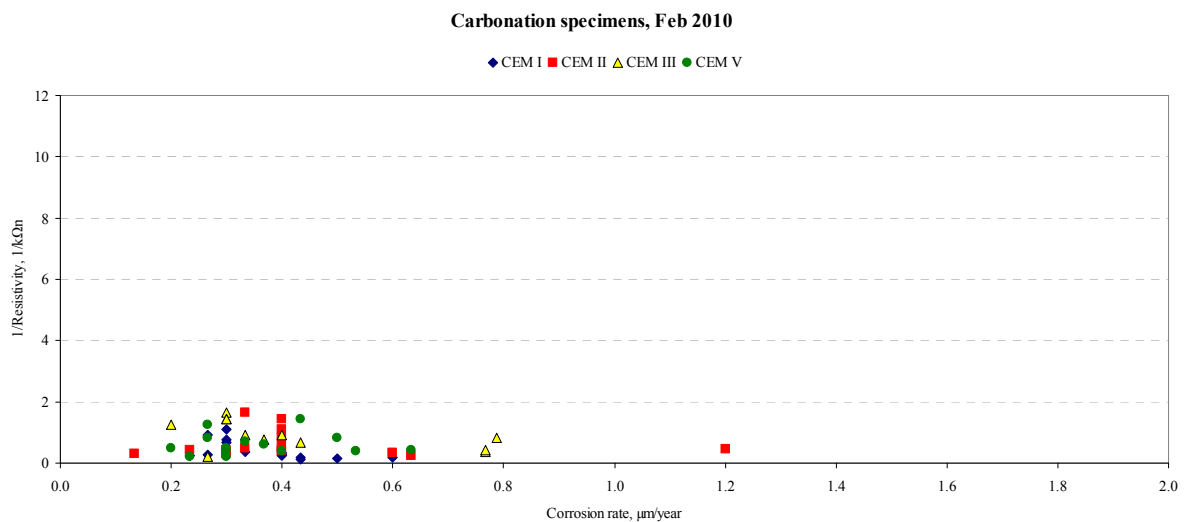


Figure 6.9 Corrosion rate and concrete resistivity of carbonation specimens, February 2010.

During April 2010 a second period of testing was done for specimens exposed to accelerated carbonation and results are presented in Figure 6.10. In this second period, values of both resistivity and corrosion rate show considerable differences when compared to those obtained during February. In an overall view, all corrosion rate values have increased in around one order of magnitude. For CEM I, the values of concrete resistivity have increased considerably as with CEM III. This behavior shows that carbonated concrete containing slag cement is sensitive to significant variations of concrete resistivity due to changes in moisture content in concrete. For the rest of the specimens, the increase in resistivity is attributed to this drying process. However, there is not a clear way to affirm if this drying process is at its end. Additional measurements during summer (July-August) would clarify this hypothesis, but they are not part of this report.

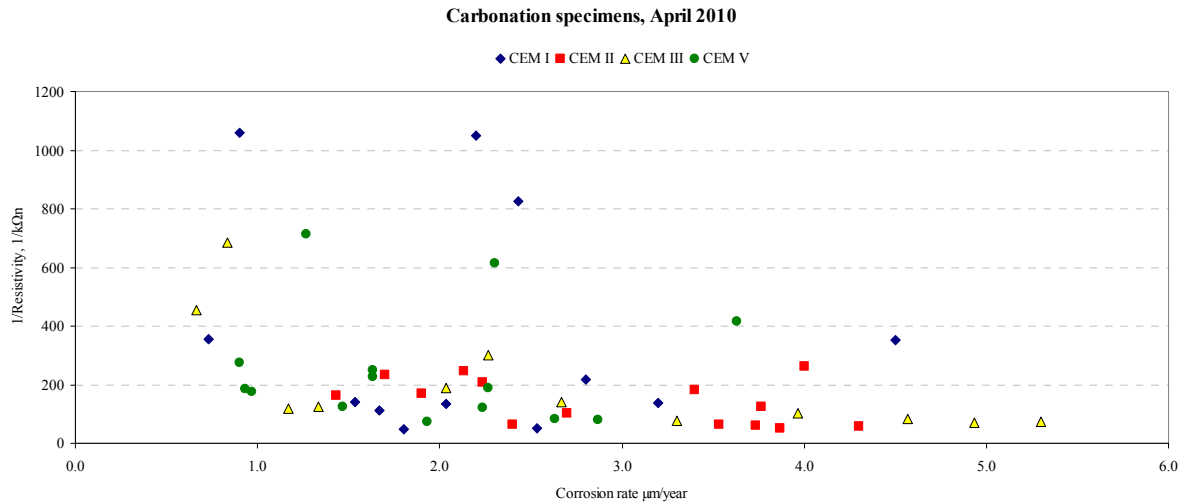


Figure 6.10 Corrosion rate and concrete resistivity of carbonation specimens, April 2010.

6.4.4 Mixed-in chloride specimens

Results of concrete resistivity and corrosion potential in mixed-in chlorides specimens are shown in Figure 6.11. These results were obtained during the month of November 2009. This figure shows a significant difference between concrete cast with Portland cement (CEM I) and blended cements (CEM II, CEM III and CEM V). Values of concrete resistivity of specimens with CEM I are on the lowest range of values with a clear difference that separates them from the rest of the specimens. Specimens with higher values of resistivity correspond to those cast with CEM III and CEM V, with specimens with CEM II in a lower degree of values. This behavior suggests that the pore structure of specimens containing CEM I is considerably different than the rest of the specimens. The accelerating effect of CaCl_2 influences the hardening process during hydration in concrete with Portland cement to an extent where the pore structure is much coarser than the rest of them. Previous information regarding the properties of these mixtures in both fresh and hardened state sustains this belief. Another reason is attributed to the chloride-binding capacity of cements with additional cementing materials (fly ash, slag) in which the increase in CSH gel constitutes an increase in the chloride-binding capacity (Tang 1993).

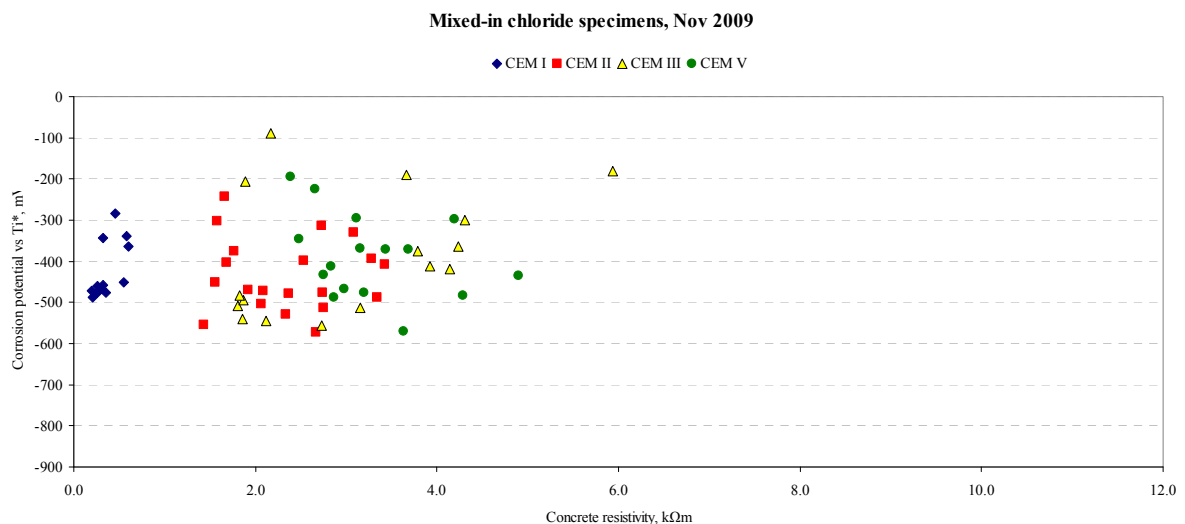


Figure 6.11 Concrete resistivity and corrosion potential of mixed-in chloride specimens, November 2009.

Figure 6.12 shows the results of concrete resistivity and corrosion potential of mixed-in chloride specimens during the month of February 2010. As the figure shows, there are not any significant changes with respect to the previous figure. This behavior suggests that mixed-in chloride specimens were most probably already

saturated since the month of November 2009. Because of their porous structure, moisture inside them was almost near full amount and the increase in relative humidity during the winter has not produced any changes in this property and therefore, concrete resistivity remains almost the same. The potential values fluctuate between -300 to -600 mV for most of the specimens. There are still some values more positive than -300 mV and they were found in specimens containing blended cements at 30 mm of cover depth. In those bars, the surrounding environment is completely soaked and therefore, the availability of oxygen is reduced.

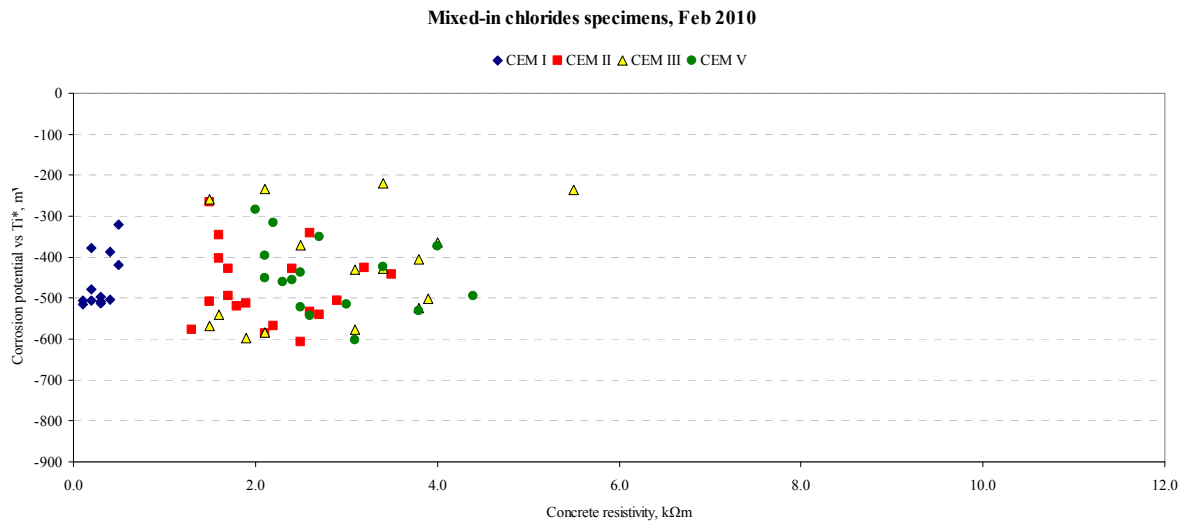


Figure 6.12 Concrete resistivity and corrosion potential of mixed-in chloride specimens, February 2010.

Figure 6.13 shows the relationship between values of corrosion potential and concrete resistivity during the month of April 2010. In this figure, significant changes of concrete resistivity are observed in specimens cast with CEM III and CEM V and in a lesser degree for CEM II. Specimens with CEM I remain in the lowest values of concrete resistivity even when concrete is drying out. The increase in concrete resistivity of specimens with CEM III and CEM V is attributed to the reduced moisture content in the specimens during this period of testing. Apparently, the accelerating effect of chloride admixture does not influence in the same degree the development of the pore structure. In this sense, transport of moisture is the most influent parameter for concrete resistivity measurements. On the other hand, for specimens with CEM I the admixture effect has influenced the coarseness of the pore structure in such a way that even when the concrete is drying out the resistivity remains low. This evidence suggests that the total pore volume and the connectivity of such pores is significantly higher for specimens with CEM I.

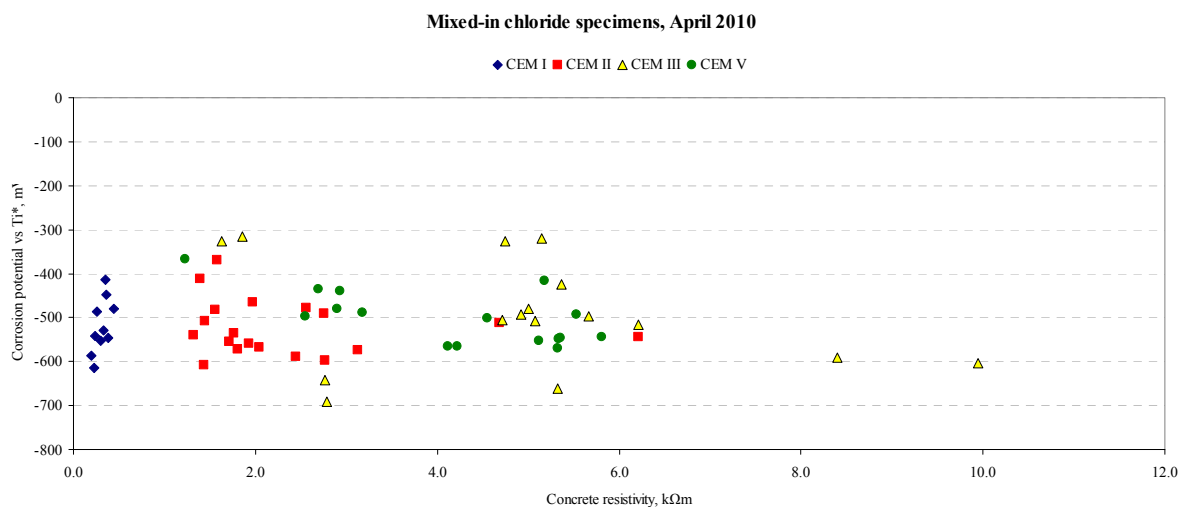


Figure 6.13 Concrete resistivity and corrosion potential of mixed-in chloride specimens, April 2010.

Results of corrosion rate and concrete resistivity during the month of February are shown in Figure 6.14. In this figure, the values of corrosion rate remain low as with salt/dry and carbonation specimens. The range of corrosion rate values fluctuates between 0.1 and 1.0 $\mu\text{m}/\text{year}$. For specimens with CEM I, values of concrete resistivity are lower than the rest of the specimens but the corrosion rate remains in the same range. This suggests that concrete resistivity is not a controlling factor in the propagation phase in mixed-in chloride specimens. This behavior is contradictory to the one found for salt/dry loading specimens.

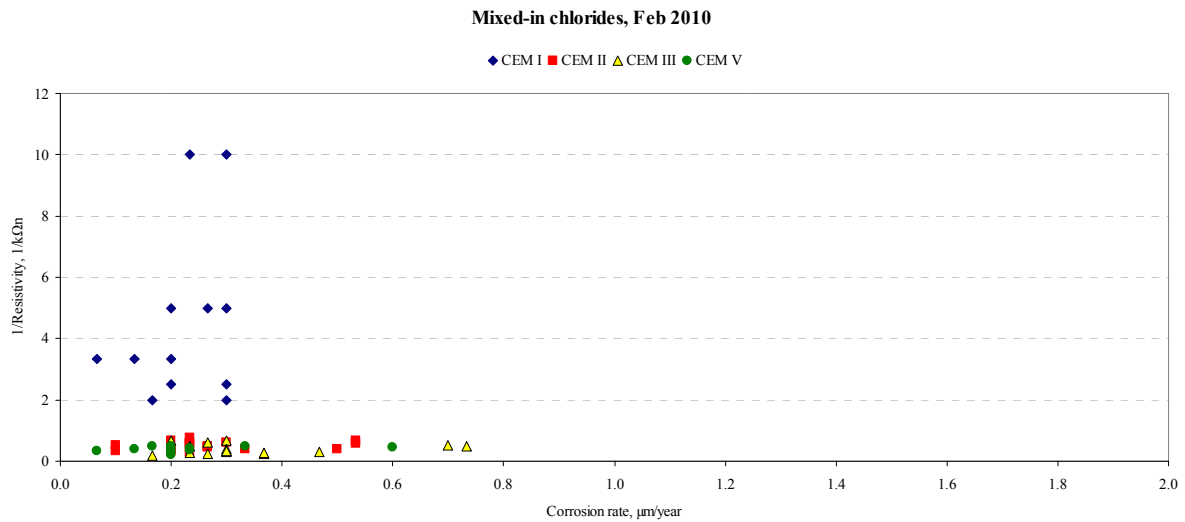


Figure 6.14 Corrosion rate and concrete resistivity of mixed-in chloride specimens, February 2010.

Figure 6.15 shows the values of corrosion rate and concrete resistivity of mixed-in chloride specimens during April 2010. At first instance, values of corrosion rate have increased one order of magnitude with respect to those obtained during February 2010. Higher values of corrosion rate are found in specimens with CEM I and CEM II with values between 2 and 8 $\mu\text{m}/\text{year}$, while for CEM III and CEM V remain in the lower range of corrosion rate with values around 2 $\mu\text{m}/\text{year}$.

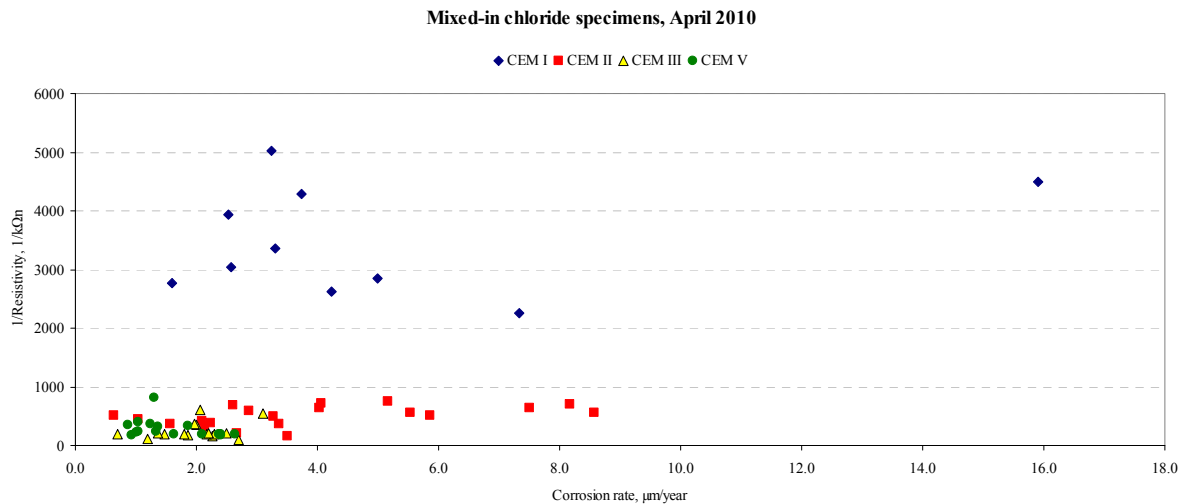


Figure 6.15 Corrosion rate and concrete resistivity of mixed-in chloride specimens, April 2010.

Synopsis

In the evaluation of corrosion of steel in concrete, results have shown that the propagation of corrosion is strongly dependant to environmental action cement type and cover depth. Changes in environmental conditions influence parameters like corrosion potential, concrete resistivity and corrosion rate from unfavorable (high relative humidity and low temperature) to favorable (moderate temperature and relative humidity) with regard to the rate of steel deterioration.

In the case of specimens exposed to salt/dry cycles, the influence of cement type has proven that blended cements have significantly reduced the damage due to pitting corrosion. Concrete specimens cast with blended cements have shown better performance against corrosion deterioration by means of corrosion rate and improved resistance to chloride penetration due to high concrete resistivity. With respect to corrosion potentials, differences were found because of environmental action (moisture and temperature changes), but it must also be noted that blended cements had higher number of bars with potentials more positive than -300 mV. With regard to cover depth, the position of the reinforcement may be determinant when the ingress of chloride due to diffusion has reached that cover level. In this sense, results of electrochemical properties in concrete and bars at a cover depth of 30 mm showed better performance than at 10 mm. This is both caused by the lesser influence of environmental action at 30 mm and delayed ingress of chlorides at such level.

Carbonation specimens showed less influence of environmental action than those exposed to salt/dry. This behavior suggests that once that the carbonation front has reached the bars; the thermodynamical conditions surrounding the steel reinforcement develop corrosion at a certain rate. While the environmental influence cannot be neglected, this is not as considerable as with salt/dry exposure. In this sense, in carbonation exposure, the cover depth was only significant when the carbonation front did not reach the cover level of reinforcement. After the carbonation depth had reached the bars, the influence of such cover was irrelevant.

For mixed-in chloride specimens, specimens cast with Portland cement showed the worst performance against this kind of exposure. This performance is related to the accelerating effect of the chloride admixture, the coarseness of the hardened pore structure and chloride-binding capacity of each cement type. In this sense, blended cements reported improved behavior when chlorides are added in the mix. Environmental action had a similar impact level as in salt/dry exposure, influence of both temperature and moisture content resulted in higher degrees of corrosion rate during the month of April 2010.

This evidence may be of particular interest to engineers involved in the design phase of civil infrastructure. A correct choice of materials will provide considerable improvement in properties related to durability that will reduce costs related to both maintenance and repair. For material scientists, the influence of cement type choice has resulted in improved performance of concrete specimens subject to chloride loading. As measurements were carried out, considerable scatter was found in all concrete mixes and tests. While this cannot be avoided to a certain degree, professionals involved in projects related to consultancy of civil infrastructure must provide an opinion and proposed action even under a degree of uncertainty due to this scatter. In this sense, during the elaboration of this report, the average of measurements of corrosion potential and corrosion rate at 10 and 30 mm of cover depth were considered for formulating comments and conclusions. In most cases, differences in potentials during potential mapping provide a huge arrange of different zones where corrosion has been developed at different degrees. However, engineers must come to a realistic and economical solution; therefore, this conclusions were extracted from the engineering thinking of the author.

7 Electrochemical repair of concrete specimens deteriorated by corrosion.

7.1 Overview

Four concrete specimens were separated from their groups for a short-term CP experiment. The purpose of this experiment was to study the current flow in the circuit, monitor potentials and concrete resistivity and study the effect of the application of current on the pH inside corrosion pits. For this, four concrete specimens were selected: 1450-B, 3550-C, 1550-B and 1552-B. Therefore, two specimens of salt/dry cycles (one cast with CEM I and CEM III), one carbonated specimen (CEM I) and one mixed-in chlorides (CEM I) were selected. Important keynotes must be made:

- Specimens exposed to salt/dry cycles showed different deterioration conditions, while 1450-B shows big rust stains on the concrete surface; the specimen 3550-C did not show any signs of corrosion products on the concrete surface.
- The carbonated specimen 1550-B did not show any signs of corrosion stains on the surface. Nevertheless, it was selected because of the high water-binder ratio which will be most probably corroded.
- The specimen 1552-B with mixed in chlorides, had small cracks in the bottom of the specimen. These cracks were not present in other specimens, thus, the cracks were not due to bad compaction or handling.

The purpose of this experiment is to study the effect of current flow in cathodically protected bars that have been deteriorated by corrosion, the pH inside corrosion pits, the visual state of the steel bars after CP treatment, evaluate the volume loss of metal in those bars and the chloride content in the steel-concrete interface. Recent literature has been developed in order to study the early benefits of applying cathodic protection to corroded steel bars in concrete (Polder 2009; Polder 2010).

7.2 Cathodic protection setup and initial conditions

After the concrete specimens were selected, the CP system was built up. A carbon fiber strip anode was attached to the exposed face of concrete with a Portland cement mortar paste layer and kept inside a fog room (20°C, >90% RH) for 24 hours. After that, the reinforcing steel bars were connected through electric wire to a resistance of 10Ω in order to measure voltage over it and therefore, obtain the electrical current on each bar by Ohm's Law. The Data logger would record the current passing to each bar in this way.

In all specimens, two bars out of three for each cover depth were subjected to cathodic protection, leaving the central bar unprotected (10C and 30C). The reason because these bars were not treated is to have a reference value of unprotected steel for the measurements of potentials, chloride content and pH inside the pits.

Before any CP current was applied to the specimens, each specimen was stored in a plastic box with a water level of 10 mm on the bottom of the boxes. In other words, each specimen was stored inside a box and separate from the others in order to avoid electrolytic contact between specimens. After 24 hours, electrochemical values of corrosion potential versus the embedded Ti* reference electrodes, corrosion rate by LPR and cell electrical resistance at 120 Hz were measured. The values of these electrochemical parameters are shown in Table 7.1.

Table 7.1 Electrochemical parameters of concrete specimens before CP, after 24 hr in contact with water.

Code	1450- B CEM I salt/dry			3550-C CEM III salt/dry			1550-B CEM I Carbonated			1552-B CEM I Mixed-Cl		
	E vs Ti* (mV)	CR ($\mu\text{m}/\text{year}$)	R (k Ω)	E vs Ti* (mV)	CR ($\mu\text{m}/\text{year}$)	R (k Ω)	E vs Ti* (mV)	CR ($\mu\text{m}/\text{year}$)	R (k Ω)	E vs Ti* (mV)	CR ($\mu\text{m}/\text{year}$)	R (k Ω)
10L	-429	20.8	1.46	-409	2.5	8.3	-622	3.3	2.1	-428	12.8	2.7
10C	-452	47.5	1.24	-393	2.8	8.29	-623	3.3	2.1	-330	12.2	2.5
10R	-429	21.1	1.36	-394	2.7	7.29	-622	3.4	2.0	-325	5.9	2.5
Anode	-72	--	--	-120	--	--	-274	--	--	-102	--	--
30L	-414	10.9	2.58	-277	1.2	14.5	-547	2.8	3.2	-407	18.2	2.1
30C	-348	32.5	2.6	-273	1.2	15.3	-626	2.9	3.2	-448	20.5	2.2
30R	-328	10.5	3.5	-276	1.9	17.4	-627	2.6	3.2	-422	8.2	2.5
Anode	-58	--	--	-138	--	--	-235	--	--	-109	--	--
10R	--	--	5.8	--	--	15.3	--	--	3.5	--	--	1.6
50R	--	--	2.5	--	--	18.4	--	--	4.9	--	--	1.3

According to the previous table, significant differences among the concrete specimens are visible. First, corrosion potential of steel bars shows that the most negative potentials are observed in the bars embedded in the carbonated Portland cement concrete. This trend is also found when measuring the potential of the anode with regard to the activated titanium electrode. This behavior is caused by changes in the pH and chemical composition of pore solution and pore structure. The most positive values of potential are found in the CEM III salt/dry specimen. In this specimen, the highest values of electrical resistance are also found. In this sense, the presence of slag has maintained better conditions for slowing down the deterioration of steel reinforcement due to corrosion. In the case of Portland cement, the highest value of corrosion rate was found in the salt/dry specimen followed by the mixed-in chloride specimen. In these two specimens, the potentials are more negative than the value of -350 mV vs Ti* which is the boundary for considering high probability of corrosion according to Table 2.10. On the other hand, values of electrical resistance found in these specimens are the lowest of the four. Therefore, the presence of chloride in specimens made with Portland cement has caused conditions of high deterioration of steel due to corrosion. Still, this has to be confirmed by results of pH inside corrosion pits, visual inspection of the bars and volume loss. The anode potential in both cases (in front of the 10 mm and 30 mm group of bars) showed differences in the potential before any current was applied. Since the anodes were placed on the specimens for a short time when compared to the history of those specimens, these variations are most probably related to changes in the potential of the Ti* electrodes themselves due to differences in pH of pore solution inside the concrete specimens.

In order to check changes in the Titanium reference electrode potential due to variations in pH, an additional set of tests against a external Ag/AgCl 3M KCl reference electrode were done. The results of such measurements are shown in Table 7.2. In this table, variations in the potential of embedded Ti* electrodes are found in all specimens. According to Table 2.9, the difference between Ag/AgCl and Ti* electrodes should be about 50 mV in ordinary conditions. However, similar values are only found in the 1450-B salt/dry specimen. In the case of specimen 3550-C, the pH variations in the pore solution occur due to the cementing action of slag that has reduced the pH of the pore solution; therefore, differences in the reported potential of Ti* electrode are found. Obviously, the carbonated specimen reported the highest difference between Ti* and Ag/AgCl electrodes due to neutralization of the pH in the pore solution. Finally, 1552-B specimen reported values that are intermediate when compared to 1450-B and 3550-C, 1550-B specimens. In this case, changes in the structure of the pore network and the influence of chloride concentration in the pore solution have influenced the pH of the pore solution.

Table 7.2 Electrochemical potential of steel, carbon (Anode) and Ti* electrodes vs Ag/AgCl 3M KCl electrode.

Specimen	10L	10C	10R	Anode	Ti*-a	30L	30C	30R	Anode	Ti*-b
1450-B	-114	-214	-191	+90	+69	-226	-133	-94	+92	+58
3550-C	+26	+5	-31	+131	+224	+71	+94	+74	+134	+223
1550-B	+31	-56	-23	+153	+378	-199	-148	+0	+153	+376
1552-B	-74	-239	-112	+86	+117	+57	-205	-263	+78	+127

Note: Ti*-a is near bars at 10 mm depth; Ti*-b is near bars at 30 mm

7.3 Monitoring of current in CP system

7.3.1 General

The recorded values of electrical current flowing to each protected bar were recorded during the time period of cathodic protection. According to a preliminary model (Polder 2009; Polder 2010), on design of cathodic protection systems, the CP current passing during first hours after the start of CP have a significant effect on the neutralization of acidic solution inside corrosion pits (Polder 2009; Polder 2010). Therefore, the first 24 hours are the most important for changes in pH inside corrosion pits. Each bar with cathodic protection of all specimens was monitored for current measurements. The exposed area of the steel bars was 11 cm² (0.0011 m²), therefore, the current that has passed through each bar is presented in mA/m². The CP treatment of steel bars was divided in two different stages. First the specimens were kept inside their storage with a water level of 10 mm and during 18 days a driving voltage of 1.4V was applied on all treated bars. The current flow was stopped for measuring depolarization of the system for 48 hours. In the second stage, the water level inside the containers was removed and the driving voltage was reduced to 1.2 V for 15 days of CP application. Finally, depolarization measurements were done again to check the effectiveness of CP. In all cases, the driving voltage applied to each bar (cell) was 1.4V during the first stage and 1.2V in the second stage.

7.3.2 Short-term CP results

Figure 7.1 shows the electrical current consumption of cathodically protected bars in specimen 1450-B. In this figure, bars at 10 mm of cover depth show high values of current at time (t=0) which is immediately after starting CP. The current consumption of bars at 30 mm depth is about half of that consumed by bars at 10 mm. After the first peak has occurred, a gradual reduction of current flow on each bar is between t=0 and 7 hours for bars at 10 mm and 4 hours for bars at 30 mm of depth. This is a transition zone where the neutralization of pH inside corrosion pits must likely take place. However, it was not possible to determine changes in pH during time because the specimens were not prepared for this. The point in time at which the gradual reduction is finished (7 hours for bars at 10 mm and 4 hours at 30 mm) is considered as a turning point. After this turning point, the current remains stable during the rest of the day with almost no variation. However, the current consumption of bars at 10 mm remains higher (with a factor of around 1.8-2) compared to bars at 30 mm cover depth. This behavior is also found in the rest of the specimens subjected to CP current. As corrosion rate values showed, bars at 10 mm have higher deterioration than those at 30 mm by means of corrosion rate. This reasoning seems logical when considering that the chloride profile reach the bars at 10 mm earlier than those at 30 mm. As CP current is being consumed, the difference between current demands of bars at 10 mm and 30 mm is due to this effect.

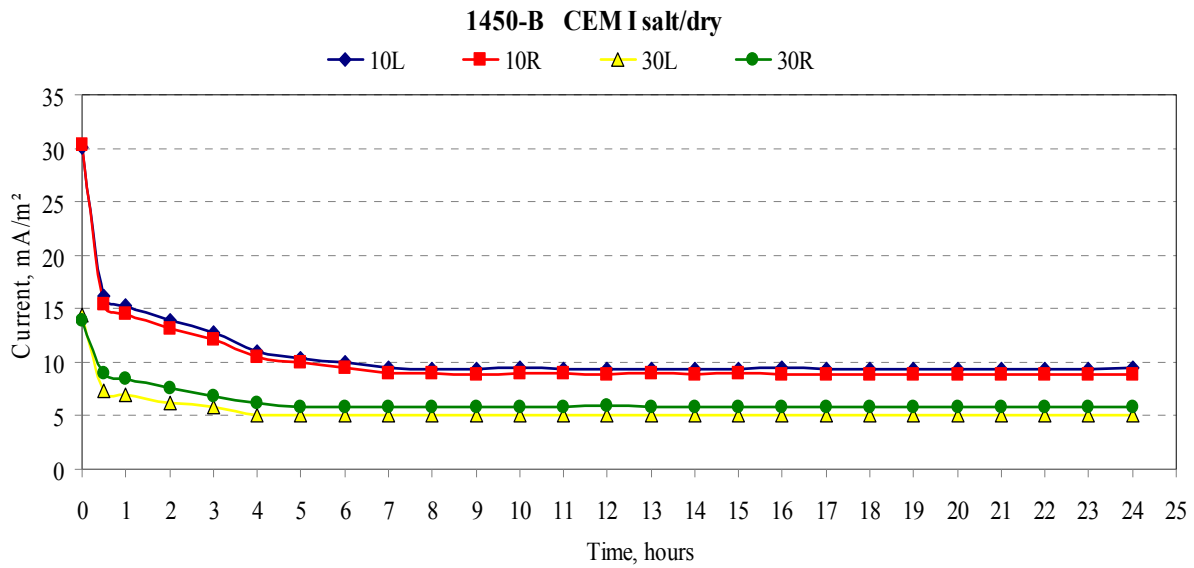


Figure 7.1 Electrical current of cathodic protected bars in specimen 1450-B, mA/m² over 24 hrs.

In the case of specimen 3550-C, the initial current consumption at t=0 is considerably less than in specimen 1450-B as shown in Figure 7.2, even though both were exposed to salt/dry cycles. Again, bars at 10 mm required more current immediately after starting CP while bars at 30 mm required less current. The ratio between current requirements of bars at 10 mm and 30 mm is 2:1. The transition zone where gradual reduction of current is observed until 4 hours, for bars at 10 mm, and until 2 hour for bars at 30 mm. The turning point at which the current becomes stable is in the same proportion as the reduction in required current in specimen 1450-B. This means that required initial current and time for current stabilization are probably related to each other. After the turning point in the current stabilization, there are no significant changes in electrical current flow in the steel bars. As in the previous specimen, the required current of bars at 10 mm in the stable phase is still higher than bars at 30 mm depth. Also, the ratio between the current consumption at 10 and 30 mm is around 1.8-2.

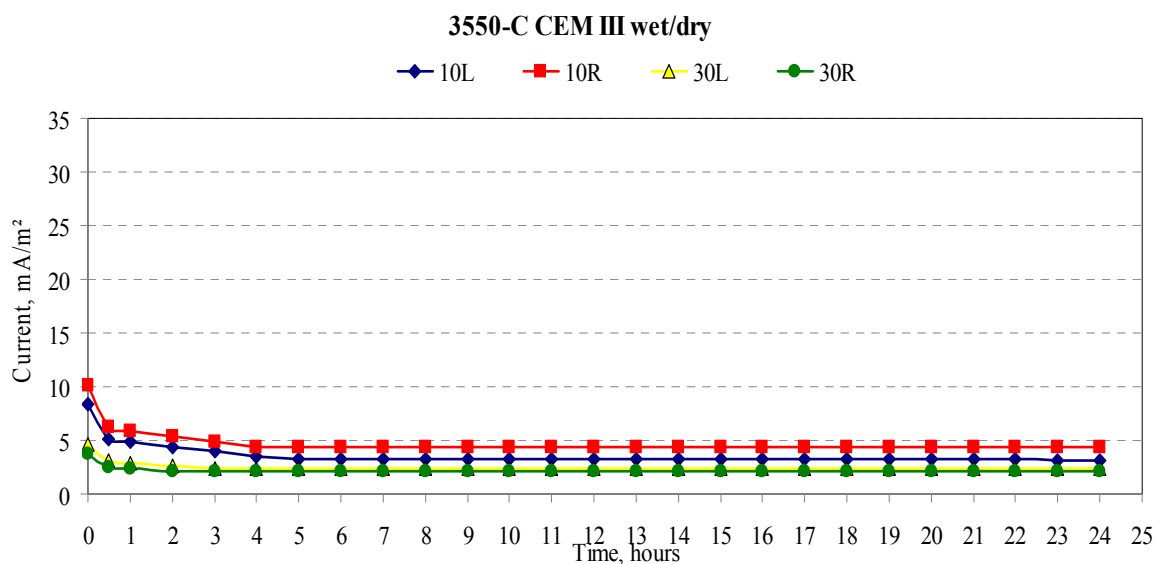


Figure 7.2 Electrical current of cathodic protected bars in specimen 3550-C, mA/m² over 24 hrs.

As a summary of specimens exposed to salt/dry cycles, concrete containing Portland cement has shown that demands in electrical current in all bars is significantly higher than in concrete made with slag cement. As described before, the corrosion rate of the bars embedded in specimen 3550-B was lower than in specimen 1450-B. The influence of slag in the development of the pore network in concrete has delayed the time at which

corrosion has started and most probably, the diffusion of chlorides from the salt/dry cycles. Once that the cycles were stopped, from week 30 and until 12 years, the diffusion or redistribution of chlorides inside these specimens is interesting with regard to corrosion of steel reinforcement. Another condition for the reduction of the current flow is the increased resistivity of such specimen. Since electrical flow may only be transported through ions the amount and connectivity of those pores is reduced for this concrete type. This reduction in conductivity is significant enough to be considered^{*}. For that, after the CP experiment the specimens will be subjected to destructive analysis for chloride content in the whole depth of the specimens. Results of that study are described below.

Results of electrical current demands of steel bars embedded in carbonated concrete are shown in Figure 7.3. Initial values of electrical current at $t=0$ are in the range between 8-13 mA/m² for bars at 30 mm and 10 mm respectively with a ratio between these values of current of around 1.6. The gradual reduction of current in the transition stage lasts until 5 hours for bars at 30 mm and 7 hours for bars at 10 mm depth. The length of the transition zone in carbonated concrete is longer than in salt/dry concrete, because the corrosion mechanism in this carbonated concrete is different. Since corrosion is not caused by chlorides but due to reduction of pH, the breakdown of the passive layer occurs with significant differences. Because the lack of chlorides, it is most probable that there are no corrosion pits in the bars embedded in carbonated concrete, therefore, neutralization of acidic solutions inside them is not possible. However, the anodic parts of the steel bar are probably larger than in chloride-pitting corrosion in which the cathodic reaction and the production of OH⁻ ions takes place. The production of these hydroxyl ions will certainly increase the pH in the concrete-steel interface and since the anodic area is larger, the evolution of pH increase may lead to higher time demands for stabilization of electrical current. Nevertheless, these assumptions must be tested in further detail for confirming or denying them. However, such experiments were not part of this study.

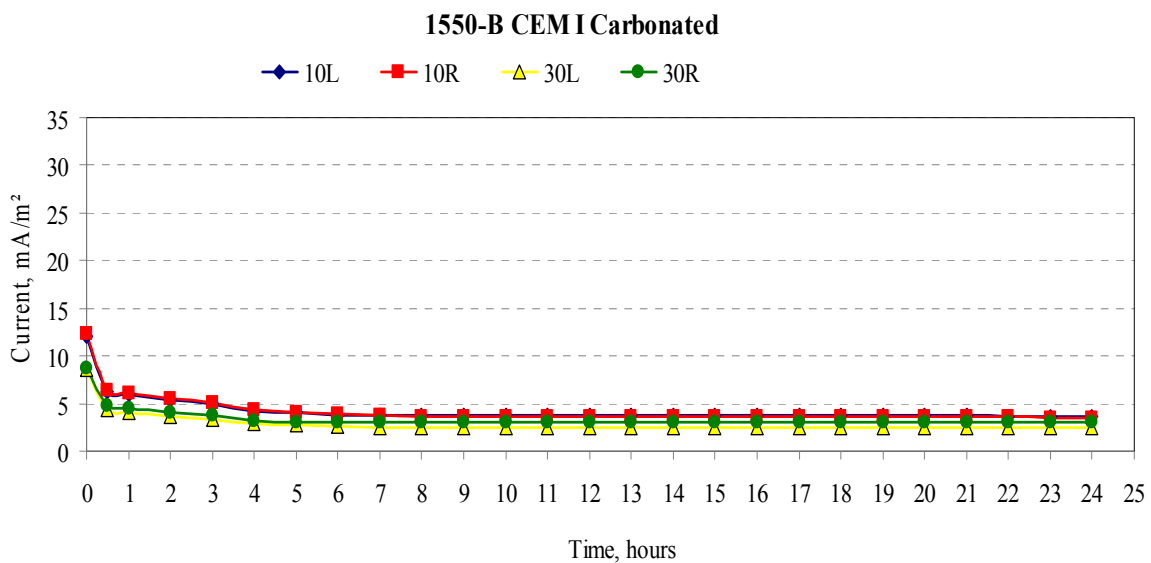


Figure 7.3 Electrical current of cathodic protected bars in specimen 1550-B, mA/m² over 24 hrs.

The behavior of electrical current of steel bars in specimen 1552-B is shown in Figure 7.4. This specimen containing Portland cement reported similar values of electrical current of bars at 10 mm and the bar at 30R. On the other hand, bar 30L demanded more current than the other three protected bars. Chlorides were added to the fresh mix of this concrete specimen, thus, all the bars have been exposed to an equal amount of chlorides during same time. Nevertheless, one bar at 30 mm demanded more current compared to the rest of the bars in this specimen. In the transition phase, the stabilization of current in these bars lasts until four hours in all cases. Even the bar 30L which had higher current demand stabilized its current at this time. In the later stage, the current remains almost constant after 4 hours. Still, the current demand in the bar 30L is around twice as much as the rest of the bars. This may be due to the presence of air voids in the concrete-steel interface due to poor compaction. As described before, the accelerating effect of CaCl₂ produced lower values of specific density in

^{*} In the case of concrete structures containing CEM III, this aspect has to be considered when other electrochemical repair techniques (realkalisation or ECE) are applied.

both fresh and hardened states. Therefore, an air void of considerable size may be present in the vicinity of the bar producing differences in oxygen concentration or pH that could accelerate the degradation of steel.

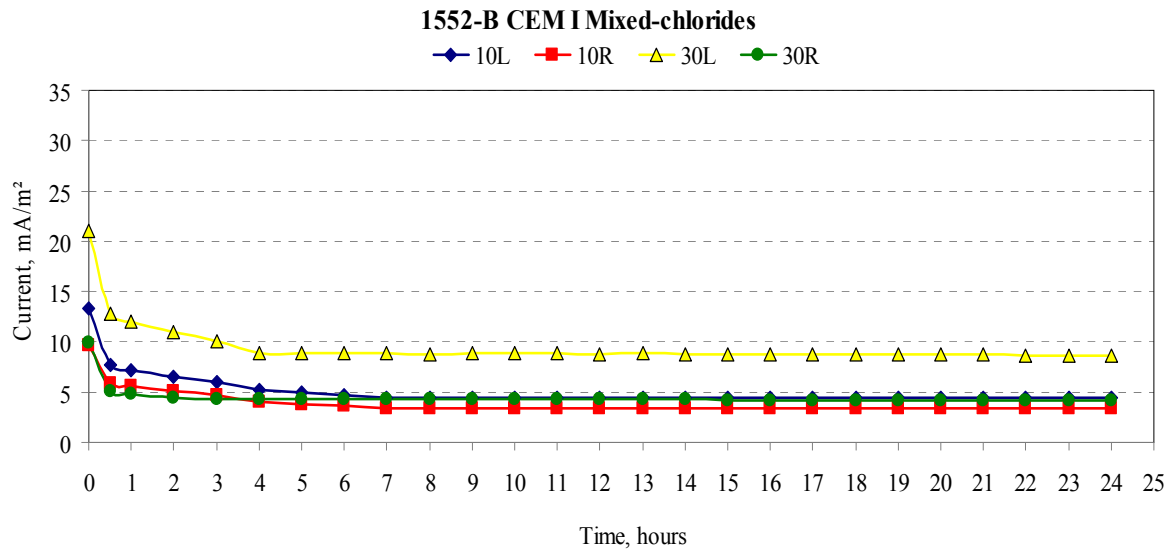


Figure 7.4 Electrical current of cathodic protected bars in specimen 1552-B, mA/m² over 24 hrs..

This behavior gives a few important aspects to consider. For example, an appropriate evaluation of the deterioration of steel bars in concrete structures is very important when designing a CP system. An optimized CP system should consider the differences in damage due to corrosion in bars in order to apply sufficient current to the system such that the bars with higher demands will still be protected. In concrete containing chlorides, the time during which the current is gradually reduced is dependent of this parameter. Bars with more damage caused by corrosion would be expected to have deeper and bigger corrosion pits with acidic solutions inside them. Therefore, the volume of acid that will be neutralized is more than in less damaged bars. The time at which all acid has been neutralized inside corrosion pits most likely will be the same at which the current flow becomes stable (turning point). In the case of carbonated concrete, it is not possible to assume the same behavior due to changes in pore structure and chemical composition of the pore solution. The pH of carbonated concrete will still be determining the conditions of either passivation or corrosion. In this study, the application of CP in carbonated concrete is more related to realkalisation of concrete than to cathodic protection of steel itself. A reason for this is that the required time to stabilize current for a particular value of corrosion rate is longer than for the chloride containing specimens. Corroding steel in carbonated concrete with values of corrosion rate similar to those found in the specimen 1450-B would most probably require more time to stop corrosion and provide successful protection against corrosion.

7.3.3 Long-term results of CP treatment

The behavior of electric current was monitored over 18 days of CP at 1.4 V in the four investigated specimens,. Figure 7.5 shows the long term behavior of current flow through cathodic protected bars embedded in specimen 1450-B. The behavior found during the first 24 hours for such bars in this specimen is still present after 18 days. However, the difference between the current demand of bars at 10 mm and bars 30L mm is reduced, but less so for bar 30R. In the long term, the total charge consumption of bars at 10 mm is higher than those at 30 mm depth. This will be discussed below.

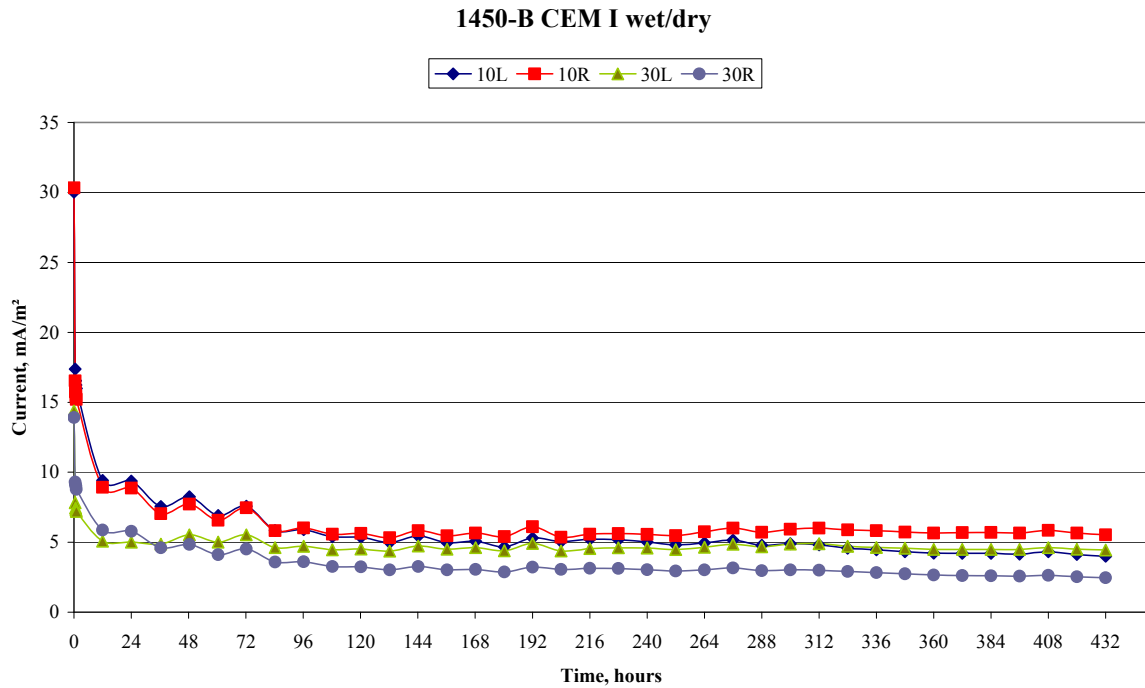


Figure 7.5 Electric current of CP protected bars in specimen 1450-B, mA/m² over 18 days.

The behavior of electric current demand in bars embedded in specimen 3550-B is shown in Figure 7.6. In this case, the current flow of bars at 10 mm and 30 mm depth is very similar on the longer term. When compared with specimen 1450-B, the total charge that has passed through the bars in this specimen is substantially less. The fact that charge for bars at 10 mm and 30 mm depth is similar may be attributed to the fact that the corrosion rates of all bars were similar before CP was applied.

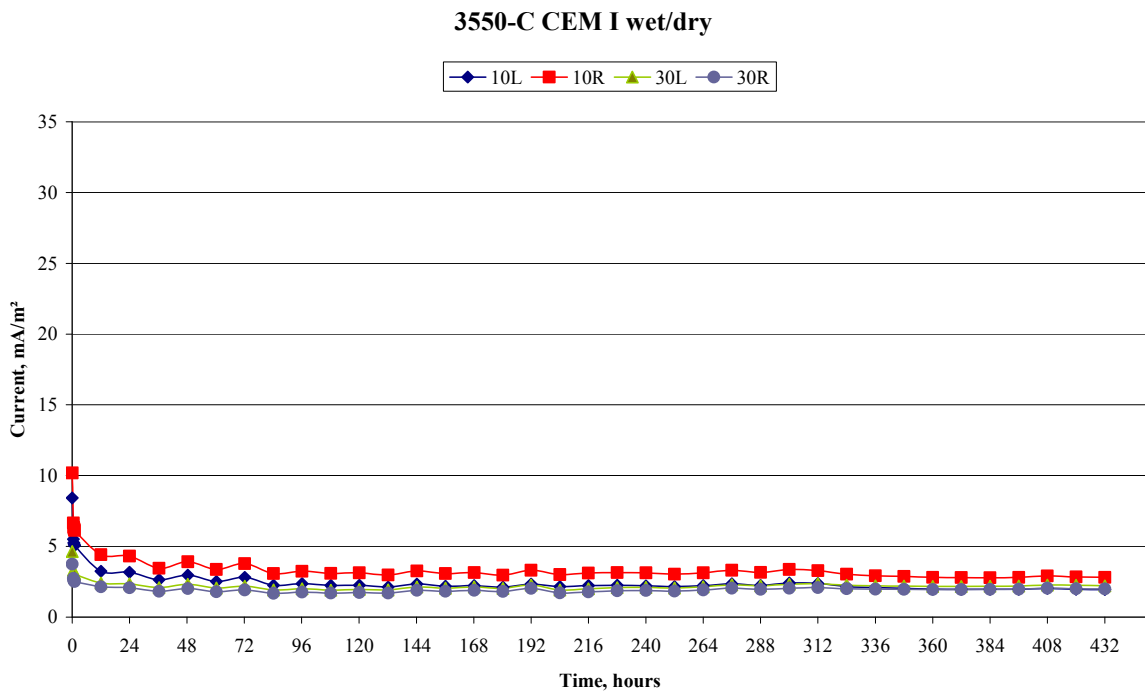


Figure 7.6 Electric current of CP protected bars in specimen 3550-C, mA/m² over 18 days.

In the case of carbonated concrete, the current consumed by steel bars is shown in Figure 7.7. The behavior of current consumption is very similar to the one found with specimen 3550-B. A reason for this is probably low corrosion rates before the application of CP. Apparently, as the degradation of steel due to corrosion is increased, the electric current required to stop corrosion is higher. In this concrete specimen, the values of current consumption of bars at 10 mm and 30 mm depth are practically the same. This means that both groups of bar would have similar deterioration due to corrosion.

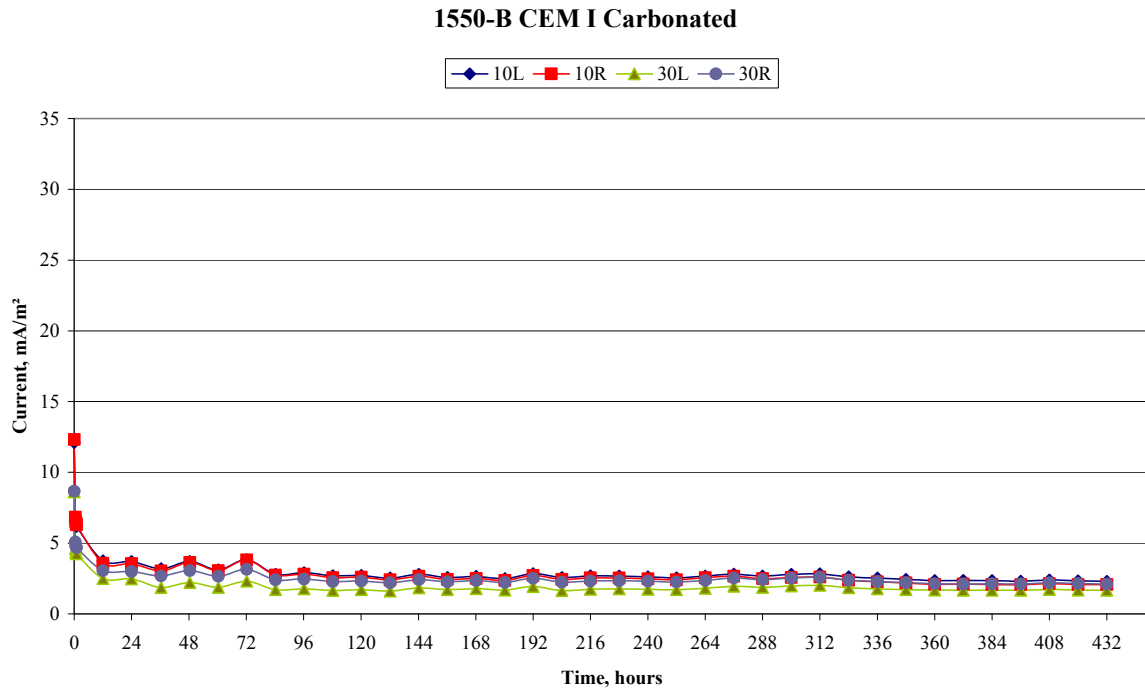


Figure 7.7 Electric current of CP protected bars in specimen 1550-B, mA/m² over 18 days.

Figure 7.8 shows the current consumption of bars embedded in specimen 1552-B. In this specimen, the behavior was different from the other three specimens. Since the beginning, bar 30L demanded significantly more current than the rest of CP treated bars. However, in the long-term, the current consumption of bars at 30 mm has not decreased by the same rate as bars at 10 mm. For the bars at 10 mm depth, the long-term current demand is substantially lower than for bars at 30 mm.

1552-B CEM I Mixed-chlorides

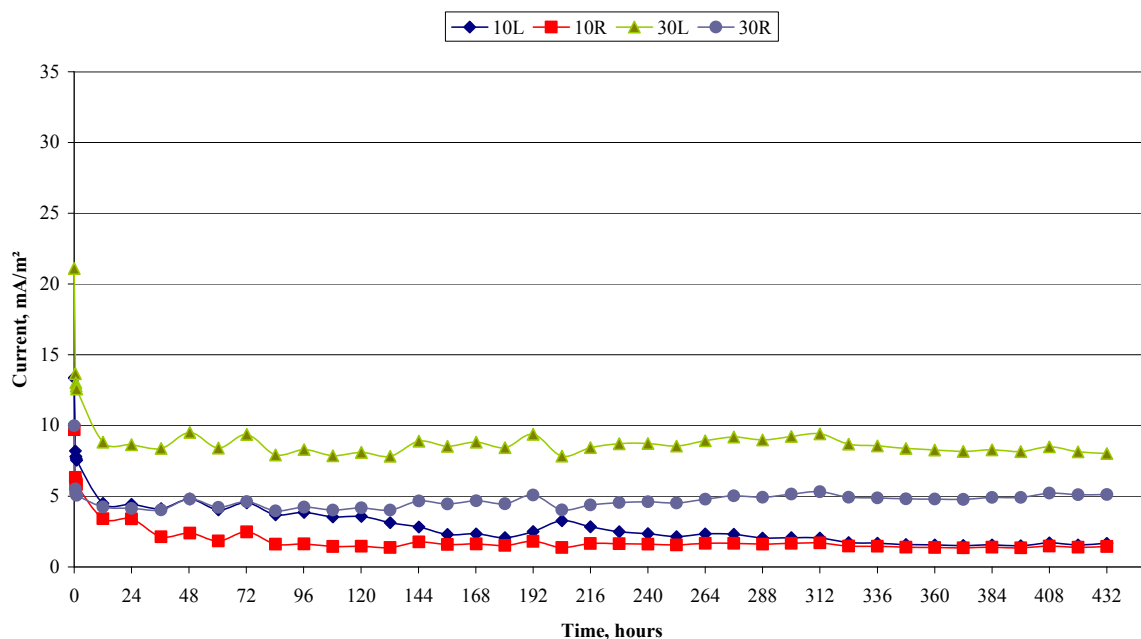


Figure 7.8 Electric current of CP protected bars in specimen 1552-B, mA/m² over 18 days.

The significant difference of bar 30L with respect to the rest of the treated bars in this specimen is certainly interesting. The behavior of this bar does not represent the rest of the bars in the specimen; even though all bars have been exposed to roughly the same amount of chlorides (see below). On the other hand, moisture variations present at 30 mm depth are possible, however, this behavior would also be found in the bar 30R. With this evidence, the only possible conclusion is that an air void of considerable size is present in the steel-concrete interface.

The area under the curve (integral) of the current consumption by each bar is equal to the total charge that has passed through it during the application of CP. Table 7.3 shows the total charge of CP treated bars up to 18 days. In this table, values of charge show a clear relation with the current demand during the whole treatment period. For bars at 10 mm cover depth, those embedded in specimen 1450-B reported the highest values of total charge. This was expected because corrosion rates of those bars were the highest for this cover depth in all specimens. Also, the instantaneous current demand after applying CP showed that the current demand was the highest for this cover depth.

Table 7.3 Total charge of CP treated bars over 18 days at 1.4V.

Specimen	10L	10R	30L	30R
	Charge, mAh/m ²	Charge, mAh/m ²	Charge, mAh/m ²	Charge, mAh/m ²
1450-B CEM I salt/dry	2342	2619	2028	1430
3550-C CEM III salt/dry	992	1379	929	825
1550-B CEM I Carbonated	1193	1121	793	1043
1552-B CEM I Mixed-in chlorides	1158	744	3703	2000

When combining the results of corrosion rate from Table 7.1 with total charge consumption from Table 7.3, it seems that these results are related to each other. Bars that reported higher values of corrosion rate (particularly in at 10 mm in specimen 1450-B and 30 mm in 1552-B) also consumed higher values of electrical charge over 18 days at 1.4V. These two specimens share two common conditions: both are Portland cement concrete and have been exposed to chlorides. As corrosion deterioration occurs in steel bars, the presence of corrosion pits will most probably occur first in these concrete specimens. As discussed before, the solution inside corrosion pits is believed to have an acidic pH. The neutralization of this solution inside corrosion pits is obtained due to the cathodic reaction (and consequent production of hydroxyl ions) in the surface of the steel bar. Bars with

bigger and deeper pits may probably contain higher volumes of acid inside them. These considerations will be discussed in the Discussion section.

The total charge that passed through bars after 15 days with a driving voltage of 1.2V is shown in Table 7.4. In this table important variations in the total charge flow are seen. First, in the case of salt/dry exposure, the total charge in all bars is reduced considerably when compared to the first CP period of treatment. The total charge in the second phase is roughly half of the charge during the first stage of CP treatment. In this case, the reduction of charge is most probably related to an efficient neutralization of pH in pits and stop of corrosion processes. On the other hand, the carbonated and mixed-in chloride specimens show a completely different behavior. In the carbonated specimen the reduction in the total charge in the second stage of CP is about 20% to 40% of the charge at 1.4V. These conditions show that different processes are occurring during the second stage in this specimen. One possible explanation is that the cathodic reaction (and production of OH-) causes concrete realcalisation in the steel-concrete interface. Therefore, the current in these bars is not only consumed to prevent further corrosion but also, due to the demand in OH⁻ ions to raise the pH in the pore solution. In other words, part of the total charge that flowed through the bars was consumed by cathodic reaction at the steel's surface and the rest to increase pH of the pore solution in the surrounding of the bars. Unfortunately, this was not expected due to the low current that was applied on the specimens. In the case of mixed-in chlorides, the bars at 10 mm showed a negative charge over 15 days. Possibly, contact problems in the wires are responsible of this erratic behavior. These results are discarded and do not form part of the analysis of the efficiency of CP. On the other hand, the total charge for bars at 30 mm depth is just about 5 to 10% lower than in the first stage. As in the carbonated specimen, other mechanisms are affecting the charge demand of such bars, but in this case, chloride extraction may be the cause of such demand.

Table 7.4 Total charge of CP treated bars over 15 days at 1.2V.

Specimen	10L	10R	30L	30R
	Charge, mA-hr/m ²	Charge, mA-hr/m ²	Charge, mA-hr/m ²	Charge, mA-hr/m ²
1450-B	1029	1962	1707	696
3550-C	490	926	1015	843
1550-B	971	678	505	795
1552-B	-57	-153	3337	1906

For more practical considerations, Table 7.5 shows the current density at two different points in time: immediately after CP current begins to flow through the bars and before depolarization measurements. In this table, it is clear that the differences between the values of current density immediately after CP is being applied and before depolarization are higher for 18 days at 1.4V. In this period, specimens 1450-B and 1552-B report bigger drops of current density than in 3550-C and 1550-B. For values after 15 days at 1.2V show that the current density of most bars is near zero. This evidence suggests that an electric field of 1.2V is not enough to sustain a proper CP current density in these specimens.

Table 7.5 Current density of steel bars due to CP, mA/m².

Specimen	Time	18 d @ 1.4V				15 d @ 1.2V			
		10L	10R	30L	30R	10L	10R	30L	30R
1450-B	Immediately after CP	30	30	14	14	5	6	5	3
	Before Depolarization	4	6	4	2	1	0	0	1
3550-C	Immediately after CP	9	10	5	4	2	3	2	2
	Before Depolarization	2	3	2	2	0	0	0	0
1550-B	Immediately after CP	12	12	9	9	3	3	2	3
	Before Depolarization	2	2	2	2	1	1	0	0
1552-B	Immediately after CP	13	10	21	10	3	2	10	5
	Before Depolarization	2	1	8	5	1	1	1	0

Values of current density before depolarization are relevant for such process because the drop of potential will be determined by the strength of the current density before CP current is turned off. Next, results obtained during depolarization measurements are given.

7.3.4 Depolarization

After 18 days, the CP current was stopped and depolarization measurements were done. According to literature (Pedefferri 1995; NEN-EN 2001; COST 534 2009), the quality of protection offered by a CP system is positive if

the potential of steel has depolarized from its value at switch-off by least 100 mV after 24 hours. Therefore, the values of depolarization of steel bars in specimens subjected to CP, measured at the end of the first period at 1.4 V, are shown in Table 7.6.

Table 7.6 Depolarization values of steel bars in concrete specimens after two weeks at 1.4 V.

Specimen	Current	10L	10C	10R	Anode	30L	30C	30R	Anode
1450-B CEM I S/D	On	-749	-483	-747	724	-761	-426	-762	700
	Off	-714		-703	612	-722		-740	585
	1 hr	-719	-487	-719	349	-731	-431	-731	335
	4 hr	-709	-488	-709	172	-707	-422	-707	173
	24 hr	-687	-497	-686	51	-692	-436	-692	44
Depolarization		-27	14	-17	561	-30	10	-48	541
3550-C CEM III S/D	On	-908	-372	-896	545	-828	-294	-829	603
	Off	-772		-750	456	-577		-573	512
	1 hr	-729	-363	-728	326	-657	-278	-656	396
	4 hr	-690	-358	-690	183	-620	-275	-620	252
	24 hr	-638	-353	-637	94	-580	-272	-579	151
Depolarization		-134	-19	-113	362	+3	-22	+6	361
1550-B CEM I CO₂	On	-1188	-715	-1189	287	-1152	-722	-1145	314
	Off	-1114		-1123	256	-1091		-1073	275
	1 hr	-1080	-715	-1077	-19	-1055	-718	-1050	3
	4 hr	-1076	-718	-1074	-196	-1053	-724	-1052	-174
	24 hr	-1036	-727	-1035	-293	-1011	-723	-1003	-268
Depolarization		-78	12	-88	549	-80	1	-70	543
1552-B CEM I Mix-C1	On	-831	-385	-829	645	-799	-503	-797	677
	Off	-822		-820	487	-751		-754	516
	1 hr	-795	-383	-794	262	-758	-501	-758	297
	4 hr	-776	-381	-776	103	-739	-500	-739	140
	24 hr	-728	-382	-727	12	-696	-496	-696	41
Depolarization		-94	-3	-93	475	-55	-7	-58	475

In this table, it is shown that, for most bars, depolarization has not reached the required minimum of 100 mV shift in order to consider the CP treatment as effective. Bars in specimen 1450-B have depolarized less than 50 mV, which suggests a poor success for the CP system. This behavior may be caused by lack of oxygen at the surface of steel due to high moisture content in the specimens. Since they were stored inside a box with a 10 mm water level, the moisture inside them may have slowed down oxygen transport that is needed for depolarizing reactions. If that is true, waiting longer might have shown stronger depolarization. The quite negative potentials (in all specimens) support this view.

In the case of specimen 3550-C, the bars at 10 mm depth have depolarized above 100 mV; however, the bars at 30 mm did not depolarize more than 100 mV. In this case, the combined action of dense pore structure and saturation by water may prevent oxygen transport into those bars and, therefore, depolarization is slowed down.

In the carbonated specimen 1550-B, none of the bars have depolarized more than 100 mV. At first glance, this may suggest an improper application of CP, however, the depolarization values are closer to the 100 mV shift, than in 1450-B and changes in the pore structure and pore solution must be taken into account. As described before, the potential of carbonated specimens was significantly more negative than -350 mV; and as the specimens were wet the drop of such potentials may be even higher. Nevertheless, potentials below -900 mV must be considered as dangerous for embrittlement of prestressing steel (*not* for reinforcing steel). These potential values may be detrimental for prestressed concrete structures in which high-strength tendons are used.

The depolarization in specimen 1552-B is near a value of 100 mV for bars at 10 mm of cover depth and around 50 mV for bars at 30 mm. In both cases, the depolarization suggests an unsuccessful application of the CP treatment. Nonetheless, these values in all specimens may reach the 100 mV shift after more than 24 hours depolarization. This was considered for the second stage of CP treatment.

For reference bars (without CP current application) differences in potential are most probably attributed to changes in temperature and moisture content inside the specimens. The range of difference fluctuates between -22 to +14 mV. In the case of specimen 1450-B changes in potential of reference bars is towards more negative potentials, which was expected because of the presence of chlorides at their level and increase of moisture due

to water absorption of the water level in the storage box. For specimen 3550-C, potentials shift towards more positive values. This suggests that electrochemical repair of steel by CP had a better effect in slag concrete. As discussed before, transport of moisture in this concrete specimen is surely lower than in Portland cement concrete. Therefore, some pores remain without water, favoring transport of oxygen towards the steel bar surface. In carbonated concrete, the potential shift occurs towards more negative values. However, these considerations must be taken with care because carbonated concrete showed less sensitivity to changes in temperature or moisture. In this specimen, the influence of external conditions is not as strong as the reduction of pH due to carbonation. Finally, for specimen 1552-B the potential of reference bars remains almost constant. This behavior suggests that the increase of moisture content during the CP treatment did not show any detrimental effect on depolarization. Apparently, this specimen was near complete saturation before it was stored inside the container, so the water level at the bottom of it was irrelevant.

After the first depolarization of steel bars, it was decided that the water inside the storage boxes must be removed and another two weeks of CP were necessary. At that time it was also determined to reduce the voltage in the power supply to 1.2 V DC. After two weeks of CP, another set of depolarization measurements was done and results are shown in Table 7.7.

Table 7.7 Depolarization over 48 hours of steel in concrete specimens after a second period of CP, two weeks at 1.2 V.

Specimen	Current	10L	10C	10R	A10	30L	30C	30R	A30
1450-B CEM I S/D	On	-408	-342	-410	822	-412	-291	-372	1033
	Off	-376		-388	813	-378		-320	831
	1 hr	-357	-342	-385	511	-386	-288	-290	513
	21 hr	-336	-341	-376	274	-392	-279	-251	278
	24 hr	-321	-339	-365	183	-380	-271	-235	188
	48 hr	-281	-340	-293	79	-309	-268	-218	85
Depolarization		-95	-2	-95	734	-69	-23	-102	746
3550-C CEM III S/D	On	-510	-245	-489	869	-505	-182	-524	856
	Off	-357		-360	680	-395		-342	639
	1 hr	-312	-362	-315	369	-253	-180	-215	369
	21 hr	-292	-229	-296	164	-204	-175	-180	166
	24 hr	-285	-217	-291	90	-196	-168	-176	92
	48 hr	-251	-215	-261	41	-165	-168	-141	55
Depolarization		-106	-30	-99	639	-230	-14	-201	584
1550-B CEM I CO₂	On	-1048	-667	-1038	362	-1035	-684	-1035	369
	Off	-660		-762	268	-860		-762	234
	1 hr	-592	-649	-687	69	-813	-682	-716	75
	21 hr	-530	-642	-623	-82	-772	-679	-669	-75
	24 hr	-497	-634	-593	-138	-753	-673	-639	-130
	48 hr	-486	-636	-577	-186	-732	-671	-618	-143
Depolarization		-174	-31	-185	454	-128	-13	-144	377
1552-B CEM I Mix-C1	On	-449	-324	-463	943	-464	-375	-492	908
	Off	-417		-438	698	-456		-471	676
	1 hr	-368	-322	-382	366	-430	-374	-454	356
	21hr	-324	-327	-331	178	-403	-369	-451	168
	24 hr	-300	-323	-306	109	-388	-364	-448	99
	48 hr	-289	-325	-300	88	-354	-358	-430	88
Depolarization		-128	1	-138	610	-102	-17	-41	588

After two weeks with a voltage of 1.2 V, the depolarization values at 48 hours of steel bars show that in most cases the bars have depolarized above 100 mV or they are very close to do it. It is difficult to assure if changes in depolarization values compared to depolarization after two weeks at 1.4 V are due to either changes in moisture content or decrease of voltage. In depolarization values, the drying effect in concrete specimens without changes in voltage would lead to more negative potential values. On the other hand, for constant moisture content subject to changes in voltage, the bars would present lesser values of overpotential shift during depolarization. The evidence suggests the first effect, so most probably the specimens have been drying out during these two weeks, which constitutes a corresponding behavior of moisture transport in concrete. Values of depolarization at 1.2V show in general more positive values than after 18 days at 1.4V. The reason is that an electric driving force of 1.2V is not strong enough to apply sufficient cathodic polarization in bars.

Nonetheless, there are still bars that have not depolarized above 100 mV in specimen 1450-B. Bars at 10 mm depth are very close to 100 mV depolarization so it is probable that those bars will reach the required potential shift to assure a successful CP treatment. This happens also with a bar of specimen 3550-C. The rest of the bars have depolarized according to recommendations so it may be assumed that CP after four weeks has been successful.

For unprotected bars, the values of potential show minor differences over the 48 hours depolarization period. However, in general they are also more positive than during the first period of CP treatment. The difference lays upon changes in moisture content inside the specimen. As the specimens have been drying out, these potentials are more related to those found in the outside environment and reported in Chapter 6. In the case of the anodes, results show that they have been polarized to the same level as the CP protected bars. Since the overall polarization at 1.2V was lower than at 1.4V, the polarization of the anodes was reduced as well.

7.4 Destructive analysis

7.4.1 General

After the CP experiment, destructive analysis of the specimens was carried out. During this part of the research, measurements of carbonation depth, chloride content, pH of corrosion products, visual inspection of steel bars and evaluation of volume loss were carried out. Since a few of these experimental techniques were new, a dummy specimen was used in order to check the reliability of those measurements. Figure 7.9 shows a few steps of the destructive analysis.



Figure 7.9 Destructive analysis of specimens after CP.

The bars were extracted from the specimens by breaking the cover by mechanical action. Then, each bar was removed individually and stored in plastic bags. The remaining pieces of concrete were saw-cut for chloride profile analysis and carbonation depth. Once the bars were collected, the corrosion products on their surface and the vicinity of concrete were removed by mechanical action and collected for pH and chloride analysis.

7.4.2 pH measurements

During the propagation phase of corrosion of steel in concrete, it is believed that the pH of the solution contained in corrosion pits is acidic (Arup 1983). However, quantitative information about measured pH of acidic liquids in pits in reinforcing steel in concrete was not found in literature. In this sense, an experimental test of pH of corrosion products obtained during the destructive analysis of steel bars was attempted.

After the bars were removed from the concrete specimens, the remaining corrosion products on the surface of the bar were removed and collected. A pH measurement using a pH meter involved a sample of corrosion products and distilled water to make a “test solution”. Two measurements of pH were done per each bar of the dummy specimen. Unfortunately, measurements of pH inside corrosion pits are difficult to make with accuracy. The mechanical action while removing the bars may produce loss of acidic solution that cannot be recovered. Another unfavorable circumstance is the unknown size of the pits. Collecting corrosion products of small pits (and especially the lack of pits like in carbonation-induced corrosion) made this procedure more difficult. Measurements of pH in small pits surely require more sophisticated equipment. Specimen 1400-B was used in order to do a rough pH measurement by extracting the bars and removing the corrosion products on its surface. Table 7.8 shows the outcome of the pH measurements in the dummy-test.

Table 7.8 Measurements of pH of corrosion products by mechanical means.

Bar	10L	10C	10R	30L	30C	30L
pH	8.4	9.2	11.4	8.6	11.4	11.2
	8.8	10.3	12.1	9.2	10.8	10.9

Results of pH measurement show values that are not in the range of the expected pH in acidic pit liquids. This result suggests that this technique has not given reliable results. The main reason behind the failure of this technique is that when the corrosion products were removed from the bars, the presence of tiny particles of concrete raised the values of pH to alkaline values closer to those of concrete. On the other hand, it is believed in literature that pH inside corrosion pits due to chlorides has is acidic (Arup 1983), and most probably values around 3 (Polder 2009; Polder 2010). In this sense, the values of pH obtained during this test are unsatisfactory. For further research on this topic, a technique which involves a higher degree of technology may be suitable, for example, ESEM microscopy.

7.4.3 Carbonation depth

The carbonation depth of concrete specimens after CP is shown in Table 7.9. It is observed that carbonation in specimen 1450-B is present until 18 mm which is beyond the group of bars at 10 mm depth. These conditions of combined action of both chloride and carbonation represent the worst conditions for controlling or repairing corrosion. Also, these findings may be related to the fact that depolarization in bars at that depth was not above 100 mV. In the case of specimen 3550-C made with slag cement, the carbonation front reached 8 mm which is near the group of bars at 10 mm depth. This behavior was expected because the pore structure of this specimen is more dense than the one in specimen 1450-B.

Table 7.9 Carbonation depth of specimens after CP.

Specimen	Carbonation depth, mm
1450-B CEM I salt/dry	18
3550-C CEM III salt/dry	8
1550-B CEM I Carbonated	>30
1552-B CEM I Mixed-chlorides	3

The behavior of carbonation depth of concrete specimens with chlorides is interesting, because of the deep carbonated front in specimen 1450-B, which was considered to have higher resistance in terms of durability than the others because of its lower water:binder ratio. When comparing specimen 1450-B with 3550-C two differences are seen, cement type and water:binder ratio. As described before, Portland cement has higher resistance to carbonation than blended cements like CEM III, resulting in a supposedly lower carbonation depth in the same exposure conditions. However, this is not the case. Nevertheless, chlorides may be the cause of this behavior. Since the values of corrosion rate and total charge consumption in specimen 1450-B were higher than 3550-C, a higher and deeper degree of corrosion in steel bars is expected. This was confirmed later with the visual inspection of the bars (see below). An increased number of corrosion pits with higher volume results also in higher volumes of acidic solution inside the pits. Now, specimen 1450-B showed visible rust stains in the concrete surface before CP. This means that transport of corrosion products towards the surface of the specimen had occurred. A transported volume of acid from a corrosion pit through the pore network may result in

neutralization of the pH in the pore solution. A neutralized pore solution may be favorable for carbonation of concrete under environmental conditions of outside exposure. Another possible cause for the behavior of this specimen is the effect of dryer exposure that may have happened to this specimen; if exposed outside, in 20 °C 80% RH from 30 weeks to 2.5 years. This is the most probable environment to which this specimen was exposed, however, this only speculation because it is not possible (with the only use of NDT) to determine the exposure environment after 30 weeks. For this, microscopy would be required.

In the case of 3550-C cast with slag cement, the increase of density in the pore structure is controlling the ingress of chlorides into the specimen. Since the corrosion rate and charge demand of this specimen was low when compared to 1450-B, the corrosion damage on the embedded steel is less than in Portland cement concrete. This increase in density also results in reduced transport of matter through the pore structure. A specimen that has been wet during time in these conditions would contain higher levels of moisture during more time than a specimen with a coarser pore structure. The rate of carbonation is strongly depending on moisture content inside concrete, with a highest rate between 60-70% of RH (Baron 1992). When the internal moisture is higher than 70%, the carbonation rate decreases because the diffusion of carbon dioxide is reduced and therefore, the carbonation reaction occurs at much lower rate.

7.4.4 Chloride profile

Measurements of chloride profile as a function of depth from the surface that was formerly exposed face were carried out in specimens subject to CP after the treatment period. Results of chloride content are shown in Table 7.10. In this table, it is shown that the content of chlorides of specimen 1450-B had the highest values between 15 and 89 mm which are higher than a nominal threshold value of 0.4% related to initiation of corrosion according to literature (Thomas 1994; ACI 365 2000; Bertolini 2004; Broomfield 2007; Angst 2009). These results show that the resistance to chloride transport in concrete cast with CEM I is low when exposed to salt/dry cycles, even though the chloride loading was stopped after 30 weeks.

Table 7.10 Chloride content of saw-cut slices of concrete specimens.

Specimen	Distance from exposed face, mm	Chloride content	
		gr/samp	%
1450-B CEM I salt/dry	0-10	0.07	0.40
	15-25	0.10	0.80
	30-40	0.10	0.80
	45-55	0.11	0.70
	60-70	0.07	0.60
	75-85	0.07	0.60
	90-100	0.02	0.10
3550-C CEM III salt/dry	0-10	0.03	0.20
	15-25	0.06	0.50
	30-40	0.01	0.10
	45-55	0.00	0.00
	60-70	0.00	0.00
	75-85	0.01	0.10
	90-100	0.00	0.00
1552-B CEM I Mixed-in Chlorides	0-10	0.10	0.60
	15-25	0.19	1.40
	30-40	0.21	1.50
	45-55	0.25	1.50
	60-70	0.21	1.50
	75-85	0.25	1.60
	90-100	0.19	1.60

In the previous table, the chloride content of the first slice (0-10 mm) reported lower values than the second slice (15-25 mm) or deeper. This effect may be caused by different reasons. As described in Table 7.10, the carbonation depth of specimen 1450-B was of 18 mm; therefore, the carbonation front has surpassed the group of bars at 10 mm of cover depth, but has not reached the group at 30 mm. This carbonated layer (18 mm) would provide a “pushing” effect on chloride content towards the rest of the specimen. This effect is seen in Figure 7.11 where the chloride content in specimen 1450-B is shown. In this figure, the average chloride content in the

first 10 mm is 0.4% per cement weight. As described before, the carbonation front in this specimen has surpassed this cover depth; therefore, carbonation products may block pores and ions contained in the pore solution of such pores are moved towards inside the specimen. This is a combined effect of internal diffusion and pore volume reduction. At a distance of 15 to 25 mm the chloride content is 0.8% per cement weight. This behavior is also found until a distance of 90 mm from the exposed face. This evidence suggests that internal diffusion of chloride had occurred during 12 years. For future research, it is most probable that the chloride content will stabilize in time in a value above the chloride threshold of 0.4%.

1450-B salt/dry

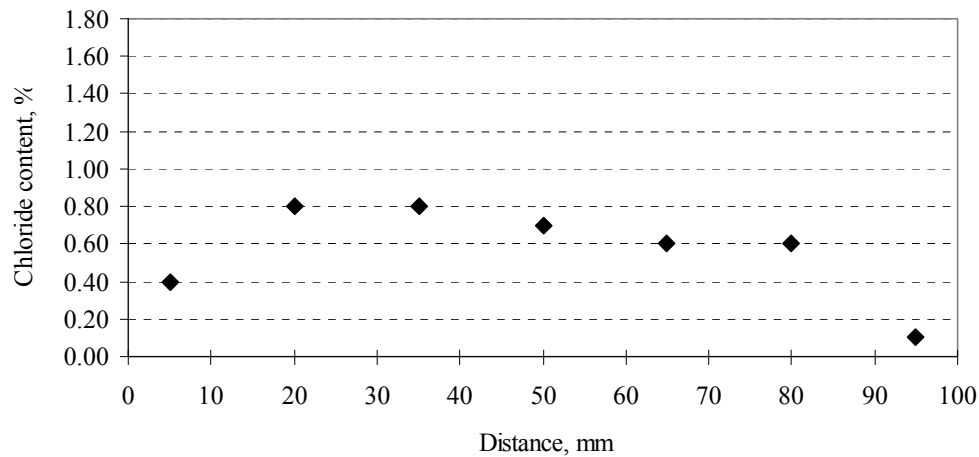


Figure 7.10 Chloride content in specimen 1450-B.

For specimen 3550-C, Figure 7.11 shows the average chloride content through the depth of the specimen. In this figure, it is clear that chloride content is significantly lower than in specimen 1450-B. The reason is that the ingress of chloride into the specimen has been slowed and delayed over the whole life span of the specimen. It is important to notice that even with a higher water/binder ratio than specimen 1450-B, this specimen contains less chlorides in it. This evidence suggests that cement type has more influence on the diffusion properties of chlorides than water cement ratio. As described in the previous specimen, a skin effect is observed in the first 10 mm of cover depth. Environmental action is also considered as the responsible of the reduced chloride content in this specimen, because carbonation has not reached the bars at 10 mm. Nonetheless, the influence of the carbonation depth on the internal diffusion of chlorides must not be discarded.

3550-C salt/dry

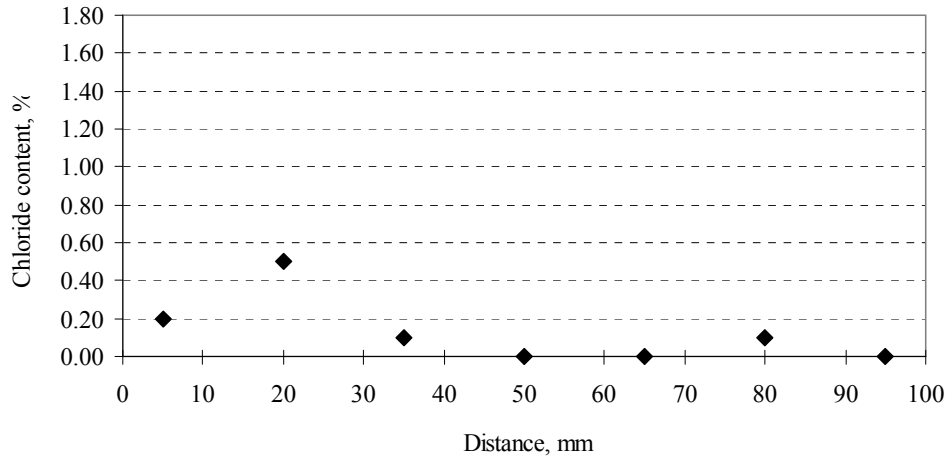


Figure 7.11 Chloride content in specimen 3550-C

Finally, Figure 7.12 shows the average chloride content in specimen 1552-B. It is clear that the chloride content in the overall depth of the specimen is significantly higher than in the previous two. However, the measured value does not correspond to those reported of 2% in Table 3.1. The difference is caused by errors during the casting of the concrete mix.

1552-B mixed-in chlorides

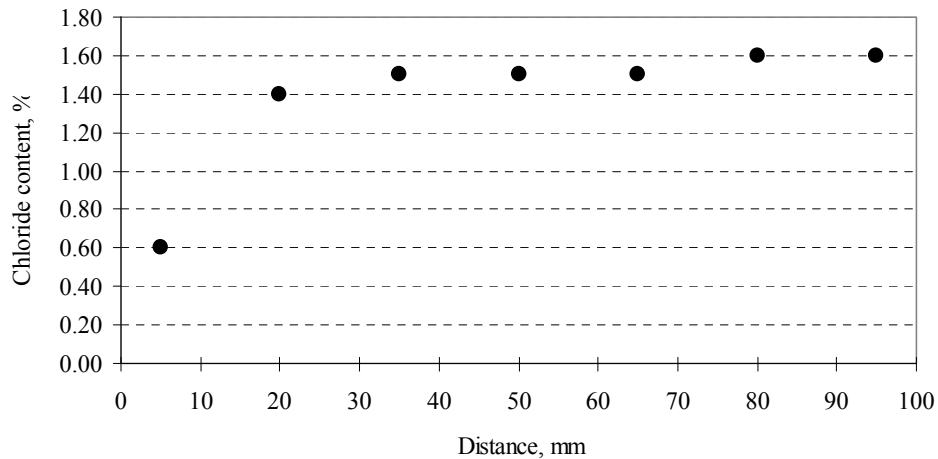


Figure 7.12 Chloride content in specimen 1552-B

7.4.5 Corrosion pit measurement and volume loss

The visual inspection of extracted bars involved the physical measurement of corrosion pit size and an estimated loss of volume of iron in the steel bars. Then, the assumption is that all liquid inside those pits has a low pH and thus the total amount of acid is proportional to the total pit volume. Next, the amount of charge needed to neutralize that amount of acid is calculated. Then, the total neutralizing charge is used to calculate the pH in the liquid. For this, the considered accumulated charge was determined at the time for which the current flow became stable during the first stage of the CP treatment. In this sense, variations of values of charge are different for each bar. The determination of pH based on a previous model is the following (Polder 2009; Polder 2010):

$$M_{H^+} = \frac{Q}{F} \quad (7.1).$$

$$a_{H^+} = \frac{M_{H^+}}{V_{H^+}} \quad (7.2).$$

$$pH = -\log(a_{H^+}) \quad (7.3).$$

Where M_{H^+} is the amount of hydrogen ions in mole, Q is the charge in A*s (Coulomb), F is Faraday's constant (9600 A*s/mole) and V_{H^+} is the volume of dissolved metal in liter.

A summary of pit size measurements are shown in Table 7.11. Full data regarding to this measurement and images of the visual inspection of bars are given in Appendix 3. It must be again noted, that the central bars 10C and 30C were not subject to CP treatment. In almost all cases, the central bar reported higher values of corroded surface and volume of iron dissolution. However, there is considerable scatter in results of pit measurement (surface, volume, mean depth). It must be noted that only the exposed area of steel bars (11 cm²) was considered when measuring the pit size and volume loss. Nonetheless, visual inspection of bars showed that corrosion pits were found underneath the coating. Since this was not meant to happen, the variations of pit size, current demand and volume loss would be influenced by the presence of pits of considerable size below the coating.

Table 7.11 Corrosion pit size measurement and estimation of volume loss.

Specimen		10L	10C	10R	30L	30C	30R
1450-B CEM I salt/dry	surface (mm ²)	250	720	340	60	320	70
	volume (mm ³)	220	1000	140	120	890	130
3550-C CEM III salt/dry	surface (mm ²)	40	30	20	20	10	10
	volume (mm ³)	30	40	20	30	20	20
1550-B CEM I carbonation	surface (mm ²)	90	130	60	50	120	60
	volume (mm ³)	80	60	40	20	100	40
1552-B CEM I Mixed in chlorides	surface (mm ²)	200	220	20	120	190	50
	volume (mm ³)	260	220	20	240	290	100

According to a proposed model (Polder 2009; Polder 2010), the time required for neutralizing the acidic solution inside corrosion pits is function of the pH of the acid, the volume of solution and the applied current. Since the loss of metal volume and the total charge at the time at which current became stable during the first 24 hours are known, it is possible to estimate the pH inside the corrosion pits of steel bars protected with CP with the use of formulas 7.1, 7.2 and 7.3. Results of estimated pH inside corrosion pits are shown in Table 7.12. Results using this model show values that are on the lowest estimation of pH inside pits. Values of pH from this model are rather extreme values for solution inside corrosion pits. On the other hand, some very low pH (<2) values are found in bars where the volume of metal loss is small. However, these results correspond to carbonated-induced corrosion which does not make sense for acid inside corrosion pits. In this case, the corrosion conditions are different and they are not part of this model for predicting pH in pits.

Table 7.12 Estimation of pH inside corrosion pits for charge values at individual turning points.

Specimen	Bar	Charge*	Volume	M(H)/liter	pH
		mA*s	mm ³		
1450-B CEM I salt/dry	10L	870	220	0.002682	2.57
	10R	560	140	0.003988	2.40
	30L	480	120	0.001947	2.71
	30R	510	133	0.002071	2.68
3550-C CEM III salt/dry	10L	120	32	0.005676	2.25
	10R	80	16	0.009306	2.03
	30L	120	28	0.002904	2.54
	30R	40	14	0.006732	2.17
1550-B CEM I Carbonated	10L	120	32	0.00726	2.14
	10R	80	18	0.012078	1.92
	30L	120	28	0.004488	2.35
	30R	60	14	0.012163	1.91
1552-B CEM I mix-in chlorides	10L	790	202	0.001327	2.88
	10R	80	20	0.010098	2.00
	30L	950	241	0.001634	2.79
	30R	400	98	0.001465	2.83

7.5 Discussion

7.5.1 Corrosion state of steel bars before CP.

The relationship between corrosion rate and corrosion potential of these concrete specimens is shown in Figure 7.13. For specimen 1450-B all bars have potentials that are more negative than -350 mV, which implies a high probability of corrosion. This was confirmed by results of corrosion rate in which all bars at 10 and 30 mm depth reported high values of corrosion rate. In the case of specimen 3550-B, the potentials are divided in two groups, one with values above -350 mV which is related to a passive state of steel for steel bars at 30 mm depth and the other group of bars at 10 mm depth with potential values below -350 mV. Corrosion rate of bars embedded in this concrete specimen are the lowest of the four, which confirms that the activation time for corrosion in this specimen has been delayed when compared to specimen 1450-B.

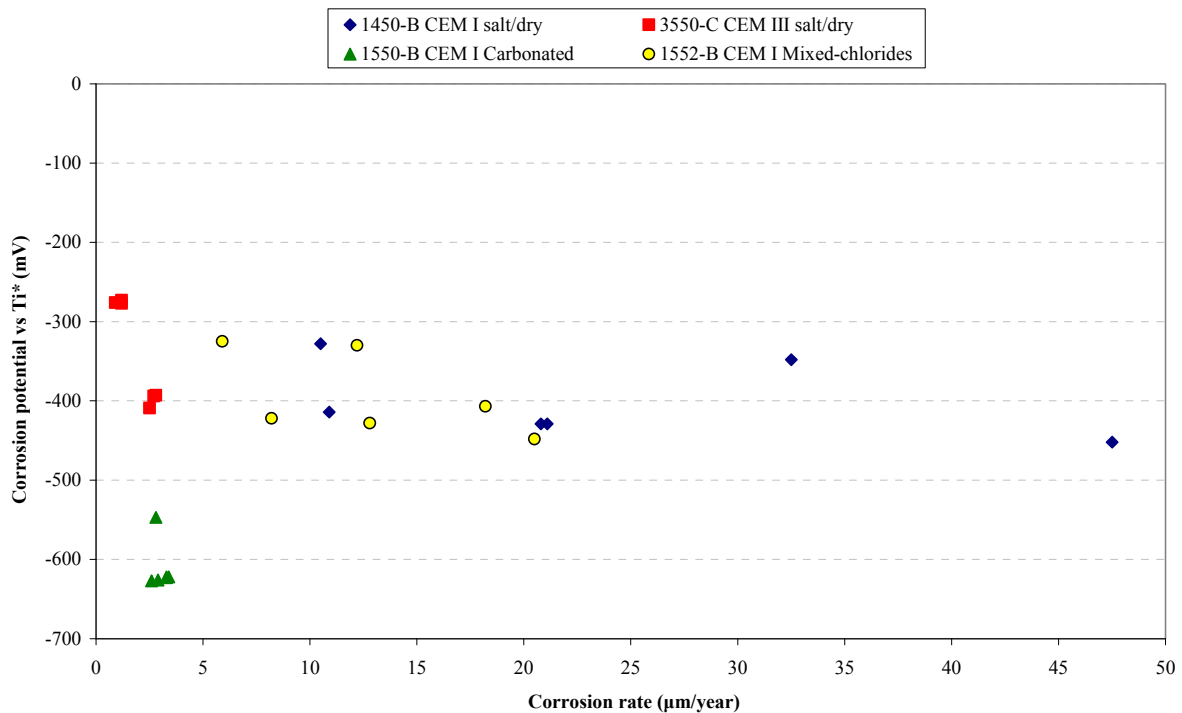


Figure 7.13 Corrosion rate and corrosion potential of concrete specimens before CP.

The carbonated specimen, 1550-B reported the most negative values of potential as described above, while the corrosion rate remained also at low values. The conditions in the surroundings of bars embedded in carbonated concrete seem to be responsible of such negative potential values. As for corrosion rate, corrosion due to carbonation seems to have a lower rate of deterioration in this specimen. Again, the unknown environmental exposure after 30 weeks may play a role. From this, it may be suggested that the specimen was stored in a wet environment that delayed oxygen penetration and therefore, slowed down the corrosion process. Finally, the specimen 1552-B cast with chlorides showed potential values similar to those found in specimen 1450-B. Corrosion rate in this specimen is lower when compared to the Portland cement specimen exposed to salt/dry cycles but higher than the slag cement concrete and carbonated concrete.

When considering the influence of carbonation (neutral pH) in values of corrosion potential, it must be considered the influence of such environment in the embedded Ti* electrodes. As potentials of Ti* in 1550-B seem to deviate from other specimens (Table 7.2), by 300 mV. This evidence strongly suggests that all potentials measured with Ti* electrodes are shifted, even those during the evaluation of corrosion in Chapter 6. Actually, steel potentials by Ag/AgCl are more positive than by Ti* (for all bars). This suggests that potential values as measured by Ti* are probably shifted by up to 300 mV into negative direction due to shift of the reference electrode.

However, potential values in carbonated concrete indicate that the degradation state of steel bars could be more significant than it appears and changes in either moisture or chemical composition of the pore solution may produce conditions that would degrade steel in a much faster rate. Finally, the specimen 1552-B cast with chlorides showed potential values similar to those found in specimen 1450-B. Corrosion rate in this specimen is lower (but still higher) when compared to the Portland cement specimen exposed to salt/dry cycles but higher than the slag cement concrete and carbonated concrete.

Results show that the relationship between corrosion rate and corrosion potential is not straightforward, especially in the propagation phase of corrosion of steel in concrete. In this phase, the corrosion rate is more related to the influence of concrete resistivity than to corrosion potential. However, important information regarding to the state of corrosion can still be acquired from this parameter. For example, the most negative values of potential were found in carbonated concrete, with values between -550 and -650 mV vs Ti* (or -250 to -350 when considering the real values of Ti* potential shift). Such negative potentials were previously reported in literature (Arup 1983); therefore, by measuring corrosion potential and combining it with a visual inspection on-site may give to the material scientist an idea of the ongoing degradation mechanism. In concrete that has

been exposed to chlorides, the distinction between cement types is hardly found. In this case, additional non-destructive testing is recommended.

As discussed previously, in the propagation phase the values of corrosion rate and electrical resistance are related due to the characteristics of the pore network. As literature has shown, concrete resistivity (which is related to electrical resistance of the pore network) has significant influence on the rate at which corrosion may propagate after initiation phase (Andrade 1996; Polder 2001b). Portland cement specimens 1450-B exposed to salt/dry cycles and 1552-B cast with mixed-in chlorides reported the highest values of corrosion rate in all embedded bars. Also, their electrical resistance of the cell between the anode and the bars were the lowest. These results show that propagation of corrosion due to low resistivity has been higher in these specimens. On the other hand, specimen 3550-C cast with slag cement has the highest values of electrical resistance. This is correlated to low corrosion rates and more positive potentials than the rest of the specimens. Finally, carbonated concrete in specimen 1550-B reported low values of both corrosion rate and electrical resistance. As discussed before, these conditions may not be held when changes in moisture or further carbonation may be present. Until now, carbonated concrete specimens have shown characteristic properties that make predictions of the damage state of the bars more difficult. Figure 7.14 shows the relationship between corrosion rate and inverse of electrical resistivity of concrete specimens before CP.

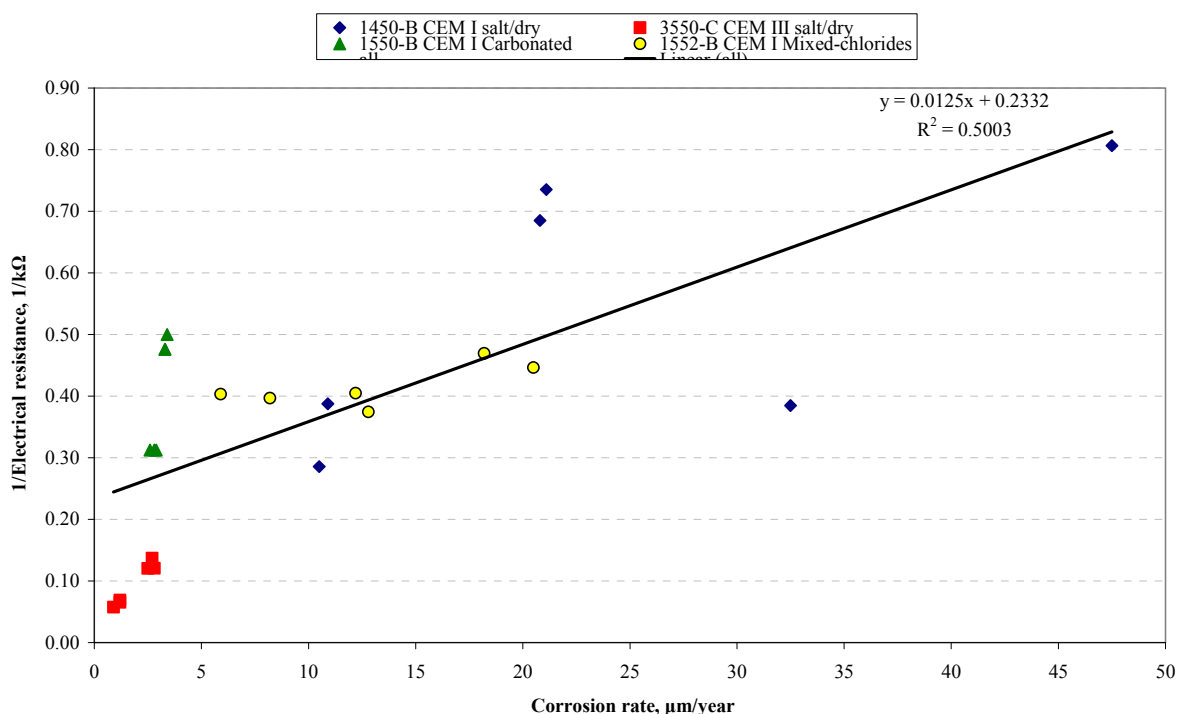


Figure 7.14 Corrosion rate and electrical resistance of concrete specimens before CP.

In this figure, the correlation between corrosion rate and the inverse of electrical resistance was found to be around 0.5. This correlation factor suggests that there is no serious correlation between concrete resistivity and corrosion rate in these specimens. The values of electrical resistivity and corrosion rate of steel in concrete under the propagation phase shows that after 12 years, there is no direct correlation between concrete resistivity and corrosion rates for specimen 1450-B. However, for concrete cast with CEM III, there is a linear correlation between corrosion rate and resistivity. In the case of carbonated concrete, the corrosion rate remained low even though the concrete resistivity was low as well. This confirms that in the carbonation process the rate of corrosion depends on other mechanisms than in chloride induced pitting corrosion. Therefore, the corrosion rate in this specimen is lower. In the case of Portland cement concrete with mixed-in chlorides and salt/dry exposure, the relationship between corrosion rate and concrete resistivity is stronger. In this sense, for Portland cement concrete structures the concrete resistivity and its relationship with the pore structure controls the ingress of both chlorides and the propagation due to ion transport between anodes and cathodes. In the case of mixed in-chlorides, the composition of the pore structure and the binding capacity has a significant influence in the corrosion rate of such specimen.

7.5.2 Measurements during CP treatment.

The relationship between initial current demand ($t=0$) and corrosion rate before CP is shown in Figure 7.15. As discussed before, the demand of current immediately after applying CP depends on the state of corrosion in each bar. Bars with high corrosion rate are related to higher current demands with a correlation factor of 0.86. This suggests that when CP is applied on the structure, the current flow will be distributed according to the comparative corrosion state of individual bars (which is more straightforward).

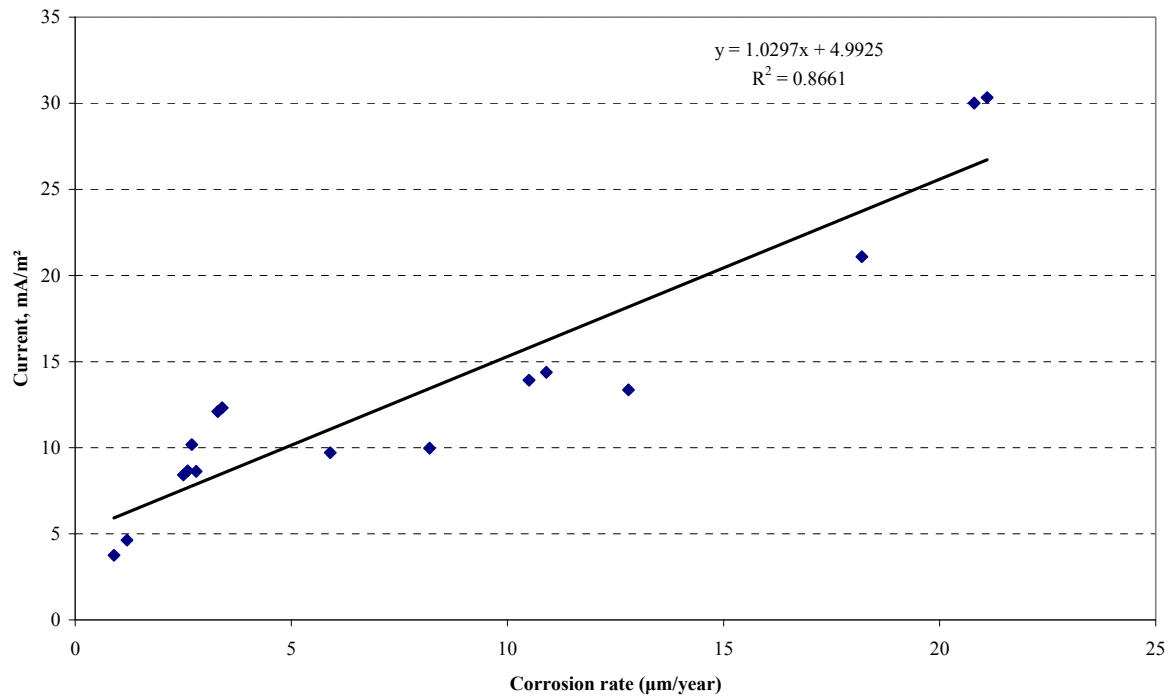


Figure 7.15 Relationship between initial current at $t=0$ and corrosion rate before CP.

The correlation between corrosion rate and total charge over 18 days in CP treated bars is shown in Figure 7.16. The relationship between these two parameters is not as good as with the correlation of corrosion rate and initial current demand as shown in Figure 7.8. This evidence suggests that the effectiveness of CP is determined by the corrosion state of the bars, modified by external parameters (Temperature, moisture content, etc.) A model to predict such behavior may have the form:

$$y = ax + b \quad (7.4).$$

Where y is the electric current demand of CP, x is the corrosion rate of bars and factors a and b are dependant to other external mechanisms. Factor a is most probably related to concrete related parameters like cement type, water:binder ratio and concrete resistivity; while factor b is probably related to external conditions like temperature and moisture changes. The low correlation of these two parameters may be due to the gradual reduction of current consumption of steel bars over time. A group of bars that had low corrosion rates still consumed significant charge after treatment. It is uncertain the level of influence when all these parameters interact between themselves. When corrosion has been stopped by imposed current, still on-going cathodic reactions occur over the surface of steel. The continuous consumption of current sustains this behavior.

It is difficult to say if transport of chlorides in specimen 3550-C or concrete realkalisation in carbonated specimen 1550-B has anything to do with these values, but for certain, they differ with values found in concrete cast with CEM I exposed to both salt/dry cycles or mixed-in chlorides.

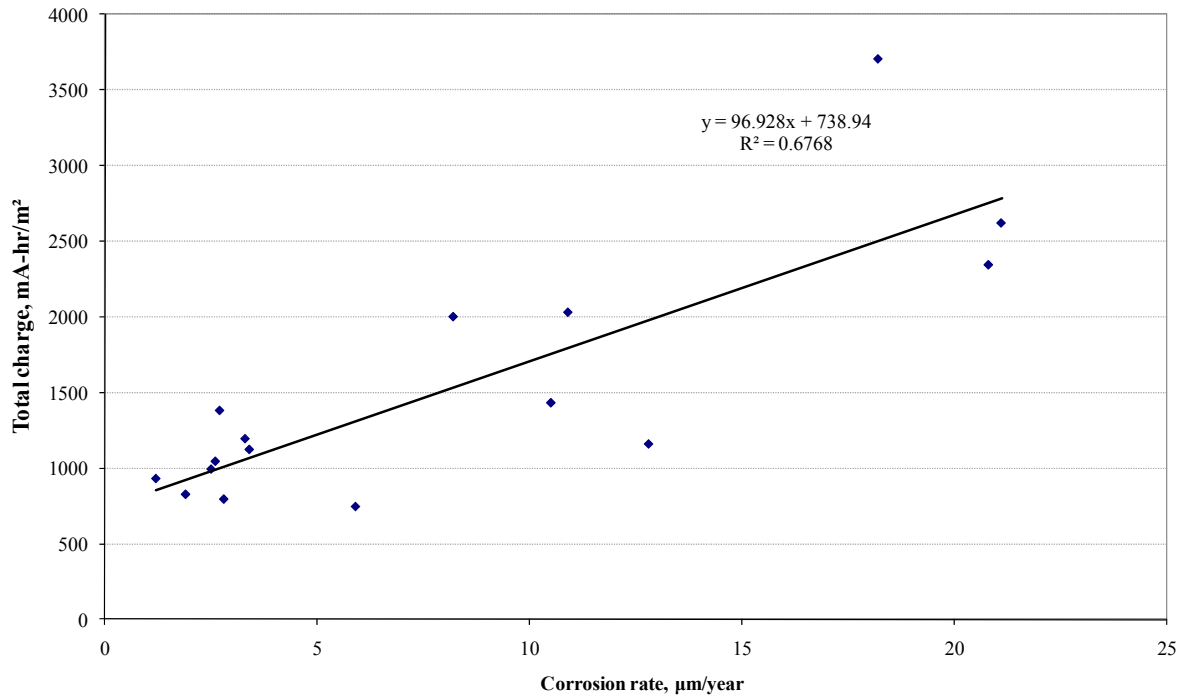


Figure 7.16 Corrosion rate and total charge in CP treated bars after 18 days.

As described before, the second stage of CP was carried out with a driving force of 1.2V during 15 days. The immediate current demand during this period (after 24 hours of depolarization, thus without current) is shown in Figure 7.17. When comparing these values to the current at the beginning of the first CP period (thus, actively corroding), the present values are significantly lower. There is hardly any relationship between previous corrosion rate and CP current, considering the low slope and the rather high scatter around it. This evidence suggests that corrosion processes probably have been stopped and that the pH of acidic liquids inside the corrosion pits is neutralized.

However, even after 18 days of CP the current demand of steel bars is dependant of the corrosion rate before CP in a lower degree. In this sense, bars with higher corrosion rate still demanded more current immediately after applying the second stage of CP treatment. On the other hand, the influence of cement type is clearly seen in this figure. Portland cement concrete reported higher values of corrosion rate which again, influence the immediate consumption of electric current due to CP. This behavior suggests that the previously discussed model has indeed a relationship between the gradient is in relationship with concrete parameters like cement type, water-binder ratio and concrete resistivity.

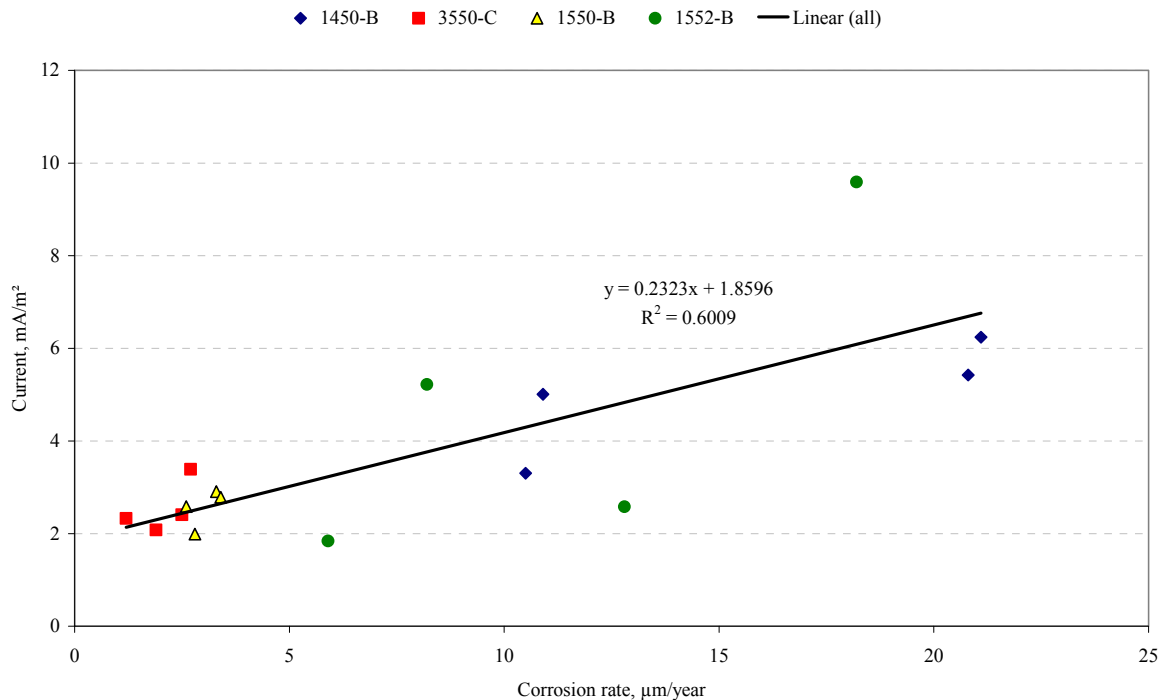


Figure 7.17 Immediate current demand of CP treated bars at 1.2V.

7.5.3 Depolarization

The behavior of bars under depolarization in specimen 1450-B may be caused by lack of oxygen at the surface of steel due to high moisture content in the specimens. Since they were stored inside a box with a 10 mm water level, the moisture inside them may have slowed down oxygen transport that is needed for depolarizing reactions. If that is true, waiting longer might have shown stronger depolarization. The quite negative potentials (in all specimens) support this view.

Overall results suggests that electrochemical repair of steel by CP had a better effect in slag concrete. As discussed before, transport of moisture in this concrete specimen is surely lower than in Portland cement concrete. Therefore, some pores remain without water, favoring transport of oxygen towards the steel bar surface. In carbonated concrete, the potential shift occurs towards more negative values. However, these considerations must be taken with care because carbonated concrete showed less sensitivity to changes in temperature or moisture. In this specimen, the influence of external conditions is not as strong as the reduction of pH due to carbonation. Finally, for specimen 1552-B the potential of reference bars remains almost constant. This behavior suggests that the increase of moisture content during the CP treatment did not show any detrimental effect on depolarization. Apparently, this specimen was near complete saturation before it was stored inside the container, so the water level at the bottom of it was irrelevant.[‡]

7.5.4 Chloride profiles

Figure 7.18 shows the chloride profiles in chloride exposed specimens. The chloride profile in specimen 1450-B s/d appeared rather flat. After 12 years, the chloride content inside this specimen seems to be in equilibrium over nearly the whole depth of the specimen. This is supposedly due to a high diffusion coefficient of chlorides for this type of concrete. This findings coincide with others previously reported in the North-sea (Polder 1995). In the case of specimen 3550-C, the chloride content reached a high value in the interval between 15-29 mm. The rest of the specimen reported low values of chloride content which are below the threshold value. Apparently, CEM III/B has a low chloride diffusion coefficient on the long term (Polder 1995). In this sense, the results of corrosion rate of this specimen, which were lower than in 1450-B, are corresponded by the chloride distribution. In the case of specimen 1552-B, the added chloride contained was nominally 2% by mass of cement, but results

[‡] This seems to suggest that CP in concrete undersea level may not depolarize at 100 mV due to the lack of oxygen for this reaction.

show values somewhat below this level. Since the test analyzes all chlorides in the concrete matrix, it is possible to infer that the addition of chloride was slightly lower than reported.

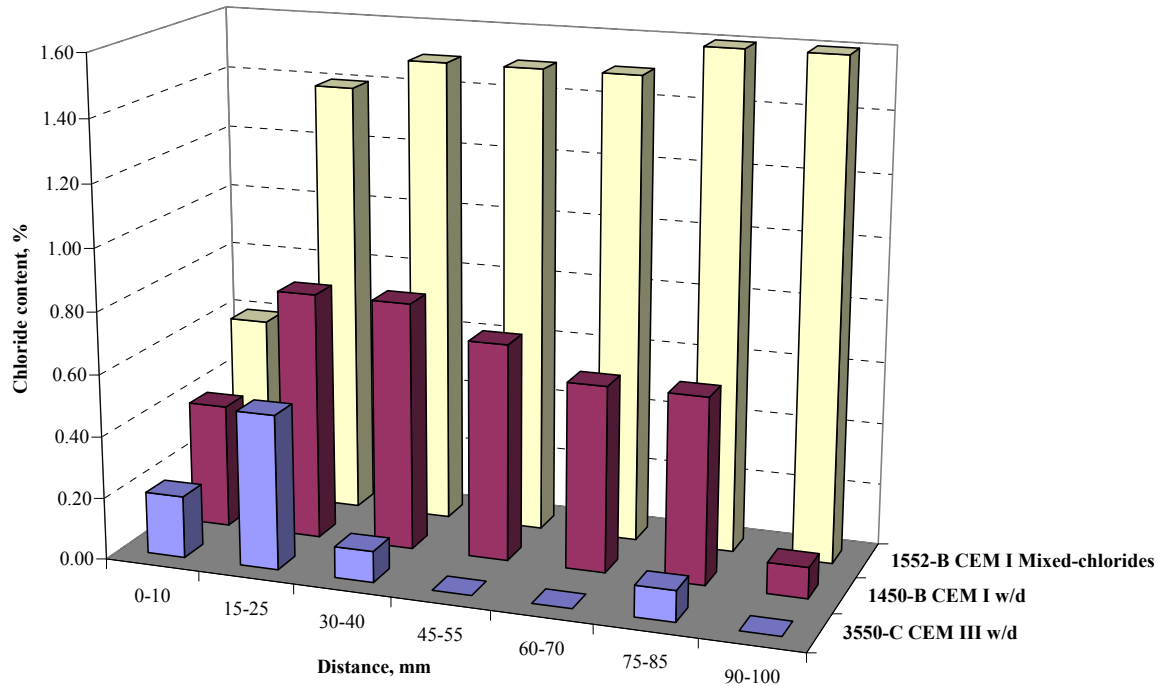


Figure 7.18 Chloride content of specimens exposed to chlorides.

7.5.5 Corrosion pit measurements and CP

The correlation between the individual accumulated charge of steel bars and volume loss after CP is shown in Figure 7.15. Since the neutralization of acid inside corrosion pits occurs during the first hours after applying CP, the total charge considered for this relationship was taken over the first 24 hours of cathodic protection. The correlation of these values show significant scatter, especially at high charge consumption values. The values of volume loss are also influenced by the presence of pits underneath the coating, which were not considered when calculating the pit size. However, those pits were mainly found in bars 10C which had values of volume loss which were low considering the corrosion rate. However, these bars served for reference so there are no records of current for these bars.

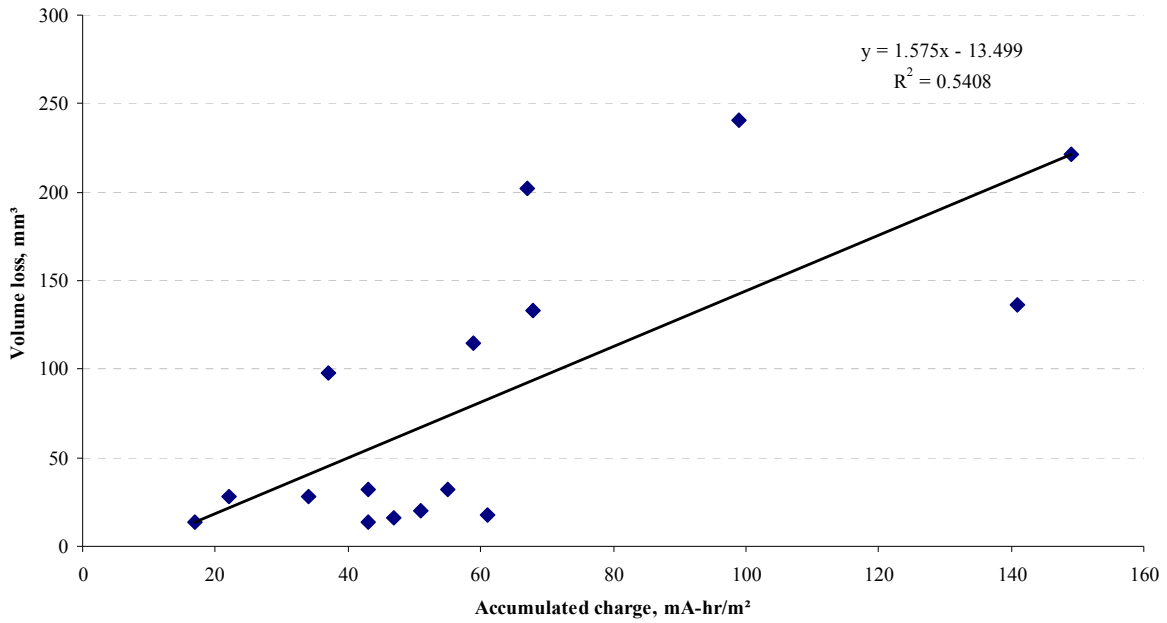


Figure 7.19 Total charge over the first 24 hours of CP current flow and volume loss of steel from destructive analysis after CP.

The relationship between volume loss of steel and estimated pH is shown in Figure 7.21. It is clear that there is no clear correlation between these two parameters. However, estimation of pH concerns idealized conditions that are probably not present in the specimens. In this sense, the estimation of pH does not constitute a reliable outcome, at least under these circumstances. For a proper correlation between loss of volume and pH, measurements of pH with a better technique may prove that the beliefs by (Arup 1983; Polder 2009; Polder 2010) can be quantified.

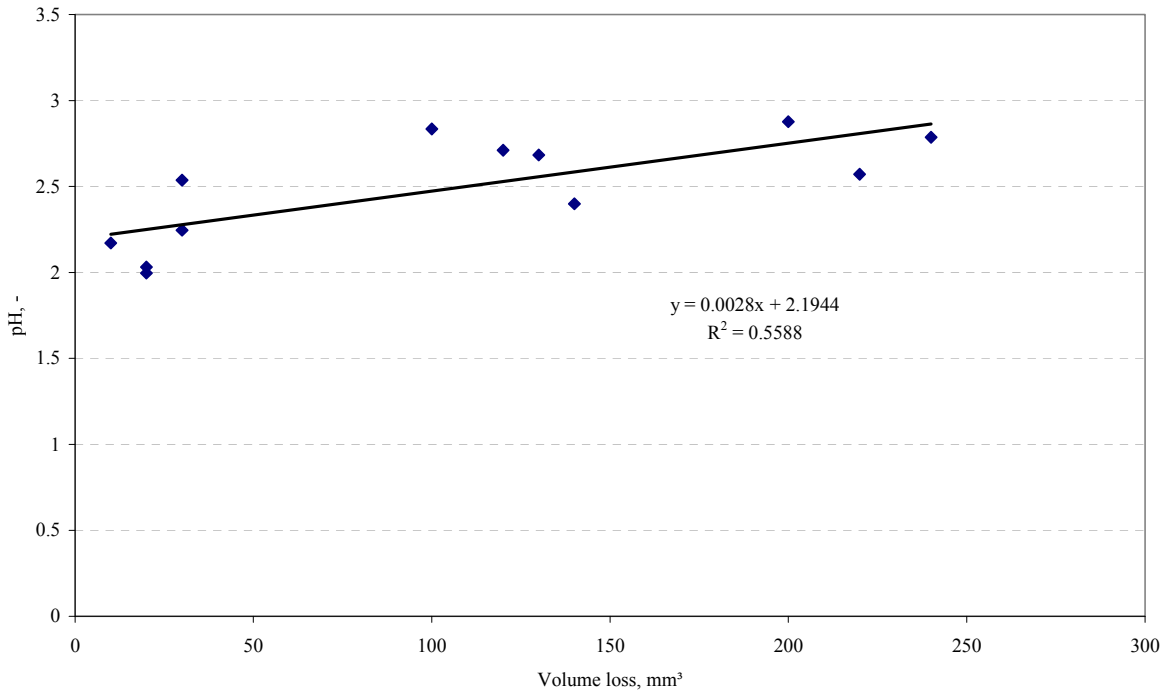


Figure 7.20 Volume loss and pH estimation of corrosion pits.

Synopsis

In this chapter, a study of electrochemical repair on steel reinforcement in concrete was carried out. Before any repair procedure was applied, measurements of electrochemical parameters were obtained of four selected concrete specimens: Portland cement and CEM II concrete exposed to salt/dry cycles, Portland cement carbonated concrete and Portland cement concrete with mixed-in chlorides.

In the short-term benefits of CP, it was found that the electric current consumption of bars under treatment right after CP was turned on is strongly related on corrosion rate before CP. During the first 4 to 8 hours, the electric current decreased gradually until a transition point in time when the current became stable until 24 hours. These transition points were different for each individual bar. The evidence suggests that neutralization of acidic pools in corrosion pits occurs in this time interval.

On the long-term benefit, Portland cement concrete exposed to chlorides (salt/dry and mixed-in) reported higher degrees of electrical current demands. The relationship between corrosion damage before CP and the electrical current and total charge flow in these specimens seems to be related in these specimens. However, this was not the case for slag cement concrete or Portland cement carbonated concrete. In the latter, the environmental surroundings nearby the reinforcement sustain different conditions that influence the electrical charge and current demands.

The depolarization measurements showed that over 18 days at 1.4V after being stored with a 10 mm water level, the shift in potential after turning off the CP current did not reached a value of 100 mV. The reason behind this was the near complete saturation of the specimens which slowed down the ingress of oxygen necessary for depolarization reaction. After another two weeks of CP treatment at 1.2V without water level, values of depolarization reached the 100 mV shift in almost all bars. As the specimens were drying out, the oxygen availability was increased.

Results in specimens with chloride-exposure showed that for specimens exposed to salt/dry cycles, Portland cement concrete contained higher amount of chlorides than CEM III. Also, the overall distribution of such chlorides in Portland cement concrete was about the same until a 90 mm depth. In slag concrete, the highest amount of chlorides was found until a depth of 25 mm. In both cases, the content surpassed 0.4% per cement weight. In mixed-in chloride specimen, the chloride content was below 2% per cement weight. The reason was attributed to errors during the addition of the admixture in the fresh mix.

Carbonation depth results showed that Portland cement concrete exposed to chlorides was carbonated until 18 mm depth. This represents conditions of both chlorides and carbonation for bars at 10 mm depth. This condition also influenced the chloride profile. Concrete with mixed-in chlorides reported the lowest values of carbonation depth. Apparently, the carbonation reaction is disturbed or slowed down by the presence of chlorides in high levels of concentration.

Measurements of pH were carried out in corrosion products on the surface of steel from a dummy specimen. Results showed that the technique was too rudimentary and affected by external parameters like presence of mortar in the corrosion products. The results were not concluding in all cases. Estimations of pH were attempted with the use of total charge consumption after each period of CP treatment. Results reported values on the lower extreme and probably are not representative of the pH of acidic pools. However, they do show that values inside pits are very acidic (around 2).

Conclusions

The state of corrosion of embedded steel in concrete has been studied in this project. This research was carried out in a three levels: inspection, evaluation and electrochemical repair of corrosion. In each level involved different goals and expected outcome. In this sense conclusions are drawn apart in each level of study and described as follows:

Inspection of concrete specimens: Identification after 12 years of exposure

- Visual inspection resulted in a useful tool when separating “apparent” cement types and exposure conditions. In combination with previous reports, it constituted a good way to start further analysis of this research.
- Statistical analysis has resulted in a powerful tool for analyzing values of concrete resistivity in order to identify cement types. The combination of NFD test and previous reports proved that in exposure to salt/dry and mixed-in chlorides, cement type is the most influencing parameter. However this tool could not identify with certainty cement type in carbonated concrete.
- Schmidt hammer testing was useful in order to provide a reasonable approach of water/binder ratio. However for an analysis with a higher degree of confidence, microscopy and image processing may result in better and more precise outcome.

Evaluation of corrosion and electrochemical parameters: measurements of potential, resistivity and corrosion rate.

- Corrosion potential of specimens fluctuated between -200 to -600 mV vs Ti* in specimens containing either penetrating or mixed-in chlorides. In carbonation specimens, corrosion potential reached values around -700 mV. Also, these values were most sensitive to changes in environmental conditions of temperature and relative humidity. Most negative values were found in conditions of low relative humidity and moderate temperature.
- Concrete resistivity of specimens exposed to salt/dry fluctuated according to cement type. Lowest values were found in concrete with CEM I and CEM II. Higher values in specimens with CEM III and CEM V were found. This behavior was also found in mixed-in chloride specimens. Also, changes in environmental conditions have influenced considerably the values of concrete resistivity in specimens exposed to penetrating or mixed-in chlorides. However, for carbonation specimens, changes in values of concrete resistivity are significantly lower.
- In wet/dry specimens, higher corrosion rates were attributed to Portland cement, high w/b ratio and 10 mm of cover depth. In carbonated concrete, high corrosion rates were found in CEM V, 0.45 w/b ratio and 30 mm of cover depth. In mixed-chloride specimens, high corrosion rates were obtained in CEM I & CEM II, 0.55 w/b ratio and either cover depth. In freezing temperatures (around 0°C) measurements of corrosion rate reported very low values when compared to reports after 2.5 years. At average temperature in The Netherlands (10°C), corrosion rate values were similar than those reported after 2.5 years.

Electrochemical repair of corrosion: short and long term benefits of CP:

- CEM I salt/dry concrete had the highest corrosion rates before CP, consumed higher values of electrical charge during the treatment, had higher values of carbonation depth, and higher values of volume loss of steel. CEM III salt/dry reported higher values of resistivity, low corrosion rate, low lost volume of steel and lower consumption of electrical charge. CEM I carbonated concrete, had low corrosion rates, low resistivity, lesser volume lost of steel and low charge demand. CEM I mixed-chlorides, had the lowest values of resistivity, high corrosion rates, higher demands of charge and high values of volume loss of steel.
- The initial current demand and total charge consumption are related to the initial state of corrosion of steel bars subject to CP. The volume of metal lost due to dissolution in chloride environment is somewhat related to the damage state of bars before CP. Neutralization of pH inside corrosion pits most likely take place in the first 8 hours of CP.
- Total charge over 18 days at 1.4V and 15 days at 1.2V is dependant of the conditions of corrosion deterioration of steel (corrosion rate).
- Values of pH measurements were not concluding due to limitations of the measuring technique. However, evidence obtained during the recording of the current demand of steel bars suggests that is

- Chloride content of concrete specimens showed that internal diffusion was found in specimens exposed to salt/dry cycles.
- Estimations of volume loss of metal in bars are related to corrosion damage in Portland cement concrete exposed to chlorides (salt/dry and mixed-in). However, this was not the case for CEM III concrete exposed to salt/dry and Portland cement carbonated concrete.

As a personal opinion, this project has showed a significant scatter in measured values of almost all properties. From the research point of view, this is not desired due to difficulties to explain and prove the behavior of concrete specimens and properties. However, this challenge is more related to real-life consulting of civil infrastructure. Also, this report intended to combine both aspects: interpretation of properties and behavior in a material scientist's point of view with practical comments from an engineering approach.

Recommendations for future research

There are plenty of areas of opportunity for further research in this project. During the inspection phase, after specimens have been identified, a probabilistic model that studies other electrochemical parameters in concrete is useful. It is advised to first study the behavior of such properties at 2.5 years of age and comparing it with the performance of concrete specimens at present. If behavior at the present is reproducible from that found at 2.5 years, a probabilistic model that could predict future behavior of the same specimens is motivating. On the testing field, non-destructive testing for concrete characterization is also recommended. These tests might include ultrasonic pulse velocity and CT scanning. For destructive analysis, certainly microscopy of hardened and deteriorated concrete is appealing for geologists and material scientists in general.

During the evaluation phase, research done in the field of characterization of corrosion rate in terms of environmental conditions might be useful. It is recommended to study the effect of seasonal variations in order to provide contractors guidelines to perform testing that is more representative to the highest rate of deterioration during a year. Additionally, the propagation of corrosion in cracked concrete is interesting because changes in environmental and loading conditions may be favorable for corrosion deterioration in previously damaged structures.

Finally, in the electrochemical repair field, it is advised to study the effect of pH inside pits while imposed CP current is being applied. This research may prove that the neutralization of pH in acidic pools is certainly obtained during the first hours of application of CP. It must also involve a more developed and technological mean to inspect deteriorated steel in concrete after extraction. Another interesting direction is the development of a model that describes the behavior of steel bars under CP with regard to concrete parameters and corrosion state before repair.

References

- ACI-201 (1991). "Proposed revision of guide to durable concrete." ACI Journal of Materials **88**(5).
- ACI 365 (2000). Service-Life Prediction. 365.1R-00, American Concrete Institute.
- ACI, Ed. (2008). Concrete Repair Manual, American Concrete Institute.
- Aitcin, P.-C. (2008). Binders for Durable and Sustainable Concrete. New York, Taylor & Francis.
- Alonso, C., Andrade C., González J., (1988). "Relation between concrete resistivity and corrosion rate of the reinforcements in carbonated mortar made with several cement types." Cement and concrete research **18**(5).
- Andrade, C., Alonso, C. (1996). "Corrosion rate monitoring in the laboratory and on-site." Construction and Building Materials **10**(5): 315-328.
- Angst, U., Elsener, B., Larsen, C.K, Vennesland O. (2009). "Critical chloride content in reinforced concrete - A review." Cement and Concrete Research **39**.
- Arup, H. (1983). The mechanism of the protection of steel by concrete. Corrosion of Reinforcement in Concrete, Society of Chemical Industry.
- Arya, C., Buenfeld N.R., Newman, J.B. (1989). "Factors influencing chloride-binding in concrete." Cement and Concrete Research **20**.
- ASTM C666-08 (2008). Standard Test Method for Resistance of Concrete to Rapid Freezing and Thawing, American Society of Testing Materials.
- ASTM C876-09 (2009). Standard Test Method for Half-Cell Potentials of Uncoated Reinforcing Steel in Concrete, American Society of Testing Materials.
- Atiş, C. D. (2003). "Accelerated carbonation and testing of concrete made with fly ash." Construction and Building Materials **17**(3).
- Atkins, P., De Paula, J., (2006). Physical Chemistry, Oxford University Press.
- Baron, J., Ollivier, J.P., (1992). La Durabilité des bétons. Paris, Presses de l'École Nationale des Ponts et Chaussées.
- Bedford, T., Cooke, R.M. (2001). Probabilistic Risk Analysis – Foundations and Methods, Cambridge University Press.
- Bertolini, L. (2004). Corrosion of steel in concrete, Wiley-VCH.
- Broomfield, J. P. (2007). Corrosion of steel in concrete: understanding, investigation and repair. London, Taylor & Francis.
- Byfors, K. (1985). "Carbonation of concrete with silica fume and fly ash." Nordic Concrete Research **4**.
- Caballero, J. (2009). Chloride diffusion in concrete at early age. Materials and Environment. Delft, Delft University of Technology. **Master in Science**.
- Campbell, D. H., Sturm, R.D., Kosmatka, S.H., (1991). "Detecting carbonation." Concrete Technology Today **PL911**.
- Chess, P. M. (1998). Cathodic protection of steel in concrete. New York.
- Colleparidi, M., Marcialis, A., and Turriziani, R., (1972). "Penetration of Chloride Ions into Cement Pastes." Journal American of Ceramics Society **55**: 534.
- Corrosion costs. (1997). "Costs of corrosion: Infrastructure."
- COST-521, Ed. (2003). Corrosion of steel in reinforced concrete structures. Final report, COST.
- COST 509 (1997). Corrosion and Protection of Metals in Contact with Concrete - Final Report. R. C. R.N. Cox, O. Vennesland, T. Valente, COST.
- COST 534 (2009). New Materials, Systems, Methods and Concepts for Prestressed Concrete Structures. R. B. Polder, Alonso, M.C., Cleland, D.J., Elsener, B., Proverbio, E., Vennesland, O., Raharinaivo, A., Brussels, cost.
- De Sitter, W. R. (1984). Costs of Service Life Optimization: The Law of Fives. Durability of Concrete Structures Workshop Report.
- Emmons, P. H., Sordyl D.J. (2006). "The state of the concrete repair industry, and a vision of its future." Concrete Repair Bulletin **July/August 2006**.
- Glass, G. K., Reedy, B., Lim, P.J., Buenfeld, N.R. (2002). "On the corrosion risk presented by chloride bound in concrete." Cement & Concrete Composites **24**.
- González, J., Andrade C., Alonso C., Feliú S., (1995). "Comparison of rates of general corrosion and maximum pitting penetration on concrete embedded steel reinforcement." Cement and Concrete Research **25**(2).
- Guerreri, M., Polder, R.B. (2002). Comparison of corrosion of steel bars in blended cement concrete from linear polarization resistance and visual examination after destructive analysis. TNO Bouw. Delft, TNO.

- Haque, M. N., Kawamura, M., (1992). "Carbonation and chloride-induced corrosion of reinforcement in fly ash concretes." ACI Journal of Materials **89**(1).
- Jones, D. A. (1996). Principles and prevention of corrosion, Upper Saddle River: Prentice Hall.
- Khunthongkeaw, J., Tangtermsirikul, S., Leelawat, T., (2006). "A study on carbonation depth prediction for fly ash concrete." Construction and Building Materials **20**.
- Kolek, J. (1958). An appreciation of the Schmidt Rebound Hammer. Magazine of Concrete Research. London. **10**: 27-36.
- Koninklijk Nederlands Meteorologisch Instituut. (2010). "Mean temperature and average moisture content."
- Kosmatka, S. H., Kerkhoff, B., Panarese, W.C., Tanesi, J. (2004). Design and control of concrete mixes. Skokie, IL, Portland Cement Association.
- Malhotra, V. M. (1968). Nondestructive Methods for testing concrete. Mines Branch Monograph. Ottawa: 66.
- Malhotra, V. M. (1976). Testing Hardened Concrete: Nondestructive methods. Detroit, MA.
- Maslehuddin, M., Saricimen, H., Al-Mana, A.I. (1987). "Effect of fly ash addition on the corrosion resisting characteristics of concrete." ACI Journal of Materials.
- Mietz, J. (1998). Electrochemical rehabilitation methods for reinforced concrete structures. London, European Federation of Corrosion Publications.
- NEN-EN (2001). 12504-2: Beproeving van beton in constructies. Deel 2: Niet-destructief onderzoek
- Neville, A. (1995). Properties of concrete, Harlow Longman.
- Nijland, T. G., Siemes, A.J.M. (2002). "Alkali-silica reaction in the Netherlands: Experiences and current research." HERON **47**(2).
- Pedefferri, P. (1995). "Cathodic protection and cathodic prevention." Construction and Building Materials **10**(5).
- Peelen, W., Polder, R.B. (2003). Accelerated aging tests of the zinc-hydrogel anode for galvanic cathodic protection of steel in concrete. 2003-CI-R0033. TNO Building and Construction Research. Delft, TNO.
- Polder, R. B. (2000). Corrosion protection of concrete with fly ash cement and other binders. 2000-BT-MK-R0018/02. TNO Building Construction Research. Rijswijk, TNO.
- Polder, R. B. (2001a). Corrosion protection of reinforcement in concrete with fly ash cement and other binders subjected to salt/dry loading, accelerated carbonation and addition of chloride: Results until 2.5 years age and destructive analysis. 2001-CI-R1029-02. TNO Building and Construction Research. Delft, TNO.
- Polder, R. B. (2001b). "Test methods for on site measurement of resistivity of concrete – a RILEM TC-154 technical recommendation." Construction and Building Materials **15**: 125-131.
- Polder, R. B., Larbi, J.A., (1995). "Investigation of Concrete Exposed to North Sea Water submersion for 16 Years." HERON **40**(1): 31-56.
- Polder, R. B., Peelen, W.H.A., (2002). "Characterisation of chloride transport and reinforcement corrosion in concrete under cycling wetting and drying by electrical resistivity." Cement & Concrete Composites **24**.
- Polder, R. B., Peelen, W.H.A., (2009). Numerical modeling of cathodic protection in concrete structures. Int. Conf. Concrete Solutions, London, Taylor & Francis Group.
- Polder, R. B., Russo P. (1998). Concrete resistivity, corrosion potential and corrosion rate at young age as a function of cement type. 98-BT-R1664. TNO Building and Construction Research. Rijswijk, TNO.
- Polder, R. B., Stoop, W.H.A., Neeft, B.J.Th., (2010). "Early stage beneficial effects of cathodic protection in concrete structures." Materials and Structures Submitted.
- RILEM (1996). REPORT 14: Durability design of concrete structures. London, E&FN SPON.
- RILEM CPC-118 (2006). Measurement of hardened concrete carbonation depth, RILEM.
- RILEM TC 104 (1994). "Draft recommendation for damage classification of concrete structures." Materials and Structures **27**(170): 362-369.
- Rodriguez, J., Ortega, L.M., Garcia, A.M., Johansson, L. and Petterson K. (1994). On site corrosion measurements in concrete structures using a device developed under the Eureka project EU-401. International Conference, Concrete across borders, Odense.
- Schiring, E. (2008). Falen of Presteren - Omgaan met het proces Corrosie, Energie Onderzoek Centrum Nederland, ECN.
- Stern, M., Geary, A.L. (1957). "A theoretical analysis of the shape of polarization curves." Journal of Electrochemical Society(104): 56.
- Tang, L., Nilsson, L-O. (1993). "Chloride binding capacity and binding isotherms of OPC pastes and mortars." Cement & Concrete Research **23**.
- The Concrete Society (1988). Permeability testing of site concrete: a review of methods and experience. Crowthorne.
- Thomas, M. D. (1994). "Chloride thresholds in marine concrete." Cement and Concrete Research **26**(4): 513-518.

- Tuutti, K. (1982). Corrosion of steel in concrete, Swedish Cement and Concrete Research.
- Vennesland, Ø., Raupach, M., Andrade, C. (2007). "Recommendation of Rilem TC 154-EMC: "Electrochemical techniques for measuring corrosion in concrete"—measurements with embedded probes." Materials and Structures **40**(8).
- Vries, d. J., Polder, R.B., Borsje, H., (1998). Durability of hydrophobic treatment. Concrete under severe conditions, Tromsø.

Appendix A: Inspection of concrete specimens

Appendix B: Evaluation of corrosion of steel in concrete

Appendix C: Electrochemical repair of corrosion